Université de Montréal

Importance of the HSP90 molecular chaperoning pathway for antibody diversification by determining AID stability

Détermination de la stabilité d'AID par la voie de chaperonnage moléculaire HSP90 : importance pour la diversification des anticorps

par
Alexandre Orthwein

Département de Microbiologie et Immunologie
Faculté de Médecine

Thèse présentée à la Faculté de Médecine
en vue de l'obtention du grade de doctorat/Ph.D
en microbiologie et immunologie

Janvier 2012

Université de Montréal

Faculté des études supérieures et postdoctorales

Cette thèse intitulée:

Importance of the HSP90 molecular chaperoning pathway for antibody diversification by determining AID stability

Présentée par :
Alexandre Orthwein

a été évaluée par un jury composé des personnes suivantes :

Dr Hugo Soudeyns, président-rapporteur
Dr Javier M. Di Noia, directeur de recherche
Dr Jacques Thibodeau, membre du jury
Dr Alberto Martin, examinateur externe

Résumé

La protéine AID (déaminase induite par l'activation) joue un rôle central dans la réponse immunitaire adaptative. En désaminant des désoxycytidines en désoxyuridines au niveau des gènes immunoglobulines, elle initie l'hypermutation somatique (SHM), la conversion génique (iGC) et la commutation isotypique (CSR). Elle est essentielle à une réponse humorale efficace en contribuant à la maturation de l'affinité des anticorps et au changement de classe isotypique. Cependant, son activité mutagénique peut être oncogénique et causer une instabilité génomique propice au développement de cancers et de maladies autoimmunes. Il est donc critique de réguler AID, en particulier ses niveaux protéiques, pour générer une réponse immunitaire efficace tout en minimisant les risques de cancer et d'auto-immunité. Un élément de régulation est le fait qu'AID transite du cytoplasme vers le noyau mais reste majoritairement cytoplasmique à l'équilibre. AID est par ailleurs plus stable dans le cytoplasme que dans le noyau, ce qui contribue à réduire sa présence à proximité de l'ADN.

Le but de cette thèse était d'identifier de nouveaux partenaires et déterminants d'AID régulant sa stabilité et ses fonctions biologiques. **Dans un premier temps**, nous avons identifié AID comme une nouvelle protéine cliente d'HSP90. Nous avons montré qu'HSP90 interagit avec AID dans le cytoplasme, ce qui empêche la poly-ubiquitination d'AID et sa dégradation par le protéasome. En conséquence, l'inhibition d'HSP90 résulte en une diminution significative des niveaux endogènes d'AID et corrèle avec une réduction proportionnelle de ses fonctions biologiques dans la diversification des anticorps mais aussi dans l'introduction de mutations aberrantes. **Dans un second temps**, nous avons montré que l'étape initiale dans la stabilisation d'AID par la voie de chaperonnage d'HSP90 dépend d'HSP40 et d'HSP70. En particulier, la protéine DnaJa1, qui fait partie de la famille des protéines HSP40s, limite la stabilisation d'AID dans le cytoplasme. La farnésylation de DnaJa1 est importante pour l'interaction entre DnaJa1 et AID et moduler les niveaux de DnaJa1 ou son état de farnésylation impacte à la fois les niveaux endogènes d'AID mais aussi la diversification des anticorps. Les souris *DNAJA1*-/- présentent une réponse immunitaire compromise en cas d'immunisation, qui est dûe à des niveaux réduits d'AID et un défaut de commutation de classe. **Dans un troisième temps**, nous avons montré que la protéine AID est intrinsèquement plus instable que ses

protéines paralogues APOBEC. Nous avons identifié l'acide aspartique en seconde position d'AID ainsi qu'un motif semblable au PEST comme des modulateurs de la stabilité d'AID. La modification de ces motifs augmente la stabilité d'AID et résulte en une diversification des anticorps plus efficace.

En conclusion, l'instabilité intrinsèque d'AID est un élément de régulation de la diversification des anticorps. Cette instabilité est en partie compensée dans le cytoplasme par l'action protective de la voie de chaperonnage DnaJa1-HSP90. Par ailleurs, l'utilisation d'inhibiteurs d'HSP90 ou de farnésyltransférases pourrait être un outil intéressant pour la modulation indirecte des niveaux d'AID et le traitement de lymphomes/leucémies et de maladies auto-immunes causés par AID.

Mots-clés : Déaminase induite par l'activation (AID); hypermutation somatique; commutation de classe; lymphocyte B; diversification des anticorps; protéines de choc thermique (HSP40 /HSP90); stabilité protéique;

Abstract

Activation induced deaminase (AID) plays a central role in adaptive immunity. AID deaminates deoxycytidine to deoxyuridine in defined regions of the immunoglobulin (Ig) genes and initiates somatic hypermutation (SHM), gene conversion (iGC) and class switch recombination (CSR). While being essential for an effective immune response by underpinning antibody affinity maturation and isotype switching, the mutagenic activity of AID can also be oncogenic and causes genomic instability leading to the development of cancer, or exacerbate autoimmune diseases. Therefore, AID regulation, including the control of its protein level, is central to balancing effective immunity with cancer/autoimmunity. Notably, AID shuttles between the cytoplasm and the nucleus but is predominantly cytoplasmic at steady-state, with cytoplasmic AID being much more stable than nuclear AID. These regulatory steps contribute to limit the exposure of the genome to AID but their mechanisms are unknown.

This thesis aimed at identifying AID partners and intrinsic determinants regulating its stability and modulating its biological functions. **Firstly**, we identified AID as a novel HSP90 client protein. We demonstrated that HSP90 interacts with AID in the cytoplasm and prevents its polyubiquitination and subsequent proteasomal degradation. Consequently, HSP90 inhibition results in a significant reduction of endogenous AID levels and correlates with a proportional reduction in both AID-mediated antibody diversification and off-target mutations. **Secondly,** we showed that the first step in the HSP90 molecular chaperoning pathway and stabilization is the interaction of AID with the HSP40 and HSP70 system. In fact, a specific HSP40 protein, DnaJa1, is the limiting step in cytoplasmic AID stabilization. DnaJa1 farnesylation is required for DnaJa1-AID interaction and modulation of DnaJa1 levels or its farnesylation impacts endogenous AID levels and antibody diversification. *In vivo*, DnaJa1-deficient mice display compromized response to immunization, resulting from reduced AID protein levels and isotype switching. **Thirdly**, we found that AID is intrinsically less stable than its APOBEC paralogs. We identified the AID N-terminal aspartic acid residue at position two and an internal PEST-like motif as destabilizing modulators of AID protein turnover. Disruption of these motifs increases AID protein stability and antibody diversification.

We conclude that AID's intrinsic instability directly contributes to regulating antibody diversification. This intrinsic instability is at least partially compensated for in the cytoplasm by the protective action of the DnaJa1-HSP90 molecular chaperoning pathway. Pharmacologically targeting AID in an indirect way, by using HSP90 or farnesyltransferase inhibitors, could be relevant for treating some AID-associated lymphomas/leukemias and/or autoimmune diseases.

Keywords : Activation-Induced Deaminase (AID); B-lymphocyte; Antibody gene diversification; Somatic hypermutation; Class switch recombination; Humoral immunity; HSP90; HSP40/DnaJa1; protein stability.

Table of contents

List of Tables

CHAPTER 2:

CHAPTER 3:

CHAPTER 4:

List of Figures

CHAPTER 1:

CHAPTER 2:

CHAPTER 3:

CHAPTER 4:

CHAPTER 5:

Abbreviations

ADAR: RNA-specific adenosine deaminase

ADAT: **t**RNA-specific adenosine deaminase

Ag: antigen

Ago: Argonaute

AID: Activation-induced deaminase

ALL: Acute lymphoblastic leukemia

17-AAG: 17-N-Allylamino-17-Demethoxygeldanamycin

APC: Antigen-presenting cell

APE: Apuric/Apyrimidic endonuclease

ApoB48: apolipoprotein B48

ATE: arginyl-tRNA protein transferase

ATP: Adenosine triphosphate

ATM: ataxia telangiectasia mutated

ATR: ATM- and Rad3-related

BER: base excision repair

CCR: chemokine C-C motif receptor

C/A-NHEJ: classical/alternative non-homologous end-joining

CDA: cytidine deaminase

CDR: complementary determining region

CHIP: C-terminus of Hsc70-interacting protein

CHX: cycloheximide

CML: chronic myeloid leukemia

CRTC2: CREB regulated transcription coactivator 2

CSR: class switch recombination

Ctrl: control

dC: deoxycytidine

DCDT: dCMP deaminase

DLBCL: Diffuse large B cell lymphoma

DNA-PK: DNA-dependent protein kinase

DSB: double-strand break

Ds/ssDNA: double-stranded /single-stranded deoxyribonucleic acid

dU: deoxyuridine

DUB: deubiquitinating enzyme

Fsk: forskolin

FTase: Farnesyltransferase

FTI: farnesyltransferase inhibitor

GA: geldanamycin

GFP: green fluorescent protein

GR: glucocorticoid receptor

HPD: histidine-proline-aspartic acid motif

HSP: heat shock protein

IBD: inflammatory bowel disease

IC_{50}: inhibitory concentration 50

iGC: IgV gene conversion

IgH/L: Immuglobulin heavy/light

chain
IgV: Immunoglobulin variable region
IL: interleukin
IP: immunoprecipitation
IUP: intrinsically unstructured protein
LMB: leptomycin B
MALT: mucosal-associated lymphoid tissue
MBD4: methyl-CpG binding domain 4
MDM2: mouse double minute 2
MetAP: methionine aminopeptidase
MFI: mean fluorescence intensity
MHC: major histocompatibility complex
miR: microRNA
MMR: mismatch repair
MRN: MRE11-RAD50-NBS1 complex
mRNA: messenger ribonucleic acid
MZ: mantle zone
NES: nuclear export signal
NLS: nuclear localization signal
NMR: nuclear magnetic resonance
PAX5: paired box protein 5
PCNA: proliferating cell nuclear antigen
PGC: primordial germ cell
Ph+: Philadelphia-positive
PKA/PKC: protein kinase A/C
PTBP2: polypyrimidine tract binding protein 2
RAG: recombination activating gene
RISC: RNA-induced silencing complex
RPA: replication protein A
RSS: recombination signal sequence
SD: standard deviation
SEM: standard error of the mean
SHM: somatic hypermutation
TdT: terminal deoxynucleotidyl transferase
TGF-β: transforming growth factor β
TH: follicular helper T cell
TPR: tetratricopeptide repeat
TSS: transcriptional starting site
XRCC: x-ray cross-complementing group protein
Ub: ubiquitin
UBC: ubiquitin-conjugating enzyme
UNG: uracil N-glycosylase
Vif: viral infectivity factor

A fact is a simple statement that everyone believes. It is innocent, unless found guilty. A hypothesis is a novel suggestion that no one wants to believe. It is guilty, until found effective. Edward Teller (1908-2003)

Remerciements

J'ai été forcé sous la contrainte d'écrire ma thèse en Anglais. Je vais donc garder un espace francophone et remercier avant tout mon directeur de thèse, Dr Javier M. Di Noia. Pendant près de cinq ans j'ai appris beaucoup à ses côtés, peut-être pas assez. Il m'a redonné le goût de la science même s'il m'a souvent obstiné, mais je dois admettre qu'il avait souvent raison. Un doctorat ne se passe bien pas sans un chef de qualité et j'ai eu la chance d'en avoir un.

Un doctorat est aussi une aventure de groupe et il faut dire qu'au début il n'y avait pas grand monde dans notre laboratoire. Alors un grand merci à Anne-Marie pour sa patience et son calme légendaire et pour donner un peu de vie à l'IRCM. Je tiens aussi à remercier mes collègues de laboratoire présents et passés, particulièrement Anil Eranki, Dr Astrid Zahn, Stephen Methot, et Vanina Campo. I will miss you guys!!!

L'IRCM, c'est une grande famille. Et au cours de mon long séjour dans cette grande institution, j'ai eu le temps de me lier d'amitié avec un certain nombre de personnes. Alors merci à Amélie Fradet-Turcotte pour son soutien et son aide, Ingrid Saba pour ses discussions pas toujours très scientifiques, Manishha Patel pour hurler dans les couloirs, Mélanie Laurin pour calmer sa collègue, les anciens du labo de rétrovirologie en particulier Jonathan Richard, Francine Gérard, Johanne Mercier et Nicole Rougeau ainsi qu'Héléne Sénéchal et le pauvre Mickael Lehoux abandonné dans son laboratoire.

Au niveau scientifique j'ai rencontré des personnes exceptionnelles d'abord à l'IRCM et je voudrais remercier mon ancien superviseur, Dr Éric A. Cohen, Dr Jean-Francois Côté, Dr Jean-Phillipe Gratton, Dr Jacques Archambault, Dr Claude Lazure, Dr Woong-Kyung Suh pour leur aide et conseil. En dehors de l'IRCM j'ai pu côtoyer des personnes scientifiquement très enrichissant et je remercie tout d'abord les membres de mon jury, Dr Hugo Soudeyns, Dr Jacques Thibodeau et Dr Alberto Martin d'avoir accepté de corriger ma thèse et de m'avoir prodigué aide et conseil quand j'en avais besoin. Je souhaiterais aussi remercier nos collaborateurs qui ont été d'une aide inestimable, en particulier Dr Jason C. Young, qui m'a beaucoup conseillé au début de mon doctorat, Dr Bachir El Affar pour les litres de cellules qu'il m'a aidé à cultiver, Dr Kazutoyo Terada, Dr Alain Lamarre, Dr Silvo G Conticello. Je tiens aussi à remercier Dr Bernardo Reina-San Martin pour m'avoir permis de venir exposer mes

travaux. Je ne serais en train de rédiger ma thèse sans l'aide et la confiance de personnes qui ont cru en moi au début en particulier Dr Imed Gallouzi et Dr Vincent Lacoste.

Un grand merci aux responsables des plateaux technologiques qui ont été d'une aide inestimable en particulier Éric Massicotte, Martine Dupuis, Julie Lord et Denis Faubert.

Finalement sur le plan personnel j'ai eu la chance d'avoir une famille qui m'a toujours soutenu même dans l'incompréhension de ce que je faisais. Un grand merci à mes parents Martine Ligier et André Orthwein. Je ne serais pas là sans eux. Un grand merci à ma sœur Marie Orthwein et à ma presque sœur Isabelle future ex-Claudel. Merci à ma grand-mère Marie-Thèrese Ligier et à mes petits bouts Nina et Karl. Merci aussi à ce qui nous ont quitté en particulier Mamie Train et et mon grand père maternel. Enfin, et ce ne sont pas les moindres merci à tous mes amis de France et de Montréal qui ont été présent pour moi : Damian Smith, Bénédicte Bouchet et Ludovic Souillard, Amandine Born, Alexia Jung et Adeline Mathien, Fanny Rollin et Yann Adelaide.

CHAPTER 1: INTRODUCTION

1.1. Antibody diversification during B cell development

The immune system is composed of both an innate and adaptive arms that together protect the body from infections (bacterial, parasitic, fungal, and viral) and from the development of tumour cells [1]. While the innate immune system is programmed to detect invariant features of invading pathogens, therefore considered as non-specific, the adaptive immune system, which is composed of both T (Thymus-derived) and B (Bursal or Bone marrow–derived) lymphocytes, uses antigen (Ag)-specific receptors and is highly specific. We are mainly interested in B lymphocytes, which are a cell lineage characterized by the presence of cell surface immunoglobulin (Ig) receptors, also called antibodies, recognizing specific antigenic epitopes [2]. Plasma B cells can secrete antibodies to neutralize and eliminate invading pathogens. This antibody-mediated immune response is known as the humoral immune response.

1.1.1. Immunoglobulin gene organization and antibody structure

An antibody molecule is composed of four polypeptide chains: two identical heavy (IgH) chains and two identical light (IgL) chains that are linked through disulfide bonds [3]. The IgH and IgL chains contain distinct structural domains of ~110 amino acids in length. The IgL chain is composed of two of these domains while the IgH chain can display up to five different domains. The N-terminal domain of each chain is unique in that it contains three highly variable regions in length and sequence and is therefore designated as the variable (V) region. Together, the two IgH and IgL chains display six hypervariable loops, termed complementary determining regions (CDRs), which form a unique surface for recognition and binding to specific antigenic epitopes [4]. Each Ig molecule contains two identical Ag-binding sites.

The C-terminal domain(s) of each IgH and IgL are constant, and those of the IgH define the antibody isotype. Two different C-terminal domains can be found in IgL, termed lambda (λ) and kappa (κ). However, each single B lymphocyte can only express one type of IgL chain. In humans, IgLκ and IgLλ are encoded on two different loci (chromosome 2 and 22 respectively).

The κ/λ ratio has a potential clinical value, as the kappa-IgL is usually preferred over lambda (2:1) in healthy adults [5] and an irregular ratio is an indicator of autoimmune disease, multiple myeloma or B-cell lymphoma [6-8].

The class and the effector functions of an antibody molecule are defined by the structure of its IgH C-terminus. Five major classes of IgH exist and define nine different isotypes in humans: μ (IgM), δ (IgD), γ (IgG1, 2, 3 and 4), α (IgA1 and 2), and ε (IgE) (Figure 1.1). The IgH locus is found on chromosome 14 in humans. Mice differ from humans in that they have only one IgA isotype and their IgG nomenclature is slightly different (IgG1, 2a, 2b and 3). B cells that have successfully rearranged their Ig genes (see section 1.1.2.) initially express membrane IgM and/or IgD. IgM molecules can be secreted as oligomers (pentamers or hexamers): they are formed through the generation of inter-molecular disulfide bonds and can be found in complex with the J chain, which is required for the secretion of IgM pentamers in the mucosa. IgM is the main class of Ig secreted during a primary immune response. Its oligomeric state confers high avidity to IgM (up to 12 antigenic binding sites) and is particularly important in activating the complement system. On the other hand, IgD is only found in a monomeric state and its functions are enigmatic. Recent evidence suggests that circulating IgD is important in the immune surveillance of the upper respiratory mucosa by modulating basophil function [9]. IgG is the most abundant class of antibodies in the serum and the most versatile with regards to its functions. In fact, it is the main Ig secreted during a secondary immune response. IgGs are found as monomers and cross easily the placenta (except IgG2), conferring protection to the foetus *in utero*. They usually display high affinity for a specific antigenic epitope and are primarily implicated in opsonisation, neutralization of pathogens and activation of the complement. Despite their close similarity in amino acid sequence, IgG subclasses display specific features which have been attributed to their selective binding to Fc receptors [10-12]. IgA plays a major role in mucosal immunity and can exist as a dimer in complex with the J chain, called secretory IgA (sIgA) [13]. In its polymeric form, IgA is the main Ig found in mucosal secretions, milk, colostrum, tears and saliva. Monomeric IgA (mainly IgA1) is also found in the serum. IgA, by preventing the invasion of pathogens through the mucosal-associated lymphoid tissues (MALT), has been intensively studied to develop

news of ways of vaccination. Finally, IgE is a monomeric antibody, prominently found in epithelia and mucosa, where it binds to specific receptors on highly potent effectors cells [14]. IgE is implicated in the immune response against helminths through the recruitment of eosinophils and monocytes. IgE antibodies can also cause an immediate hypersensitivity syndrome via the activation of mast cells and basophils. Therefore, IgE is a central player in allergic reactions such as asthma.

1.1.2. V(D)J recombination

To achieve nearly universal Ag recognition, vertebrates have developed a series of genetic alterations that target the Ig genes. During B cell development in the bone marrow, the variable region of the IgH and IgL is assembled from a large number of variable (V), diversity (D), and joining (J) gene segments, a process called V(D)J recombination (Figure 1.1). This reaction is catalyzed by the recombination-activating genes 1 and 2 (RAG1 and RAG2), which together form the RAG endonuclease and are sufficient *in vitro* [15, 16] and necessary *in vivo* [17, 18] for the cleavage step of V(D)J recombination. The joining of V, D and J segments is achieved through the generation of a site-specific DNA double-strand break (DSB) at the border of two coding segments in their flanking recombination signal sequences (RSSs). The RSSs contain two well-conserved DNA elements (heptamer and nonamer) separated by a spacer region. They are recognized by the RAG endonuclease complex that cleaves the DNA between the coding sequence and the RSS, thus creating DNA DSBs. V(D)J recombination is achieved by the repair of these DSBs through the non-homologous end-joining pathway (NHEJ) (reviewed in [19]).The final stage of B cell development is characterized by the expression of a functional Ag receptor (B cell receptor; BCR) at the B cell surface surface (Figure 1.2). This immature B cell only expresses surface IgM molecules and undergoes negative selection by testing its capacity to recognize self-molecules present in the bone marrow. Immature B cells activated by self-Ags are eliminated through clonal deletion. Non-self reactive B cells can then migrate in the peripheral lymphoid organs and become mature B cells (Figure 1.2). V(D)J recombination generates the diversity of the primary repertoire of antibodies in different ways. Firstly, the large number of gene segments and their random joining give rise to a consequent combinatorial diversity. Secondly, additional diversity can

arise from nucleotidic processing of the DNA ends occurring during the recombination events which bring the V next to the J or D segment. This junctional diversity, combined to the insertion of a series of nucleotides between the D and J segments catalyzed by the terminal deoxynucleotide transferase (TdT), also contributes to the diversification of the antibody repertoire [20, 21]. Thirdly, the association of different IgH and IgL chains also contributes to the diversity of combinations.

1.1.3. Antibody diversification during the germinal-center reaction

Mature B cells continuously circulate through the secondary lymphoid organs and encounter Ags in the lymphoid follicles. The first cognate antibody-Ag recognition of naïve B cells is usually not of high affinity. This endows the immune system with enough flexibility to recognize almost any possible Ag using a large but limited primary repertoire. By contrast, high affinity antibody-Ag interactions are critical for neutralizing or disposing of Ags. Thus, there are additional mechanisms to change the antibody genes. Upon activation by a cognate Ag, follicular B cells initiate the germinal center (GC) reaction (Figure 1.2). This reaction is considered to be the starting point of a T-cell dependent humoral immune response, although certain reports suggest that GCs may also be formed during T-cell independent responses [22, 23]. However, in general, non-protein Ags, including polysaccharides, glycolipids, and nucleic acids, induce a T-cell independent antibody response, consisting mainly in the activation of marginal zone B cells (MZ) and the subsequent secretion of low affinity IgM and IgG3 antibodies [24, 25].

Upregulation of the chemokine receptor CCR7 on activated B cells is the starting point of the GC reaction [26], leading to the migration of activated B cells from primary follicles to the T zone where they become distributed along the B/T border [27]. This facilitates the interaction between follicular helper T cells (TH) and B cells and results in an extensive B cell proliferation and the formation of GCs [28]. In fact, GCs are composed of proliferating Ag-specific B cells, Tfh cells and specialized follicular dendritic cells [29]. The costimulatory molecule CD40, which is constitutively expressed at the B cell surface, and its ligand CD40L

(CD154), which is expressed on activated TH cells, play a crucial role in the formation of GCs [30, 31]. During the GC reaction, B cells undergo diversification of the genes encoding for IgH and IgL by the mechanisms of somatic hypermutation (SHM) and antibody class switch recombination (CSR), which underpin antibody affinity maturation and isotype switching. Furthermore, GC B cells differentiate into high-affinity antibody-secreting plasma cells as well as into memory B cells, which ensure a sustained immune protection and a rapid response against previously encountered Ags.

1.1.3.1. Somatic hypermutation

SHM consists in the introduction of point mutations in the Ig variable exon (VDJ or VJ region) [32-34] (Figure 1.1). The mutations introduced are predominantly single base pair changes, although insertions and deletions have also been reported [35]. All four bases (A, T, G and C) are targeted for mutation; A:T and C:G pairs are targeted with comparable frequencies, at least in humans and mice. Nevertheless, neither the targeting of individual bases nor the nature of the substitution are random: mutations at A:T pairs preferentially occur if the A is present in the coding strand and transition mutations (A to G or C to T) usually occur twice as frequently as transversions (reviewed in [36, 37]). Furthermore, a high proportion of the mutations occurs in the hotspot motif DGYW (where D=A/G/T, Y=C/T, W=A/T) or its reverse complement sequence WRCH (R=A/G, H=T/C/A) [38-40]. Finally, specific domains in the IgV region encoding the amino acids constituting the Ag binding sites (CDR domains) are more targeted than others [41].

This mutagenic process depends on a B cell specific factor, activation-induced deaminase (AID), which initiates SHM by deaminating deoxycytidine into deoxyuridine in the IgV region [42-45] (Figure 1.3). The introduction of a uracil, which is a foreign base for DNA, can be processed in two ways [36, 37]. The introduced uracil can either be replicated over to produce C to T transitions or processed by components of the base excision repair pathway (BER) (Figure 1.3). The uracil can be excised by uracil-DNA glycosylase UNG, leaving an abasic site that is repaired in an error-prone manner through the recruitment of translesion polymerases [46, 47].

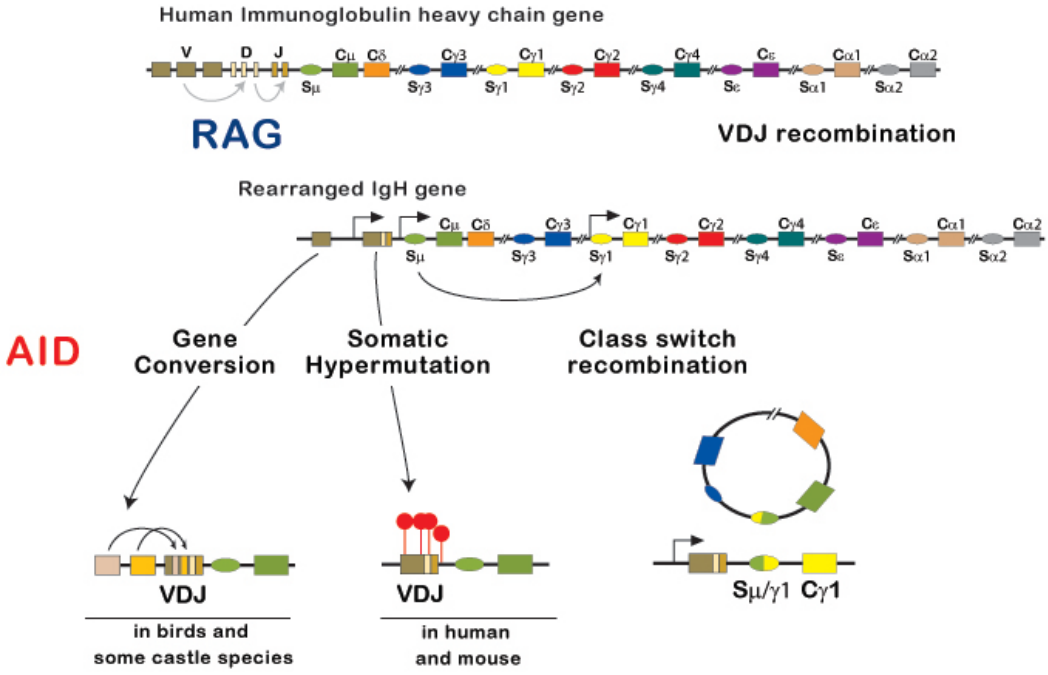

Figure 1.1. Human IgH gene organization. *The IgH locus is composed of several V, D and J segments that encode part of the functional IgV region of an antibody molecule after RAG-catalyzed VDJ recombination. The IgH region is composed of several constant region (C) exon sets, each coding for a different isotype: Cμ (IgM), Cδ (IgD), Cγ3 (IgG3), Cγ1 (IgG1), Cγ2 (IgG2), Cγ4 (IgG4), Cε (IgE) and Cα (IgA). Each C region is preceded by a switch region (S), where transcription takes place to generate AID ssDNA substrate. The AID-catalyzed dC>dU are processed by DNA repair enzymes resulting in DNA double-strand breaks that are intermediates for class switch recombination. CSR occurs between the Sμ region and a downstream S region (f.i. here Sγ1), which results in the switching from IgM to IgG1. The intervening DNA region that is eliminated upon CSR is predominantly released as a circular episome called a switch circle. Somatic hypermutation consists in the introduction of point mutations in the rearranged IgV region. Gene conversion is an alternative IgV diversification process that is used by birds and cattle species, consisting in the transfer of random stretches of adjacent pseudo-genes into the rearranged IgV region. SHM, CSR and iGC are initiated by AID.*

This process produces both transition and transversion mutations. Alternatively, the U:G mistmatch can be recognized by components of the mismatch repair pathway (MMR), notably MSH2 and MSH6, that recruits the exonuclease EXO1 and DNA polymerase η, which preferentially generates mutations at A:T pairs (Figure 1.3). Inactivation of BER components (f.i. UNG [48-50] and XRCC1 [51]), of certain error prone DNA polymerases [52-56], or of key players in the MMR system [57-66] affect the pattern or frequency of SHM. A:T mutagenesis during the diversification of the IgV region also requires the ubiquitination of the proliferating cell nuclear antigen protein (PCNA) [67-69] and both the UNG- and the MSH2-dependent pathways seem to depend on this intermediate [70]. Although many details are still unclear, SHM of the IgV region is achieved through DNA deamination, processing of the uracil and introduction of point mutations during the repair of abasic sites or single-stranded DNA tracts.

During the GC reaction, antibody variants produced by SHM are selected for improved Ag recognition. This selection process underlying affinity maturation consists in a stepwise re-entry model, where the B cell undergoing cell division and SHM in the dark zone of the GC can migrate to the light zone, where it interacts with Ag-presenting dendritic cells and TH cells. B cells expressing high-affinity antibodies at their surface are preferentially selected and can re-enter the cycle of proliferation, mutation and subsequent selection. A large number of cells fail this selection, enter into apoptosis and are eliminated by a subset of macrophages that reside in the GCs [29] (Figure 1.2).

1.1.3.2. Gene conversion

In many farm animals, diversification of the antibody repertoire is achieved by both SHM and a process called IgV gene conversion (iGC). The best model to study iGC is the chicken Ig loci. Chicken have a single functional light chain V segment (Vλ), which recombines with a single Jλ segment, thus limiting the primary repertoire of antibodies generated by RAG-mediated VDJ recombination [71-74]. However, during B cell development in the bursa of Fabricius of avian species, the rearranged IgV undergoes an additional step of diversification, the iGC [71, 75]: during iGC, random stretches of adjacent pseudo-genes are recopied onto the rearranged IgV

region by homologous recombination (Figure 1.1). Indeed, the chicken Ig loci are composed of a large number of pseudo-gene segments that precede the rearranged IgV region [71]. In this case AID also contributes to the primary diversification of the antibody repertoire by initiating iGC (Figure 1.1) [76, 77]. Pseudo-genes that are more homologous, closer, or in the opposite orientation to the IgV segment, are usually preferred as donors [71, 78]. The IgV region is subsequently diversified by both iGC and SHM during the GC reaction in chicken [79, 80].

iGC has been extensively studied in the chicken DT40 B cell lymphoma line, which continuously diversifies its Ig loci by iGC *in vitro*. Disruption of the AID gene (*Aicda*) in this cell line completely blocks iGC [76, 77]. Thus, although iGC and SHM are two distinct processes, they are both initiated through a common intermediate (i.e. AID-catalyzed deamination of deoxycytidine into deoxyuridine) and share similarities [81]. UNG mediates the major pathway to create abasic sites which in some way trigger homologous recombination [76, 77, 81] (Figure 1.3). In contrast to SHM [49], UNG inactivation almost completely abrogates iGC in the DT40 cell line [82]. Completion of iGC requires the RAD51 paralogs XRCC2 and XRCC3 or RAD51B and BRCA2 to promote the transfer of sequence information from an upstream donor pseudogene to the IgV region [83, 84] (Figure 1.3). Several lines of evidence also suggest that the MRE11-RAD50-NBS1 complex (MRN) is implicated in iGC [85, 86]. Chicken B cells not only diversify their IgV region by iGC but also accumulate untemplated mutations during the GC reaction in peripheral lymphoid organs.

1.1.3.3. Class switch recombination

Activated B cells, which express IgM and/or IgD at their surface, also undergo class switch recombination (CSR) during the GC reaction. CSR consists in the exchange of the default Cμ constant region to another downstream constant region (γ, ε or α) and results in the expression of a different isotype of antibody (IgG, IgE or IgA) with different effector functions (Figure 1.1). AID also initiates CSR [42, 43] through deamination of deoxycytidines in switch regions, which are repetitive sequences preceding each constant region (except Cδ). Switch regions are enriched in AID hotspot motifs and are preferentially targeted by this enzyme. AID-

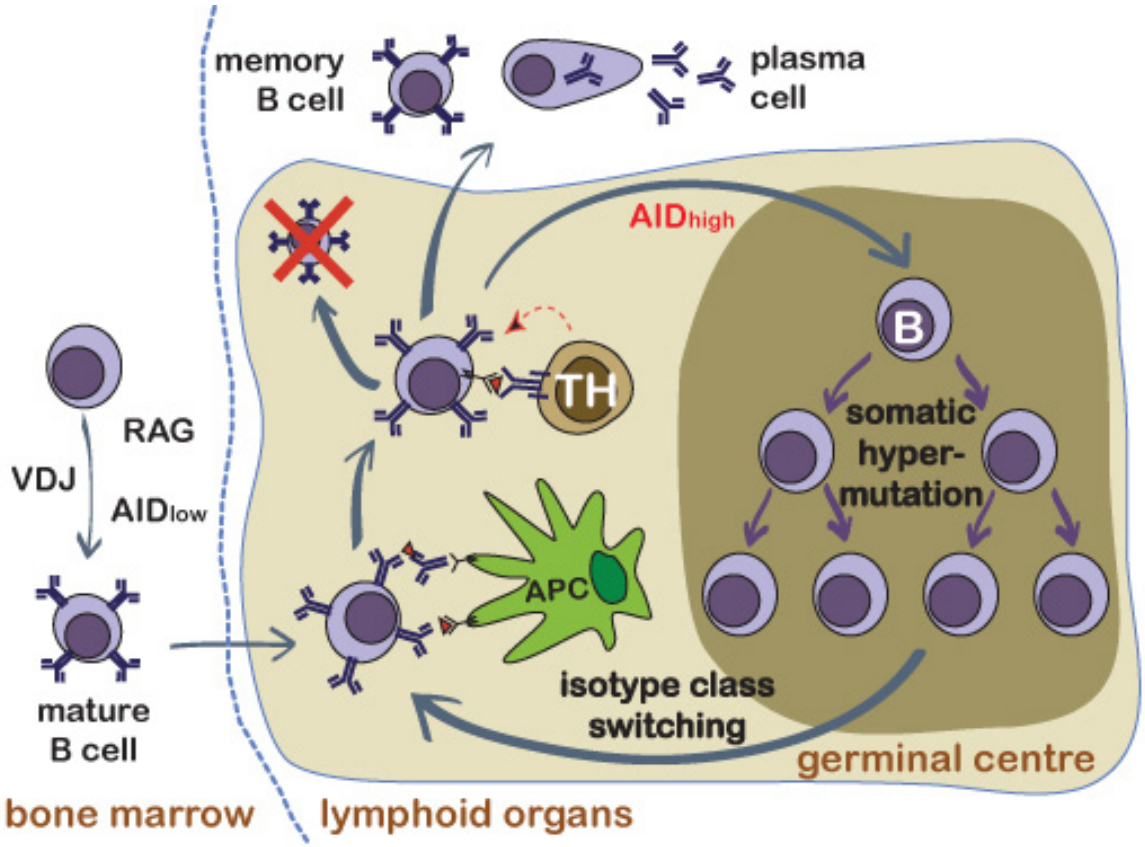

Figure 1.2. The germinal center reaction. *Rearrangement of the IgV region takes place in the bone marrow and results in the expression of functional IgM and IgD molecules at the B cell surface. Low expression of AID has been reported in this compartment, which plays a role in central tolerance. In the peripheral lymphoid organs, antibody gene diversification in mature B cells takes place in the GC in the form of somatic hypermutation (SHM), which underpins affinity maturation, and class switch recombination (CSR), which changes the isotype of the antibody. Upon presentation of an Ag by specialized Ag presenting cells (APC), mature B cells are activated and undergo the GC reaction, controlled by follicular helper T cells (TH). B cells proliferate extensively and are subsequently selected for a better Ag affinity by APC. B cells that fail this positive selection die by apoptosis. The selected B cells can undergo additional rounds of diversification or differentiate into memory or plasma cells.*

generated uracils are subsequently removed by UNG [48, 49, 87] and the apurinic/apyrimidinic endonucleases APE1 and APE2 [88], leading to DNA DSBs (Figure 1.3). Alternatively, uracils can be recognized as U:G mismatches by the MMR pathway (Figure 1.3). The MSH2/MSH6 complex in collaboration with MLH1/PMS2 recruits the exonuclease Exo1, which can also generate a DSB intermediate [89]. Indeed, disruption of genes involved in BER (*ung*, *ape1* or *ape2*) [48-50, 87, 88] or in MMR (*Msh2, Msh6, Mlh1, Pms2, Exo1*) [59, 63, 90-94] inhibits CSR. In absence of both UNG and MSH2, CSR is in fact completely abolished [95], indicated that both the BER and MMR pathways contribute to CSR.

Early sensors of DNA DSBs are required to coordinate the downstream repair pathways leading to CSR. The MRN complex, which travels along DNA and scans for DNA breaks, is present within seconds at the site of DSBs [96]. As expected from its central role in sensing DNA damage and CSR, mutations affecting MRE11 and NBS1 cause immunodeficiency, chromosomal instability and a high incidence of lymphoid malignancies, which are characteristics of the Nijmegen breakage syndrome [97]. Patients affected by this syndrome exhibit reduced levels of CSR to IgA *in vivo*, which is recapitulated in *Nbs1*-haploinsufficient mice that display a two- to three-fold reduction in CSR *in vitro* [98, 99]. Once bound to the DSB, the MRN complex recruits the ataxia telangiectasia mutated kinase (ATM), which becomes activated and phosphorylates several substrates including NBS1, MRE11, 53BP1, MDC1 and γ-H2AX [100]. Ablation in mice of ATM, or its interactor protein ATMIN, compromise CSR *in vitro* [101-103], and results in patients in a rare immunodeficiency disorder as well as a predisposition to cancer (ataxia–telangiectasia syndrome) [104]. Moreover, mice deficient in 53BP1, H2AX, MDC1, or the ubiquitination machinery RNF8/RNF168, which is critical to propagate the DNA damage signal [105], display compromised CSR *in vitro* [106-110]. Interestingly, most of these sensors are abundantly expressed in a constitutive manner in the B cell lineage [111, 112]. This is thought to contribute to a repair-prone environment that renders activated B cells less susceptible to DNA damage-induced apoptosis. The DNA DSBs are resolved by a “region-specific” recombination process involving the donor and acceptor S regions. It occurs through the recruitment of ubiquitous proteins from the classical non-homologous end-joining pathway (C-NHEJ), including

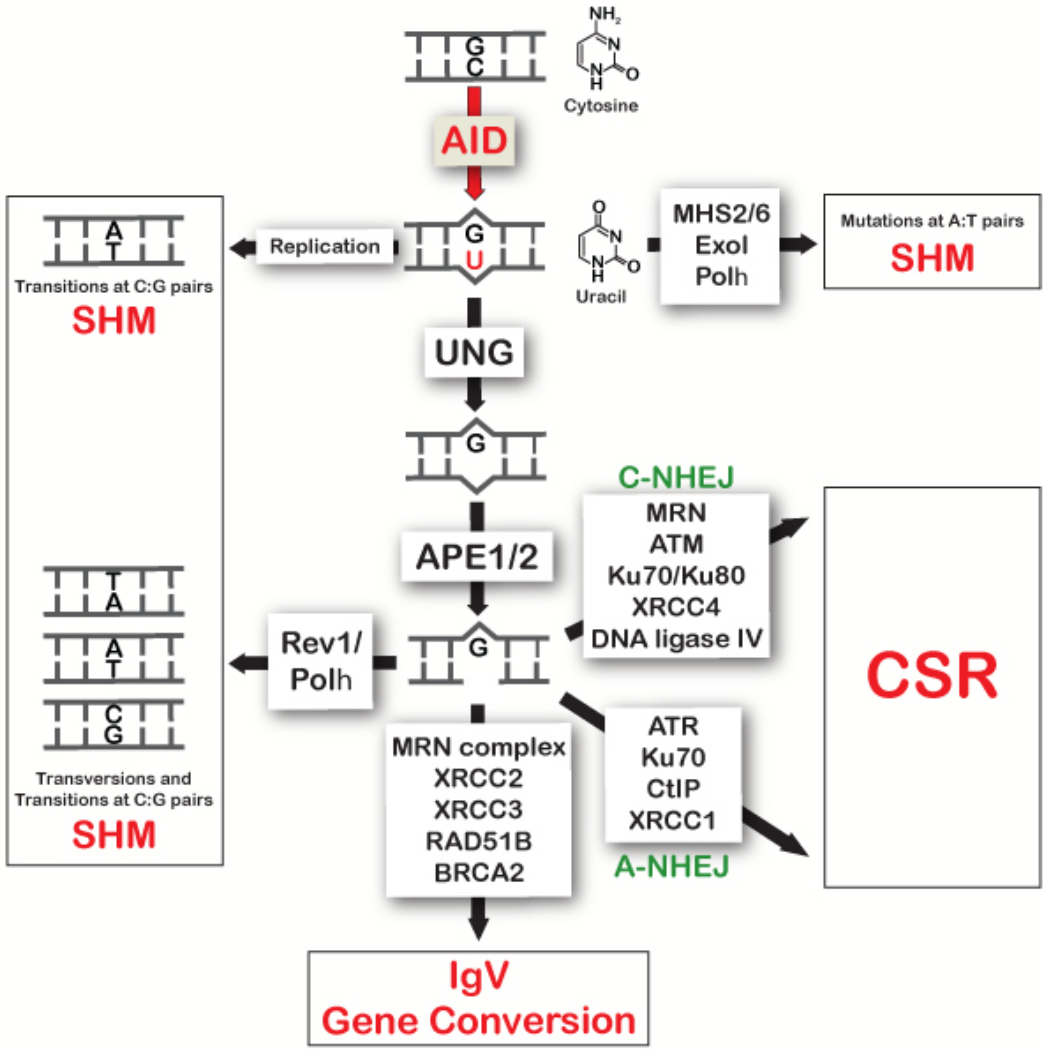

Figure 1.3. Differential processing of AID-catalyzed dU lesions leads to SHM, iGC or CSR. *AID deaminates deoxycytidines in the Ig loci leading to U:G mismatches that can be either replicated over, processed by the uracil-DNA glycosylase (UNG) or recognized by the mismatch repair proteins MSH2/6. UNG or MSH2/6 cooperate with distinct sets of DNA repair factors that will result in mutations for SHM and IgV gene conversion or DNA double-strand breaks and repair for CSR. SHM can be divided into several pathways, depending on the type of mutations introduced. Similarly, DNA DSBs can be repaired by either the classical (C-) or alternative (A-) non-homologous end-joining pathways (NHEJ). Adapted from [36].*

Ku70/80, DNA-PKcs, XRCC4 and DNA ligase IV (Figure 1.3). Studies in mice have shown that Ku70 and Ku80 are essential for CSR [113, 114], while XRCC4 is important but not essential for CSR [115]. DNA-PKcs is also implicated in CSR [116-119], but has a redundant role with ATM [120]. The fact that the Ku70/80 complex is essential for CSR, but not XRCC4 or DNA ligase IV, suggested the contribution of an alternative pathway for the resolution of the DSBs [115, 121-123]. In fact, Ku70 collaborates with the DNA end-processing factor CtIP, ATR (ATM and Rad3-related protein) and the DNA damage sensor PARP1 to promote an alternative end joining pathway (A-NHEJ) that makes more frequent use of microhomology at the ends for resolving the DSB [124-126] (Figure 1.3). The factors composing the A-NHEJ pathway are still under investigation. Resolution of the DSB by C-NHEJ or A-NHEJ ensures IgH loci functionality and allows the expression of an antibody with the same specifity but a new isotype with different effector functions.

GC B cells are particularly interesting since they have to balance extensive DNA damage and apoptosis. B cells upregulate or express at high levels a series of proteins implicated in the MMR, BER and DNA damage sensing to be protected from DNA damage-induced apoptosis [111, 127-129]. Activated GC B cells also express a transcriptional repressor, BCL6 [130, 131], which negatively regulates DNA damage response and check point genes [132-136]. Altogether, GC B cells generate an anti-apoptotic environment to favour the diversification of the Ig loci and limit DNA-damage induced apoptosis. Nonetheless, they become more susceptible to extrinsic apoptosis induced by negative selection in order to eliminate non-productive mutations [137].

1.2. AID and its physiological functions

1.2.1. The AID/APOBEC family

AID is a member of a family of cytidine deaminase-related enzymes comprising APOBEC1, APOBEC2, the APOBEC3 group, APOBEC4 and the recently identified APOBEC5 (Figure 1.4) [138, 139]. The AID/APOBEC proteins have the unique capacity of

deaminating (deoxy)cytidine in DNA and/or RNA, thus converting it into (deoxy)uridine (reviewed in [140]). They also exhibit diverse physiological functions. AID and its paralogs APOBEC share the structural and catalytic backbone of the zinc-dependent deaminases that are involved in the metabolism of purines and pyrimidines (Figure 1.4). It is composed of two motifs H(A/V)E and PCxxC (where x is any amino acid) separated from each other by 24-36 amino acids [140]. The histidine (H) and the two cysteines (C) coordinate a zinc atom and form the catalytic core of the deaminase. During the deamination reaction, the cytidine is bound in this pocket and a nucleophilic attack on the NH_2 in its carbon 4 occurs. The nearby glutamic acid residue (E) serves as the proton donor while a water molecule serves as an activator in this reaction [141].

The AID/APOBEC group appeared with the vertebrate lineage and the evolution of adaptive immunity. AID and APOBEC2 are thought to be the ancestral members of the AID/APOBEC group, although the RNA-editing APOBEC1 enzyme was the first member to be discovered and characterized [142] (Figure 1. 4).

APOBEC2 and APOBEC4 functions remain elusive. APOBEC4 is primarily expressed in testis but its function is unknown [143]. APOBEC2 has been reported to be expressed specifically in skeletal and cardiac muscle [144, 145], although broader analysis suggested a low but ubiquitous expression of APOBEC2 in human and mouse [146]. Little is known about APOBEC2 substrates or its physiological functions. Its deamination activity is in fact controversial [145, 147] and *Apobec2*-deficient mice display no developmental, survival or fertility problems [147]. There is genetic evidence supporting a role of APOBEC2 in muscular development [148]. Knockdown of *Apobec2* in zebrafish embryos led to a dystrophy in skeletal musculature and impaired heart function. The chaperone UNC45B is essential for APOBEC2 folding in zebrafish and disruption of *Unc45b* recapitulates the phenotype observed in APOBEC2-knockdown zebrafish embryos [149].

On the other hand, APOBEC1 mRNA editing functions are well characterized. This enzyme is mostly expressed in the human small intestine and in the liver in rodents [142, 150], and is the only known RNA-editing enzyme of the AID/APOBEC group. Functionally, APOBEC1 generates a premature stop codon in apolipoprotein B mRNA that leads to the expression of a tissue-specific truncated apolipoprotein B polypeptide chain (ApoB48). Beside abnormalities in

lipoprotein metabolism, *Apobec1-/-* mice are viable and do not display any particular phenotype [151, 152]. Conversely, hepatic overexpression of APOBEC1 in mice and rabbits is oncogenic and results in liver hyperplasia and the development of hepatocellular carcinomas [153]. These could result from aberrant editing of hepatic mRNAs [154], but could also reflect the ability of APOBEC1 to mutate DNA [155]. Thus, APOBEC1 activity needs to be tightly regulated. This is in part achieved by the APOBEC1 complementation factor (ACF) that targets specifically APOBEC1 to an AU-rich motif in the apolipoprotein B mRNA and restrict deamination to a specific cytosine (C_{6666}). Despite acting in the nucleus, APOBEC1 is a nucleo-cytoplasmic shuttling protein [156]. It contains a poorly characterized nuclear localization signal (NLS) and a carboxy-terminal nuclear export signal (NES) [157, 158]. Restricting nuclear access to APOBEC1 may be an additional way to limit its biological activity.

The APOBEC3 subgroup plays a central role in the intrinsic immunity to retroviruses [159, 160], and protects against the transposition of endogenous retroelements [161-163]. Mouse encodes for only one APOBEC3 protein, whereas humans have at least eight different APOBEC3 members, named APOBEC3A to H. Ablation of APOBEC3 in mouse does not impact development, survival or fertility [147]. However, APOBEC3 proteins can restrict retroviral infection. Indeed, APOBEC3G is packaged into HIV virions and deaminates deoxycytidine in deoxuridine on the nascent first cDNA strand produced by the reverse transcriptase in the newly infected cell [159, 160]. Consequently, the viral genome is heavily mutated and becomes non functional. HIV encodes an accessory protein, the viral infectivity factor (Vif), that overcomes APOBEC3G restriction by recruiting the E3 Ub ligase Cullin5 and ElonginB/C proteins, thus targeting APOBEC3G for proteasomal degradation [164-166]. Anti-retroviral functions have been attributed to several other human and primate APOBEC3 proteins [167]. Additionally, APOBEC3G restriction may also occur through a deamination-independent mechanism [168, 169]. APOBEC3G activity is regulated notably by post-translational phosphorylation. Two APOBEC3G residues have been found to be phosphorylated *in vitro* and *in vivo*: Thr32 and Thr218 [170, 171]. These residues are evolutionary conserved in AID. Phosphorylation of Thr32 by protein kinase A (PKA) promotes APOBEC3G antiviral activity by reducing the binding of APOBEC3G to Vif and its

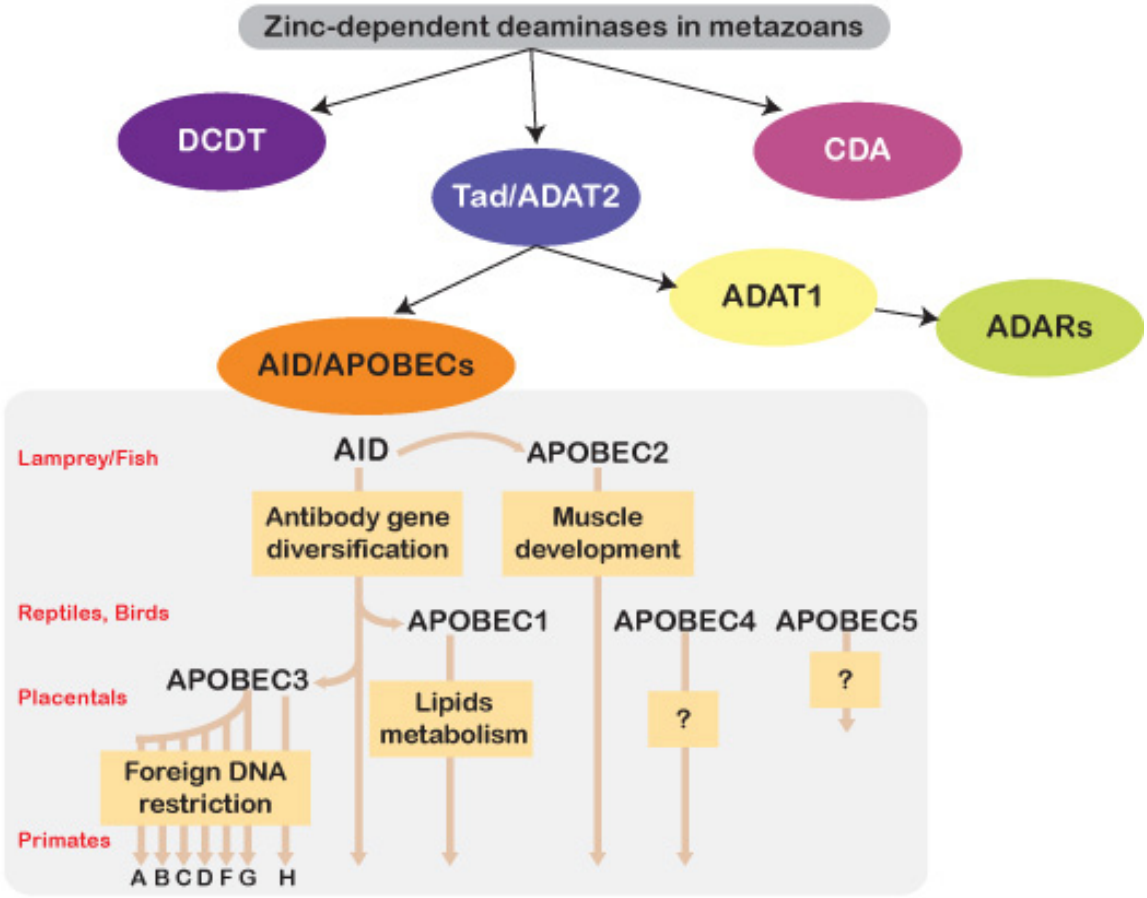

***Figure 1.4*. Phylogenetic organization of the zinc-dependent cytidine deaminase family.** *The AID/APOBEC subgroup shares the structure and catalytic backbone of the zinc-dependent deaminases. Cytidine deaminases (CDA) are not likely the ancestors of the AID/APOBEC subgroup because of the differences in gene organization and catalytic domain. The gene structure of most AID/APOBEC is reminiscent of the genetic organization of dCMP deaminases (DCDT) and tRNA adenosine deaminases (Tad/ADAT2). AID and APOBEC2 are the oldest members of the AID/APOBEC family, which exhibit diverse physiological functions. AID has a high similarity and a conserved 3D structure with its APOBEC paralogs. The tRNA adenosine deaminase ADAT1 and the mRNA adenosine deaminases (ADARs) are thought to originate from the Tad/ADAT2 family independently of the AID/APOBECs. Adapted from [140].*

subsequent polyubiquitination and degradation [170]. On the other hand, phosphorylation at Thr218 inhibits APOBEC3G biological activity *ex vivo* by reducing its catalytic activity but its role and importance *in vivo* are unknown [171]. Furthermore, APOBEC3G proteins can be entrapped in high-molecular-mass ribonucleoprotein complexes found in cytoplasmic structures called P-bodies and stress granules [163, 172, 173], where APOBEC3G catalytic activity is greatly inhibited, or in low-molecular-mass complexes important for retroviral restriction [174]. Recently, an additional member of the AID/APOBEC subgroup, named APOBEC5, has been identified in non-placental animals. It has been suggested that APOBEC5 may be a functional homologue of the APOBEC3 proteins in non-placental animals [175].

Despite their great biological divergence, AID/APOBEC proteins share reasonably high level of primary sequence and structural similarities. The crystal and NMR structures of APOBEC2 and the C-terminal domain of APOBEC3G confirmed the structural conservation between the members of this family and revealed the active-site loops implicated in substrate binding [176-178]. Furthermore, APOBEC2 and APOBEC3G crystal structures suggest that AID/APOBEC proteins may dimerize/oligomerize, which could be relevant for their biological functions [179, 180].

1.2.2. AID in antibody diversification

The AID gene *Aicda* is composed of 5 exons and has been found in all vertebrates. Its chromosomal localization is syntenically conserved at least among mammals [138]. Furthermore, its genomic structure is well conserved among chimpanzee, mouse, cattle, chicken, urodele amphibian, frog, fugu and zebrafish, particularly in the last three exons [138, 181-185]. The full-length mammalian AID is composed of 198 amino acids but splice variants of AID in both normal human and mouse B cells have been described [181]. As expected from its central role in antibody diversification, loss of function mutations affecting AID cause an immunodeficiency syndrome called hyper-IgM syndrome type 2 (HIGM-2). HIGM2 is characterized by the absence of switched antibody isotypes, recurrent infections and lymphoid tissue hyperplasia [42], which is recapitulated in *Aicda-/-* mice [43]. Due to its close similarity

with APOBEC1, AID was initially hypothesized to be a RNA-editing cytidine deaminase (RNA-editing hypothesis) [43, 139]. Alternatively, Michael Neuberger's group postulated a model where AID directly deaminates DNA [45], and several studies confirmed this DNA deamination model [45, 49, 50, 186-192].

In this thesis, we are mainly interested in the amount of AID protein necessary for an efficient antibody diversification. In fact, AID levels are limiting for antibody diversification as indicated by studies in *Aicda*+/- mice. AID haploinsufficient mice have ~40% of AID mRNA and protein levels compared to wt [193, 194] and several groups have found reduced CSR and SHM in *Aicda*+/- mice [193-196]. The decrease in CSR and SHM is roughly proportional to the decrease in AID levels. But *in vivo*, the effect is greatly compensated by selection [193, 194]. Conversely, higher levels of AID protein translate into more CSR and SHM. Indeed, AID overexpression increased the rate of SHM in human B cell lines [197, 198]. Mouse models with modified AID expression levels also provided evidence for a rate-limiting role of AID in antibody diversification. First, several transgenic mice overexpressing AID have been made, which all show increased CSR and SHM [199-202]. The two transgenic lines in which AID was expressed from a ubiquitous promoter showed a significant but modest effect on antibody diversification [199, 200, 202]. In contrast, transgenic AID under the control of the Igκ enhancer, which showed maximal expression in GC B cells, displayed a very high increase in CSR and SHM levels [201]. Secondly, upregulation of AID expression in B cells by removing the negative post-transcriptional regulation of AID by microRNA miR-155, also leads to higher levels of CSR [203, 204] (see section 1.4.2). Nonetheless, none of these mice showed an increase in switched serum Ig levels. This may be regulated at another level (selection, homeostatic proliferation) and does not necessarily reflect the intrinsic CSR capacity of the B cells. Interestingly, mice in which higher levels of AID were achieved by removing the miR-155 negative post-transcriptional regulation showed compromised affinity maturation but no differences in quantity or quality of SHM at the IgV region [203].

1.2.3. AID expression profile

Initially, AID was thought to be a B cell-restricted factor. In fact, high AID mRNA levels have been reported in the spleen, in MALT (Peyer's patches, mesentery lymph nodes,

auxiliary lymph nodes) and in the chicken bursa, in line with AID functions in antibody diversification [76, 139, 205]. *Aicda* transcription is induced by cytokines and cell-cell interactions in the context of Ag-triggered B cell activation during the immune response (reviewed in [206]). Thus, *Aicda* is highly transcribed in GC cells but repressed in plasma and memory B cells [207, 208], and this correlates with measurements of AID mRNA and protein levels in the B cell lineage as well as with the analysis of an AID-GFP reporter mouse [139, 207, 209, 210]. However, the original belief of AID being exclusively expressed in GC B cells has been now revised.

AID is expressed outside of the B cell compartment in normal conditions. One example is the ovaries, in which basal AID mRNA levels are ~50-70% of those found in spleen [211, 212]. Furthermore, *Aicda* is induced by estrogens which increases AID mRNA a few fold in the spleen but by >20-fold in the ovaries [213]. Breast tissue also expresses AID when stimulated with estrogens [213] and several human breast cancer cells express AID mRNA [214], but the basal levels in normal breast tissue have not been reported. AID expression was reported in other normal non-lymphoid cells, including prostate, heart and lung [211, 212, 215]. It is unclear whether AID expression in these tissues has any physiological role. Furthermore, infectious agents like Epstein-Barr virus, Abelson murine leukemia virus and Moloney murine leukemia virus are able to induce AID in the infected cells, which has been proposed as the result of an ancestral function in restricting retroelements [211, 216-219].

Low AID mRNA levels have also been measured during B cell development [220, 221]. Convincing evidence suggests that AID plays a role in B cell tolerance by eliminating autoreactive B cells [220, 221] but the mechanism of AID-mediated B cell tolerance is unknown. Genetic evidence suggested that AID expression during B cell development results in mutations in the IgV region [222, 223]. This is reminiscent of what is observed in sheep, rabbits, and cattle, where SHM or iGC contribute to the diversity of the primary antibody repertoire [224-226], and could be an evolutionary relic or may contribute to tolerance by mutating autoreactive clones, thus changing their specificity. Similarly, extremely low levels of AID mRNA (~1/10 of AID mRNA levels in immature B cells) have been measured in a subset of CD4+ T cells [227], but the biological significance of AID expression in T cells in unclear.

SHM on the T-cell antigen receptor loci was reported [228], however, it is difficult to imagine that the 10^3-10^4-fold lower levels of AID expressed in immature B and T cells when compared to GC B cells [221] could contribute to SHM, given the relative proportionality between AID protein levels and SHM in GC B cells.

AID has also been detected in cell types such as oocytes, spermatocytes, primordial germ cells (PGCs) or embryonic stem cells [211-213, 229-232]. As mentioned, oocytes express AID mRNA to comparable levels as B cells [211, 212]. AID mRNA is very low in testis [207, 211, 212] but AID protein has been detected by IF in spermatocytes [230], which would suggest higher levels. The timing of AID expression in PGCs is controversial, although there is agreement that AID mRNA levels are substantially lower than in B cells (5-10%) [212, 229, 232]. Similarly, AID mRNA levels in stem cells are ~5-10% of those found in B cells [212, 231]. Furthermore, AID is expressed during early development in *Danio rerio* [233], *Xenopus laevis* [234] and *Pleurodeles waltl* [183], which could suggest a role of AID during cellular differentiation and development.

1.2.4. AID demethylation activity

Evidence is accumulating to suggest that AID could be part of a mechanism to demethylate methylated cytidine (5-mC) at CpG sites in the genome, thereby influencing gene expression [212, 231, 232]. In fact, AID and its paralogs APOBEC can convert 5-mC to thymidine with similar efficiency *in vitro* [212, 235]. Functionally, cytosine methylation is a major covalent DNA modification in mammals and plays important roles in transcriptional regulation [236]. Its main function is to stabilize or lock-in transcriptional silencing. It participates in tissue-specific gene expression, gene imprinting, nuclear reprogramming, X chromosome inactivation, but also in the suppression of retrotransposons. DNA methylation patterns are established early during cell development and maintained in adult somatic cells. Nevertheless, changes in methylation pattern occur during mammalian development and cell differentiation, as reported in mice where significant waves of demethylation/remethylation occur in germ lines and early embryos [237]. Genome-wide demethylation has also been observed in PGCs around embryonic days 11.5-12.5, followed by a gamete-specific methylation [238-240].

Consistent with a role of AID in epigenetic reprograming during development, AID mRNA has been detected in cell types such as oocytes, spermatocytes, PGCs or embryonic stem cells [211-213, 229-232]. In interspecies heterokaryons of mouse embryonic stem cells and human fibroblasts, AID downregulation results in a hypermethylated state of *oct4* and *nanog* promoters [231]. Furthermore, genetic evidence supports a role for AID in demethylating the genome of PGCs. AID-deficient PGCs are up to three times more methylated than their wt counterparts. In *Danio rerio*, AID downregulation results in hypermethylation of the *neurod2* promoter in embryos and a severe defect in neurogenesis [233]. Mechanistically, AID may collaborate with a group of proteins previously implicated in demethylation, Gadd45 and the T:G glycosylate MBD4, to target specific genomic regions for demethylation [241]. But the amount of AID required for its proposed role in epigenetic programming seem to be considerably lower than that required for antibody diversification. Furthermore, the absence of any additional phenotype in AID-deficient humans and mice, beside a severe immunodeficiency syndrome, tends to favor a model where AID is redundant with other APOBEC deaminases in demethylation.

1.3. Pathological consequences of AID

Due to AID mutagenic activity, secondary antibody diversification is accompanied by a higher incidence of potentially transforming genomic lesions. The fact that AID is limiting for antibody diversification may be a consequence to its pathological side effects. Mice overexpressing AID have demonstrated its oncogenic capacity. Ubiquitous transgenic overexpression of AID leads to the development of T cell lymphomas and lung adenomas and adenocarcinomas, but not B cell malignancies [202]. In accordance with its role in central and peripheral tolerance, AID levels also influence antibody-mediated autoimmune diseases [195, 242-244].

1.3.1. Off-targets mutations

AID can introduce mutations outside of the Ig loci. Several genes such as *Bcl6*, *Cd95*, *Pim1*, *Pax5*, *RhoH*, *Cd79a,* and *Cd79b,* have been reported to be hypermutated in post-GC B cells from healthy human donors, although at a significantly lower frequency than the IgV region [245-250]. *In vitro*-stimulated human primary B cells or human B cell lines displayed mutations in non-Ig genes, including *Bcl6* and *c-myc* [251, 252]. AID is directly responsible for these mutations [253] (Figure 1.5). In fact, overexpression of AID in B and non-B cell lines results in off-target mutations in *Aicda* and a GFP reporter genes [254, 255], and as indicated before, AID-transgenic mice develop T-cell lymphomas characterized by the presence of point mutations in the T cell receptor, *c-myc,* and *Pim1* genes [202, 256]. Indeed, increased levels of AID in B cells lead to a higher mutation rate in some non-Ig targets [201, 203, 257], although this does not always have oncogenic consequences *in vivo* [200, 204].

Extensive sequencing of the GC-B cell genome demonstrated that AID is mistargeted to a larger extent than initially hypothesized [253]. AID is recruited to 5910 genes in activated B cells and mutates ~25% of the genes transcribed in GC-B cells [257]. AID preferentially targets actively transcribed genes where RNA polII and trimethylated histone H3 Lys4 (H3K4me3) are present and AID occupancy correlates with the localization of transcription elongation factor SPT5 [257]. Nonetheless, only a reduced number of genes (~23) displayed a high rate of mutations ressembling Ig SHM. *Bcl6* is the primary AID off-target in activated B cells with a rate of mutation about 25-fold lower than the IgV region [253, 257]. Interestingly, some genes, such as *c-myc* or *Pim1*, which are frequently hit by AID in $Ung^{-/-}$ $Msh2^{-/-}$ B cells, display a significantly lower rate of mutations in wt B cells [253]. These results indicate that AID off-target activity is in some cases counteracted by faithful repair to prevent the accumulation of mutations. Still, more than 50% of the GC-derived diffuse large B cell lymphomas (DLBCL) display aberrant hypermutation in *Bcl6*, *Pim, Btg1*, *RhoH*, and *Pax5* [258]. Moreover, AID can be a disease progression factor by accelerating leukemia clonal evolution in Ph+ ALL (Philadelphia chromosome-positive B cell acute lymphoblastic leukemia) [259] and by mutating the BCR-ABL1 oncogene in CML (chronic myelogenous leukemia) and ALL [129, 259, 260], thus underpinning resistance to the therapeutic drug imatinib [129].

1.3.2. Chromosomal translocations

AID oncogenicity is probably in large part a consequence of its capacity to produce DNA breaks, thus initiating chromosomal translocations at a number of locations in normal B cells [261-265] (Figure 1.5). In fact, a recurrent hallmark in B cell lineage tumors is the presence of chromosomal translocations involving Ig loci and another partner. AID initiates DSBs in the IgH loci that lead to chromosomal translocations in activated B cells, and artifically increased levels of AID in B cells lead to a large increase in the frequency of IgH-cMyc translocations [201, 204], a characteristic of Burkitt's lymphomas. In addition, endogenous AID levels contribute to chromosomal translocations of multiple partners with the Ig locus, such as the IgH-Igβ [266] or IgH-Pax5 [264, 265], a hallmark of lymphoplasmacytic lymphoma. It can even occur between two non-Ig genes [201, 264, 265]. Indeed, most of the translocations occurring in a p53-deficient background involve *c-Myc* and miR-142 [201], a molecular hallmark of acute prolymphocytic leukemia [267]. Normally, apoptotic control eliminates cells with AID-induced translocations [261] and prevents B cell lymphomas in the AID-Igκ transgenic model [201]. In absence of p53, AID-Igκ induced B cell lymphomas with high frequency, even outpacing the T cell lymphomas that usually kill p53-deficient mice [201]. Curiously, GC B cells have reduced levels of p53 to allow for the necessary DNA damage that accompanies antibody gene diversification [134] so there are probably other mechanisms to prevent AID-initiated lymphomagenesis. For instance, AID-catalyzed lesions are more frequent in the absence of a number of DNA repair pathways, even with normal endogenous AID levels [253, 257, 268].

It does not seem that AID overexpression is necessary for lymphomagenesis, as demonstrated in the Balb/Bcl-xL mouse model of plasmacytoma. In this model, AID is required for most pristane-induced plasmacytomas, where it underpins the oncogenic IgH-cMyc translocation [34, 39]. AID haploinsufficient mice show reduced incidence of lymphoma compared to *Aicda*+/+ but still significantly higher than the *Aicda*-/- [193], demonstrating that 50% lower than normal levels of AID can be oncogenic in combination with another predisposing condition. Similarly, AID haploinsufficient B cells still display IgH-cMyc chromosomal translocations, albeit at a reduced frequency compared to wt [193, 194].

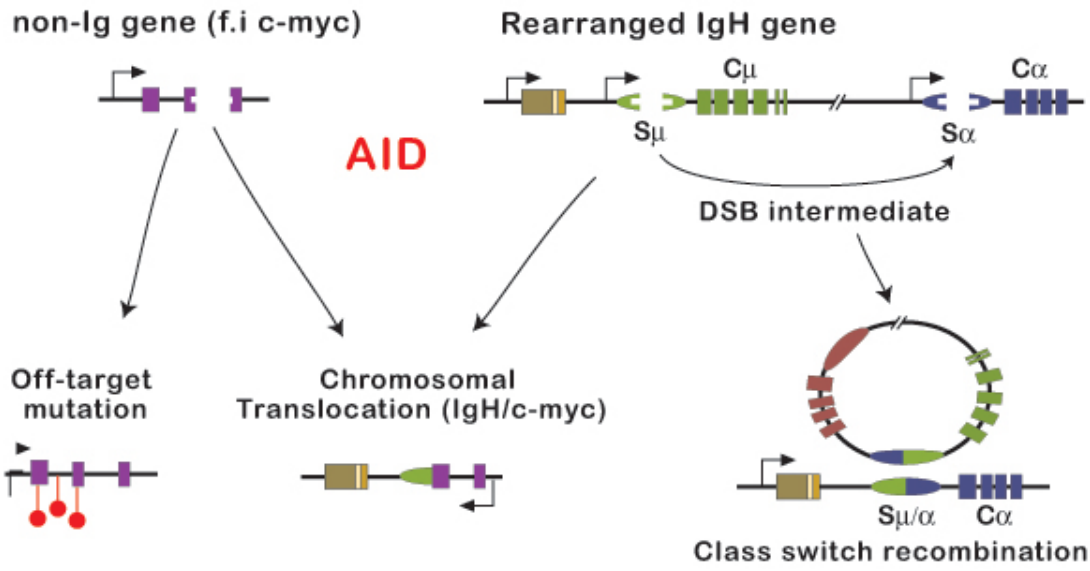

Figure 1.5. AID-mediated off-target mutations and chromosomal translocations. *Although AID preferentially acts at the Ig loci, other genes (f.i. c-myc, p53, BCR-Abl, etc) can be targeted at a lower but significant frequency, leading to oncogenic mutations and chromosomal translocations. The DNA double-stranded break (DSB) generated after AID deamination and processing can be resolved through the joining of switch regions in the Ig loci but can also lead to the joining of the Ig locus with a non-Ig gene (illustrated here with c-myc), resulting in a chromosomal translocation.*

Altogether, AID levels are critical in modulating the extent of off-target mutations and chromosomal translocations. Still, these are inherent to AID activity and contribute to cancer development.

1.3.3. AID expression in B-derived cancer cells

AID expression has been reported in several B lymphoid malignancies and endogenous levels of AID initiate B cell transformation, albeit infrequently. AID expression outside the GCs, f.i. in interfollicular large B lymphocytes, may give rise to precursors of mature B-cell malignancies [269]. Interestingly, the etiological role of AID in B cell lymphomas originating from GC B cells was demonstrated using the IμHABCL6 transgenic oncogene model, which deregulates BCL6 in B cells and results in mature B cell lymphomas. In an AID-deficient background, these transgenic mice did not develop mature B cell lymphomas [258]. IμHABCL6 lymphomas are akin to human DLBCL, which shows the highest prevalence of AID expression [210, 270-273], strongly suggesting an etiological role for endogenous AID in this lymphoma. In general, DLBCL but also follicular lymphoma samples show similar or lower AID levels than GC B cells [210, 270-272]. Near to normal AID levels are also expressed in Ph+ ALL and CML [129, 259, 260]. In these cases, BCR-ABL1 oncogene itself could be involved in inducing *Aicda*. Chronic lymphocytic leukemia is another B cell malignancy expressing variable levels of AID due to population heterogeneity where a defined subpopulation of cells can express most of the AID mRNA [274, 275]. The presence of this subpopulation correlates with a worsa prognosis but AID mRNA levels in these cells are not higher than in normal B cells [274, 275].

1.3.4. Ectopic expression of AID: link with inflammation

AID expression is induced in several malignant epithelial cells including colonic epithelium [276], hepatocytes [277, 278], biliary cells [279] and gastric cells [280]. This

ectopic AID expression is usually associated to chronic inflammation, and there is often an underlying infection such as with hepatitis C virus [277, 281], *Helicobacter pylori* [280, 282], or human immunodeficiency virus [218, 283]. It is likely that NF-κβ is involved, given that it is an important transcription factor in B and other cells for *Aicda* induction [277, 280, 284] (see section 1.4.1). Solid tumors originating from epithelial cells are usually associated with genetic alterations in *p53*, which appears to be an early event during tumorigenesis. Genetic evidence supports a role for AID in the pathogenesis of inflammation-associated carcinogenesis. As mentioned previously, AID overexpressing mice develop T cell lymphomas but also lung adenomas and hepatocellular carcinomas [202]. Disruption of *Aicda* in the IL-10$^{-/-}$ mouse model, which recapitulates human inflammatory bowel disease (IBD), reduces the frequency of mutations in *p53* and correlates with a reduced incidence of colon cancer. Thus, AID may play a central role in chronic inflammation-associated cancers by mutating non-Ig genes.

1.3.5. AID and autoimmunity

AID also influences antibody-mediated autoimmune diseases. AID is important in determining the severity of the pathology as demonstrated in mouse models of lupus and arthritis in which AID deficiency, or even haploinsufficiency, results in a more moderate disease [195, 242-244]. In keeping with this, increased levels of AID correlate with higher levels of autoantibodies in the MRL/fas$^{lpr/lpr}$ and BXD2 mouse models of lupus and rheumatoid arthritis (RA), respectively [242, 285-287]. Interestingly, AID-deficient mice also have autoimmune disorders albeit of a different nature [288]. This fits well with the predisposition to autoimmune disorders noted in AID-deficient human patients [289]. The recent finding that low AID expression levels during B cell development play a role in establishing B cell tolerance could explain these findings [220, 221]. Although, like in cancer, there are predisposing conditions beyond AID for developing autoimmunity, here again AID levels are important in balancing an efficient immune response with disease. Several autoimmune diseases, including rheumatoid arthritis and lupus, feature chronically inflamed tissues, where ectopic GC-like structures are present [290]. These structures express high levels of AID and can produce autoantibodies in a RA-SCID mouse chimera model [291]. It is therefore unclear whether high

AID expression plays an etiological role in the development of autoimmune diseases, or whether it is a consequence of the chronic inflammation associated with these diseases and thus a disease progression factor.

1.3.6. AID and allergies

AID is required for switching to the IgE isotype, which is the main antibody isotype involved in atopic allergy. Local expression of AID and antibody diversification was reported in the nasal musoca of rhinitis patients [292], in the bronchial mucosa of asthma patients [293], and within the oesophageal mucosa of chronic oesophagitis patients [294], which could be driven by the local presence of the allergen [295]. Furthermore, gene expression pattern analysis from patients affected by chronic rhinosinusitis with nasal polyps suggests a central role of AID in the etiology of this disease [296]. However, there is no direct genetic evidence for a link between abnormal AID expression and the development of allergies.

1.4. AID regulation

The data summarized above illustrates how the optimal expression levels of AID in GC B cells reflect a compromise between being able to mount an effective adaptive immune response and delaying the onset of cancer or autoimmune diseases. A strikingly complex network of regulatory mechanisms exist to ensure that the optimal amount of biologically active AID protein gets to the Ig locus much more preferentially than to any other genomic location. Any alteration in the performance of these mechanisms could predispose to immunodeficiency, autoimmunity, or B cell lymphomas. This thesis studies aspect of AID post-translational regulation. These will be introduced in greater details than the transcriptional regulation of AID.

1.4.1. Transcription regulation and cell-type specific expression

A combination of promoter, enhancers and silencers, which are located within four evolutionary-conserved regulatory regions, determines AID expression in GC B cells of the spleen and MALT (Peyer's patches, tonsils, lymph nodes) [206, 297]. These regulatory elements are found within 9kb upstream of the first exon and 25kb downstream of the last exon of the AID gene. The 5' most region of the *Aicda* locus contains binding motifs for NF-κβ, STAT6, C/EBP and SMAD3/4 proteins. This region is responsive to cytokines, co-stimulatory molecules, and stimulation through the NF-κβ pathway [297]. The second region, located 1kb upstream of the transcription start site (TSS), contains a ubiquitously active promoter and binding sites for NF-κβ, STAT6, SP proteins, and HOXC4-OCT [284, 298-300]. It may also contain a PAX5-binding site but its location is controversial [299, 300]. The third portion is located in the intronic region between exons 1 and 2 of *Aicda* and contains sites for NF-κB, E proteins (E-box) and PAX5 [297, 299-301]. Regions 1 and 3 cooperate to restrict AID expression to Ag-activated GC B cells. Finally, the fourth regulator region is located about 6kb in mouse and 25kb in human downstream of exon 5. It plays an enhancer role and is required for normal AID expression [207].

AID expression is also controlled by ubiquitous silencer proteins. For instance, region 1 contains binding motifs for c-MYB and E2F proteins, which can function as transcriptional repressors [297]. Furthermore, the inhibitor of differentiation (Id) proteins ID1, ID2 and ID3 repress *Aicda* transcription by binding to PAX5 and other stimulatory factors and preventing their association to DNA [299, 301]. Indirect repressors such as the transcription factor Blimp-1 or the DSBs-initiated ATM/LKB1 signaling pathway, which inhibits the transcription factor CRTC2, can also limit AID expression to the GC compartment [208, 302].

1.4.2. Post-transcriptional regulation

AID is post-transcriptionally regulated by micro-RNAs (miR). miR are short (20-23 nucleotides), noncoding RNAs that bind to complementary sequences in mRNAs and are key post-transcriptional regulators of gene expression. They are part of an active RNA-induced silencing complex (RISC) that contains the RNase III-type endonuclease Dicer and the

Argonaute proteins (Ago), which are important for mRNA silencing. The latter occurs either by mRNA degradation or by preventing mRNA from being translated. MiR-155 and miR-181b bind to conserved sites in the 3'untranslated region of AID mRNA and regulate its levels. This results in lower AID protein levels and reduced antibody diversification [203, 204, 303]. The different miR-155 and -181b expression patterns suggest two ways of regulating and restricting AID mRNA expression. MiR-155 is induced along with AID after B cell activation, and is expressed in GC B cells [203]. On the other hand, miR-181b is highly expressed in unstimulated B cells, decreases after B-cell activation and reaches its normal levels 3 days post-stimulation [303]. Therefore, miR-181b may restrict AID expression to the GC B cell compartment while miR-155 may limit AID levels during antibody diversification.

1.4.3. Post-translational modifications

AID activity is modulated at the post-translational level by phosphorylation. Five AID residues, for the most part conserved throughout evolution, have been found to be phosphorylated in B cells: Ser3, Thr27, Ser38, Thr140 and Tyr184 [196, 304-308]. The biological significance of Tyr184 remains unknown. On the other hand, phosphorylation of Thr27 inhibits AID deamination and CSR *in vitro*, suggesting it modulates AID specific activity [304, 305, 309] but whether this is used *in vivo* to regulate AID is unknown. Phosphorylation at Ser3 reduces AID biological activity *ex vivo* but does not impact its catalytic activity and again its role and importance *in vivo* are unknown [306]. Phosphorylation at Ser3 is controlled by the serine/threonine phosphatase PP2A *in vitro*. Conversely, phosphorylation of Ser38 and Thr140 are not essential for AID catalytic activity *in vitro* but both significantly increase AID biological activity *in vivo* [196, 304, 307, 310, 311]. Ser38 is phosphorylated by PKA in the chromatin, which allows AID interaction with RPA and greatly facilitates CSR and SHM [196, 304, 305, 307, 311, 312]. The effect of mutating Ser38 and Thr140 *in vivo* was much more pronounced when combined with AID haploinsufficiency [196, 310], thus suggesting that even if important, these modifications are not limiting for AID activity.

1.4.4. AID Subcellular localization

AID nuclear exclusion is an additional step of regulating its mutagenic activity. AID is predominantly cytoplasmic at steady-state, as first reported for AID-GFP in Ramos B cells [313] and confirmed by subcellular fractionation and immunohistochemistry in primary B cells [87, 209, 210]. In fact, AID subcellular localization is dynamic and reflects the equilibrium between active nuclear import [314, 315], active nuclear export [314, 316, 317], and cytoplasmic retention (see annexe 1 for ref.[315]). The deletion or mutation of the C-terminal 10 amino acids of AID led to its nuclear accumulation, thus identifying this region as a nuclear export signal (NES). This demonstrated that AID is a nuclear-cytoplasmic shuttling protein [316, 318, 319]. This leucine-rich NES is a typical recognition motif for the CRM1 exportin, as was demonstrated by using the CRM1-specific inhibitor leptomycin B [316, 319] and by coimmunoprecipitation [315, 320].

The mechanism by which AID gains access to the nucleus is still unclear. Due to its small size (24 kDa), AID could in principle diffuse passively through the nuclear pores. However, it is actively imported into the nucleus, as demonstrated by its capacity to confer nuclear localization to large proteins, which requires energy [315]. The nuclear localization signal (NLS) of AID has not been completely defined. AID N-terminal region (roughly residues 5-50) contains multiple basic residues, a characteristic of many NLS, and it is clearly a major part of it [315, 319]. However, it is not by itself sufficient to mediate nuclear import of heterologous proteins, which actually requires the first 181 out of the 198 AID amino acids [315]. So, there are other residues elsewhere in the protein that form part of and/or are critical in displaying the NLS, which prompted the suggestion that AID has a conformational NLS [315]. The factors mediating AID nuclear import are even less defined. AID binds *in vitro* to several importin-αs, which are dedicated nuclear import factors, but their functionality in AID import has only been indirectly inferred [315]. AID also interacts with CTNNBL1, a nuclear protein presumed to work in mRNA splicing, which binds to NLS through an armadillo-like domain [321, 322]. Nuclear accumulation of an AID variant with mutated NES is partially compromised in DT40 *CTNNBL1-/-* cells, suggesting a role for CTNNBL1 in AID nuclear import [322]. Still, CH12 *CTNNBL1-/-* cells did not show any reduction in CSR, demonstrating that it is at least redundant with another mechanism for importing AID into the nucleus [323].

Since CTNNBL1 interacts with importin-αs [322], they could be part of the same pathway. GANP, a protein associated with the RNA shuttling machinery and induced in GC B cells, has also been proposed to mediate active nuclear import of AID [324].

AID seems to be actively imported into the nucleus to counteract cytoplasmic retention, which prevents its diffusion [315]. Indeed, a motif in AID C-terminal region, overlapping with but distinct from the NES, is able to limit the passive diffusion of GFP into the nucleus [315]. Separation of function mutations exist to corroborate that these two signals are distinct and mediate different protein-protein interactions [315]. The translation factor eEF1α could participate in retention at least in part since it is stoichiometrically associated with AID in the cytoplasm and mutating the proposed AID cytoplasmic retention motif can disrupt this interaction [315, 325].

Any modification in the balance of forces determining AID subcellular distribution should impact antibody diversification. Whether this is regulated (f.i. to increase diversification after some signaling event, at a particular cell cycle stage [326]), or whether the proportion of AID in the nucleus is constant at all times [206, 327], is unresolved. Drastic alterations or truncation of AID NES abolish CSR, most likely because this region also contains a domain mediating interactions required for CSR [316, 319, 328, 329]. Nevertheless, the relocalization of AID into the nucleus by mutating or deleting the NES increases SHM and immunoglobulin gene conversion [319, 328, 329]. This could partially be explained by a higher catalytic activity of nuclear AID variants [316, 328, 330], although these latter are less expressed [316, 329, 331]. Nevertheless, mutating the C-terminal cytoplasmic retention signal of AID led also to faster nuclear import and higher SHM and CSR [315, 329]. Therefore, nuclear exclusion limits the biological activity of AID.

1.4.5. AID stability

The stability of AID is directly linked to its subcellular localization. Cytoplasmic AID is much more stable than nuclear AID [331]. The ~8 h half-life of AID in B cells represents in fact a rough average of its ~2.5 h nuclear and 18-20 h cytoplasmic half-life [331]. Indeed,

inhibition of AID nuclear export with leptomycin B and mutation or deletion of the NES, as well as disruption of AID cytoplasmic retention, increase the nuclear fraction of AID and correlate with a decrease in its half-life [315, 325, 329, 331, 332]. On the other hand, restricting AID to the cytoplasm resulted in increased AID half-life [315, 331]. The mechanistic explanations for this difference in stability are unclear.

Inside the nucleus, AID seems to be constantly targeted to the proteasome by ubiquitin (Ub)-dependent and -independent pathways [331, 333]. Proteasomal inhibition suffices to detect an important increase in polyubiquitinated nuclear AID [331]. The Ub ligases modifying nuclear AID are unknown. The murine double minute 2 (MDM2) E3 ubiquitin ligase interacts with AID and could be one of them [334]. However, DT40 cells deficient in or overexpressing MDM2 show very modest increase and decrease in Ig gene conversion, respectively [334]. Thus, MDM2 is either redundant with some other Ub ligase or not relevant for AID. Interestingly, AID with no internal lysine residues is still significantly polyubiquitinated [331], suggesting either N-terminal ligation or a non-canonical pathway of polyubiquitination for AID. A proportion of AID interacts with and is targeted for degradation by the nuclear protein REG-γ, which brings proteins for proteasomal degradation in Ub- and ATP-independent fashion [333] (see section 1.6.1 and figure 1.8). In fact, REG-γ deficiency results in higher AID steady-state levels, increased nuclear AID stability, and increased CSR in mice, demonstrating the physiological role of this protein in reducing nuclear AID levels [333]. Thus, modulating AID stability seems to be one more way of limiting AID expression and yet another mechanism restraining antibody diversification. It remains unclear whether cytoplasmic AID is protected from this active degradation process.

1.4.6. Targeting specificity to the Ig loci

AID gets to the Ig locus much more preferentially than to any other genomic location. The reasons for this preferential targeting are still unclear. AID activity is highly dependent on transcription *in vitro* and *in vivo*, which transiently exposes unpaired bases in the transcription bubble [186-192, 254, 255, 335-340]. However, transcription alone cannot account for the preferential targeting of AID to the Ig loci. Indeed, AID contains a domain (residues 113-123)

that contributes to the preferential deamination at WRCH motifs, which are highly enriched in the switch and the IgV regions and therefore function as mutational hot-spots [341, 342]. AID equally deaminates both the transcribed and non-transcribed strands [343], due to its interaction with the RNA exosome complex [344]. Given the abundance of actively transcribed genes containing RGYW/WRCY motifs, the substrate specificity of AID cannot fully explain the preferential targeting to the Ig loci.

Epigenetic modifications of histones, which control the chromatin architecture, may contribute in defining a window where AID can be preferentially recruited. Histone modifications are associated with CSR and SHM, although the nature of these modifications may differ between CSR and SHM [345-350]. They may play a role in AID targeting by modulating the structure of the chromatin and/or providing binding motifs for factors implicated in antibody diversification. Indeed, a proportion of nuclear AID interacts with KRAB domain-associated protein 1 (KAP1) and the heterochromatin protein 1 (HP1) and is targeted to H3K9me3 (trimethylated histone H3 at lysine 9) present at the Sμ region [351]. KAP1 deficiency results in impaired binding of AID to the Su region and reduced CSR in mice [351]. Still, KAP1 is dispensable for SHM and therefore cannot account alone for the specific targeting of AID to the Ig loci.

Genetic evidence supports a contribution of the transcription machinery in AID targeting. The most promising targeting factor is the transcription elongation factor SPT5, which associates with stalled RNA polIIand recruits AID near the transcription start site [352]. In fact, RNA polII behaves differently in the Ig loci than in other genes and appears to stall and accumulate due to the high frequency of R-loops in that region [345, 353]. AID occupancy at transcribed regions depends on SPT5 and RNA polII. Problematically, SPT5 occupancy correlated with both the Ig loci and off-targets genes. Selective recruitment of AID to the variable and switch regions may in part depend on the polypyrimidine tract binding protein 2 (PTBP2) and the 14-3-3 scaffold proteins. Normally, PTBP2 inhibits RNA splicing by binding to the polypyridimidine RNA tracts. In B cells, PTBP2, which preferentially binds RNA transcribed from the Sμ region, interacts with AID and promotes its specific recruitment to Sμ and Sγ1 regions [354]. On the other hand, the 14-3-3 scaffold proteins can bind dsDNA regions

that contain AID hotspot motifs and associate with transcribed switch regions in activated B cells [355]. They interact directly with AID through its C-terminus and may contribute to the preferential recruitment of AID to switch regions.

As mentioned previously, PKA is present in switch regions in an AID-independent fashion but can interact with AID in the Ig loci, thus phosphorylating and enabling the local association of AID with the single-stranded binding protein RPA [311, 312]. In fact, RPA plays a role in SHM, CSR and iGC [196, 304, 305, 310, 312]. Nonetheless, neither PKA nor RPA are required for physically recruiting AID to DNA [311]. In conclusion, the preferential targeting of AID to the Ig loci results from the contribution of several elements including AID's intrinsic substrate specificity, AID's association with the transcription machinery, epigenetic modifications, and local post-translational modifications of AID.

1.4.7. AID co-factors

It is clear that AID interacts with co-factors critical for either SHM or CSR. Deletion/mutation of the amino-terminal domain of AID abolishes SHM without drastically affecting CSR [356]. On the other hand, deletion/mutation of AID C-terminal NES leads to defective CSR but retains SHM [357-359]. Nonetheless, the nature of the interactions mediated by AID's N- and C-terminal domains and their functional importance remain to be determined. Beside the 14-3-3 adaptor proteins that recruit AID to the switch regions, AID C-terminus binds to the Ub ligase MDM2 [334] and DNA-PKcs [360], but the functional relevance of these interactions are unclear.

In this thesis, we will show that AID interacts with several members of the HSP90 molecular chaperoning pathway. Therefore, we will introduce the important points of this pathway that are relevant to our work.

1.5. The HSP90 molecular chaperoning pathway

AID is predominantly cytoplasmic at steady-state and requires nuclear translocation for proper activity [361]. Consistent with the fact that cytoplasmic AID is more stable than its

nuclear counterpart, it was suggested that AID is protected and/or retained in the cytoplasm by specific chaperones [362]. Indeed, the heat shock 70-kDa protein HSC70 was coimmunoprecipitated with AID from HeLa cell extract [360], but the functional relevance of this interaction in B cells remains unclear. HSC70 is a ubiquitous molecular chaperone, which is mainly implicated in the folding of nascent proteins and the refolding of denatured proteins.Two major forms of this chaperone have been identified: the constitutive form, named HSC70, and the stress- and heat shock-induced form, HSP70. Both are often considered to have similar cellular functions. Indeed, HSC70/HSP70 play a central role in protein triage and controls the balance between (re)folding and degradation of denaturated proteins (reviewed in [363]). HSC70 is also part of the HSP90 molecular chaperoning pathway, which includes the HSP40 and HSP90 chaperones, as well as additional cofactors. These heat shock proteins (HSPs) are highly conserved throughout evolution and their role extends beyond *de novo* protein folding and protection in stressful situations. In fact, HSP90 participates in the stabilization and the activation of a large range of proteins, referred to as HSP90 clients, rather than interacting with unfolded proteins to facilitate their (re)folding. The best characterized HSP90 clients are involved in cell signalling and transcriptional regulation (i.e. kinases and steroid hormone receptors) [364-366], but recent proteomic and genetic studies suggest that the HSP90 molecular chaperoning pathway may be implicated in broader cellular processes [367-369].

1.5.1. HSP90

HSP90 is highly conserved throughout evolution and is present in four different isoforms in humans [370]: two cytosolic (HSP90α and β), one mitochondrial (TRAP1), and one in the endoplasmic reticulum (GRP94). HSP90 functions as a flexible dimer and each monomer is constituted of three domains: an N-terminal domain which possesses an ATP-binding pocket and catalyzes ATP hydrolysis; a flexible and highly charged linker sequence which connects the N-terminal domain to the middle (M) region; and a C-terminal dimerization domain [370]. Genetic evidence indicates that the M region plays a key role in the binding of many HSP90

clients. It also modulates ATP hydrolysis [371, 372]. HSP90 interacts with the co-chaperone AHA1 (activator of HSP90 ATPase homologue 1), that promotes the association of the N- and the M-domains, thus accelerating the ATP-hydrolysis rate [373, 374] (see section 1.5.3.). The ability of HSP90 to recognize and stabilize a large repertoire of clients depends on its intrinsic flexibility and on highly dynamic conformational shifts catalyzed by ATP hydrolysis. These structural rearrangements are essential for client maturation and are modulated by certain co-chaperones, including AHA-1 and p23 (reviewed in [375]).

Little is known about the molecular basis of HSP90 client recognition. All the known HSP90 clients are different in structure and even close variants of the same protein do not necessarily depend on HSP90 stabilization in the same way. The two SRC kinase variants, the cellular form (c-SRC) and the viral form (v-SRC), are the perfect example. Although both are almost identical (95%), v-SRC requires HSP90 stabilization while c-SRC is largely independent of this chaperone [376-378]. This may partially be explained by the differential intrinsic instability of the two forms, with v-SRC being highly instable. But it remains unclear whether the requirement for the HSP90 chaperoning pathway is dictated by a specific motif or general biophysical properties of the client.

1.5.2. HSP40/DnaJ proteins

The specific recognition of client proteins for stabilization by the HSP90 pathway may be controlled by the HSP40/DnaJ proteins. In fact, they are the most diverse family of co-chaperones and consist of 41 members in humans, while there are only 11 different HSC70 isoforms and 4 different HSP90 isoforms. The canonical role of HSP40/DnaJ proteins is to present clients to HSC70 and stimulate HSC70 ATP hydrolysis [379]. This latter process is dependent on a highly conserved 70 amino acid J-domain, which is the defining feature of all HSP40/DnaJ proteins [380, 381]. Indeed, the J domain contains a histidine–proline–aspartic acid (HPD) motif that is essential for the stimulation of ATP hydrolysis by HSC70 [382]. HSP40/DnaJ proteins are structurally divided into three subclasses based on the presence or absence of conserved domains: type I (DnaJa/DjA), type II (DnaJb/DjB), and type III (DnaJc/DjC) [379] (Figure 1.6). In this thesis, we are primarily interested in type I HSP40/DnaJ

proteins (DnaJa1–4), which are orthologues of *E. coli* DnaJ and yeast YDJ1. DnaJa1, -a2 and –a4 are cytoplasmic proteins, while DnaJa3 is found in the mitochondria (reviewed in [383]), and cytosolic DnaJa1 and –a2 are ubiquitously expressed [384]. Besides the conserved J domain, HSP40/DnaJ may contain a Gly/Phe-rich (G/F) linker and a C-terminal substrate-binding region (Figure 1.6). The G/F rich region contributes to the interaction with HSC70 but is not involved in stimulating the ATPase activity of HSC70 [385-390] (Figure 1.6). The C-terminal substrate-binding region can be subdivided into a hydrophobic pocket that can confer substrate binding specificity (CTDI), a cysteine-rich region, also known as the zinc finger (CTDII), and a dimerization domain, at least for type I-DnaJ proteins [391, 392] (Figure 1.6). Substrate specificity of type I and II-DnaJ proteins is considered to be dependent on their C-terminal domain [393-395]. In fact, type I-DnaJs and their yeast ortholog YDJ1 are farnesylated at their C-terminus [396, 397]. Farnesylation is a posttranslational modification catalyzed by a farnesyltransferase (FTase), which consists in the addition of a 15-carbon isoprenoid group (farnesyl group) at the carboxyl terminus of a protein containing a CAAX motif (C=cysteine, A=aliphatic, and X=any amino acid) (reviewed in [398]). FTase, which catalyzes the formation of a thioether bond between the farnesyl group and the thiol group of cysteine, is a heterodimer but its substrate specifity is unclear. In fact, ~300 proteins terminate with a CAAX motif in the human proteome, but only a small fraction is actually post-translationally modified [398]. Nevertheless, farnesylation plays an important role in membrane association and protein-protein interaction of a number of proteins. In the case of type-I DnaJ proteins, farnesylation largely contributes to protein-protein interactions [399] and is functionally important for the interaction between YDJ1 and HSP90 clients [400, 401]. The diversity of HSP40/DnaJ proteins and their implications in a large range of biological functions suggest a functional specialization and the recognition of a specific subset of substrates (see section 1.5.4.).

1.5.3. Stabilization of HSP90 client proteins: the maturation process

HSP90 and its co-chaperones HSP40/DnaJ and HSC70 interact with clients in an ordered ATP-dependent pathway. This maturation process has been extensively characterized

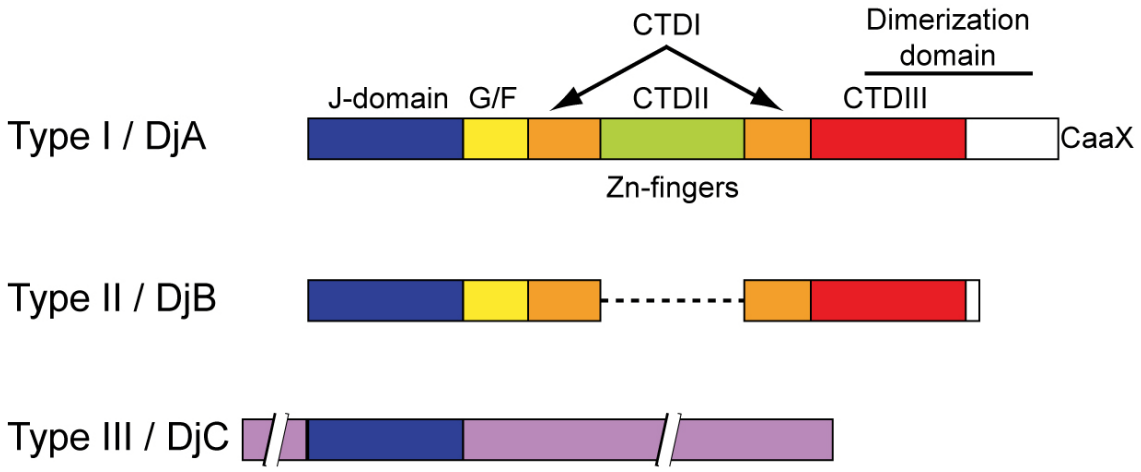

Figure 1.6. HSP40/DnaJ proteins. *Schematic structure of the three types of J-proteins indicating their different domains (except for type IIIs, which do not share a common organization). They all share a highly conserved J domain, which is important of the ATPase activity of HSC70. Type I- and type II-HSP40/DnaJ proteins contain a glycine/phenylalamine-rich domain (G/F), which is involved in the binding to HSC70. The C-terminal domain of HSP40/DnaJ protein varies largely depending on the subtype. Carboxyl-terminal domain I (CTDI) can confer substrate specificity; CTDII contains a zing-finger domain, and CTDIII encompasses a dimerization domain. CAAX indicates the farnesylation motif present in type I J-proteins.*

in the context of steroid hormone receptors, and consists in the initial recognition of the newly synthesized or misfolded client by HSP40/DnaJ and HSC70/HSP70 [363, 402] (Figure 1.7). When bound to ATP, HSC70 has a low affinity for client proteins. Stimulation of HSC70 ATPase activity by the J-domain of HSP40/DnaJ increases the affinity of HSC70 for its substrate and promotes the formation of a stable HSC70-client complex [402]. HSC70

1.5.4. Limiting step of the HSP90 chaperoning pathway

Consistent with the view that the HSP90 molecular chaperoning pathway stabilizes a functions as a monomer but can be associated with several co-chaperones beside HSP40/DnaJ proteins. Transfer of the client from HSC70 to HSP90 is mediated by HOP/STI, which simultaneously binds HSC70 and HSP90 through two distinct tetratricopeptide repeat (TPR) domains [403] (Figure 1.7). It remains unclear how the client is transferred from HSC70 to HSP90. For the progression of the maturation cycle, HSC70 and HOP/STI are replaced by other TPR-containing co-chaperones including p23 [404-406]. This latter step promotes ATP-binding and the formation of a closed conformation of HSP90 with its client (Figure 1.7). The closed conformation of HSP90 maintains its client in a metastable state (Figure 1.7; reviewed in [407]). ATP hydrolysis results in the reopening of HSP90 and the dissociation of the client from HSP90. The client can then undergo additional maturation until it reaches a stable conformation (Figure 1.7). In the context of the steroid hormone receptors, hormone binding leads to a conformation change in the receptor [407]. Chaperone components are released and the steroid hormone receptor bound to its specific hormone can be translocated to the nucleus to perform as a transcription factor. Similarly, post-translational modifications (f.i. phosphorylation, acetylation or s-nitrosylation) of both HSP90 and its clients influence their association [375, 408, 409].broad range of proteins, HSP90 is implicated in several cellular processes, f.i. protein activation, translocation across membranes, and quality control in the endoplasmic reticulum or immunogenic peptide processing. HSP90 is very abundant, representing up to 2% of the cytosolic proteins, and is required for cellular viability in eukaryotes [410, 411]. This chaperone rarely functions alone and requires the help of other co-

chaperones. For instance, HSP40/DnaJ proteins are less abundant and limiting in the chaperoning pathway. Although *dnaJ* and the HSP70 orthologue *dnaK* genes are both transcribed from the same strong promoter in *E. coli,* DnaJ proteins are 10 times less abundant than DnaKs [412]. Similarly, YDJ1 (HSP40/DnaJ orthologue) is estimated to be present in yeast at a 1:2:4 ratio relative to SSA1 (HSP70 orthologue) and HSP82 (HSP90 orthologue), respectively [413]. HSP40/DnaJ proteins are also functionally limiting in mammalian systems [390, 414, 415]. HSP40/DnaJ binding to the client is not only the first step in the maturation cycle; it is also the only co-chaperone that binds intrinsically to these clients without assistance of other co-factors [416-418]. Since HSP40/DnaJ proteins are the largest and most diverse family of co-chaperones, they could be indirect regulators of the HSP90 molecular chaperoning pathway by selecting specific client proteins. In line with this, *in vitro* studies indicate a certain level of functional specialization for HSP40/DnaJ proteins, despite some redundancy [416, 419-423]. *In vivo*, all the HSP40/DnaJ-deficient mice show different phenotypes. *DNAJA1*-/- mice have a defect in spermatogenesis with aberrant androgen receptor signalling [424]. *DNAJA3* deficiency results in embryonic lethality [425] and heart-specific *DNAJA3* deletion causes dilated cardiomyopathy [426]. *DNAJB1* disruption compromises thermotolerance in mice [427]. *DNAJB6*-deficient mice are embryonic lethal and show defects in placental development [428]. *DNAJC3*-/- mice develop diabetes [429]. Finally, *DNAJC5* deficiency results in progressive neurodegeneration [430]. These genetic evidences suggest substrate specialization of HSP40/DnaJ proteins. But the identity of these *in vivo* substrates and the mechanistic details beyond their specific recognition by DnaJ proteins are largely unknown.

1.5.5. Pharmacological interventions

The HSP90 pathway is not only involved in normal cellular processes but can also contribute to the development of cancer by stabilizing oncogenic proteins. Indeed, several HSP90 clients are implicated in cellular proliferation (f.i. HER-2, RAF-1, CDK4) [431-433], in immortalization (telomerase TERT) [434, 435], or in the prevention of apoptosis (AKT) [436], and the list is expanding. HSP90 also stabilizes specific B cells transcription factor such as BCL6 [437], which is oncogenic in DLBCL. Moreover, HSP90 stabilizes the constitutively

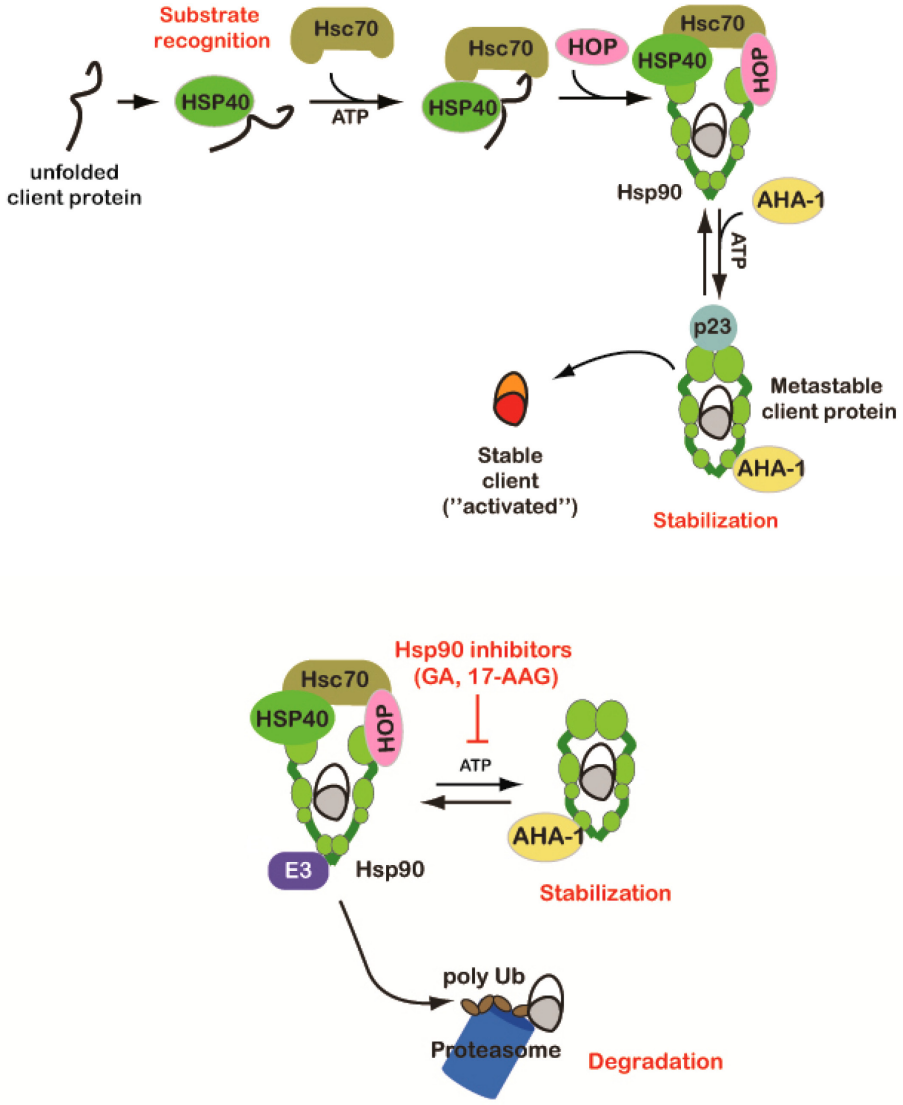

Figure 1.7. The HSP90 maturation process: pharmacological intervention. *HSP90 modulates the function of proteins by stabilizing a meta-stable intermediate. HSP40/DnaJ protein initiates this maturation pathway by recognizing the client protein. Subsequently, HSP40/DnaJ transfers the substrate to HSC70 and stimulates HSC70 ATPase activity. HSC70 can associate with HSP90 via the co-chaperone HOP. The client protein is stabilized in a metastable complex with*

HSP90. p23 locks HSP90 in a closed conformation until AHA-1 stimulates HSP90 ATPase activity. This results in the release of the client protein. This latter can be stabilized by post-translational modifications or the presence of its substrate (f.i. steroid hormone), becomes activated, or undergoes an additional round of maturation. HSP90 chaperone activity depends on ATP hydrolysis, which can be inhibited by the drug geldanamycin (GA) and its derivatives 17-AAG, leading to polyubiquitination and degradation of its clients.

active tyrosine kinase BCR-ABL in CML [438, 439]. Mutations in BCR-ABL that can arise during treatment with tyrosine kinase inhibitors (f.i. imatinib) result in a stronger dependence toward HSP90 [440]. In fact, HSP90 has been proposed to act as a capacitor in cancer by stabilizing mutated proteins that otherwise would not be functional [441, 442].

Increased expression of one or more HSP proteins is also a common feature of both solid tumors and haematological malignancies [408, 409]. Thus, targeting HSP90 for cancer therapy has been an expanding area of research and HSP90 is now considered to be a *bona fide* anti-cancer drug target. The N-terminal ATP-binding pocket of HSP90 can also bind natural products such as geldanamycin (GA) and radicicol [443] (Figure 1.7). These compounds interact with greater affinity with HSP90 N-terminus than ATP and prevent the chaperone from cycling between its open and closed states. Synthetic GA derivatives such as 17-AAG have been developed and are currently in clinical trials [444]. HSP90 inhibition results in the recruitment of E3 Ub ligases such as CHIP (carboxy-terminus of HSP70-interacting protein) [445-447]. HSP90 clients are therefore destabilized by polyubiquitination and targeting for proteasomal degradation (Figure 1.7). It is unlikely that CHIP is the only E3 Ub ligase involved in the degradation of HSP90 clients [447, 448]. Genetic evidence suggests that Cullin5 may be one alternative E3 ligase [449].

The identification of a specific substrate for a given HSP40/DnaJ protein may also be a promising avenue of research in targeting this pathway for therapy. Unfortunately, there is limited information on the expression and function of most HSP40/DnaJ in cancer [379, 450], and very few specific substrates are known. Of note, there are currently 8 different HSP40/DnaJ proteins that have been implicated in the development of cancer and metastasis [379], but how mechanistically they play a role in influencing cancer properties is unknown. DnaJa1, a type-I HSP40/DnaJ protein, is an interesting example. Modulation of DnaJa1 levels in a human glioblastoma cell line modulates its resistance to radiation [451]. As mentioned previously, DnaJa1 is farnesylated at its C-terminus, which is important for its association with client proteins. Use of farnesyltransferase inhibitors (FTI) that are currently in clinical trials led to the accumulation of non-farnesylated DnaJa1 and correlated with increased radiosensitivity [451]. Although FTI may affect other farnesylated proteins, the use of these drugs may be an

interesting tool to target substrates recognized by a farnesylated HSP40/DnaJ proteins.

1.6. Instrinsic motifs dictating protein turnover

The differential stability between cytoplasmic and nuclear AID may also result from its intrinsic biochemical properties or the presence of degradation motifs in AID that may be more relevant in one subcellular compartment than another. AID is targeted by both an Ub-dependent and independent degradation pathway in the nucleus [331, 333], and one could speculate that specific motifs may direct AID to one or the other pathway.

1.6.1. Ubiquitin-dependent and –independent degradation pathways

The proteasome performs the majority of the proteolysis in higher eukaryotic cells and therefore plays a central role in protein homeostasis. It is found in both the cytoplasm and the nucleus and contributes in the destruction of abnormal/unwanted proteins but also to the maturation of polypeptide precursors [452, 453]. It is also involved in the generation of peptides presented by MHC class I molecules, which is crucial for initiating an immune response. The proteasome is composed of a proteolytic core, the 20S proteasome, which is highly conserved throughout evolution [452]. The 20S proteasome has a typical barrel-shape that results from the assembly of 28 subunits in 4 heptameric rings [454, 455]. The two inner rings form the catalytic sites while the outer rings associate with a variety of regulatory complexes. Substrates access the central catalytic sites through axial ports at the end of the 20S proteasome [456]. But these pores are closed in absence of the regulatory complexes. Three activators of the 20S proteasome have been characterized: the 19S regulatory complex (PA700) [457-460], the 11S activating complex (REG activator PA28) [461, 462], and the proteasome activator P200 [463]. Two inhibitory proteins, PI31 [464] and Pr39 [465], have also been described. Their mechanism of action is still under investigation but it is clear that the 19S complex is necessary for the processing of ubiquitinated proteins, although it has also been implicated in a Ub-independent pathway [466]. The 20S proteasome can associate with two 19S regulatory complexes to form the 26S proteasome [467] (Figure 1.8A), which is directly

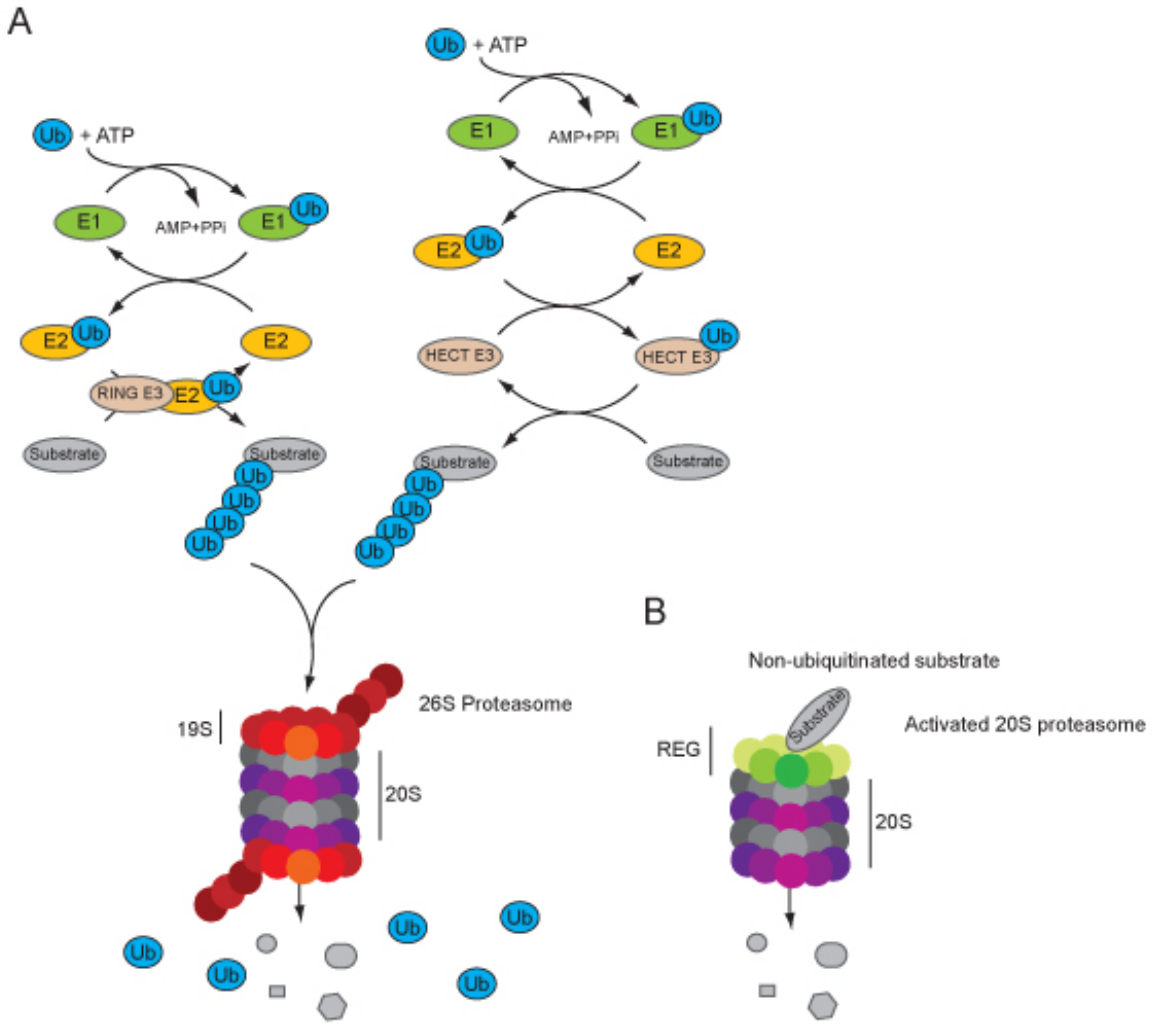

Figure 1.8. The ubiquitin-dependent and -independent proteasome system*. (A) Conjugation of ubiquitin (Ub) is catalyzed by the RING/U-box or the HECT E3 ligase. Ub is activated in an ATP-dependent manner by the Ub-activating enzyme, E1. The activated Ub is subsequently transferred to the Ub-conjugating enzyme E2. In the case of a RING/U-box E3 ligase, Ub-charged E2 binds to E3 and transfers the activated Ub moiety directly to the substrate that is also bound to E3. For the HECT E3 ligase, the Ub is transferred from E2 to a cysteine residue in E3 and then to the substrate .The conjugated substrate is degraded into short peptides by the 26S proteasome, composed of the core 20S proteasome and the 19S activator subunits. (B)*

Alternatively, a substrate can be directly recognized by the REG complex (also called PA28/11S), which acts as an activator of the 20S proteasome and can initiates the degradation of intact proteins through an Ub- and ATP-independent pathway.

involved in the degradation of ubiquinated proteins. Nevertheless, this complex is not necessarily the most abundant proteasomal complex in the cell. It is also unclear what the subcellular distribution of all these complexes is and how they manifest substrate specificity.

The Ub-dependent proteasome degradation pathway requires the initial conjugation of single or polymeric Ub moieties to the substrate. This most often occurs through the formation of an isopeptide bond between the C-terminal group of Ub and the ε-amino group of an internal lysine residue. Ubiquitination can also occur at alternative sites, including the N-terminal group of a protein [468-470] or unconventional non-lysine residues (cysteine, serine or threonine) [471-475]. Importantly, this process is reversible through the action of deubiquitylases (DUB) [476]. Protein ubiquitination is carried out by an enzymatic cascade, where Ub is first activated by a Ub-activating enzyme (E1) in an ATP-dependent manner (Figure 1.8A) [453, 470]. A thioester bound is formed between the C-terminus of Ub and a cysteine residue in E1. Activated Ub is subsequently transferred to a Ub-conjugating enzyme (E2/UBC). Despite partial redundancy, E2 can confer some specificity to substrate ubiquitination. However, in most cases, the E3 Ub ligase provides the layer of specificity for a substrate. HECT E3 ligases form a thioester bond with activated Ub before transferring it to the substrate [477]. On the other hand, RING/U-box E3 ligases facilitate the transfer of the Ub moiety from the E2 to the substrate [478]. Ub moieties can then bind efficiently and specifically to the 19S regulatory complex, thus targeting the protein substrate for degradation.

Interestingly, there are a number of proteins that can be degraded in a Ub-independent (Figure 1.8B) manner but still require the proteasome, including ornithine decarboxylase (ODC) [479, 480], cyclin-dependent kinase inhibitor p21 [481, 482], or c-JUN [483]. The fact that p21 or c-Fos can be degraded by both a Ub-dependent and –independent pathways [476] suggest that both pathways can contribute to the protein turnover of a specific substrate and may be selected depending on the context or subcellular localization. However, it remains unclear what are the intrinsic protein determinants that dictate this choice. Absence of an Ub acceptor NH2 group on the substrate may be an obvious element, although proteins that have lysine redisues, including AID [484], are also subjected to this pathway (reviewed in [476]).

Furthermore, the proteasomal subunits involved in this pathway are still controversial. The REG complex (11S/PA28), which is an ATP- and Ub-independent proteasome activator, strongly enhances the catalytic activity of the proteasome *in vitro* [485]. In particular, REGγ resides primarily in the nucleus and can directly interact with intact protein substrates for targeting to the 20S proteasome in an ATP- and Ub-independent manner [452] (Figure 1.8B). But the determinants implicated in the recruitment of REG-γ are unclear. *In vitro* studies have shown that proteins containing intrinsically unstructured regions undergo degradation by the 20S proteasome. In fact, up to 20% of all cellular proteins can be degraded or cleaved at unstructured domains by a Ub-independent 20S-dependent proteasomal pathway [476, 486-488]. However, the REGγ-20S proteasome seems to be highly selective and its recruitment may require additional structural or sequence motifs for substrate degradation [489, 490] .

1.6.2. The N-end rule

Although the general steps implicated in protein turnover are defined, it is less clear what are the actual signals dictating protein stability and whether they influence an Ub-dependent or –independent proteasomal targeting. Several biochemical and biophysical properties of proteins have been described as determinants of protein turnover, including molecular weight [491], isoelectric point [492, 493], hydrophobicity [494, 495], and the presence of certain motifs [496-499]. The simplest degradation motif, the N-degron, has been extensively studied and illustrates that the nature of a protein's N-terminal amino acid determines its half-life [499, 500]. Newly synthesized proteins contain an N-terminal methionine which is considered as a stabilizing residue according to the N-end rule, but proteins can be enzymatically modified at their N-terminus to reveal a primary, secondary or tertiary destabilizing residue depending on the number of steps required before polyubiquitination [500].

There are two cytosolic methionine aminopeptidases in mammals, MetAP1 and MetAP2, which remove the initial methionine, thus exposing the secondary residue of a protein. Interestingly, MetAP2 is highly expressed in GC B cells and its inhibition led to suppression of T-cell dependent Ag-specific antibody response by disrupting GC formation [501, 502]. Indeed, N-terminal cleavage is quite a common post-translational modification that can affect between 55 and 70% of the proteins depending on the organism and the subcellular

compartment [503]. Processed proteins that contain an N-terminal cysteine residue are subsequently modified by an arginyl-tRNA protein transferase (ATE1) to introduce an arginine, which targets it to the N-end rule pathway. ATE1 can actually modify several proteins without necessarily creating a N-degron, suggesting that multiple determinants could influence the half-life of a protein. In fact, high-throughput analysis suggested that the half-life of a protein is influenced by multiple factors (f.i. structural disorder) *in vivo* [504].

1.6.3. PEST and other degradation motifs

Other degrons predisposing a protein to increased instability have been identified, including the PEST motifs (P=proline, E=glutamic acid, S=serine, T=threonine) [498, 505]. These regions are enriched in proline, aspartic/glutamic acid, serine and threonine, and are generally flanked by positive residues. They have been predicted to be solvent-exposed regions, which would make them more susceptible to proteolysis [505]. In fact, PEST motifs are abundant in intrinsically unstructured proteins [506, 507]. Most of the proteins containing a PEST motif are short-lived [508-511], which could result from the contribution of both the Ub-dependent and independent proteasomal degradation pathway [512]. However, whether PEST motifs interact with specific E3 Ub ligases or substrate recognition proteins for the Ub-independent proteasome is unknown.

Beside PEST motifs, additional degrons have been characterized such as the APC/C-dependent D- and KEN boxes [497, 513-516] and the TrCP recognition box (DSGXXS) [470, 517-519]. These motifs seem to be present in more defined and smaller subsets of proteins. The D- and KEN boxes are recognized by the anaphase-promoting complex/cyclosome (APC/C), an E3 Ub ligase involved in the polyubiquitination of regulatory proteins such as securin, cyclin A and geminin [520]. Proteasomal degradation of these proteins through the action of APC/C is important for cell-cycle progression. On the other hand, the DSGXXS motif is recognized by β-transducin repeats-containing proteins (β-TrCP), which serve as a substrate recognition for the $SCF^{\beta\text{-}TrCP}$ E3 Ub ligases [521]. This motif is mainly found in phosphorylated proteins and plays a role in the regulation of cell division and signal transduction. For instance, the regulatory

protein Iκβ and the E-cadherin-associated β-catenin protein contain such a motif and can be targeted to the proteasome through the action of the β-TrCP-$SCF^{\beta\text{-}TrCP}$ complex. The D/Ken box and the β-TrCP motifs are highly dependent on Ub for their substrate degradation, which makes them improbable candidates for targeting to the other pathway.

In summary, the rate of degradation of a protein results from the combination of multiple factors, including the presence of one or several degradation motifs as well as intrinsic domains of disorders. Whether these degradation motifs may influence the targeting of a substrate to the Ub-dependent or –independent proteasome remains unclear.

1.7. Rationale of the research

Given that AID is limiting for antibody diversification, and that ectopic and normal expression of AID results in off-target mutations which contribute to cancer/autoimmune diseases, it is critical to precisely define the post-translational regulations that determine the optimal levels of AID. Since AID is found at steady-state in the cytoplasm, where it is more stable than in the nucleus, we asked whether cytoplasmic AID could be protected by binding to specific factors in this compartment. A pull-down assay, using AID as bait, revealed interactions with several molecular chaperones, including DnaJa1, HSC70 and HSP90. Our hypothesis is that the HSP90 molecular chaperoning pathway protects AID from degradation in the cytoplasm. We first investigated the role of HSP90 in cytoplasmic AID stabilization and its biological importance in antibody diversification (Chapter 2). Analysis of the role of DnaJa1 revealed a limiting step in the stabilization of cytoplasmic AID by the HSP90 molecular chaperoning pathway (Chapter 3). This may influence the optimal levels of AID required for antibody diversification. Finally, we investigated whether AID stability is only linked to its subcellular localization or whether there is a direct contribution of intrinsic protein motifs to AID stability, in the context of the regulation of antibody diversification (Chapter 4).

CHAPTER 2: REGULATION OF ACTIVATION-INDUCED DEAMINASE AND ANTIBODY GENE DIVERSIFICATION BY HSP90

Alexandre Orthwein, Anne-Marie Patenaude, El Bachir Affar, Alain Lamarre, Jason C. Young

and Javier M. Di Noia

This article has been published in the *Journal of Experimental Medicine* (2010), 207(12):2751-65

2.1. Authors contribution

Alexandre Orthwein designed and performed most of the experiments. Anne-Marie Patenaude performed the immunofluorescence experiments. Dr Bachir El Affar contributed to the AID-FLAG/HA purification and provided with useful advice. Dr Alain Lamarre provided patients samples for the purification of human B cells and useful advice. Dr Jason C. Young contributed in the conception of the project, the design of experiments and provided useful advice. Dr Javier M. Di Noia conceived the project and wrote the paper. All authors discussed and interpreted the data and contributed to the final manuscript.

2.2. Abstract

Activation-induced deaminase (AID) is the mutator enzyme that initiates somatic hypermutation and isotype switching of the antibody genes in B lymphocytes. Undesired byproducts of AID function are oncogenic mutations. AID expression levels seem to correlate with the extent of its physiological and pathological functions. In this study, we identify AID as a novel HSP90 (heat shock protein 90 kD) client. We find that cytoplasmic AID is in a dynamic equilibrium regulated by HSP90. HSP90 stabilizes cytoplasmic AID, as specific HSP90 inhibition leads to cytoplasmic polyubiquitination and proteasomal degradation of AID. Consequently, HSP90 inhibition results in a proportional reduction in antibody gene diversification and off-target mutation. This evolutionarily conserved regulatory mechanism determines the functional steady-state levels of AID in normal B cells and B cell lymphoma lines. Thus, HSP90 assists AID-mediated antibody diversification by stabilizing AID. HSP90 inhibition provides the first pharmacological means to down-regulate AID expression and activity, which could be relevant for therapy of some lymphomas and leukemias.

2.3. Introduction

Antibody genes are first rearranged by V(D)J recombination during B lymphocyte development and then further diversified in the periphery after encountering cognate Ag. The latter is achieved by the mechanism of somatic hypermutation (SHM), which introduces random mutations over the exon that encodes the antibody variable region. Coupled to phenotypic selection during the GC reaction, SHM results in the overall maturation of the antibody response. SHM is initiated by activation-induced deaminase (AID), which deaminates dC to dU in the Ig loci. Processing of the dU by specific DNA repair enzymes produces the full spectrum of SHM (Di Noia and Neuberger, 2007; Peled *et al.*, 2008). In addition, AID also targets the DNA immediately preceding the constant exons that encode for the different antibody isotypes in the IgH locus. Processing of the dU in these switch regions leads to the DNA breaks necessary for class switch recombination (CSR; Stavnezer *et al.*, 2008).

AID being a mutator enzyme sufficient to cause cancer in transgenic models (Okazaki *et al.*, 2003; Pasqualucci *et al.*, 2008), there has been a well-deserved emphasis in studying its regulation. Gene expression regulation is an important step during normal B cell development, with AID being mostly restricted to GC B cells (Muramatsu *et al.*, 1999; Crouch *et al.*, 2007). However, AID can normally be expressed outside of the B cell compartment, the exact physiological relevance of which is still unclear, although it may influence the expression of many genes by affecting DNA methylation (Morgan *et al.*, 2004; Macduff *et al.*, 2009; Pauklin *et al.*, 2009; Bhutani *et al.*, 2010; Popp *et al.*, 2010). Importantly, there is ample evidence that AID is expressed in a variety of human lymphomas (Greeve *et al.*, 2003; Pasqualucci *et al.*, 2004) and leukemias (Albesiano *et al.*, 2003; Feldhahn *et al.*, 2007; Klemm *et al.*, 2009; Palacios *et al.*, 2010). In fact, AID plays a role in malignant transformation by initiating DNA double-strand breaks at various non-Ig loci, most prominently c-Myc, which in murine experimental plasmacytoma, and therefore most likely also in human Burkitt's lymphoma, leads to the hallmark oncogenic c-Myc–IgH chromosomal translocation (Ramiro *et al.*, 2004, 2006; Robbiani *et al.*, 2008,2009). A role for AID in the etiology of diffuse large B cell lymphoma is also very likely (Pasqualucci *et al.*, 2001, 2004, 2008). In chronic myeloid leukemia (CML), AID mutates the BCR-ABL1 oncogene, leading to resistance to the tyrosine

kinase inhibitor imatinib, the main therapeutic drug (Klemm *et al.*, 2009). Moreover, AID expression in nonlymphoid tumors has also been shown (Endo *et al.*, 2008). Therefore, it is important to understand AID posttranslational regulation, which may differ between normal and transformed cells and have important and varied implications in the several cell types that can express AID.

Multiple mechanisms seem to contribute to restrain AID protein. Subcellular localization is an important step in regulating AID that also impinges on its stability because AID has a significantly shorter half-life in the nucleus than in the cytoplasm (Aoufouchi *et al.*, 2008). In steady-state, the bulk of AID is cytoplasmic as a result of the integration of three mechanisms: nuclear import (Patenaude *et al.*, 2009), nuclear export (Ito *et al.*, 2004; McBride *et al.*, 2004), and cytoplasmic retention (Patenaude *et al.*, 2009). However, it is unknown whether AID stability is regulated in the cytoplasm. Several studies, including the analysis of AID-haploinsufficient mice (Sernández *et al.*, 2008;Takizawa *et al.*, 2008) or mice with altered AID levels resulting from manipulating microRNA regulation (de Yébenes *et al.*, 2008; Dorsett *et al.*, 2008; Teng *et al.*, 2008) or enforcing transgenic overexpression (Robbiani *et al.*, 2009), have suggested that AID protein levels are limiting for and correlate with the efficiency of antibody diversification but also B cell lymphomagenesis. Therefore, any mechanism impinging on the overall AID steady-state levels is important for balancing an efficient humoral immune response with the associated risk of B cell transformation.

We report the physical and functional interaction of AID with the HSP90 (heat shock protein 90 kD) molecular chaperone pathway. HSP90 is thought to be more selective of its range of substrates than other chaperones, playing a prominent role in the structural stabilization and functional modulation of many of its client proteins, rather than in their initial folding (Pratt and Toft, 2003; Whitesell and Lindquist, 2005; Pearl and Prodromou, 2006; Picard, 2006; Wandinger *et al.*, 2008). Indeed, the interaction with HSP90 prevents proteasomal degradation of AID in the cytoplasm, thereby determining the steady-state levels of functional AID.

2.4. Results

2.4.1. AID specifically interacts with HSP90

Immunopurification of AID-Flag/HA from cell extracts of Ramos B cells produced a complex but reproducible pattern of copurifying proteins (Fig. 2.1 A). Of note, we used a stable cell line expressing only 2.5-fold the amount of endogenous AID (Fig. S2.1 A). After identification of the associated proteins by mass spectrometry, we noticed the presence of several members of the HSP90 molecular chaperone pathway (Whitesell and Lindquist, 2005), including the two major isoforms of HSP90 (α and β), the HSP90 cochaperone AHA-1, HSP70/HSC70, and one HSP40 cochaperone (DnaJa1), as well as several proteasome subunits (Table 2.1). The HSP90, HSP70, and HSP40 proteins are known to cooperate in a multichaperone system (Picard, 2006; Wandinger *et al.*, 2008). Given the importance of HSP90 in regulating the function of many signal transduction and nucleocytoplasmic shuttling proteins, we decided to further explore this interaction. We confirmed the binding of AID to endogenous HSP90 by coimmunoprecipitation of AID-GFP from stably expressing Ramos cells (Fig. 2.1 B). We also confirmed that AID coimmunoprecipitated similarly with tagged versions of HSP90-α and HSP90-β (Fig. 2.1 C). Both isoforms are constitutively expressed in the B cell lines we used, although HSP90-β is the predominant form in resting primary mouse B cells, with HSP90-α increasing after cytokine activation (Fig. S2.1, B and C). These results are in keeping with various studies indicating that mitogenic and cytokine stimuli up-regulate HSP90-α, whereas HSP90-β is constitutively expressed (Hansen *et al.*, 1991; Metz *et al.*, 1996; Csermely *et al.*, 1998;Sreedhar *et al.*, 2004). HSP90-α and HSP90-β share ~90% similarity, and although they may have some nonoverlapping roles, for most functions, they are largely equivalent (Csermely *et al.*, 1998; Sreedhar *et al.*, 2004).

We then characterized the interaction between HSP90 and AID. Notably, the AID paralogue proteins APOBEC1, APOBEC2 (A2), and APOBEC3G, which share ~50–60% similarity with AID (Conticello *et al.*, 2005), did not coimmunoprecipitate with Myc–HSP90-β (Fig. 2.1 D). This is consistent with a recent study showing that zebra fish A2 interacts with the

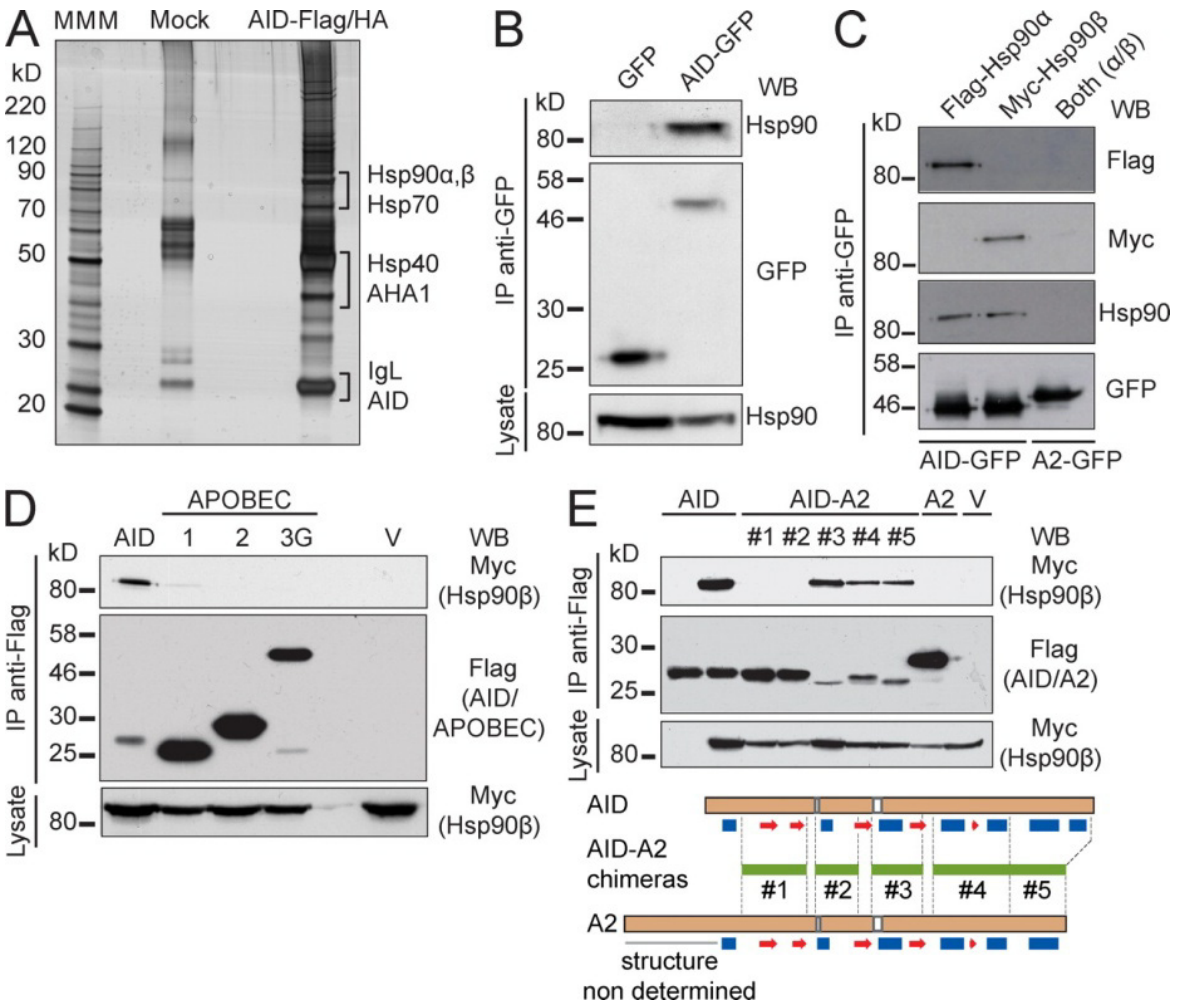

Figure 2.1. AID interacts with HSP90. *(A) Ramos B cells stably expressing AID-Flag/HA were subjected to consecutive immunoprecipitation with anti-Flag and anti-HA. Precipitated material was eluted with the specific peptides and separated by SDS-PAGE. Proteins were identified by mass spectrometry of tryptic peptides. The proteins relevant to this work are indicated next to the bands from where they were identified. One of two independent experiments is shown. MMM, molecular mass marker. (B) GFP and AID-GFP were immunoprecipitated from extracts of stably expressing Ramos cells and analyzed by Western blot (WB) to detect coimmunoprecipitated endogenous HSP90. One of three independent experiments is shown. (C) APOBEC2 (A2)-GFP and AID-GFP were immunoprecipitated with anti-GFP from transiently expressing HEK293T cells cotransfected with Flag–HSP90-α and/or Myc–HSP90-β. Immunoprecipitates (IP) were probed with anti-Flag and anti-Myc in Western*

blots. The filters were then probed with anti-HSP90, which recognizes both isoforms, to verify that the overall HSP90 level was similar after transfection. Anti-GFP confirmed similar immunoprecipitation of the bait. One of two independent experiments is shown. (D) Lysates from HEK293T cells cotransfected with Myc–HSP90-β and Flag-tagged versions of AID or the indicated APOBECs or vector alone (V) were immunoprecipitated using anti-Flag and analyzed by Western blot with anti-Myc to verify the presence of HSP90-β and anti-Flag to confirm the immunoprecipitation of the baits. One of four independent experiments is shown. (E) Lysates from HEK293T cells cotransfected with Myc–HSP90-β and either vector only (V) or Flag-tagged AID, A2, or AID-A2 chimeras (#1–5, described below in schematic form) were immunoprecipitated with anti-Flag. Immunoprecipitates were analyzed by Western blot using anti-Myc and anti-Flag antibodies. One of three independent experiments is shown. In schematics, horizontal green lines between dashed lines identify the fragments of AID replaced by the homologous region of A2 in each construct. Based on experimental A2 (Prochnow et al., 2007) and predicted AID (Patenaude et al., 2009) secondary structures, blue rectangles indicate α helixes, and red arrows indicate β sheets. Where indicated, aliquots (5%) of the whole cell lysates were probed to control for expression.

Table 2.1. Proteins copurifying with AID-Flag-HA from Ramos B cells identified by mass spectrometry

HUGO name	Mascot Score[a]	Coverage (%)	Description
*HSP90AB1**	2178	44	Heat shock 90 kDa protein 1, beta
	300	8	
*HSP90AA1**	1668	35	Heat shock 90 kDa protein 1, alpha
	151	6	
HSPA8	1338	39	Heat shock 70 kDa protein 8 isoform 1
HSPA6	327	8	Heat shock 70 kDa protein B
*AHSA1**	81	3	AHA1, Activator of heat shock 90kDa
	27	9	protein ATPase homolog 1
DNAJA1	212	26	HSP40 homolog, subfamily A, member 1
PSMD2	242	14	Proteasome 26S non-ATPase subunit 2
PSMD1	105	2	Proteasome 26S non-ATPase subunit 1
*PSMD6**	105	5	Proteasome 26S non-ATPase subunit 6
	46	6	
PSMC2	75	3	Proteasome 26S ATPase subunit 2

* Proteins identified in two independent experiments.

A threshold Mascot score of 50 was used as cut-off, indicating a 95% confidence of being a true identification. For AHSA1 in the second experiment the MS profile was manually examined to confirm the reliability of the observation.

chaperone Unc45b but not with HSP90-α (Etard *et al.*, 2010). The region of AID interacting with HSP90-β could be mapped to the N-terminal half of the molecule by using AID-A2 chimeric proteins (Fig. 2.1 E). An AID mutant showing impaired oligomerization (Patenaude *et al.*, 2009) was still recognized by HSP90 (Fig. S2.1D). Phosphorylation can modulate client binding to HSP90 (Dickey *et al.*, 2007), but the known protein kinase A (PKA) sites within the N-terminal region of AID, Thr27, and Ser38, were not essential for the interaction (Fig. S2.1 D). These results suggest that HSP90 specifically binds to AID by its N-terminal region in an oligomerization- and phosphorylation-independent fashion.

2.4.2. HSP90 maintains the steady-state level of AID

The chaperone activity of HSP90 depends on an ATP hydrolysis cycle, which is inhibited by geldanamycin (GA) and its derivatives, like 17-allylamino-17-demethoxygeldanamycin (17-AAG; Prodromou *et al.*, 1997; Stebbins *et al.*, 1997; Panaretou *et al.*, 1998; Young and Hartl, 2000). Treating Ramos cells with GA prevented the interaction of AID-GFP with HSP90, as indicated by the lack of coimmunoprecipitation (Fig. 2.2 A). More importantly, treatment of human, chicken, and mouse B cell lymphoma lines with GA caused a clear reduction in the levels of endogenous AID at 12 and 24 h. We probed for the known HSP90 client kinase LCK, which was also reduced, as positive control (Giannini and Bijlmakers, 2004). Other enzymes involved in antibody diversification, including UNG (uracil-DNA ***N***-glycosylase) and MSH6, were not sensitive to HSP90 inhibition (Fig. 2.2 B). Finally, endogenous AID in stimulated human primary B cells from multiple donors was also sensitive to HSP90 inhibition (Fig. 2.2 C), confirming that the functional interaction between AID and HSP90 is physiologically relevant.

To use a more sensitive assay to monitor AID decay at shorter times and to be able to compare AID variants, we established stable Ramos transfectants expressing various AID-GFP constructs from a heterologous promoter. The levels of AID-GFP could thus be monitored over time and accurately quantified by flow cytometry. We confirmed that AID-GFP but not GFP was destabilized upon HSP90 inhibition in these cell lines with kinetics consistent to that

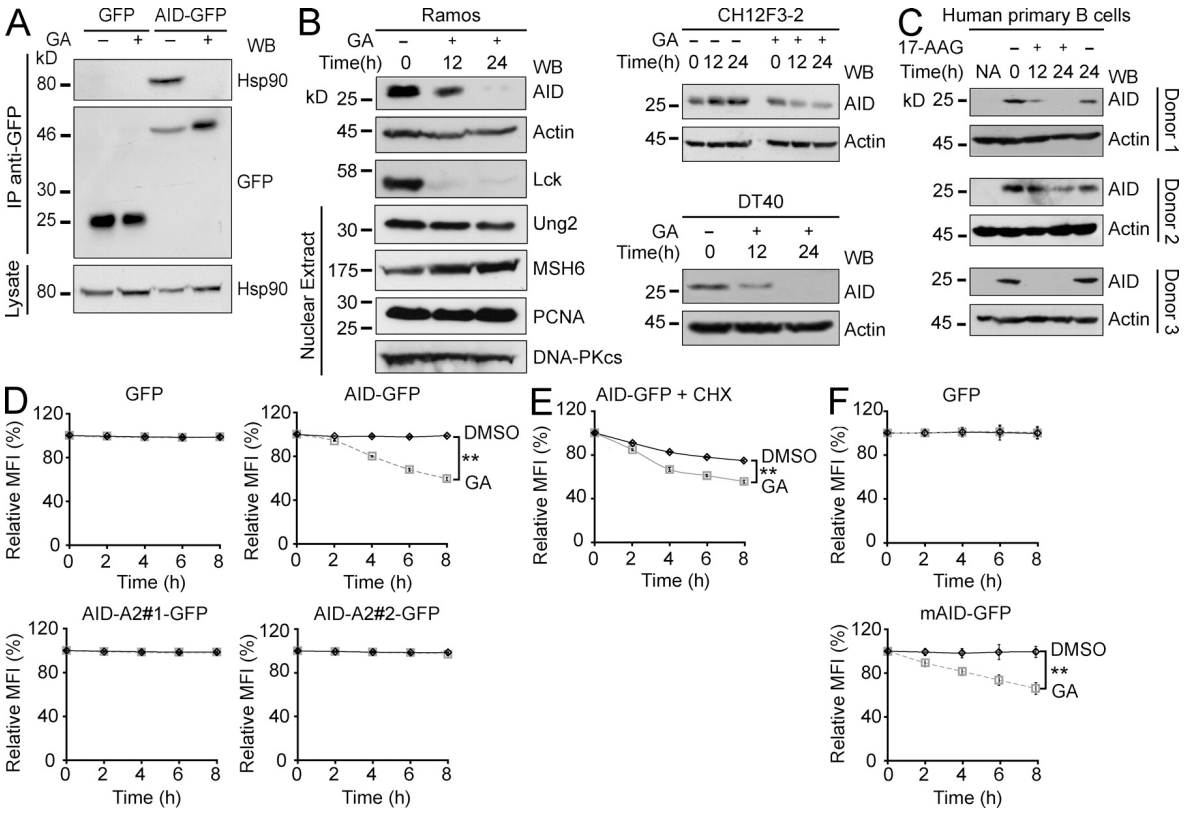

Figure 2.2. HSP90 actively maintains the steady-state levels of AID. *(A) Ramos cells stably expressing AID-GFP or GFP alone were treated with 2 μM GA (+) or DMSO (−) for 2 h. Anti-GFP immunoprecipitates (IP) were fractionated on SDS-PAGE, and blots were probed with anti-HSP90 and anti-GFP. Aliquots (5%) of the whole cell lysates were probed to control for HSP90 expression. One of two independent experiments is shown. (B) Human Ramos, mouse CH12F3-2 (pretreated for 16 h with IL-4, TGF-β1, and anti-CD40 to induce AID expression), and chicken DT40 B cell lines were treated with 2 μM GA (+) or DMSO (–) and harvested at the indicated time points after GA. The expression level of the indicated proteins was analyzed by Western blot (WB) in total or nuclear (where indicated) extracts. Identical effect was observed with 17-AAG in all cell lines (not depicted). Representative panels from one of two or three independent experiments (depending on the antibody) are shown. (C) Resting B cells purified from blood of three donors were activated with IL-4 and anti-CD40 and 4 d later treated and analyzed as in B except that the HSP90 inhibitor 17-AAG (+) was used instead of GA. (D) Ramos cells stably expressing GFP, AID-GFP, or chimeras AID-A2 #1 or #2 were treated in triplicate with 2 μM GA or DMSO. The GFP mean fluorescence intensity (MFI) was*

*monitored by flow cytometry and normalized to t_0 = 100%. MFI ± SD is plotted over time. One of three independent experiments is shown (**, P < 0.01). (E) AID-GFP was monitored as in D except that Ramos cells were pretreated with 100 ng/ml CHX for 30 min before HSP90 inhibition. One of five independent experiments is shown (**, P < 0.01). (F) Purified naive B cells from Aicda$^{-/-}$ mice were activated and retrovirally transduced with mouse AID-GFP or GFP control. Cells were analyzed as in D 2 d after transduction. One of three independent experiments is shown (**, P < 0.01)*

observed for endogenous AID (Fig. 2.2 D). This indicated a direct action on AID protein rather than on ***Aicda*** transcription, which was confirmed by Northern blot of ***Aicda*** in Ramos cells (unpublished data). As would be expected, the AID-A2 chimeras that did not interact with HSP90 were insensitive to GA treatment (Fig. 2.2 D). Treatments inhibiting or exacerbating PKA activity had no effect on the sensitivity of AID-GFP to GA, further suggesting that these two pathways are not connected (Fig. S2.2). We then measured the decay kinetics of AID-GFP after pretreating the cells with cycloheximide (CHX) so as to follow the pool of AID that had already been synthesized and not the nascent AID that might be more sensitive to folding requirements. CHX caused the expected decay of AID-GFP (compare control DMSO-treated AID-GFP levels in Fig. 2.2, D vs. E), which was clearly accelerated by GA (Fig. 2.2 E), indicating a role for HSP90 in stabilizing fully synthesized AID. We confirmed that both mouse and human AID-GFP were similarly sensitive to HSP90 inhibition when expressed in AID-deficient mouse primary splenic B cells (Fig. 2.2 F and not depicted), thus ruling out any effect of the transformed cell environment of Ramos on our observations. We conclude that functional HSP90 is necessary to stabilize and maintain the steady-state levels of AID in vivo in primary as well as in transformed cells.

2.4.3. HSP90 protects cytoplasmic AID from being degraded

Binding to HSP90 can regulate protein subcellular localization (DeFranco, 1999;Galigniana *et al.*, 2004). Indeed, our results could be explained by increased AID nuclear import after HSP90 inhibition and therefore AID destabilization in the nucleus (Aoufouchi *et al.*, 2008). However, we did not observe any changes in AID localization after HSP90 inhibition, even when combined with a proteasome inhibitor to prevent degradation of nuclear AID (Fig. S2.3). So, we compared the effects on AID-GFP of inhibiting HSP90 versus inhibiting nuclear export with leptomycin B (LMB), which enriches AID-GFP in the nucleus (Ito *et al.*, 2004; McBride *et al.*, 2004), in the stable Ramos transfectants. The kinetics of AID-GFP decay after GA or LMB treatment were different (Fig. 2.3 A). Combined GA and LMB treatment showed an apparently additive effect (Fig. 2.3 A). Similar results were obtained using DT40 and HeLa cells stably expressing AID-GFP (Fig. S2.4). The lack of detectable nuclear translocation of AID after HSP90 inhibition, together with the different decay kinetics after GA and LMB,

raised the possibility that AID degradation after each of these treatments happened in different compartments and therefore would involve different pathways. To test this, we used Ramos cells expressing GFP-AID because the N-terminal GFP fusion blocks nuclear import of AID (Patenaude *et al.*, 2009) but not its binding to HSP90 (Fig. S2.1E). Consistently, with its exclusively cytoplasmic localization, GFP-AID did not respond to LMB, but it was still sensitive to GA (Fig. 2.3 B). HSP90 clients are in dynamic equilibrium with proteasomal degradation (Pearl and Prodromou, 2006). Indeed, the proteasome inhibitor MG132 prevented the HSP90 inhibition–induced degradation of AID-GFP as well as of endogenous AID in Ramos and DT40 cells (Fig. 2.3, C and D; and Fig. S2.4 A). We obtained identical results using lactacystin, another proteasome inhibitor (unpublished data). A reproducible ~3.5-fold increase in AID polyubiquitylation was observed in Ramos and primary mouse B cells after combined HSP90 and proteasome inhibition versus inhibiting only the proteasome (Fig. 2.3 E). This was not particular to B cells because it was also true for AID-GFP in stably transfected HeLa cells (unpublished data). These experiments show that HSP90 stabilizes cytoplasmic AID by protecting it from proteasomal degradation.

The E3 Ub ligase CHIP (C terminus of HSC70-interacting protein) is physically associated with HSP90 and triages many HSP90 clients (McDonough and Patterson, 2003). Of note, CHIP is constitutively expressed in Ramos and induced upon activation in primary mouse B cells (Fig. S2.1, B and C). Furthermore, CHIP coimmunoprecipitated with AID-GFP from extracts of stably transfected HeLa cells (Fig. 2.4 A). The interaction was only apparent when the cells were pretreated with a proteasome inhibitor, which allows the accumulation of this rapid turn over interaction (Li *et al.*, 2004). We reasoned that if HSP90 was normally stabilizing AID in B cells, the overexpression of CHIP could reduce AID levels by shifting the equilibrium of the pathway from stabilization to degradation. Indeed, all subclones from three independent transfectants of Ramos B cells overexpressing Myc-CHIP showed a significantly reduced steady-state level of AID (Fig. 2.4, B and C) but not of ATM (ataxia telangiectasia mutated), which is not an HSP90 client. Altogether, these results indicate that cytoplasmic AID

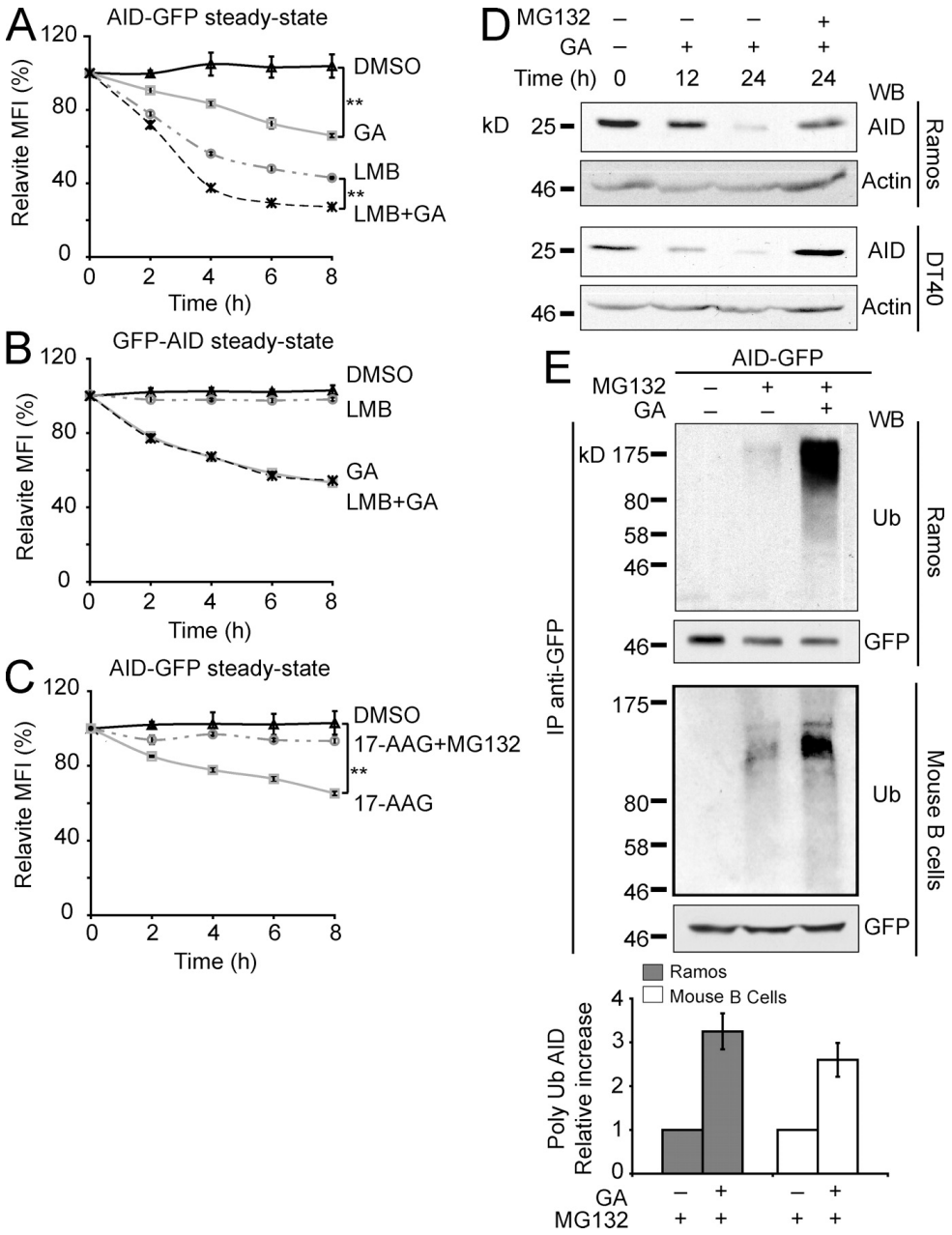

Figure 2.3. Cytoplasmic ubiquitination and proteasomal degradation of AID after HSP90 inhibition. *(A) Ramos cells stably expressing AID-GFP were treated in triplicate with DMSO, 2 μM GA, and/or 50 ng/ml LMB, and the GFP signal was monitored over time by flow cytometry. The MFI normalized to t_0 = 100% ± SD is plotted for each treatment (**, P < 0.01). One of five independent experiments is shown. (B) Ramos cells stably expressing GFP-AID, which is completely impaired for nuclear import (Patenaude et al., 2009), were analyzed as in*

*A. One of three independent experiments is shown. (C) Ramos cells stably expressing AID-GFP were pretreated or not for 30 min with 10 μM MG132 before adding DMSO or 2 μM 17-AAG and analyzed as in A (**, P < 0.01). One of five independent experiments is shown. (D) Human Ramos and chicken DT40 B cell lines were treated with 2 μM GA. Where indicated, 10 μM MG132 was added only during the last 12 h of incubation to avoid excessive cell death. Cells were harvested at different time points, lysed, and analyzed by Western blot (WB). One of two independent experiments is shown for each cell line. (E) Ramos B cells stably expressing human AID-GFP or primary mouse B cells transduced with mouse AID-GFP were pretreated with 10 μM MG132 for 30 min before addition or not of 2 μM GA for 5 h. Anti-GFP immunoprecipitates (IP) were analyzed by Western blot using anti-ubiquitin (Ub) and anti-GFP. Polyubiquitinated AID was quantified by densitometry, and the relative means ± SD were plotted for three independent experiments for each cell type.*

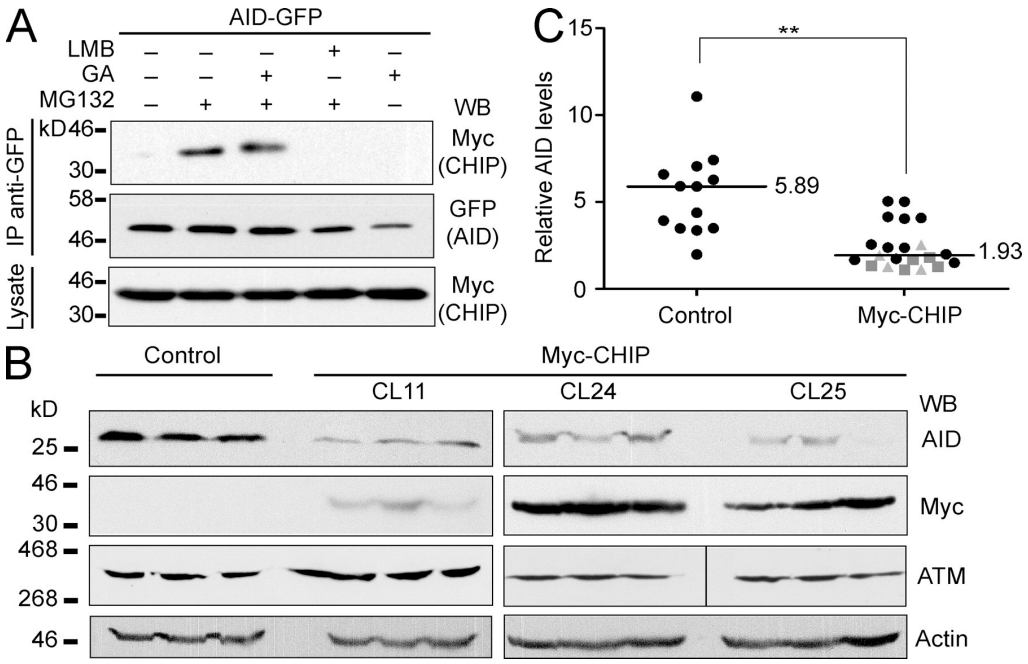

Figure 2.4. The HSP90-associated E3 ubiquitin ligase CHIP can destabilize AID. *(A) HeLa cells stably expressing AID-GFP were transfected with Myc-CHIP and 48 h later treated for 5 h with DMSO (–), 2 μM GA, 50 ng/ml LMB, and/or 10 μM MG132 (30 -min pretreatment) in the indicated combinations. Anti-GFP immunoprecipitates (IP) were analyzed by Western blot (WB) with anti-GFP and anti-Myc. Aliquots (5%) of the total cell lysates were used to control for Myc-CHIP expression. One of two independent experiments is shown. (B) Endogenous AID was analyzed by Western blot in single cell subclones from untransfected control or three independent Myc-CHIP Ramos transfectants (CL11, CL24, and CL25) after expansion. ATM was used as an HSP90-independent control, antiactin as loading control, and anti-Myc to confirm the expression of CHIP. Three representative subclones from each transfectant are shown. The vertical black line indicates that intervening lanes have been spliced out. (C) AID protein levels in all control or Myc-CHIP Ramos subclones (distinguished by different symbols) were estimated from nonsaturated Western blots. The signal was normalized to each corresponding actin signal obtained from equivalent exposures and plotted. Median values are indicated (**, $P < 0.01$).*

requires constant stabilization by HSP90 and that altering the balance of this reaction, either by inhibiting HSP90 or favoring the degradative side of this pathway through CHIP overexpression, leads to greatly diminished AID protein levels through proteasomal degradation in the cytoplasm.

2.4.4. Inhibition of HSP90 results in reduced antibody diversification

We first used the chicken B cell lymphoma line DT40 to monitor AID-dependent antibody diversification by gene conversion. The frequency of Ig gene conversion is estimated by using a DT40 line with a frameshift mutation in the *IgV*λ gene that prevents surface IgM expression. Some gene conversion events correct this frameshift, restoring IgM expression. The median percentage of IgM^+ cells generated during expansion of several initially IgM^- populations is proportional to the rate of Ig gene conversion (Arakawa *et al.*, 2002). The problem is that HSP90 is essential for eukaryotic cells (Borkovich *et al.*, 1989;Cutforth and Rubin, 1994), which precludes its genetic ablation or complete inhibition. However, we observed that AID decay after HSP90 inhibition was dose dependent (Fig. S2.4 C for GA and not depicted for 17-AAG). We used 17-AAG for these assays because we found it to be less toxic than GA for lymphocytes (unpublished data). Low doses of 17-AAG had minimal impact on DT40 cell growth but still caused a robust decrease in AID protein levels (Fig. 2.5 A). This partial reduction in AID levels was proportional to a reduction in Ig gene conversion (Fig. 2.5 A). In similar experiments using a DT40 line that diversifies the IgVλ by SHM (Arakawa *et al.*, 2004), we could also confirm a reduction in SHM (this time by monitoring the appearance of sIgM-loss cells from originally $sIgM^+$populations but also by direct IgVλ sequencing) that was proportional to the decrease in AID protein levels (Fig. 2.5, B and C). We then analyzed the effect of HSP90 inhibition on CSR by using the mouse CH12F3-2 cell line, which efficiently switches from IgM to IgA after cytokine stimulation (Nakamura *et al.*, 1996). Because these assays take place over a few days, we used CFSE staining to monitor cell proliferation. Thus, we could compare the efficiency of switching between cells that have undergone the same number of cell divisions, accounting for any cell growth defect that continuous exposure to 17-

AAG could cause. There was a clear and dose-dependent reduction in CSR caused by 17-AAG, overall and for each cell division tested (Fig. 2.5 D). Alternatively, we performed a 12-h treatment with higher doses of 17-AAG, after which the drug was removed (Fig. 2.6 A). A drastic reduction in CSR to IgA was observed when the CH12F3-2 cells were treated with 17-AAG at day 1 after stimulation, coincident with the time when the peak of AID protein was observed (Fig. 2.6, B and C). As would be expected, 17-AAG treatment at day 2 had a less but still statistically significant effect on CSR. Importantly, we obtained identical results in switching assays using normal mouse splenic B cells (Fig. 2.6 D). A drastic decrease of CSR to IgG1 was observed when cells were treated with 17-AAG at day 1 after stimulation. This higher dose of 17-AAG delayed growth of primary B cells, but the effect on CSR was nevertheless very clear when comparing the efficiency of switching per cell division. Again, treating the cells at day 2 after stimulation caused a smaller but statistically significant effect. As expected, treating the cells at day 3 had no effect on the efficiency of CSR measured at day 4 (unpublished data). We conclude that cytoplasmic AID degradation after HSP90 inhibition has a direct and proportional effect on all antibody diversification mechanisms.

2.4.5. HSP90 inhibition prevents off-target mutation by AID

We assayed AID off-target mutation using the recently described role of AID in generating resistance of the oncogenic kinase BCR-ABL1 to the drug imatinib in CML cells (Klemm *et al.*, 2009). We transduced the BCR-ABL1$^+$ K562 cell line with AID-ires-GFP or GFP control retroviruses and, for each construct, prepared mixed populations with uninfected (GFP$^-$) cells at a defined ratio. Mutations in *BCR-ABL1* that confer resistance are selected by culturing the cells in the presence of imatinib. This is readily observed by flow cytometry as an increased ratio of GFP$^+$/GFP$^-$ cells over time. Indeed, we observed a higher proportion of GFP$^+$ cells within 2–3 wk only in AID-expressing cells that were growing in the presence of imatinib (Fig. 2.7 A). This was AID dependent as it was not observed in GFP control cultures, and the imatinib-resistant cells appeared earlier in cultures expressing higher levels of AID (Fig. 2.7, A and B). More relevant to our purpose, the AID-dependent change in the

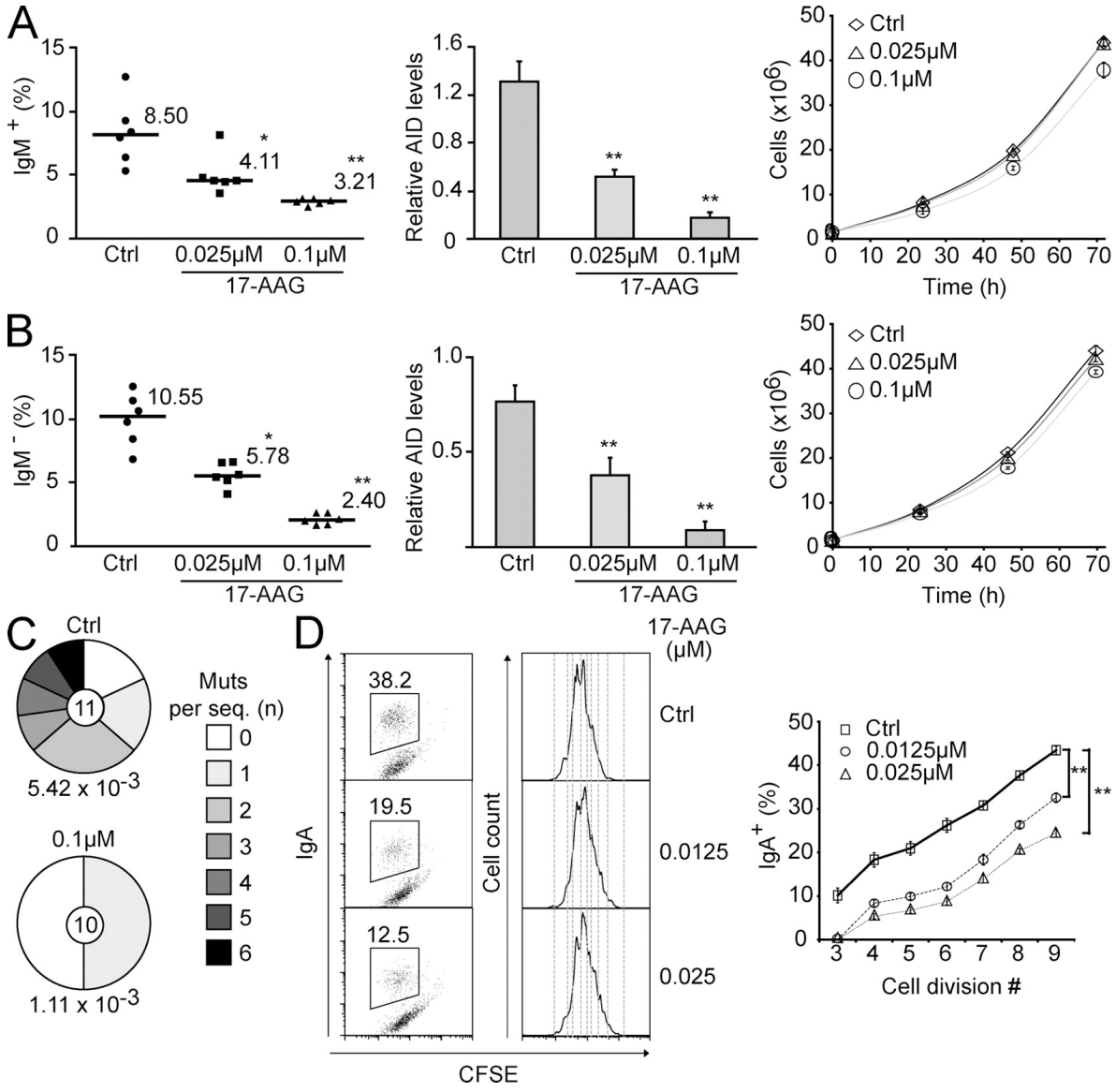

Figure 2.5. Reduced antibody diversification in chicken and mouse B cells chronically treated with HSP90 inhibitors. *(A) The rate of Ig gene conversion in DT40 cells was estimated from the proportion of sIgM-gain cells arising from sIgM$^-$ populations after 3 wk of expansion in the presence of DMSO (Ctrl) or two different concentrations of 17-AAG. The proportion of sIgM$^+$ cells for each population and the median values are indicated (left). The level of AID protein was quantified by densitometry from nonsaturated Western blots for each population at the end of the experiment and normalized to actin levels. Mean ± SD values for all populations*

*grown in each condition are plotted (middle). The effect of 17-AAG on DT40 growth was monitored by calculating the total number of cells in a culture originating from 10^5 cells (right). Mean ± SD of triplicate cultures are plotted over time. (B) SHM was monitored in analogous experiments to A except that a $sIgM^+$ ψV^- AID^R DT40 cell line, which cannot undergo gene conversion and instead uses SHM to diversify the Ig genes, was used. IgM-loss cells arise as a consequence of SHM with a certain frequency, and so the proportion of sIgM-loss cells arising over time provides an estimate of SHM rate (Arakawa et al., 2004). (C) DNA was extracted from control or 0.1 μM 17-AAG–treated unsorted cultures from B after equal expansion. The IgVλ was PCR amplified and sequenced. The fraction of sequences containing the indicated number of mutations is plotted in the pie chart with the number of sequences analyzed indicated in the center. The calculated mutation frequency (mutations/base pair) is indicated under each pie chart. (D) CH12F3-2 mouse B cells stimulated with IL-4, TGF-β1, and agonist anti-CD40 were cultured with DMSO (Ctrl) or the indicated concentrations of 17-AAG. The cells were stained with CFSE before activation to follow cell divisions. Representative plots of the proportion of IgA^+ cells in each population after 3 d (left) and CFSE profiles (middle) are shown. For each cell division, the proportion of $sIgA^+$ cells was calculated, and the results from four independent experiments are summarized in the plot as the mean ± SD values (right). In all panels: *, $P < 0.05$; **, $P < 0.01$.*

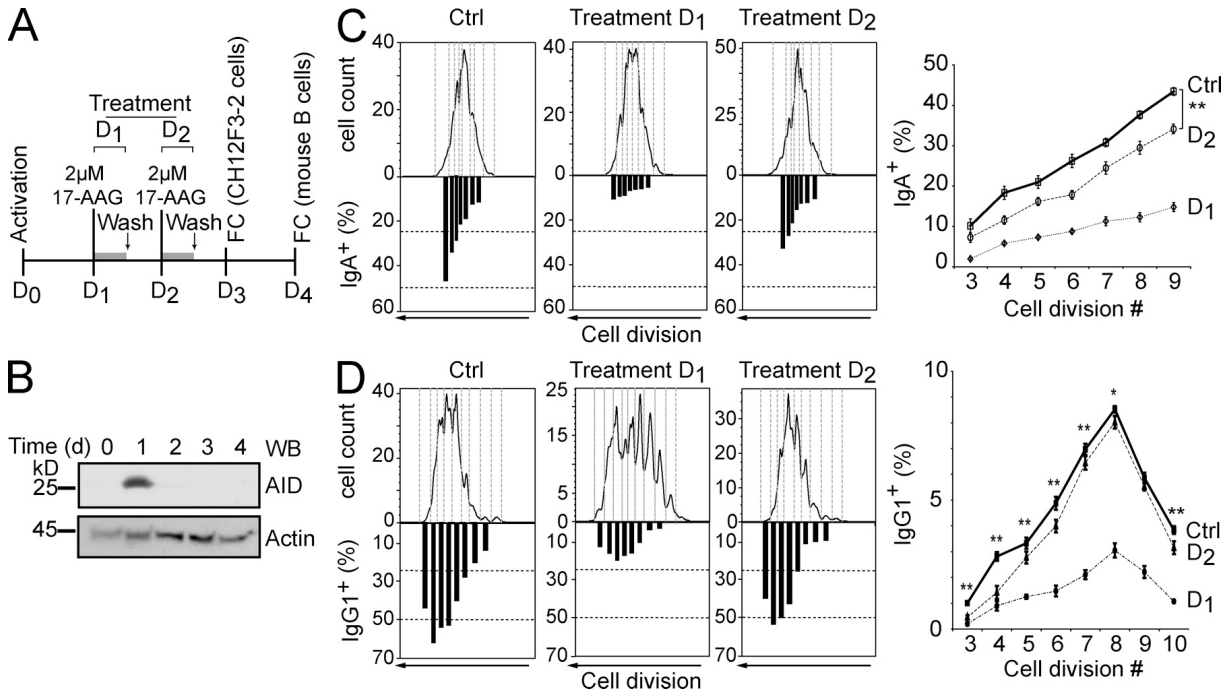

Figure 2.6. Acute inhibition of HSP90 impairs CSR in mouse B cells. *(A) Scheme of the experimental strategy fort treatment of CH12F3-2 B cells or primary naive mouse splenic B cells. D, day; FC, flow cytometry. (B) Kinetics of AID protein expression in CH12F3-2 mouse B cells determined by Western blot (WB) at different times after stimulation. One of two independent experiments is shown. (C) CH12F3-2 B cells were stained with CFSE and stimulated with IL-4, TGF-β1, and anti-CD40 to switch to IgA. Either at day 1 or 2 after activation, the cells were treated for 12 h with 2 μM 17-AAG and then returned to normal medium. The proportion of sIgA$^+$ cells per cell division determined by flow cytometry is plotted under each cell division in the corresponding CFSE plot for a representative experiment (left). The mean proportions of sIgA$^+$ cells for each cell division ± SD from four independent experiments are plotted (right; **, P < 0.01). (D) Purified mouse naive splenic B cells were loaded with CFSE and stimulated with IL-4 and LPS to induce switching to IgG1. Either at day 1 or 2 after activation, the cells were treated with 17-AAG and then returned to normal medium. The proportion of sIgG1$^+$ cells per cell division was determined and presented as in C. Data from one representative mouse are shown (left), and pooled data from five mice are*

plotted (right). To be able to compare all the mice accounting for the inter assay variability, data points were normalized with the percentage of IgG1$^+$ cells in cell division 3 of the control set as 1 (, $P < 0.05$; **, $P < 0.01$). Ctrl, control.*

GFP^+/GFP^- ratio was fully prevented by a very low dose of 17-AAG (Fig. 2.7 A). Treatment with this dose of 17-AAG visibly reduced AID but not BCR-ABL1 protein levels by day 7 (Fig. 2.7 C). We confirmed that 17-AAG prevented the AID-mediated increase in imatinib IC_{50} (Fig. 2.7 D). We also directly checked for mutations by sequencing *BCR-ABL1*. An increase in point mutations (many of them known to induce imatinib resistance; Klemm *et al.*, 2009) could be detected in AID-expressing K562 cells growing in imatinib. In contrast, the mutation level in AID-expressing cultures that were jointly treated with imatinib and 17-AAG was indistinguishable from the GFP control (Fig. 2.7 E and Table 2.2).

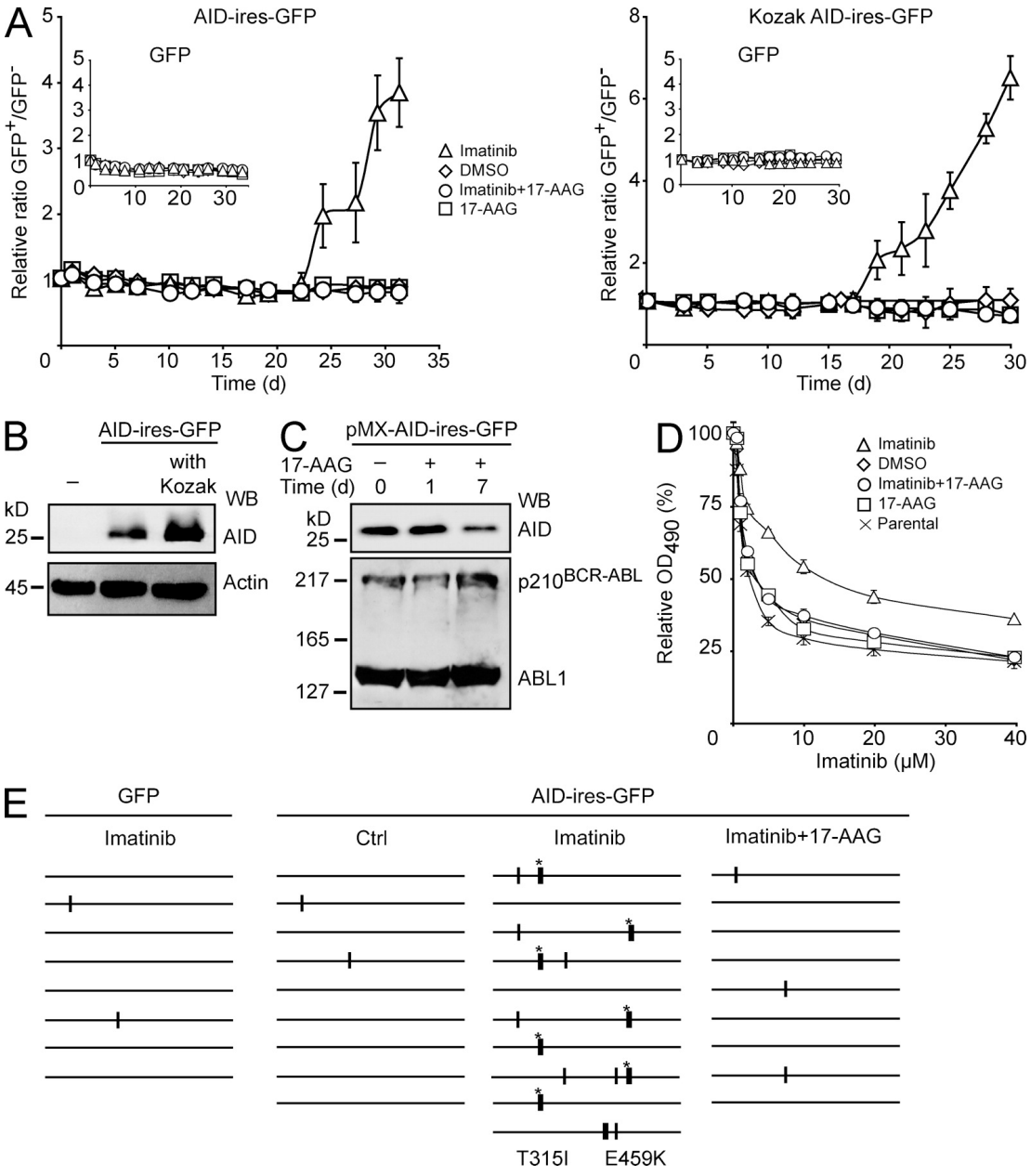

Figure 2.7. HSP90 inhibition reduces AID off-target mutations. *(A) BCR-ABL1$^+$ K562 cells were transduced with GFP control (insets) or AID-ires-GFP retroviral vectors. Mixed populations of transduced (GFP$^+$) and uninfected (GFP$^-$) cells were cultured in the presence of DMSO, 2 μM imatinib, 2 μM imatinib plus 0.1 μM 17-AAG, or 0.1 μM 17-AAG, and the proportion of GFP$^+$ cells was determined periodically by flow cytometry. Data are plotted as the mean GFP$^+$/GFP$^-$ ratio from triplicate populations ± SD, relative to the initial ratio set as*

1. Two independent experiments are shown differing only in AID protein level expression from having or not a consensus Kozak sequence before the AID start codon. (B) Western blot (WB) of parental K562 cells (–) and sorted GFP $^{+}$ populations transduced with pMX-AID-ires-GFP vectors differing only in the presence of the Kozak sequence. AID was detected using anti-AID, and antiactin was used as loading control. (C) Sorted GFP^{+} cells transduced or not with pMX-KozakAID-ires-GFP vectors as in A were cultured with 0.1 μM 17-AAG for the indicated times. The levels of the indicated proteins were analyzed by Western blot in total extracts using anti-AID and anti-ABL1. One of two independent experiments is shown. (D) GFP^{+} K562 populations were sorted after expansion from A. Cell viability after culture for 2 d with different concentrations of imatinib was determined using an MTS reduction colorimetric assay. The relative mean OD at 490 nm ± SEM of duplicate wells (untreated cells = 100%) is plotted for each concentration for cell populations transduced with pMXs-KozakAID-ires-GFP that had been treated in A with DMSO, imatinib, imatinib plus 0.1 μM 17-AAG, or 17-AAG. The parental K562 cells were included in this assay. One of two independent experiments is shown. (E) BCR-ABL1 (exon 13 of BCR and exon 9 of ABL1) was PCR amplified from cells expressing GFP control or AID-ires-GFP and expanded under the indicated conditions. Mutations, determined relative to the consensus of all sequences, are indicated on schemes of the ~700-bp ABL1 region that was directly sequenced from the PCR product. Thin vertical bars represent mutations at A:T bp, whereas thick bars represent mutations at C:G pairs. Mutations previously described to confer imatinib resistance (Branford and Hughes, 2006) are identified by an asterisk and indicated below the sequence stack.

Table 2.2. BCR-ABL1 mutations in K562 cells

Construct transduced	Treatment	BCR-ABL1 sequence analysis	Number of clones/total	Amino acid change
GFP	Imatinib	Unmutated	6/8	No changes
		894 CTA to CTG	1/8	Silent
		1062 CTA to CTG	1/8	Silent
AID-ires-GFP	Control	Unmutated	7/9	No changes
		894 CTA to CTG	1/9	Silent
		1062 CTA to CTG	1/9	Silent
AID-ires-GFP	Imatinib	Unmutated	2/10	No changes
		894 CTA to CTG	3/10	Silent
		944 ACT to ATT	4/10	**T315I**
		1062 CTA to CTG	2/10	Silent
		1334/1335 CGT to CTG	1/10	R445L
		1356 CTA to CTG	2/10	Silent
		1375 GAG to AAG	3/10	**E459K**
AID-ires-GFP	Imatinib + 17-AAG	Unmutated	6/9	No changes
		894 CTA to CTG	1/9	Silent
		1062 CTA to CTG	2/9	Silent

The BCR-ABL1 kinase domain (exon 13 of BCR and exon 9 of ABL1) was PCR amplified from single cell clones and a fragment of ~700 bp in the ABL1 domain was directly sequenced. The number to the left of the mutation indicates the mutated position respect to the ABL1 open reading frame. The mutated base is indicated underlined within the affected codon. Mutations at C:G pairs and amino acid substitutions previously described to confer clinical imatinib resistance are highlighted in bold.

2.5. Discussion

We identify and characterize herein the constitutive stabilization of AID by the HSP90 chaperone pathway. Our results show that HSP90 largely determines the overall steady-state levels of functional AID protein. Although HSP90 may also contribute to the biogenesis of AID, its key function appears to be the stabilization of the protein. This is well in accordance with the major role of HSP90 in protecting the functional competence of many of its clients, beyond simply assisting with their de novo folding (Jakob *et al.*, 1995; Nathan *et al.*, 1997; Whitesell and Lindquist, 2005; Pearl and Prodromou, 2006;Picard, 2006; Wandinger *et al.*, 2008). This is a new mechanism positively regulating AID-mediated antibody diversification that seems evolutionarily conserved, as we find it in chicken, mouse, and human B cells.

The molecular details of AID stabilization in the cytoplasm are likely incomplete because many proteins modulate the HSP90 pathway (Young *et al.*, 2004; Wandinger *et al.*, 2008). However, our experimental evidence, together with the identification of members of the HSP90 chaperone pathway that consistently copurified with AID (Table 2.1), suggests a working model in which AID would be regulated similarly to the steroid hormone receptors (Picard, 2006). These receptors first form an early complex with the HSP70/HSP40 chaperone/cochaperone, to which HSP90 and other factors are then recruited. Consecutive cycles of chaperoning are in dynamic equilibrium with proteasomal degradation unless the receptor is stabilized by ligand binding and translocates to the nucleus (Whitesell and Lindquist, 2005; Picard, 2006). Consistent with this model, we found HSPA8, the major constitutively expressed form of HSP70, among the AID-Flag/HA–interacting partners in Ramos B cells. The same isoform has been found using tagged AID expressed in HEK293 cells (Wu *et al.*, 2005). HSP40 proteins are the first agents in the HSP70/HSP90 chaperone pathway (Kimura *et al.*, 1995; Hernández *et al.*, 2002). We identified and have confirmed the functional interaction of AID with a defined subset of HSP40 proteins, which will be reported elsewhere (unpublished data). AID stabilization requires the ATP hydrolysis cycle of HSP90, and the cochaperone AHA-1, which stimulates the ATPase activity of HSP90 (Panaretou *et al.*, 2002; Lotz *et al.*, 2003), also copurified with AID. As is the case for steroid hormone receptors,

we show that cytoplasmic AID exists in a dynamic equilibrium between stabilization and proteasomal degradation. Indeed, inhibiting HSP90 or overexpressing the HSP90-associated ubiquitin ligase CHIP (Connell *et al.*, 2001; McDonough and Patterson, 2003) can shift the balance toward AID degradation. Stabilization seems to be the predominant pathway because simultaneous inhibition of the proteasome and HSP90 leads to the accumulation of much higher levels of polyubiquitinated AID than only proteasome inhibition. However, it remains possible that the destabilizing side of this pathway contributes to limit AID levels, which we are exploring. It is interesting that AID seems to be uniquely dependent on HSP90 when compared with its paralogue proteins, the APOBEC family. The intrinsic instability of uncomplexed AID probably helps to limit its mutagenic potential. This fits nicely with a study showing that the half-life of AID is highly reduced in the nucleus compared with the cytoplasm (Aoufouchi *et al.*, 2008). We speculate that AID, just as the steroid hormone receptors (Whitesell and Lindquist, 2005; Picard, 2006), might undergo some conformational change to dissociate from HSP90. An attractive possibility is that oligomerization stabilizes AID, thus emancipating it from HSP90. In line with this, the HSP90-interacting domain of AID comprises most of its proposed dimerization interface (Prochnow *et al.*, 2007; Patenaude *et al.*, 2009), and an oligomerization-deficient AID mutant can still bind to HSP90. We have proposed that dimerization/oligomerization of AID is important for its cytoplasmic retention and nuclear import (Patenaude *et al.*, 2009). However, at variance with the estrogen receptor, HSP90 does not seem to play a major role in AID cytoplasmic retention. We must hypothesize that AID forms part of another cytoplasmic complex that fulfills this role. This HSP90-independent fraction of AID might explain the slower kinetics of AID degradation in Ramos cells after HSP90 inhibition compared with other HSP90 clients such as LCK (Giannini and Bijlmakers, 2004).

The interaction of AID with HSP90 has major functional consequences. HSP90 stabilizes many proteins, and part of the effect observed on antibody diversification after inhibiting HSP90 could formally be indirect. However, there is a negative dose–response relationship between AID protein levels and HSP90 inhibition, which correlates with a proportional decrease in antibody diversification. This observation argues for a direct effect. Furthermore, HSP90 inhibition affected all AID-dependent pathways: SHM, CSR, and Ig gene

conversion as well as off-target mutation. All of these pathways are initiated by DNA deamination by AID followed by uracil processing by either UNG or MSH2/MSH6, which were not affected by HSP90 inhibition. Downstream from there, these pathways diverge (i.e., translesion synthesis for mutations, homologous recombination for gene conversion, and nonhomologous end joining for CSR), so a direct effect on AID is much more likely than an independent effect on each of these pathways. By stabilizing the bulk of AID, the HSP90 pathway determines the availability of functional AID. Indeed, AID-catalyzed DNA deamination at the Ig loci was directly proportional to the overall level of AID protein remaining after HSP90 inhibition. This is in agreement with the previously reported AID dose effect on the efficiency of antibody diversification (de Yébenes *et al.*, 2008; Dorsett *et al.*, 2008; Sernández *et al.*, 2008; Takizawa *et al.*, 2008; Teng *et al.*, 2008). Together with our findings, these observations suggest that the ratio of nuclear to cytoplasmic AID is constant. Thus, decreasing the overall level of AID would lead to a proportional decrease in the nuclear fraction and biological activity of AID. Otherwise, if AID were particularly abundant in the nucleus at any stage, a 50% decrease in total AID protein caused by partial HSP90 inhibition (or by haploinsufficiency) would not necessarily lead to a proportional decrease in antibody diversification. Our work highlights the intimate relationship between the mechanisms of AID subcellular localization and protein stability (Aoufouchi *et al.*, 2008; Patenaude *et al.*, 2009).

Finally, the HSP90-mediated mechanism stabilizing AID is operative in lymphoma-derived cell lines as well as in cells with ectopic overexpression of AID. The relative HSP90 dependence of AID in transformed versus normal cells remains to be studied. Nevertheless, our findings offer the first possibility of pharmacologically manipulating AID protein levels to prevent off-target mutation. We provide proof of principle that this is possible in a CML cell line model. A very low dose of HSP90 inhibitor completely abrogated BCR-ABL1 mutations and imatinib resistance. AID-generated lesions in non-Ig genes are widespread but much less frequent than at the Ig genes (Liu *et al.*, 2008;Robbiani *et al.*, 2009). Indeed, the AID-generated breaks in c-Myc seem to be limiting for the oncogenic c-Myc–IgH chromosomal translocations (Robbiani *et al.*, 2008, 2009). Therefore, it might be possible that very low doses of HSP90 inhibitors have a disproportionate effect on the frequency of oncogenic lesions versus antibody

diversification. It would be worth exploring whether the HSP90 inhibitors that are currently being tested in the clinic could be useful in treating those cancers in which AID contributes to disease progression (Matsumoto *et al.*, 2007; Pasqualucci *et al.*, 2008;Klemm *et al.*, 2009).

2.6. Materials and methods

2.6.1. DNA constructs

The pEGFP-N3–based (Takara Bio Inc.) expression vectors for human AID-GFP, AID FYRN-GFP, AID-Flag/HA, APOBEC2, and AID-APOBEC2 chimeras have been described previously (Patenaude *et al.*, 2009). Rat APOBEC1 and human APOBEC3G cloned in pEGFP-C3 as well as human AID T27A/T38A, which was subcloned into pEGFP-N3, were gifts from S. Conticello (Istituto Toscano Tumori, Florence, Italy; Conticello *et al.*, 2008). To construct N-terminally Flag-tagged versions of APOBEC1, APOBEC2, and APOBEC3G, enhanced GFP (EGFP) was excised NheI–XhoI from pEGFP-C3 and replaced by the annealed oligonucleotides AO1 and AO2. To construct C-terminally Flag-tagged versions of some of the proteins, EGFP was excised EcoRI–NotI from pEGFP-N3 and replaced by the annealed oligonucleotides OJ215 and OJ216. AID was subcloned as an NheI–NotI fragment under the weaker EF1-α promoter in pEF. AID-APOBEC2 chimeras #1 and #2 were excised from pTrc99a (Patenaude *et al.*, 2009) by partial digestion with NotI and EcoRI and subcloned into the pMXs retroviral vector. Untagged hAID in pMXs-ires-GFP has been described previously (Patenaude *et al.*, 2009). Mouse AID (from R. Harris, University of Minnesota, Minneapolis, MN) was subcloned EcoRI and NotI into pMXs. Flag-human HSP90-α was inserted as a KpnI–NotI fragment into pcDNA3.1. Myc-human HSP90-β in pCMV-3Tag2 was a gift of J.-.P Gratton (Institut de Recherches Cliniques de Montréal, Montréal, Québec, Canada). Construct names throughout the manuscript indicate the actual order of the fragments in fusion proteins.

2.6.2. Reagents and antibodies.

Stock aliquots of 2 mM GA, 2 mM 17-AAG, 5 mM H-89, and 25 mM forskolin (LC Laboratories) as well as 50 mM IBMX (3-isobutyl-1-methylxanthine; Sigma-Aldrich) were made in DMSO. Stocks of 5 mM MG132 (EMD) and 25 μg/ml LMB (LC Laboratories) were made in ethanol. CHX (Sigma-Aldrich) was freshly prepared before each experiment 100 mg/ml in ethanol. Stock of 2 mM imatinib (Gleevec; Novartis) in PBS was a gift of T. Moroy

and C. Khandanpur (Institut de Recherches Cliniques de Montréal). All drugs were stored at −20°C protected from light. Antibodies and dilutions used were as follows: 1:3,000 anti–EGFP–horseradish peroxidase (HRP; Miltenyi Biotec), 1:3,000 anti–Myc-HRP (Miltenyi Biotec), 1:3,000 anti–Flag-HRP (Sigma-Aldrich), 1:3,000 anti-HSP90 (sees both isoforms; BD), 1:1,000 anti–HSP90-α and 1:1,000 anti–HSP90-β (StressMarq), 1:1,000 anti-AID (Cell Signaling Technology) for human and chicken AID and 1:500 anti-mAID (a gift from F. Alt, Harvard University, Boston, MA) for mouse AID, 1:3,000 antiactin (Sigma-Aldrich), 1:1,000 anti-monoubiquitinated and -polyubiquitinated conjugates antibody (Enzo Life Sciences, Inc.) for endogenous ubiquitin, 1:1,000 mAb anti-CHIP (Sigma-Aldrich), 1:2,000 anti-UNG2 (specific for nuclear isoform; Abcam), 1:2,500 anti-MSH6 (Bethyl Laboratories, Inc.), 1:5,000 anti-PCNA (PC-10; Abcam), 1:1,000 anti–DNA-PK (Santa Cruz Biotechnology, Inc.), 1:1,000 anti-LCK (gift of A. Veillette, Institut de Recherches Cliniques de Montréal), and 1:1,000 anti–c-abl (EMD). Secondary antibodies were used according to the species of the primary antibody: 1:5,000 goat anti–mouse-HRP and 1:10,000 anti–rabbit-HRP (Dako) and 1:5,000 goat anti–rat-HRP (Millipore).

2.6.3. Mice and cell lines.

HeLa cells stably expressing AID-GFP were generated by transfecting with pEF-AID-EGFP and selecting with 2.5 μg/ml puromycin. Ramos cell lines stably expressing GFP, AID-GFP, and AID-Flag/HA have been described previously (Patenaude *et al.*, 2009). Ramos cells expressing Myc-CHIP were generated by transfecting with pcDNA3.1 Myc-CHIP (a gift of L. Petrucelli, Mayo Clinic, Jacksonville, FL) and selecting with G418. Subclones from three independent Myc-CHIP Ramos transfectants and controls were obtained by single cell deposition. Populations of Ramos cells stably expressing chimeras AID-A2 #1 or #2 and DT40 cells stably expressing GFP or AID-GFP as well as the CML cell line K562 (a gift of T. Moroy) stably expressing AID-ires-GFP or GFP control were obtained by retroviral delivery of these genes cloned in pMXs vectors. The supernatant of HEK293T cells cotransfected with pMX and vectors expressing MLV Gag-Pol and VSV-G envelope (3:1:1 ratio) was used to infect 10^6 cells by spin-infection at 600***g*** for 1 h at room temperature in the presence of 16 μg/ml polybrene and 20 mM Hepes. Infected cells were sorted to obtain GFP^+ homogeneous

populations. Primary B cells from ***Aicda***$^{-/-}$ mice (obtained from T. Honjo, Kyoto University, Sakyo-ku, Kyoto, Japan) were prepared and infected as described previously (Patenaude *et al.*, 2009). Experiments using mice followed the guidelines of the Canadian Council on Animal Care and were approved by the Animal Protection Committee at the Institut de Recherches Cliniques de Montréal. Primary human B cells were purified from PBMC obtained by Ficoll gradient centrifugation of voluntary donor blood samples. Resting B cells were isolated using a B cell isolation kit (Miltenyi Biotech) and activated with 5 ng/ml recombinant hIL-4 (PeproTech) and 5 µg/ml recombinant human sCD40L. Work with human samples was performed according to the guidelines of the Institut de Recherches Cliniques de Montréal and Institut National de la Recherche Scientifique–Insitut Armand-Frappier Ethics Committees for Research with Human Samples.

2.6.4. Identification of AID-interacting proteins.

5×10^9 Ramos B cells expressing AID-Flag/HA or empty vector were pelleted, incubated on ice for 10 min, and resuspended in hypotonic buffer I (1 mM Tris-HCl, pH 7.3, 10 mM KCl, 1.5 mM $MgCl_2$, and β-mercaptoethanol). Cells were centrifuged at 2,500 rpm for 10 min at 4°C and lysed by adding hypotonic buffer II (1 mM Tris-HCl, pH 7.3, 10 mM KCl, 1.5 mM $MgCl_2$, 1 mM trichostatin A, 50 µM β-mercaptoethanol, 0.5 mM PMSF, and protease inhibitors [Sigma-Aldrich]). The lysate was centrifuged at 3,900 rpm for 15 min at 4°C, and the supernatant was recentrifuged at 35,000 rpm for 1 h and dialyzed against 20 mM Tris-HCl, pH 7.3, 20% glycerol, 100 mM KCl, 50 µM β-mercaptoethanol, and 0.5 mM PMSF. The dialyzed lysate was incubated with anti-Flag M2 affinity gel (Sigma-Aldrich) overnight at 4°C and then extensively washed and eluted using 3× Flag peptide (Sigma-Aldrich). The eluate was incubated with anti-HA beads (Santa Cruz Biotechnology, Inc.) overnight at 4°C and then washed and eluted using HA peptides (PEP-101P; Covance). Protein was concentrated using StrataClean Resin (Agilent Technologies) before loading on a 4–12% gradient gel (Invitrogen) for SDS-PAGE. The gel was silver stained, each lane was divided into 20 slices, and the slices were submitted for tryptic digestion and peptide identification by mass spectrometry to the

Institut de Recherches Cliniques de Montréal Proteomics service using a linear quadrupole IT Orbitrap hybrid mass spectrometer (Thermo Fisher Scientific). Peak generation and protein identification were performed using the MASCOT software package (Perkins *et al.*, 1999)

2.6.5. Coimmunoprecipitation and Western blot.

HEK293T cells cotransfected at a 1:1 ratio with GFP and Myc or Flag-tagged proteins were homogenized in lysis buffer (20 mM Tris, pH 8.0, 137 mM NaCl, 10% glycerol, 2 mM EDTA, 1% Triton X-100, and 20 mM NaF) 48 h after transfection and immunoprecipitated with anti-Flag M2 affinity gel as described previously (Patenaude *et al.*, 2009). Immunoprecipitation of GFP-tagged proteins were performed using the μMACS GFP Isolation kit (Miltenyi Biotech) according to the manufacturer's instructions. Where indicated, cells were treated with 10 μM MG132 for 30 min and/or 2 μM GA or DMSO for 5 h before lysis. The eluates and lysates were analyzed by Western blot developed with SuperSignal West Pico Chemiluminescent substrate (Thermo Fisher Scientific).

2.6.6. AID stability assays.

The GFP signal of cell lines expressing AID-GFP variants was measured by flow cytometry at various time points after the indicated treatments. Dead cells were excluded by propidium iodide staining. For endogenous AID, 5×10^6 Ramos, DT40, or K562 cells in 5 ml of culture medium were treated with GA or 17-AAG, and aliquots of $1.5–2 \times 10^6$cells were harvested at various time points. Alternatively, 2×10^6 CH12F3-2 cells (a gift of T. Honjo through A. Martin [University of Toronto, Toronto, Ontario, Canada]; Nakamura *et al.*, 1996) were stimulated with 2 ng/ml recombinant human TGF-β1 (R&D Systems), 20 ng/ml recombinant murine IL-4 (PeproTech), and 5 μg/ml functional grade purified anti–mouse CD40 (BD) for 16 h before GA treatment. Human primary B cells at 2×10^6/ml were treated with 2 μM 17-AAG 72 h after activation, and aliquots of 10^6 cells were harvested at various time points. Cells were washed once with PBS and lysed in SDS-PAGE sample buffer. Lysates were analyzed by Western blotting.

2.6.7. Monitoring antibody diversification.

AID-mediated Ig gene conversion was estimated in DT40 cre1 cells by scoring the frequency of sIgM-gain phenotype, which is directly proportional to the frequency of repair of a frameshift in the IgVλ by gene conversion (Arakawa *et al.*, 2002). DT40 $sIgM^-$ cell populations were FACS sorted, and confluent cultures were grown in 24-well plates with HSP90 inhibitors. This method was favored over using single cell clones because of the effect of HSP90 inhibition on single cells growth. Cells were grown for 3 wk at 41°C in the presence of the inhibitors, and the surface IgM phenotype was measured by flow cytometry as described previously (Di Noia and Neuberger, 2004). AID-mediated SHM was monitored using the $sIgM^+$ DT40 line ψV^- AID^{R}, in which the IgV pseudogenes have been ablated (gift of H. Arakawa and J.-M. Buerstedde, Institute for Molecular Radiobiology, Neuherberg, Germany; Arakawa *et al.*, 2004). IgM^+ cell populations were FACS sorted and expanded for 3 wk in 24-well plates, and the IgM phenotype was analyzed by flow cytometry. Mutations were scored as described previously (Di Noia and Neuberger, 2004) in Vλ sequences PCR amplified from unsorted populations after expansion. To analyze CSR, CH12F3-2 cells were preincubated with CFSE (Invitrogen) according to manufacturer's instruction before activation with 1 ng/ml TGF-β1, 10 ng/ml recombinant murine IL-4, and 1 μg/ml functional grade purified anti–mouse CD40 (BD). For chronic HSP90 inhibition, 17-AAG was added 4 h after activation and kept for 3 d. For acute HSP90 inhibition, 17-AAG was added to the medium for 12 h, and then the cells were washed twice with PBS and resuspended in fresh normal medium. IgA expression was monitored at day 3 after stimulation using PE-conjugated anti–mouse IgA antibody (eBioscience). Resting B cells from AID-deficient mice were purified by MACS CD43 depletion (Miltenyi Biotech) from total splenic lymphocytes (Patenaude *et al.*, 2009). Cells were loaded with CFSE, and 10^6 cells/well were seeded in 24-well plates with 25 μg/ml LPS (Sigma-Aldrich) and 50 ng/ml mouse IL-4. At different times after activation, 17-AAG was added and washed away 12 h later with PBS, and fresh culture medium was replenished. Isotype switching was analyzed 4 d after activation by flow cytometry after staining with anti–IgG1-biotin (BD), followed by APC-conjugated antibiotin antibody (Miltenyi Biotech) and propidium iodide.

2.6.8. Imatinib resistance assay.

K562 cells stably expressing AID-ires-GFP or GFP control were mixed with the parental cell line at a fixed ratio. The ratio of GFP^+ to GFP^- cells was measured by flow cytometry every 2 d for populations under the different treatments indicated in the figure (2 μM DMSO, 2 μM imatinib, and 0.1 μM 17-AAG). GFP^+ cells were FACS sorted at the end of the experiments for the relevant conditions. Relative imatinib resistance of these populations was determined using Celltiter 96 Aqueous nonradioactive cell proliferation assay (Promega) according to manufacturer's instruction. For mutation analysis of the *BCR-ABL1* gene, single GFP^+ CML cells expressing AID or not were sorted at the end of the treatments and expanded to obtain a clone in 96-well plates. RNA was extracted with TRIZOL (Invitrogen), and cDNA synthesis was performed using M-MULV first strand cDNA synthesis kit (New England Biolabs, Inc.). A 1540-bp fragment of the BCR-ABL1 cDNA was PCR amplified using specific primers for BCR (in exon 13) and ABL1 (in exon 9; Klemm *et al.*, 2009) with KOD Hot Start Polymerase (EMD). PCR products were purified and directly sequenced using an ABL1-specific primer.

2.6.9. Statistical analysis.

The unpaired two-tailed Student's ***t*** test was used.

2.7. Acknowledgments

We thank Dr. J.-P. Gratton for useful discussions and Drs. S. Conticello, D. Muñoz, C.A. Buscaglia, and R. Casellas for comments on the manuscript. We are indebted to H. Yu for helping with AID-Flag/HA purification and to Drs. H. Arakawa, J.-M. Buerstedde, S. Conticello, R. Harris, J.-P. Gratton, T. Moroy, C. Khandanpur, A. Veillette, F. Alt, A. Martin, T. Honjo, and L. Petrucelli for providing reagents. We thank D. Faubert (Institut de Recherches Cliniques de Montréal Proteomics facility) for assistance.

This work was funded by grants from The Cancer Research Society and Canadian Institutes of Health Research (CIHR; MOP-84543) and supported by a Canadian Foundation for Innovation Leaders Opportunity Fund equipment grant to J.M. Di Noia. A. Orthwein was supported in part by a Michel Bélanger fellowship from the Institut de Recherches Cliniques de Montréal, by an Excellence Fellowship from the Department of Microbiology and Immunology, University of Montréal, and by a Cole Foundation Fellowship. A. Lamarre is supported by the Jeanne and J.-Louis Lévesque Chair in Immunovirology of the J.-Louis Lévesque Foundation and by CIHR. J.M. Di Noia and J.C. Young are supported by Canada Research Chairs Tier 2.

The authors have no conflicting financial interests.

2.8. References

1. Albesiano E., Messmer B.T., Damle R.N., Allen S.L., Rai K.R., Chiorazzi N. 2003. Activation-induced cytidine deaminase in chronic lymphocytic leukemia B cells: expression as multiple forms in a dynamic, variably sized fraction of the clone. *Blood.* 102:3333–3339. doi: 10.1182/blood-2003-05-1585.
2. Aoufouchi S., Faili A., Zober C., D'Orlando O., Weller S., Weill J.-C., Reynaud C.-A. 2008.Proteasomal degradation restricts the nuclear lifespan of AID. *J. Exp. Med.* 205:1357–1368. doi: 10.1084/jem.20070950.
3. Arakawa H., Hauschild J., Buerstedde J.-M. 2002. Requirement of the activation-induced deaminase (AID) gene for immunoglobulin gene conversion. *Science.* 295:1301–1306. doi: 10.1126/science.1067308.
4. Arakawa H., Saribasak H., Buerstedde J.-M. 2004. Activation-induced cytidine deaminase initiates immunoglobulin gene conversion and hypermutation by a common intermediate.*PLoS Biol.* 2:E179. doi: 10.1371/journal.pbio.0020179.
5. Bhutani N., Brady J.J., Damian M., Sacco A., Corbel S.Y., Blau H.M. 2010. Reprogramming towards pluripotency requires AID-dependent DNA demethylation. *Nature.* 463:1042–1047. doi: 10.1038/nature08752.
6. Borkovich K.A., Farrelly F.W., Finkelstein D.B., Taulien J., Lindquist S. 1989. hsp82 is an essential protein that is required in higher concentrations for growth of cells at higher temperatures. *Mol. Cell. Biol.* 9:3919–3930.
7. Branford S., Hughes T. 2006. Detection of BCR-ABL mutations and resistance to imatinib mesylate. *Methods Mol. Med.* 125:93–106.
8. Connell P., Ballinger C.A., Jiang J., Wu Y., Thompson L.J., Höhfeld J., Patterson C. 2001. The co-chaperone CHIP regulates protein triage decisions mediated by heat-shock proteins. *Nat. Cell Biol.* 3:93–96. doi: 10.1038/35050618.
9. Conticello S.G., Thomas C.J., Petersen-Mahrt S.K., Neuberger M.S. 2005. Evolution of the AID/APOBEC family of polynucleotide (deoxy)cytidine deaminases. *Mol. Biol. Evol.* 22:367–377. doi: 10.1093/molbev/msi026.
10. Conticello S.G., Ganesh K., Xue K., Lu M., Rada C., Neuberger M.S. 2008. Interaction between antibody-diversification enzyme AID and spliceosome-associated factor CTNNBL1. *Mol. Cell.*31:474–484. doi: 10.1016/j.molcel.2008.07.009.
11. Crouch E.E., Li Z., Takizawa M., Fichtner-Feigl S., Gourzi P., Montaño C., Feigenbaum L., Wilson P., Janz S., Papavasiliou F.N., Casellas R. 2007. Regulation of AID expression in the immune response. *J. Exp. Med.* 204:1145–1156. doi: 10.1084/jem.20061952.
12. Csermely P., Schnaider T., Soti C., Prohászka Z., Nardai G. 1998. The 90-kDa molecular chaperone family: structure, function, and clinical applications. A comprehensive review.*Pharmacol. Ther.* 79:129–168. doi: 10.1016/S0163-7258(98)00013-8.
13. Cutforth T., Rubin G.M. 1994. Mutations in Hsp83 and cdc37 impair signaling by the

sevenless receptor tyrosine kinase in *Drosophila*. *Cell.* 77:1027–1036. doi: 10.1016/0092-8674(94)90442-1.

14. de Yébenes V.G., Belver L., Pisano D.G., González S., Villasante A., Croce C., He L., Ramiro A.R. 2008. miR-181b negatively regulates activation-induced cytidine deaminase in B cells. *J. Exp. Med.* 205:2199–2206. doi: 10.1084/jem.20080579.
15. DeFranco D.B. 1999. Regulation of steroid receptor subcellular trafficking. *Cell Biochem. Biophys.* 30:1–24. doi: 10.1007/BF02737882.
16. Di Noia J.M., Neuberger M.S. 2004. Immunoglobulin gene conversion in chicken DT40 cells largely proceeds through an abasic site intermediate generated by excision of the uracil produced by AID-mediated deoxycytidine deamination. *Eur. J. Immunol.* 34:504–508. doi: 10.1002/eji.200324631.
17. Di Noia J.M., Neuberger M.S. 2007. Molecular mechanisms of antibody somatic hypermutation. *Annu.Rev.Biochem.* 76:122.doi:10.1146/annurev.biochem.76.061705.090740.
18. Dickey C.A., Kamal A., Lundgren K., Klosak N., Bailey R.M., Dunmore J., Ash P., Shoraka S., Zlatkovic J., Eckman C.B., *et al.* 2007. The high-affinity HSP90-CHIP complex recognizes and selectively degrades phosphorylated tau client proteins. *J. Clin. Invest.* 117:648–658. doi: 10.1172/JCI29715.
19. Dorsett Y., McBride K.M., Jankovic M., Gazumyan A., Thai T.-H., Robbiani D.F., Di Virgilio M., San-Martin B.R., Heidkamp G., Schwickert T.A., *et al.* 2008. MicroRNA-155 suppresses activation-induced cytidine deaminase-mediated Myc-Igh translocation. *Immunity.* 28:630–638. doi: 10.1016/j.immuni.2008.04.002.
20. Endo Y., Marusawa H., Kou T., Nakase H., Fujii S., Fujimori T., Kinoshita K., Honjo T., Chiba T. 2008. Activation-induced cytidine deaminase links between inflammation and the development of colitis-associated colorectal cancers. *Gastroenterology.* 135:889–898: 898: e1–e3. doi: 10.1053/j.gastro.2008.06.091.
21. Etard C., Roostalu U., Strähle U. 2010. Lack of Apobec2-related proteins causes a dystrophic muscle phenotype in zebrafish embryos. *J. Cell Biol.* 189:527–539. doi: 10.1083/jcb.200912125.
22. Feldhahn N., Henke N., Melchior K., Duy C., Soh B.N., Klein F., von Levetzow G., Giebel B., Li A., Hofmann W.-K., *et al.* 2007. Activation-induced cytidine deaminase acts as a mutator in*BCR-ABL1*–transformed acute lymphoblastic leukemia cells. *J. Exp. Med.* 204:1157–1166. doi: 10.1084/jem.20062662.
23. Galigniana M.D., Harrell J.M., O'Hagen H.M., Ljungman M., Pratt W.B. 2004. HSP90-binding immunophilins link p53 to dynein during p53 transport to the nucleus. *J. Biol. Chem.*279:22483–22489. doi: 10.1074/jbc.M402223200.
24. Giannini A., Bijlmakers M.-J. 2004. Regulation of the Src family kinase LCK by HSP90 and ubiquitination. *Mol. Cell. Biol.* 24:5667–5676. doi: 10.1128/MCB.24.13.5667-

5676.2004.

25. Greeve J., Philipsen A., Krause K., Klapper W., Heidorn K., Castle B.E., Janda J., Marcu K.B., Parwaresch R. 2003. Expression of activation-induced cytidine deaminase in human B-cell non-Hodgkin lymphomas. *Blood.* 101:3574–3580. doi: 10.1182/blood-2002-08-2424.
26. Hansen L.K., Houchins J.P., O'Leary J.J. 1991. Differential regulation of HSC70, HSP70, HSP90 alpha, and HSP90 beta mRNA expression by mitogen activation and heat shock in human lymphocytes. *Exp. Cell Res.* 192:587–596. doi: 10.1016/0014-4827(91)90080-E.
27. Hernández M.P., Chadli A., Toft D.O. 2002. HSP40 binding is the first step in the HSP90 chaperoning pathway for the progesterone receptor. *J. Biol. Chem.* 277:11873–11881. doi: 10.1074/jbc.M111445200.
28. Ito S., Nagaoka H., Shinkura R., Begum N., Muramatsu M., Nakata M., Honjo T. 2004.Activation-induced cytidine deaminase shuttles between nucleus and cytoplasm like apolipoprotein B mRNA editing catalytic polypeptide 1. *Proc. Natl. Acad. Sci. USA*. 101:1975–1980. doi: 10.1073/pnas.0307335101.
29. Jakob U., Lilie H., Meyer I., Buchner J. 1995. Transient interaction of HSP90 with early unfolding intermediates of citrate synthase. Implications for heat shock in vivo. *J. Biol. Chem.*270:7288–7294. doi: 10.1074/jbc.270.13.7288.
30. Kimura Y., Yahara I., Lindquist S. 1995. Role of the protein chaperone YDJ1 in establishing HSP90-mediated signal transduction pathways. *Science.* 268:1362–1365. doi: 10.1126/science.7761857.
31. Klemm L., Duy C., Iacobucci I., Kuchen S., von Levetzow G., Feldhahn N., Henke N., Li Z., Hoffmann T.K., Kim Y.M., *et al.* 2009. The B cell mutator AID promotes B lymphoid blast crisis and drug resistance in chronic myeloid leukemia. *Cancer Cell.* 16:232–245. doi: 10.1016/j.ccr.2009.07.030.
32. Li L., Xin H., Xu X., Huang M., Zhang X., Chen Y., Zhang S., Fu X.-Y., Chang Z. 2004. CHIP mediates degradation of Smad proteins and potentially regulates Smad-induced transcription. *Mol. Cell. Biol.* 24:856–864. doi: 10.1128/MCB.24.2.856-864.2004.
33. Liu M., Duke J.L., Richter D.J., Vinuesa C.G., Goodnow C.C., Kleinstein S.H., Schatz D.G. 2008. Two levels of protection for the B cell genome during somatic hypermutation. *Nature.*451:841–845. doi: 10.1038/nature06547.
34. Lotz G.P., Lin H., Harst A., Obermann W.M.J. 2003. Aha1 binds to the middle domain of HSP90, contributes to client protein activation, and stimulates the ATPase activity of the molecular chaperone. *J. Biol. Chem.* 278:17228–17235. doi: 10.1074/jbc.M212761200.
35. MacDuff D.A., Demorest Z.L., Harris R.S. 2009. AID can restrict L1 retrotransposition suggesting a dual role in innate and adaptive immunity. *Nucleic Acids Res.* 37:1854–1867. doi: 10.1093/nar/gkp030.
36. Matsumoto Y., Marusawa H., Kinoshita K., Endo Y., Kou T., Morisawa T., Azuma T., Okazaki I.M., Honjo T., Chiba T. 2007. Helicobacter pylori infection triggers aberrant

expression of activation-induced cytidine deaminase in gastric epithelium. *Nat. Med.* 13:470–476. doi: 10.1038/nm1566.

37. McBride K.M., Barreto V., Ramiro A.R., Stavropoulos P., Nussenzweig M.C. 2004. Somatic hypermutation is limited by CRM1-dependent nuclear export of activation-induced deaminase.*J. Exp. Med.* 199:1235–1244. doi: 10.1084/jem.20040373.
38. McDonough H., Patterson C. 2003. CHIP: a link between the chaperone and proteasome systems. *Cell Stress Chaperones*. 8:303–308. doi: 10.1379/1466-1268(2003)008<0303:CALBTC>2.0.CO;2.
39. Metz K., Ezernieks J., Sebald W., Duschl A. 1996. Interleukin-4 upregulates the heat shock protein HSP90alpha and enhances transcription of a reporter gene coupled to a single heat shock element. *FEBS Lett.* 385:25–28. doi: 10.1016/0014-5793(96)00341-9.
40. Morgan H.D., Dean W., Coker H.A., Reik W., Petersen-Mahrt S.K. 2004. Activation-induced cytidine deaminase deaminates 5-methylcytosine in DNA and is expressed in pluripotent tissues: implications for epigenetic reprogramming. *J. Biol. Chem.* 279:52353–52360. doi: 10.1074/jbc.M407695200.
41. Muramatsu M., Sankaranand V.S., Anant S., Sugai M., Kinoshita K., Davidson N.O., Honjo T. 1999. Specific expression of activation-induced cytidine deaminase (AID), a novel member of the RNA-editing deaminase family in germinal center B cells. *J. Biol. Chem.* 274:18470–18476. doi: 10.1074/jbc.274.26.18470.
42. Nakamura M., Kondo S., Sugai M., Nazarea M., Imamura S., Honjo T. 1996. High frequency class switching of an IgM+ B lymphoma clone CH12F3 to IgA+ cells. *Int. Immunol.* 8:193–201. doi: 10.1093/intimm/8.2.193.
43. Nathan D.F., Vos M.H., Lindquist S. 1997. In vivo functions of the *Saccharomyces cerevisiae*HSP90 chaperone. *Proc. Natl. Acad. Sci. USA*. 94:12949–12956. doi: 10.1073/pnas.94.24.12949.
44. Okazaki I.M., Hiai H., Kakazu N., Yamada S., Muramatsu M., Kinoshita K., Honjo T. 2003.Constitutive expression of AID leads to tumorigenesis. *J. Exp. Med.* 197:1173–1181. doi: 10.1084/jem.20030275.
45. Palacios F., Moreno P., Morande P., Abreu C., Correa A., Porro V., Landoni A.I., Gabus R., Giordano M., Dighiero G., *et al.* 2010. High expression of AID and active class switch recombination might account for a more aggressive disease in unmutated CLL patients: link with an activated microenvironment in CLL disease. *Blood.* 115:4488–4496. doi: 10.1182/blood-2009-12-257758.
46. Panaretou B., Prodromou C., Roe S.M., O'Brien R., Ladbury J.E., Piper P.W., Pearl L.H. 1998.ATP binding and hydrolysis are essential to the function of the HSP90 molecular chaperone in vivo. *EMBO J.* 17:4829–4836. doi: 10.1093/emboj/17.16.4829.
47. Panaretou B., Siligardi G., Meyer P., Maloney A., Sullivan J.K., Singh S., Millson S.H., Clarke P.A., Naaby-Hansen S., Stein R., *et al.* 2002. Activation of the ATPase activity of

HSP90 by the stress-regulated cochaperone aha1. *Mol. Cell.* 10:1307–1318. doi: 10.1016/S1097-2765(02)00785-2.

48. Pasqualucci L., Neumeister P., Goossens T., Nanjangud G., Chaganti R.S., Küppers R., Dalla-Favera R. 2001. Hypermutation of multiple proto-oncogenes in B-cell diffuse large-cell lymphomas. *Nature.* 412:341–346. doi: 10.1038/35085588.
49. Pasqualucci L., Guglielmino R., Houldsworth J., Mohr J., Aoufouchi S., Polakiewicz R., Chaganti R.S., Dalla-Favera R. 2004. Expression of the AID protein in normal and neoplastic B cells. *Blood.* 104:3318–3325. doi: 10.1182/blood-2004-04-1558.
50. Pasqualucci L., Bhagat G., Jankovic M., Compagno M., Smith P., Muramatsu M., Honjo T., Morse H.C., III, Nussenzweig M.C., Dalla-Favera R. 2008. AID is required for germinal center-derived lymphomagenesis. *Nat. Genet.* 40:108–112. doi: 10.1038/ng.2007.35.
51. Patenaude A.M., Orthwein A., Hu Y., Campo V.A., Kavli B., Buschiazzo A., Di Noia J.M. 2009.Active nuclear import and cytoplasmic retention of activation-induced deaminase. *Nat. Struct. Mol. Biol.* 16:517–527. doi: 10.1038/nsmb.1598.
52. Pauklin S., Sernández I.V., Bachmann G., Ramiro A.R., Petersen-Mahrt S.K. 2009. Estrogen directly activates AID transcription and function. *J. Exp. Med.* 206:99–111. doi: 10.1084/jem.20080521.
53. Pearl L.H., Prodromou C. 2006. Structure and mechanism of the HSP90 molecular chaperone machinery. *Annu.Rev.Biochem.*75:271294.doi:10.1146/annurev.biochem.75.103004.142738
54. Peled J.U., Kuang F.L., Iglesias-Ussel M.D., Roa S., Kalis S.L., Goodman M.F., Scharff M.D. 2008. The biochemistry of somatic hypermutation. *Annu. Rev. Immunol.* 26:481–511. doi: 10.1146/annurev.immunol.26.021607.090236.
55. Perkins D.N., Pappin D.J., Creasy D.M., Cottrell J.S. 1999. Probability-based protein identification by searching sequence databases using mass spectrometry data.*Electrophoresis.* 20:3551–3567.doi: 10.1002/(SICI)1522-2683(19991201)20:18<3551.
56. Picard D. 2006. Chaperoning steroid hormone action. *Trends Endocrinol. Metab.* 17:229–235. doi: 10.1016/j.tem.2006.06.003.
57. Popp C., Dean W., Feng S., Cokus S.J., Andrews S., Pellegrini M., Jacobsen S.E., Reik W. 2010. Genome-wide erasure of DNA methylation in mouse primordial germ cells is affected by AID deficiency. *Nature.* 463:1101–1105. doi: 10.1038/nature08829.
58. Pratt W.B., Toft D.O. 2003. Regulation of signaling protein function and trafficking by the HSP90/HSP70-based chaperone machinery. *Exp. Biol. Med. (Maywood).* 228:111–133.
59. Prochnow C., Bransteitter R., Klein M.G., Goodman M.F., Chen X.S. 2007. The APOBEC-2 crystal structure and functional implications for the deaminase AID. *Nature.* 445:447–451. doi: 10.1038/nature05492.
60. Prodromou C., Roe S.M., O'Brien R., Ladbury J.E., Piper P.W., Pearl L.H. 1997. Identification and structural characterization of the ATP/ADP-binding site in the HSP90 molecular chaperone. *Cell.* 90:65–75. doi: 10.1016/S0092-8674(00)80314-1.

61. Ramiro A.R., Jankovic M., Eisenreich T., Difilippantonio S., Chen-Kiang S., Muramatsu M., Honjo T., Nussenzweig A., Nussenzweig M.C. 2004. AID is required for c-myc/IgH chromosome translocations in vivo. *Cell.* 118:431–438. doi: 10.1016/j.cell.2004.08.006.
62. Ramiro A.R., Jankovic M., Callen E., Difilippantonio S., Chen H.-T., McBride K.M., Eisenreich T.R., Chen J., Dickins R.A., Lowe S.W., *et al.* 2006. Role of genomic instability and p53 in AID-induced c-myc-Igh translocations. *Nature.* 440:105–109. doi: 10.1038/nature04495.
63. Robbiani D.F., Bothmer A., Callen E., Reina-San-Martin B., Dorsett Y., Difilippantonio S., Bolland D.J., Chen H.T., Corcoran A.E., Nussenzweig A., Nussenzweig M.C. 2008. AID is required for the chromosomal breaks in c-myc that lead to c-myc/IgH translocations. *Cell.*135:1028–1038. doi: 10.1016/j.cell.2008.09.062.
64. Robbiani D.F., Bunting S., Feldhahn N., Bothmer A., Camps J., Deroubaix S., McBride K.M., Klein I.A., Stone G., Eisenreich T.R., *et al.* 2009. AID produces DNA double-strand breaks in non-Ig genes and mature B cell lymphomas with reciprocal chromosome translocations. *Mol. Cell.* 36:631–641. doi: 10.1016/j.molcel.2009.11.007.
65. Sernández I.V., de Yébenes V.G., Dorsett Y., Ramiro A.R. 2008. Haploinsufficiency of activation-induced deaminase for antibody diversification and chromosome translocations both in vitro and in vivo. *PLoS One.* 3:e3927. doi: 10.1371/journal.pone.0003927.
66. Sreedhar A.S., Kalmár E., Csermely P., Shen Y.F. 2004. HSP90 isoforms: functions, expression and clinical importance. *FEBS Lett.* 562:11–15. doi: 10.1016/S0014-5793(04)00229-7.
67. Stavnezer J., Guikema J.E.J., Schrader C.E. 2008. Mechanism and regulation of class switch recombination. *Annu. Rev. Immunol.* 26:261–292. doi: 10.1146/annurev.immunol.26.021607.090248.
68. Stebbins C.E., Russo A.A., Schneider C., Rosen N., Hartl F.U., Pavletich N.P. 1997. Crystal structure of an HSP90-geldanamycin complex: targeting of a protein chaperone by an antitumor agent. *Cell.* 89:239–250. doi: 10.1016/S0092-8674(00)80203-2.
69. Takizawa M., Tolarová H., Li Z., Dubois W., Lim S., Callen E., Franco S., Mosaico M., Feigenbaum L., Alt F.W., *et al.* 2008. AID expression levels determine the extent of *cMyc*oncogenic translocations and the incidence of B cell tumor development. *J. Exp. Med.*205:1949–1957. doi: 10.1084/jem.20081007.
70. Teng G., Hakimpour P., Landgraf P., Rice A., Tuschl T., Casellas R., Papavasiliou F.N. 2008.MicroRNA-155 is a negative regulator of activation-induced cytidine deaminase. *Immunity.*28:621–629. doi: 10.1016/j.immuni.2008.03.015.
71. Wandinger S.K., Richter K., Buchner J. 2008. The HSP90 chaperone machinery. *J. Biol. Chem.*283:18473–18477. doi: 10.1074/jbc.R800007200.
72. Whitesell L., Lindquist S.L. 2005. HSP90 and the chaperoning of cancer. *Nat. Rev. Cancer.*5:761–772. doi: 10.1038/nrc1716.

73. Wu X., Geraldes P., Platt J.L., Cascalho M. 2005. The double-edged sword of activation-induced cytidine deaminase. *J. Immunol.* 174:934–941.
74. Young J.C., Hartl F.U. 2000. Polypeptide release by HSP90 involves ATP hydrolysis and is enhanced by the co-chaperone p23. *EMBO J.* 19:5930–5940. doi: 10.1093/emboj/19.21.5930.
75. Young J.C., Agashe V.R., Siegers K., Hartl F.U. 2004. Pathways of chaperone-mediated protein folding in the cytosol. *Nat. Rev. Mol. Cell Biol.* 5:781–791. doi: 10.1038/nrm1492.

2.9. Supplementary material

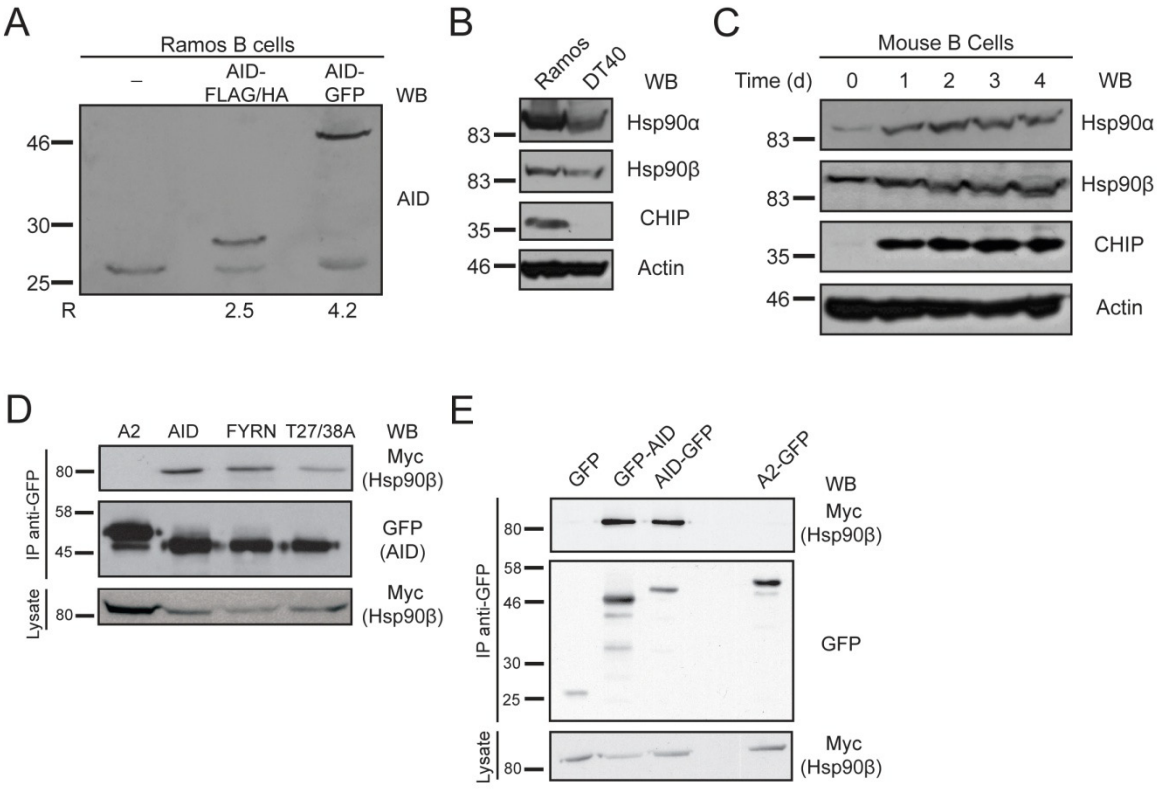

Figure S2.1. Expression levels of AID, HSP90, and CHIP in various B cells and interaction of HSP90 with various AID variants. *(A) Total extracts from parental Ramos B cells and its derived cell lines stably expressing AID-Flag/HA and AID-GFP were analyzed by Western blot (WB) with anti-AID to compare the protein level of each transgenic AID with the endogenous enzyme. Bands were quantified using ImageQuant, and the ratio (R) of tagged to endogenous AID is indicated. One of two independent experiments is shown. (B) Expression of HSP90 isoforms and of the HSP90-associated E3 ubiquitin ligase CHIP (Fig. 2.4) in human Ramos and chicken DT40 B cell lines. Total cell lysate lines were analyzed by Western blot using anti–HSP90-α, anti–HSP90- β, anti-CHIP, and antiactin. Apparent differences in expression between Ramos and DT40 cells most likely reflect variations in the chicken epitopes because anti–HSP90-α and anti-CHIP are mAbs raised against human proteins. One of two*

independent experiments is shown. (C) Kinetics of HSP90 isoforms and CHIP expression in purified naive mouse B cells activated with IL-4 and LPS. Cells were harvested at different time points, lysed, and analyzed by Western blot using anti–HSP90-α, anti–HSP90-β, anti-CHIP, and antiactin. One of two independent experiments is shown. (D) AID oligomerization or phosphorylation is not necessary for HSP90 interaction. Interaction of HSP90 was tested by coimmunoprecipitations with AID mutants carrying the F46A/Y48A/R50G/N51A simultaneous mutations (FYRN), previously shown be defective for oligomerization (Patenaude et al., 2009), or the T27A and T38A phospho-null mutations (T27/38A). (E) The position of the tag on AID does not affect the association with HSP90-β. HEK293T cells were cotransfected with Myc–HSP90-β and GFP-AID, AID-GFP, A2-GFP, or GFP. Anti-GFP immunoprecipitates (IP) were analyzed by Western blot with anti-Myc and anti-GFP. One of three independent experiments is shown.

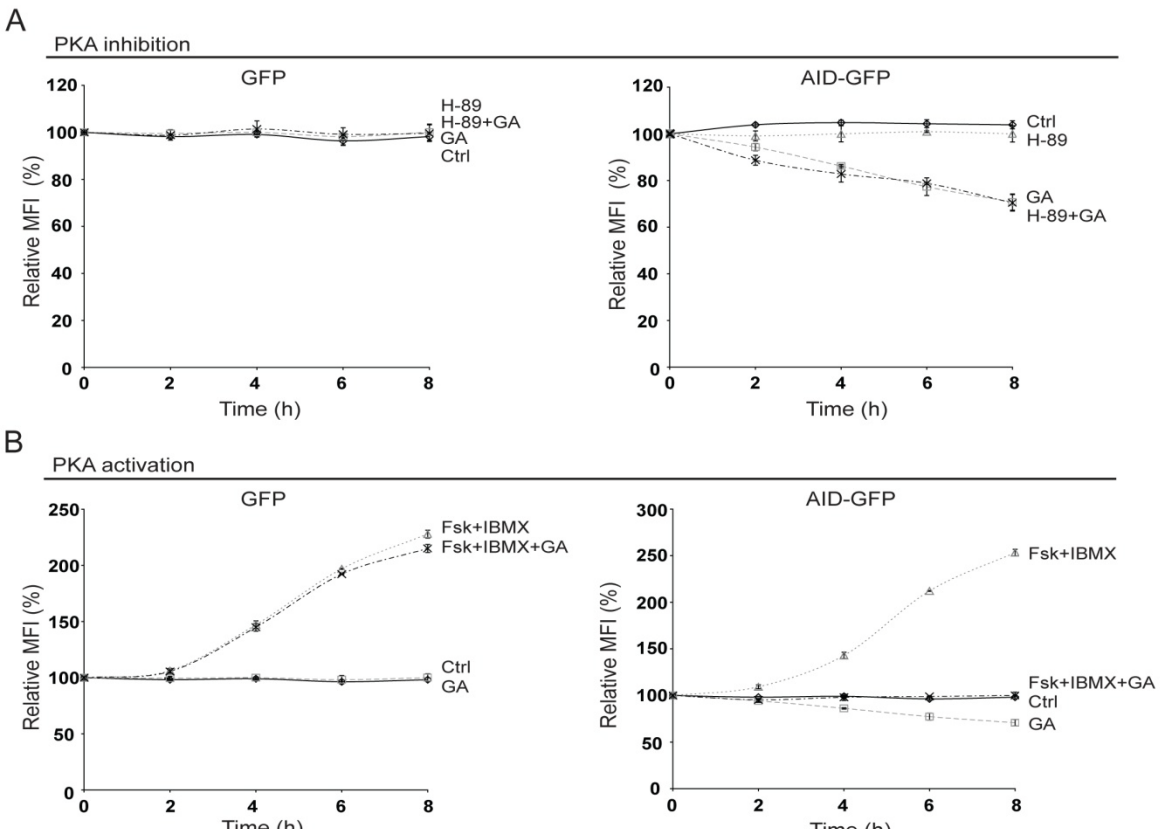

Figure S2.2. AID dependence on HSP90 is unaffected by PKA inhibition or activation. *(A and B) Ramos cells stably expressing AID-GFP were treated with 10 μM of PKA inhibitor H-89 (A) or 50 μM of adenylate cyclase activator forskolin (Fsk) in combination with 100 μM of phosphodiesterase inhibitor IBMX to boost cAMP levels (B) before treating the cells with 2 μM GA or DMSO. AID-GFP was followed by flow cytometry and the MFI (normalized to the t = 0 signal) plotted at different times for each treatment. Note that Fsk + IMBX equally increases the level of GFP and AID-GFP in Ramos cells. The reasons behind this increase are unknown, but although GFP control increases also in the presence of HSP90 inhibition, a similar increase in AID-GFP is totally prevented by GA, confirming the dependence of AID on HSP90. Mean ± SD of triplicates is plotted. One of three independent experiments is shown. Ctrl, control.*

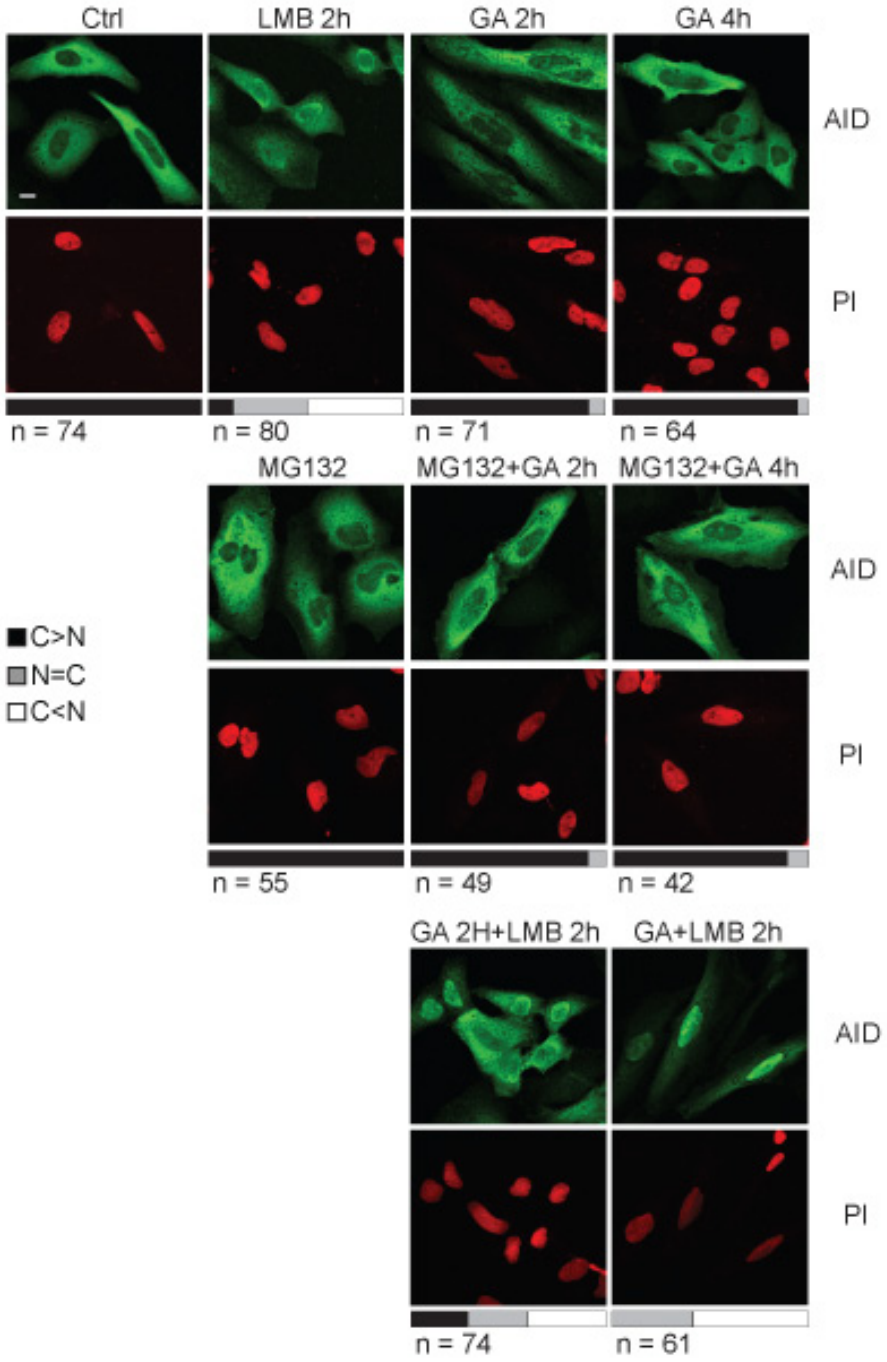

Figure S2.3. HSP90 inhibition does not affect AID compartmentalization. *HeLa cells were transiently transfected with untagged AID and 48 h later treated as indicated (control [Ctrl] = DMSO, 2 μM GA, 50 ng/ml LMB, and 10 μM MG132). AID localization was monitored by immunofluorescence using anti-AID antibody. Treatments GA 2 h + LMB 2 h and GA + LMB 2*

h differ in the time of addition of LMB; in the first case, cells were pretreated with GA before adding LMB, whereas in the latter, both drugs were added simultaneously. Simultaneous inhibition of HSP90 and nuclear export may have a small effect on the speed with which AID accumulates in the nucleus. One possibility is that a proportion of the HSP90-bound AID might be nuclear import competent. So, release of AID from HSP90 by GA treatment at the same time of nuclear export inhibition could allow nuclear import to compete with cytoplasmic AID degradation, leading to an apparent enrichment of AID in the nucleus. However, HSP90 on its own has no effect on AID subcellular distribution, indicating that it is not retaining it in the cytoplasm. C, cytoplasmic; N, nuclear. Bar, 10 μm

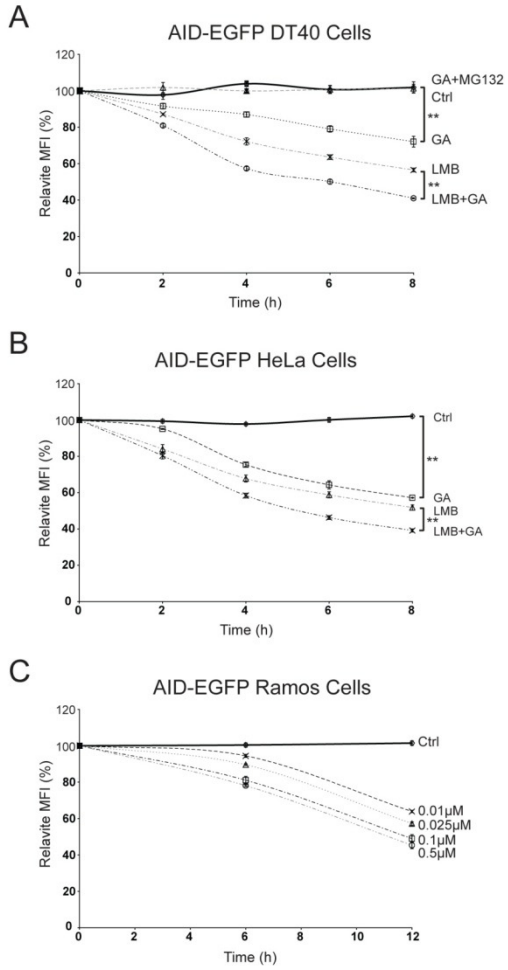

Figure S2.4. The effect of HSP90 inhibition on AID stability is conserved in chicken B cells and human non-B cells and is dose dependent. *(A and B) DT40 Aicda-/- (A) and HeLa cells stably expressing AID-GFP (B) were treated with the indicated combinations of DMSO (Ctrl), 2 μM GA, 50 ng/ml LMB, and/or 10 μM MG132 (30-min pretreatment). The GFP signal was monitored over time by flow cytometry, and the MFI was normalized to the signal at t0 = 100% for each treatment. Means ± SD of triplicates are plotted (**, P < 0.01). One of three independent experiments is shown in each case. (C) Ramos cells stably expressing AID-GFP were treated with DMSO (Ctrl) or the indicated concentrations of GA, and the GFP signal was monitored by flow cytometry. Means ± SD of triplicates are plotted. One of three independent experiments is shown.*

CHAPTER 3: OPTIMAL FUNCTIONAL LEVELS OF ACTIVATION-INDUCED DEAMINASE SPECIFICALLY REQUIRES THE HSP40 DNAJA1

Alexandre Orthwein, Astrid Zahn, Stephen P. Methot, David Godin, Silvo G. Conticello,

Kazutoyo Terada and Javier M. Di Noia

This article has been published in the *EMBO Journal* (2011), doi:10.1038/emboj.2011.417.

3.1. Authors contribution

Alexandre Orthwein designed and performed most of the experiments. Dr Astrid Zahn, Stephen P. Methot, David Godin, Dr Silvo G.Conticello, Dr Kazutoyo Terada and Dr Javier M. Di Noia performed the experiments. Dr Javier M. Di Noia conceived the project and wrote the paper. All authors discussed and interpreted the data and contributed to the final manuscript.

3.2. Abstract

The enzyme activation-induced deaminase (AID) deaminates deoxycytidine at the immunoglobulin genes, thereby initiating antibody affinity maturation and isotype class switching during immune responses. In contrast, off-target DNA damage caused by AID is oncogenic. Central to balancing immunity and cancer is AID regulation, including the mechanisms determining AID protein levels. We describe a specific functional interaction between AID and the HSP40 DnaJa1, which provides insight into the function of both proteins. Although both major cytoplasmic type I HSP40s, DnaJa1 and DnaJa2, are induced upon B-cell activation and interact with AID *in vitro*, only DnaJa1 overexpression increases AID levels and biological activity in cell lines. Conversely, DnaJa1, but not DnaJa2, depletion reduces AID levels, stability and isotype switching. *In vivo*, *DNAJA1*-deficient mice display compromised response to immunization, AID protein and isotype switching levels being reduced by half. Moreover, DnaJa1 farnesylation is required to maintain, and farnesyltransferase inhibition reduces, AID protein levels in B cells. Thus, DnaJa1 is a limiting factor that plays a non-redundant role in the functional stabilization of AID.

3.3. Introduction

Antibody genes Naive B lymphocytes display the prediversified primary repertoire of antibodies. Antibody responses are initiated when a few of them recognize their cognate Ag and proliferate. To be effective, the antibodies produced by the selected B-cell clones still need to undergo affinity maturation to better recognize the Ag; as well as isotype switching to change the default IgM isotype for IgG, IgE or IgA. Antibody affinity maturation and isotype switching absolutely depend on activation-induced deaminase (AID) (Muramatsu *et al*, 2000; Revy *et al*, 2000).

AID deaminates deoxycytidine to deoxyuridine at defined regions of the immunoglobulin (Ig) genes, which initiates somatic hypermutation or gene conversion, the molecular pathways underpinning antibody affinity maturation, as well as class switch recombination (CSR) (Di Noia and Neuberger, 2007; Peled *et al*, 2008; Stavnezer *et al*, 2008). AID deficiency compromises the antibody response resulting in a Hyper-IgM immunodeficiency syndrome (Revy *et al*, 2000). On the other hand, AID contributes to antibody-mediated autoimmune diseases (Zaheen and Martin, 2011) as well as to cancer (Okazaki *et al*, 2003; Pasqualucci *et al*, 2008). The latter ensues from AID mutating tumour suppressor and (proto)-oncogenes as well as from initiating chromosomal translocations as byproducts of CSR (Pasqualucci *et al*, 2001; Ramiro *et al*, 2004; Liu *et al*, 2008; Robbiani *et al*, 2008; Yamane *et al*, 2011). A number of regulatory pathways enforcing an appropriate AID expression pattern, optimal AID mRNA and protein levels as well as modulating its access to the nucleus, favour AID physiological functions over its pathological effects (reviewed in Stavnezer, 2011; Storck *et al*, 2011).

AID post-translational regulation is important for two reasons. First, because upwards and downwards variations in AID levels impact the frequency of both antibody diversification and pathological byproducts (Sernández *et al*, 2008; Teng *et al*, 2008; Robbiani *et al*, 2009; Orthwein *et al*, 2010). Second, because physiological and pathological expression of AID outside germinal centre B cells is well documented (Morgan *et al*, 2004; Pasqualucci *et al*, 2004; Matsumoto *et al*, 2007; Macduff *et al*, 2009; Pauklin *et al*, 2009; Kuraoka *et al*, 2011).

Prominent among AID regulation are subcellular localization and protein stability, which are linked mechanisms that limit AID access to the genome. Indeed, AID is a nucleo-cytoplasmic shuttling protein but most of AID is in the cytoplasm in steady state because nuclear export plus cytoplasmic retention outcompete nuclear import (Brar *et al*, 2004; Ito *et al*, 2004; McBride *et al*, 2004; Patenaude *et al*, 2009; Patenaude and Di Noia, 2010). In turn, cytoplasmic AID is more stable than nuclear AID (Aoufouchi *et al*, 2008; Orthwein *et al*, 2010). We have shown that AID is stabilized in the cytoplasm by the chaperone HSP90, which helps explaining the differences in AID stability depending on its localization (Orthwein *et al*, 2010). We now describe a key role for the HSP40 DnaJa1 in determining AID protein levels and stability.

The prototypical HSP40 is *Escherichia coli* DnaJ, a cochaperone of the bacterial HSP70 DnaK (Langer *et al*, 1992). DnaJ is but one member of a large protein family characterized by the J-domain, which stimulates the ATPase activity of HSP70 as part of a chaperoning cycle that allows folding, conformational changes, degradation and transport across membranes (Walsh *et al*, 2004; Qiu *et al*, 2006; Kampinga and Craig, 2010). The human genome encodes for 41 J-domain proteins, which can be divided into three groups (Qiu *et al*, 2006; Kampinga and Craig, 2010). Type I J-proteins or DjAs (DnaJa1–4) are orthologues of *E. coli* DnaJ and yeast YDJ1. DjAs have an N-terminal J-domain separated by a Gly/Phe-rich linker from the C-terminal substrate-binding region. This region contains three distinct structural domains revealed by the YDJ1 crystal structures (Li *et al*, 2003; Wu *et al*, 2005) (Supplementary Figure S3.1): CTDI, has a hydrophobic pocket that binds certain peptides found in a subset of YDJ1 substrates; CTDII, is made of two Zn-fingers; and CTDIII, which contains most residues involved in DjA dimerization. Additionally, like YDJ1, cytoplasmic DjAs have a short C-terminal extension ending in a farnesylation motive (Kanazawa *et al*, 1997). Type II J-proteins or DjBs (13 members in humans) are orthologues of yeast SIS1 and have CTDI and CTDIII structurally homologous to DjA's (Sha *et al*, 2000) but lack Zn-fingers. Type III J-proteins are very heterogeneous in structure, size and function sharing only the J-domain. Only DjAs and some DjBs behave as HSP70 cochaperones similarly to DnaJ, YDJ1 or SIS1 (Qiu *et al*, 2006; Kampinga and Craig, 2010). Some DjAs additionally work in the HSP90-mediated stabilization pathway (Caplan *et al*, 1995; Kimura *et al*, 1995; Hernández *et al*, 2002).

The expansion and divergence of J-protein paralogs during evolution contrast with the

conservation of many orthologues across vertebrate species (f.i. DnaJa1 is >95% identical between most vertebrates). This is likely to reflect functional specialization and presumably some specific subset of substrates *in vivo*, the mechanistic details of which as well as the identity of the substrates are largely unknown (Kampinga and Craig, 2010). *In-vitro* folding experiments have shown some redundancy but also clear functional differences between the major mammalian cytosolic HSP40s (DnaJa1, DnaJa2, Dnaja4, DnaJb1) (Terada and Mori, 2000; Bhangoo *et al*, 2007; Tzankov *et al*, 2008; Walker *et al*, 2010). The different phenotypes of mice deficient for DnaJa1 (Terada *et al*, 2005) and DnaJb1 (Uchiyama *et al*, 2006) support this view but have not provided yet the identity of any substrates that would depend on one particular HSP40. Here, we identify DnaJa1 as a specific limiting factor in determining AID protein levels and biological activity during the immune response in mice.

3.4. Results

3.4.1. AID interacts with a subset of HSP40 cochaperones and with HSC70

Several results pointed to the interaction between AID and type I HSP40/DjAs. A yeast two-hybrid screening using AID as bait (described in *Conticello et al, 2008*) yielded DnaJa2 (Figure 3.1A). Mass spectrometry then identified DnaJa1 among the proteins copurifying with AID–Flag/HA through two consecutive immunopurifications using agarose-conjugated antibodies (*Orthwein et al, 2010*), which we confirmed here by coimmunoprecipitation (coIP) (Figure 3.1B). Finally, DnaJa1, a2 and a3 were pulled down with AID–GFP using anti-GFP-coated magnetic beads from extracts of stably transfected Ramos B cells (Table 3.1). We verified the DnaJa1–AID interaction by coIP (Figure 3.1C). CoIP also confirmed the preferential association of AID with cytoplasmic DjAs compared with DnaJb1 and DnaJb11, two of the DjB members most similar to DnaJa1 (Figure 3.1D and E). We focused on DnaJa1 and DnaJa2, which are highly induced upon B-cell activation, excluding DnaJa4, which was undetectable (Figure 3.1F) and DnaJa3 because it is mitochondrial (*Qiu et al, 2006*). DjAs have Zn-fingers and E. coli J-proteins non-specifically bind to DNA (*Gur et al, 2005*) but nuclease treatment confirmed that AID interaction with DjAs was not mediated by nucleic acids (Figure 3.1G).

We previously showed that AID interacts with HSP90 while the AID paralogs APOBECs do not despite being up to 60% similar to AID (Orthwein *et al*, 2010). Also here, AID but not APOBEC1, 2 or 3G, interacted with DnaJa1 and DnaJa2 by coIP (Figure 3.2A and B). The major cytosolic HSP70 isoform, HSC70 (encoded by HSPA8) was identified in our three pull-down experiments (Table 3.1). Again, HSC70 coIP with AID but not with any of the APOBECs from transfected cells (Figure 3.2C). Interestingly, the binding of DnaJa1 or DnaJa2 to AID was not equivalent. We used AID–APOBEC2 chimeras, in which 30–50 amino acids long AID regions were replaced by the homologous APOBEC2 residues (Figure 3.2D) (Conticello *et al*, 2008), to probe the interaction between AID and DjAs. Most chimeras partially or completely lost interaction with DnaJa1 while they all interacted with DnaJa2 just

Table 3.1. (Co)chaperones identified by mass spectrometry copurifying with tagged AID from Ramos B cell extracts

HUGO name	Description	AID-Flag/HA Pull down[1]	AID-GFP Pull down		
			Peptide number	Mascot Score	Coverage (%)
DNAJA1	HSP40 homolog, subfamily A, member 1	×	47	1232	65
DNAJA2	HSP40 homolog, subfamily A, member 2		39	1003	60
DNAJA3	HSP40 homolog, subfamily A, member 3		9	207	14
HSPA8	Heat shock 70 kDa protein 8 isoform 1	×	19	517	19
HSP90AA1	Heat shock 90 kDa protein 1, alpha	×	39	1101	25
HSP90AB1	Heat shock 90 kDa protein 1, beta	×	81	2010	48
AHSA1	AHA1, Activator of heat shock 90kDa protein ATPase homolog 1	×	19	480	28
BAG2	BCL2-associated athanogene 2 (HSP70-cochaperone)		16	327	39
TCP1	T-complex polypeptide 1	×	5	154	6
CCT6A	T-complex protein 1 subunit zeta	×	1	84	3
CCT4	T-complex protein 1 subunit delta	×	3	60	7
CCT7	T-complex protein 1 subunit eta		1	56	5

[1] Data from ref [332].

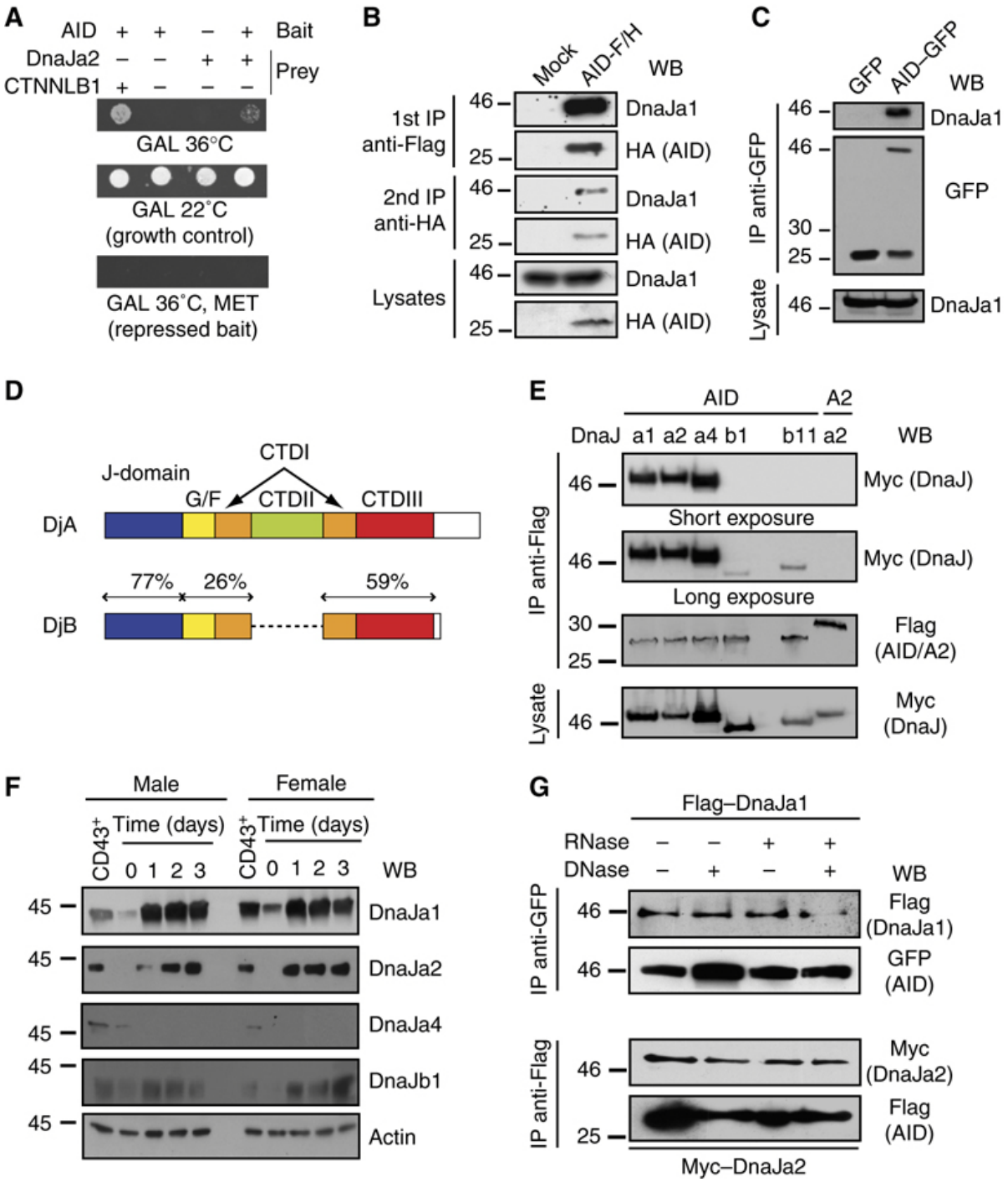

Figure 3.1. AID interacts with type I J-proteins. *(A) Yeast two-hybrid assay showing the interaction of AID with DnaJa2 (truncated clone starting at codon 198). The AID-interacting protein CTNNLB1, isolated in the same screening from a human spleen library (Conticello et*

al, 2008), was used as positive control. GAL, galactose; GLU, glucose; MET, methionine. (B) AID–Flag/HA was sequentially immunoprecipitated using anti-Flag and then anti-HA from extracts of stably expressing Ramos cells and analysed by western blot after each step to detect endogenous DnaJa1. One of the two independent experiments is shown. (C) GFP or AID–GFP were immunoprecipitated from extracts of stably expressing Ramos cells and analysed as in (B). (D) Schematic structure of type I (DjA) and type II (DjB) J-proteins. Similarity values (%) for each structural domain, calculated from the alignment between DnaJa1 and DnaJb1, are indicated. (E) Lysates from HEK293T cells cotransfected with Flag-tagged AID or APOBEC2 (A2) and Myc-tagged versions of the indicated DnaJ proteins were immunoprecipitated with anti-Flag and analysed by western blot. One of the two independent experiments is shown. (F) Expression of selected DnaJ proteins in total cell lysates of mouse naive primary splenic B cells purified by CD43 depletion (>97% CD43$^-$ B220+) either resting (0) or after 1–3 days stimulation with IL-4 and LPS, analysed by western blot using antibodies against DnaJa1, DnaJa2, DnaJa4, DnaJb1 and actin. The CD43-enriched fraction (a heterogeneous mixture including T, B and other leukocytes) was included as an additional control. Exposure times vary between panels and do not accurately reflect relative abundances. (G) AID–GFP or AID–Flag/HA were immunoprecipitated in the presence of 1 mg/ml DNase and/or 0.5 mg/ml RNase using the corresponding anti-tag antibodies from lysates of HEK293T cell contransfected with Flag–DnaJa1 or Myc–DnaJa2, respectively, and analysed by western blot.

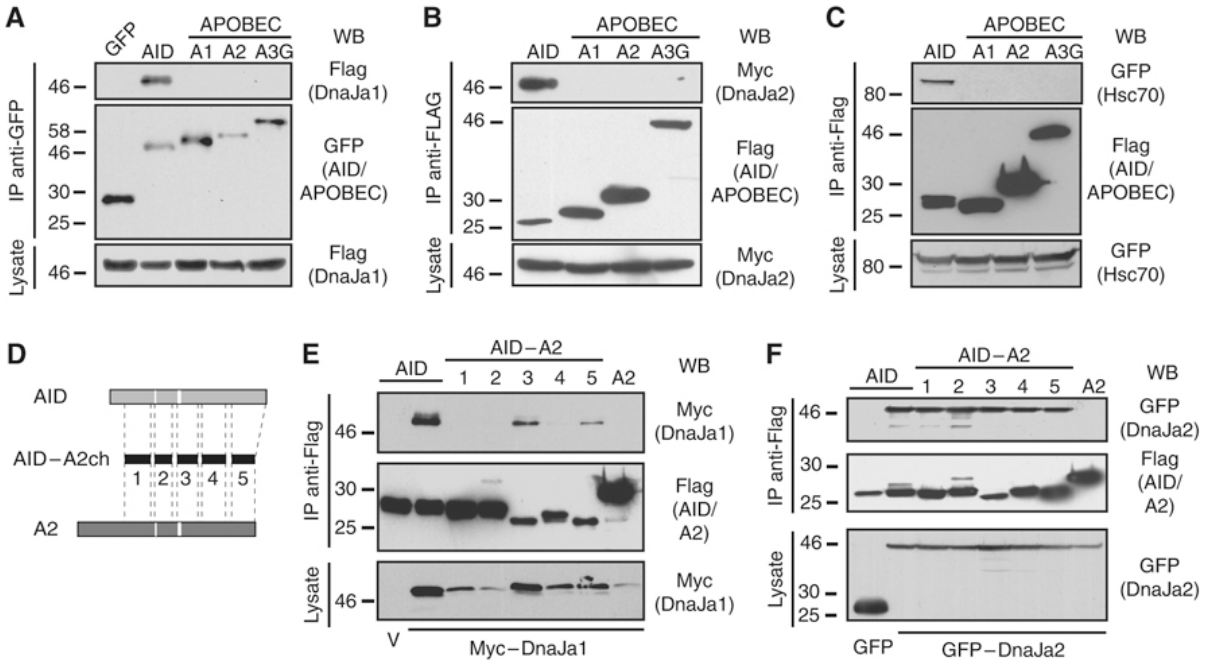

Figure 3.2. AID but not the APOBECs interacts with DnaJa1, DnaJa2 and HSC70 in vitro. *(A) GFP-tagged versions of AID, the indicated APOBECs or GFP control were transiently cotransfected with Flag–DnaJa1 into HEK293T cells and immunoprecipitated with anti-GFP. Immunoprecipitates were probed by western blot. (B) As in (A) but using Flag-tagged versions of AID and the APOBECs cotransfected with Myc–DnaJa2 and immunoprecipitated with anti-Flag. (C) As in (B) but cotransfected with GFP–HSC70. One of the two independent experiments is shown for (A–C). (D) Schematic representation of AID–APOBEC2 chimeric proteins (AID–A2ch1–5) in which either one of the regions from A2 indicated between dotted lines was substituted into the homologous AID region. (E) Flag-tagged versions of AID, A2 or the AID-2 chimeras were immunoprecipitated using anti-Flag from HEK293T cell lysates cotransfected with Myc–DnaJa1 and analysed by western blot. (F) Flag-tagged versions of AID, A2 or the AID-2 chimeras were immunoprecipitated using anti-Flag from HEK293T cell lysates cotransfected with GFP–DnaJa2 and analysed by western blot.*

as well as AID (Figure 3.2E and F). We can conclude that there is a specific association of AID to DjAs and the HSP40–HSP70 chaperoning machinery, which is not detected for the APOBEC enzymes.

3.4.2. DnaJa1 determines the protein levels and activity of AID in B-cell lines

The ability of both DnaJa1 and DnaJa2 to bind to overexpressed AID may not be surprising since they share ~70% similarity (Supplementary Figure S3.1). Notwithstanding this, several reports suggest that they are not completely redundant in their functions (Terada *et al*, 2005; Bhangoo *et al*, 2007; Tzankov *et al*, 2008). We thus tested whether DnaJa1 and/or DnaJa2 were functionally relevant for AID biology, first through overexpression. We used the mouse B-cell line CH12F3 in which stimulation with anti-CD40, TGF-β1 and IL-4 induces AID and isotype switching to IgA (Nakamura *et al*, 1996; Muramatsu *et al*, 1999). Retroviral delivery led to ~2-fold overexpression of DnaJa1 or DnaJa2 in CH12F3 cells (Figure 3.3A and B). Only DnaJa1 overexpression was associated with higher AID protein levels (~1.6-fold) and a significant increase in CSR (Figure 3.3B and C). We obtained similar results in the chicken B-cell lymphoma line DT40, which constitutively expresses AID and undergoes Ig gene conversion (Arakawa *et al*, 2002). Overexpression of DnaJa1, but not of DnaJa2, correlated with increased levels of endogenous AID (Figure 3.3D and E). This was accompanied by a similar increase in the rate of Ig gene conversion as measured by a surface IgM-gain fluctuation assay (Figure 3.3F). In this assay, a proportion of AID-dependent gene conversions in the DT40 CL18 line reverses a frameshift in the IgVλ, thus rescuing IgM expression (Arakawa *et al*, 2002). The median proportion of IgM^+ cells arising during clonal expansion of multiple populations is proportional to the Ig gene conversion activity. In contrast, overexpression of HSC70 or HSP90 had no effect on AID or Ig gene conversion in DT40 (Figure 3.3D–F).

We then asked whether depletion of DnaJa1 would have the predicted opposite effect to its overexpression. We transduced CH12F3 cells with different shRNAs targeting murine DnaJa1. Each of them decreased DnaJa1 protein to a different extent (from ~70 to 30% of the

control; Figure 3.4A and B), which was mirrored by a proportional decrease in isotype switching to IgA (Figure 3.4C and D). Importantly, the relative reductions in CSR and in DnaJa1 were linearly correlated (Figure 3.4E). Depletion of DnaJa1 reduced AID protein levels (Figure 3.4F) but did not affect *Aicda* or Iα germline transcription, nor did it impact cell growth kinetics or HSC70 or HSP90 levels (Supplementary Figure S3.2). In contrast, efficient knockdown of DnaJa2 in CH12F3 cells had no effect on CSR or AID protein levels (Figure 3.4G–J). Finally, DnaJa2 depletion had no effect on AID half-life while DnaJa1 depletion reduced it by half (Figure 3.4K and L). Altogether these results suggest a non-redundant and limiting role for DnaJa1 in determining the levels of functional AID partaking in its stabilization.

3.4.3. Compromised antibody immune response in DnaJa1-deficient mice

The only phenotype observed so far in *DNAJA1*$^{-/-}$ mice is a defect in spermatogenesis likely due to abnormal androgen receptor signalling (Terada *et al*, 2005). Our findings prompted the analysis of the antibody response in these mice. Flow cytometry analysis of lymphocyte populations showed little difference between *DNAJA1*$^{-/-}$ and control mice lymphocyte populations. The only statistically significant changes were a 10% decrease in the proportion of follicular B cells and an ~2-fold increase in marginal zone B cells in the spleen (Supplementary Figure S3.3). In contrast, there was a consistent 50% deficiency in isotype switching to IgG1 in splenic naive B cells from *DNAJA1*$^{-/-}$ mice stimulated *ex vivo* compared with their *DNAJA1*$^{+/+}$ or *DNAJA1*$^{+/-}$ controls (Figure 3.5A and B). The defect in CSR was also clear when comparing cells that have undergone the same number of cell divisions without any sign of increased cell death in *DNAJA1*$^{-/-}$ cells (Figure 3.5C; Supplementary Figure S3.4). In fact, there were no differences in proliferation, *Aicda*, Iμ or Iγ1 germline transcription in *DNAJA1*$^{-/-}$ versus control activated B cells (Supplementary Figure S3.4). Western blots showed a consistent 50% decrease in AID protein levels in activated B cells from each *DNAJA1*$^{-/-}$ mouse compared with their littermate controls (Figure 3.5D). DnaJa1-deficient

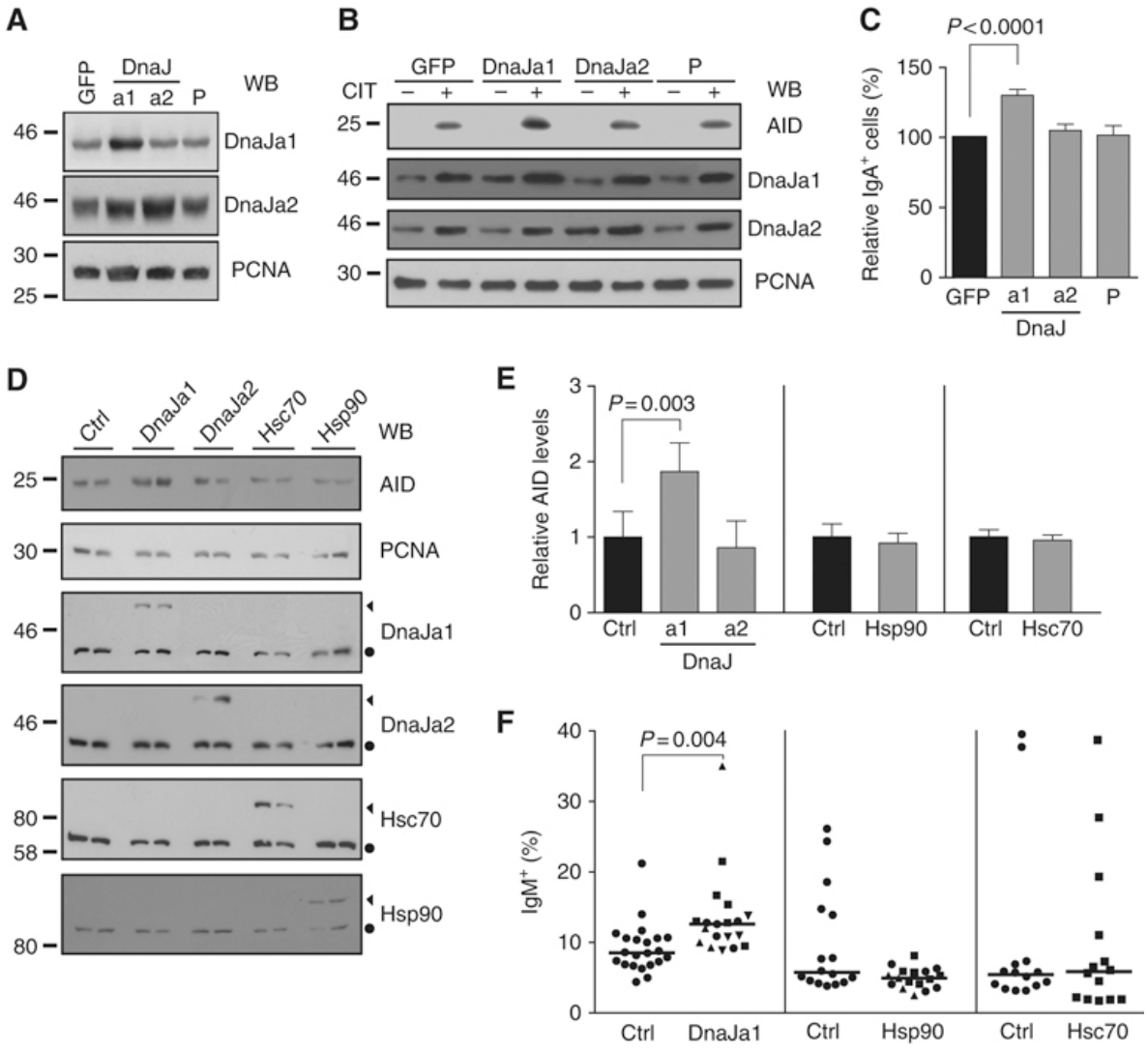

Figure 3.3. DnaJa1 overexpression increases AID levels and antibody gene diversification. *(A) CH12F3 mouse B cells transduced with pMX-ires–GFP vector either empty (GFP) or encoding untagged DnaJa1 or DnaJa2 were sorted for GFP-expressing cells, lysed and analysed by western blot using anti-DnaJa1 or anti-DnaJa2 and anti-PCNA as loading control. P, parental cells. (B) Endogenous AID from transduced and parental CH12F3 cells was analysed by western blot using the indicated antibodies before (–) and 24 h after (+) stimulation with agonist anti-CD40, IL-4 and TGF-β1 (CIT). (C) Proportion of IgA^+ CH12F3 cells at day 3 post-CIT. The mean proportion of IgA^+ cells determined by flow cytometry±s.d.*

from six independent stimulations is plotted for each population relative to the GFP controls set as 100%. (D) Endogenous AID was analysed by western blot using anti-AID on cell lysates from two representative, independently derived stable DT40 cell clones transfected with empty vector (Ctrl) or plasmids encoding myc–DnaJa1, myc–Dnaja2, myc–HSP90 or GFP–HSC70. Specific antibodies against each protein detected the transfected (triangles) and endogenous (circles) proteins. PCNA was used as loading control. (E) Endogenous AID levels quantified by densitometry from unsaturated western blots similar to those shown in (D) and normalized to the corresponding PCNA level. The mean value for AID in control samples set as 1 was used to normalize all values in each experiment. Data expressed as mean values±s.d. of multiple subclones for each construct are plotted (myc–DnaJa1 n=15 and myc–DnaJa2 n=21 versus controls n=18; myc–HSP90β n=11 versus controls n=11; GFP–HSC70 n=12 versus controls n=12). (F) Ig gene conversion frequency in transfected DT40 cells was estimated as the median proportion of IgM^+ cells arising from multiple IgM^- subclones after 4 weeks of clonal expansion. The proportion of $sIgM^+$ for each subclone and median values are plotted. Different symbols indicate subclones obtained from independent transfectants. In all panels, P-values from unpaired, one-tailed t-test are indicated only for significant differences ($P<0.05$).

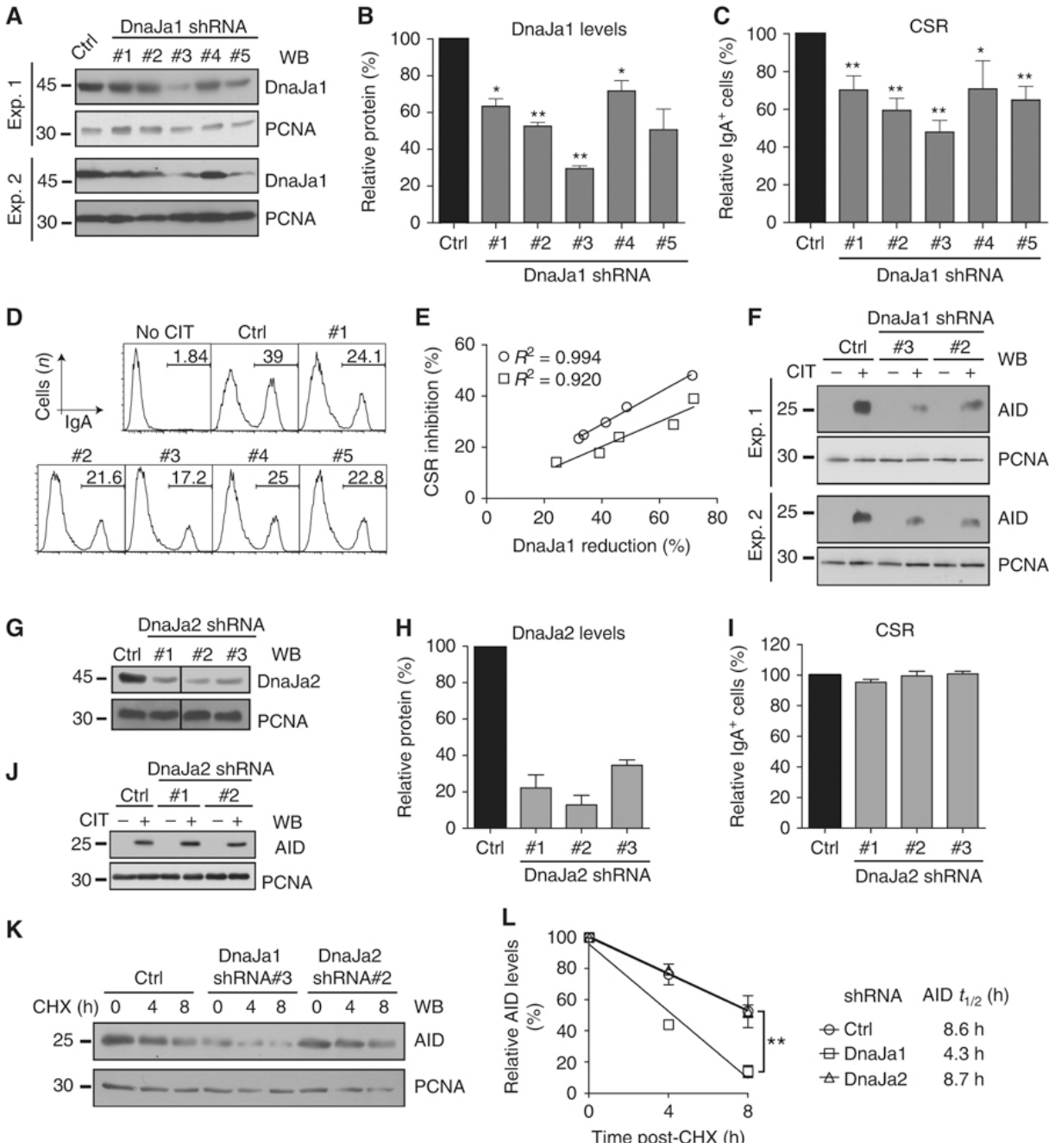

Figure 3.4. Reduced AID levels and CSR in DnaJa1-depleted CH12F3 cells. *(A) CH12F3 cells were transduced with a lentiviral vector carrying control shRNA (Ctrl) or one of five*

different mouse DnaJa1-specific shRNAs (#1–#5), selected on puromycin and analysed by western blot for DnaJa1 and PCNA as loading control. Populations obtained from two independent infections are shown. (B) DnaJa1 protein levels were estimated by densitometry from western blots of three independently infected populations and normalized to each corresponding PCNA signal. Data expressed as mean values±s.d. for each DnaJa1 shRNA are plotted relative to DnaJa1 levels in control shRNA cells set as 100% ($^{*}P<0.01$, $^{**}P<0.0005$, paired one-tailed t-test). (C) Proportion of IgA^{+} cells at day 3 post-CIT as determined for flow cytometry for the same populations used for (B). Data expressed as mean values±s.d. from six independent inductions are plotted relative to the IgA^{+} proportion in control shRNA cells set as 100% ($^{*}P<0.005$, $^{**}P<0.0005$ in paired one-tailed t-test). (D) Representative flow cytometry profiles of transduced CH12F3 stimulated with CIT for 3 days or not (no CIT) and stained with anti-IgA. The proportion of IgA^{+} cells is indicated in each histogram. (E) The mean reduction in CSR versus the mean reduction in DnaJa1 protein for each shRNA was plotted for two independent experiments (circles and squares) and analysed by linear regression. The correlation coefficients (R^2) are indicated. (F) Western blots from two independent experiments measuring AID in CH12F3 cells transduced with control or DnaJa1 shRNAs, 24 h post-CIT. (G) CH12F3 cells transduced with control shRNA (ctrl) or one of three different mouse DnaJa2-specific shRNAs (#1–#3) were analysed as in (A). One of the two independent experiments is shown. (H) DnaJa2 protein levels were estimated and plotted as in (B). (I) The proportion of IgA^{+} cells at day 3 post-CIT in control versus DnaJa2-depleted cells was determined and plotted as in (C). (J) Western blot measuring AID in CH12F3 cells transduced with control or DnaJa2 shRNAs, 24 h post-CIT. (K) AID levels were measured by western blot 24 h post-CIT in CH12F3 cells transduced with shRNA control, DnaJa1 shRNA#3 or DnaJa2 shRNA#2 at 0, 4 and 8 h after treatment with 100 ng/ml CHX. PCNA is used as a loading control. One of the two independent experiments is shown. (L) AID protein levels after CHX treatment were estimated by densitometry from western blots of two independent experiments, normalized to each corresponding PCNA signal. Data expressed as mean values±s.e.m. for each time point are plotted with AID levels at t=0 h set as 100%. AID protein half-lives were calculated and are indicated.

mice had similar IgM and IgG1 serum levels than controls (Figure 3.5E). This was expected since the long lifespan of plasma cells and Ag-mediated selection allow substantial accumulation of switched Ig isotypes in the serum of AID haploinsufficient or *MSH2*$^{-/-}$ mice, which have defects of similar magnitude in AID levels and/or CSR as those we observe (Rada *et al*, 2004; Sernández *et al*, 2008; Takizawa *et al*, 2008). DnaJa1-deficient mice had impaired response to immunization with the T-cell-dependent Ag 4-hydroxy-3-nitrophenylacetyl-conjugated chicken γ globulin (NP-CGG). There was a significant decrease in the titre of total as well as high affinity anti-NP IgG1 during the primary response in all six *DNAJA1*$^{-/-}$ mice analysed (Figure 3.5F), demonstrating a CSR defect *in vivo*. By the secondary response anti-NP titres remained lower than controls in only half of them so only a non-significant trend was apparent when analysing the group (Figure 3.5F). Unlike androgen signalling defects and slightly reduced body weight, which are only found in *DNAJA1*$^{-/-}$ males (Terada *et al*, 2005), there was no sex bias for the phenotypes reported here. We conclude that DnaJa1 deficiency causes a B-cell intrinsic defect in CSR, most likely by reducing AID protein levels, thus delaying antibody immune responses.

3.4.4. DnaJa1-mediated stabilization of AID depends on its farnesylation

Since we have shown that AID is an HSP90 client (Orthwein *et al*, 2010) and HSP40s partake in the HSP90 molecular chaperoning pathway (Kimura *et al*, 1995; Young *et al*, 2004), we sought some evidence linking DnaJa1 to HSP90, in addition to the decrease in AID stability observed after Dnaja1 depletion (see Figure 3.4L). Molecular details about the link between HSP40 and HSP90 *in vivo* are scarce but it has been shown that YDJ1 farnesylation is necessary for maintaining the protein levels of HSP90 clients in yeast (Flom *et al*, 2008). We first determined which domains of DnaJa1 mediated interaction with AID. CoIP of AID with DnaJa1 truncated variants showed that the CTDI, an YDJ1 substrate-binding site (Li *et al*, 2003), as well as the Zn-fingers domain were dispensable for the interaction. Indeed, deletion of the N-terminal 160 amino acids of DnaJa1 destroys the structure of both these domains

(Figure 3.6A and B) but still allowed AID interaction (Figure 3.6C). Mutating the farnesyl group acceptor Cys (Caplan *et al*, 1992) abolished the interaction of DnaJa1 with AID (Figure 3.6D). Thus, the CTDIII and farnesylation are the minimal requirements for DnaJa1 binding to AID. More importantly, while DnaJa1 expression was able to complement the CSR defect in *DNAJA1*$^{-/-}$ B cells, expression of the DnaJa1-C394S was not able to; nor was DnaJa2 further suggesting a specific role for DnaJa1 (Figure 3.6E–G). To confirm that the AID levels were dependent on farnesylated DnaJa1, we treated the Ramos human B-cell line and mouse primary B cells with the farnesyltransferase inhibitor FTI-277. Increasing doses of FTI-277 correlated with the accumulation of non-farnesylated DnaJa1 and a concomitant decrease in AID protein levels in both cases (Figure 3.6H) without affecting *Aicda* transcription (Supplementary Figure S3.5). Furthermore, FTI treatment was able to decrease *ex-vivo* isotype switching to IgG1 in mouse B cells (Figure 3.6I–K). Confocal microscopy of cotransfected cells showed that AID shuttled independently of DnaJa1 localization, which was not obviously affected by the C394S mutation (Figure 3.6L). In fact, DnaJa1 depletion in CH12F3 cells had no effect on AID localization or shuttling (Supplementary Figure S3.5).

Taken together, these results indicate that AID biological activity levels depend on farnesylated DnaJa1 through a mechanism that determines AID protein levels in the cytoplasm.

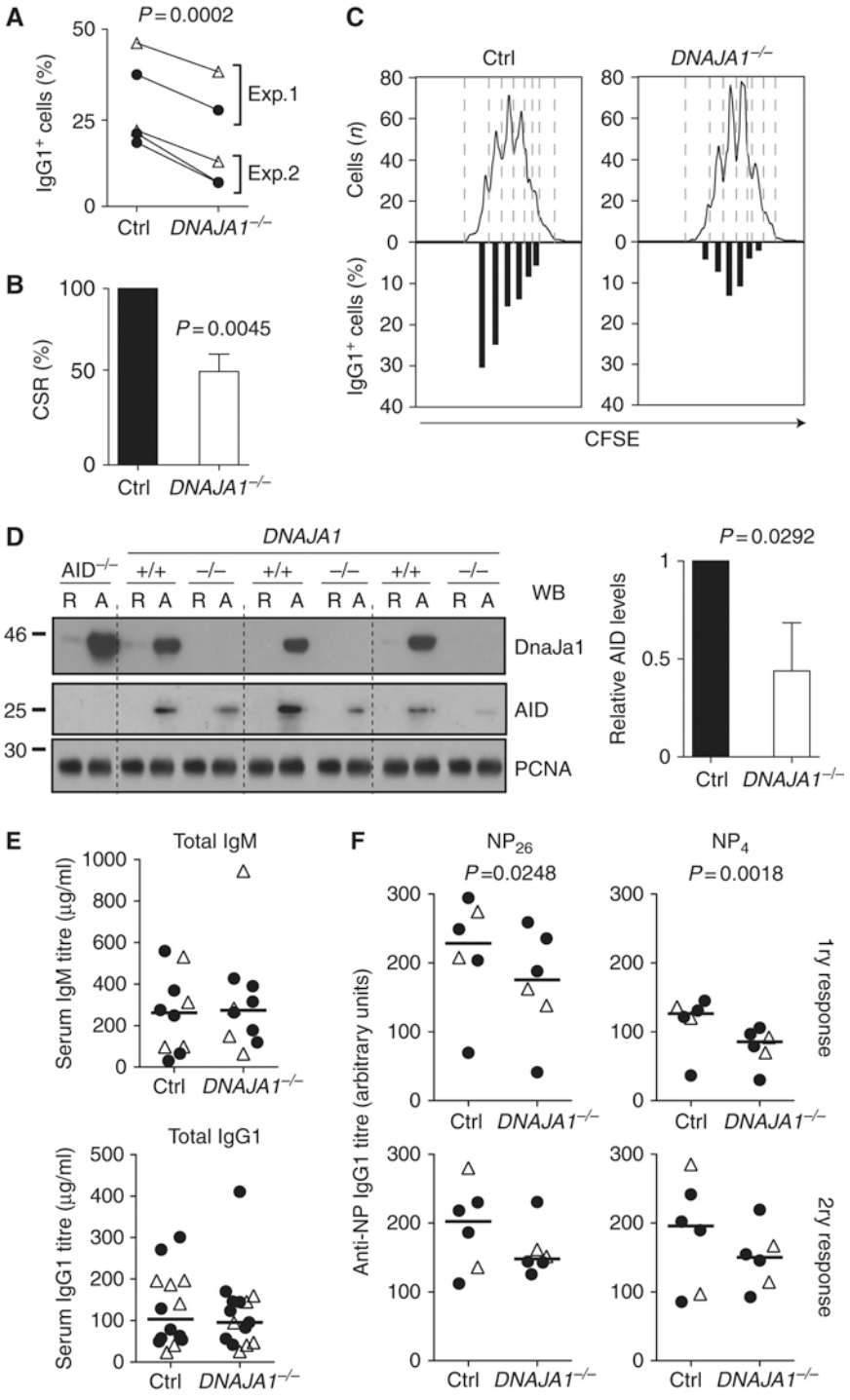

Figure 3.5. Reduced AID protein levels and isotype switching in DNAJA1$^{-/-}$ mice. *(A) Proportion of IgG1^{+} cells in purified splenic B cells from five DNAJA1$^{-/-}$ and control (+/+ or*

+/−) mice 4 days post-IL-4 and LPS stimulation, measured by flow cytometry. Two independent experiments are plotted in the same graph. A line links littermate pairs, with females (triangles) and males (circles) distinguished. (B) The data from (A) were compiled by normalizing the IgG1$^+$ B-cell proportion from each of the DNAJA1$^{-/-}$ mice to its paired control set as 100%. The mean relative CSR±s.d. value for DNAJA1$^{-/-}$ mice is plotted. (C) Splenic naive B cells from DNAJA1$^{-/-}$ mice and littermate controls were loaded with CFSE, activated with IL-4 and LPS for 4 days and the proportion of IgG1$^+$ cells for each cell division determined by flow cytometry. One representative out of four mice pairs analysed is plotted. (D) DnaJa1, AID and PCNA protein levels were analysed by western blot in lysates from resting (R) or LPS + IL-4-activated (A) splenic B cells purified from three DNAJA1$^{-/-}$ and their matched control littermates (pairs separated by dashed lines). AID levels in each mouse were quantified by densitometry, normalized to PCNA levels and the mean±s.d. AID levels for DNAJA1$^{-/-}$ mice relative to their corresponding littermate are plotted in the right-hand panel. (E) Concentration of IgM and IgG1 in sera from 3- to 5-month-old DNAJA1$^{-/-}$ or littermate control mice determined by ELISA. Each dot represents an individual mouse with females (triangles) and males (circles) distinguished. Horizontal lines indicate median values. (F) Six littermate pairs of control and DNAJA1$^{-/-}$ mice were immunized with NP_{15}-CGG and serum samples collected at day 11 post-immunization (primary response). The mice were boosted at day 30 and sera collected again at day 37 (secondary response). Anti-NP IgG1 titres were determined by ELISA using plates coated with NP_{26}-BSA (NP_{26} column, total anti-NP antibodies) or NP_4-BSA (NP_4 column, high affinity anti-NP antibodies). The value for each mouse is indicated, distinguishing females (triangles) and males (circles) with lines indicating median values. In all panels, P-values from paired, one-tailed Student's t-test are indicated only for statistically significant differences ($P<0.05$).

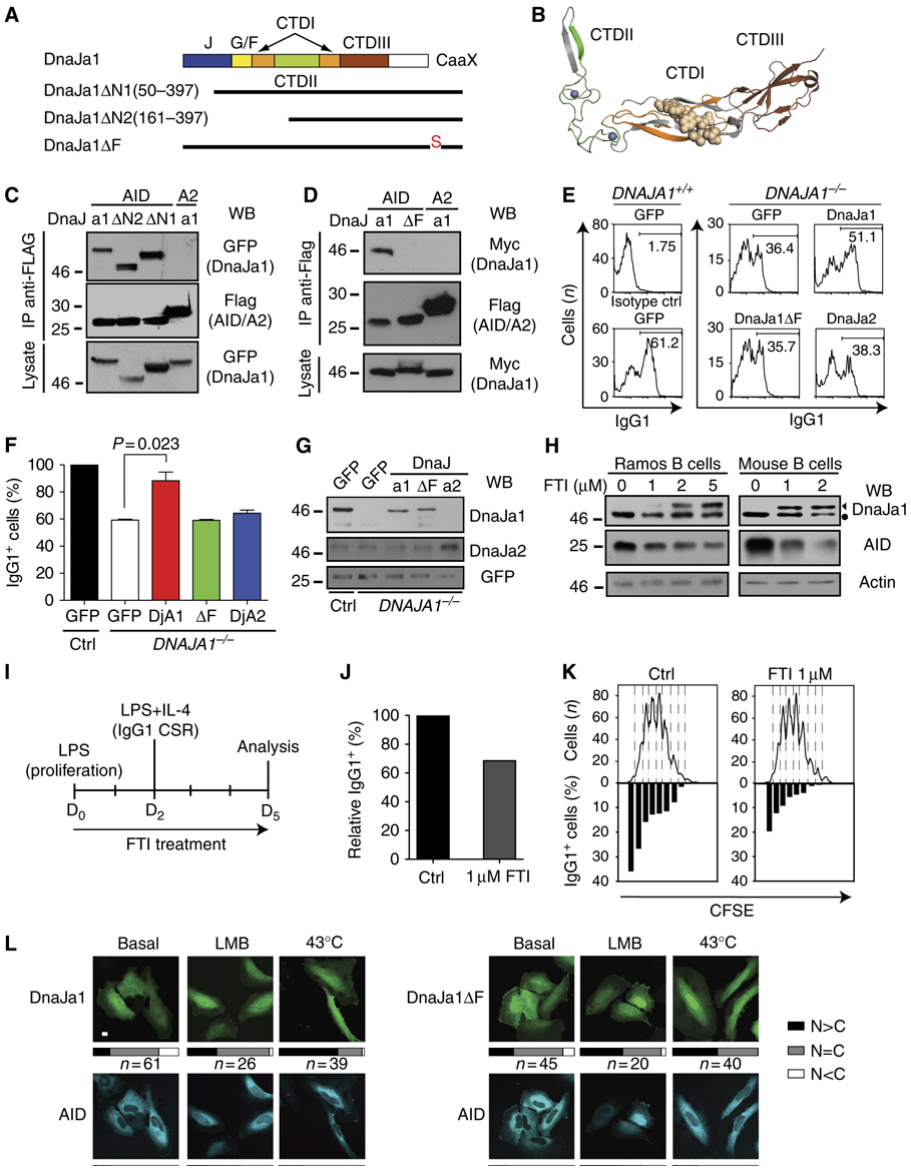

Figure 3.6. DnaJa1 farnesylation is necessary to maintain AID levels and for CSR. *(A) DnaJa1 domains illustration indicating the deletions and single point mutation variants used. CaaX indicates the farnesylation motif where Cys394 was mutated to Ser in DnaJa1ΔF. (B) Crystal structure of the yeast DnaJa1 orthologue YDJ1 substrate-binding domain using the same colour scheme as in (A). Residues homologous to those truncated in DnaJa1ΔN2, which destroy CTDI and II, are in grey. A YDJ1 substrate peptide, which cocrytstalized bound to*

CTDI, is shown as filled model. Data are from pdb1NLT (Li et al, 2003). (C) Flag-tagged AID or A2 were immunoprecipitated using anti-Flag from lysates of HEK293T cells cotransfected with the indicated GFP-tagged DnaJa1 variants and analysed by WB. One of the two independent experiments is shown. (D) Similar experiment to (C) but using Myc-tagged DnaJa1 variants. One of the two independent experiments is shown. (E) Splenic B cells purified from $DNAJA1^{+/+}$ and $DNAJA1^{-/-}$ mice activated with LPS and IL-4, transduced with retroviruses expressing control (GFP), DnaJa1–, DnaJa1ΔF– or DnaJa2-ires–GFP and analysed at day 4 post-infection by flow cytometry. Histograms show GPF-gated cells stained with anti-IgG1 indicating the proportion of $IgG1^+$ cells for one representative out of three mice analysed. (F) Compilation of ex-vivo CSR data from three $DNAJA1^{-/-}$ mice complemented as in (E). The proportion of $IgG1^+$ cells for the $DNAJA1^{-/-}$ B cells expressing each transduced protein is shown relative to the value obtained for the corresponding $DNAJA1^{+/+}$ littermate B cells infected with control GFP vector, set as 100%. Paired, two-tailed t-test was used to evaluate significance ($P<0.05$). (G) Transduced splenic B cells were analysed by western blot with anti-DnaJa1 and anti-DnaJa2 using anti-GFP as loading control. (H) Ramos B-lymphoma cells and purified mouse splenic B cells were treated with the indicated concentrations of the farnesyltransferase inhibitor FTI-277 for 72 h and the levels of AID and farnesylated (circle) and non-farnesylated (triangle) DnaJa1 analysed by western blot. PCNA was used as loading control. (I) Experimental strategy used for assaying CSR in mouse splenic B cells after farnesyltransferase inhibition. D, day. (J) Relative proportion of $IgG1^+$ cells measured by flow cytometry in mouse splenic B cells treated with the farnesyl transferase inhibitor FTI-277 or solvent control as in (I). (K) CFSE staining profile of the cells used for (I) with the proportion of $IgG1^+$ cells for each cell division plotted below. (L) Hela cells cotransfected with GFP-tagged DnaJa1 or DnaJa1ΔF and untagged AID were treated with leptomycin B or heat shocked for 90 min at 43°C, fixed, stained with anti-AID and anti-mouse Alexa-680 and imaged by confocal microscopy. Representative confocal images are shown, scale bar=10 μm. The cellular localization of each protein was classified and the proportion of cotransfected cells showing each distribution is plotted as bars with the number of cells counted indicated (n). C, cytoplasmic; N, nuclear.

3.5. Discussion

We have previously identified AID as an HSP90 client, with this interaction being critical for AID stability (Orthwein et al, 2010). We now show the interaction of AID with the HSP40–HSC70 system and with DnaJa1 in particular. The remarkable specificity of the functional interaction between AID and DnaJa1 in vitro and in vivo provides insight not only on AID biology but also into the functional specialization of HSP40s.

The HSP40–HSP70 system delivers a subset of its substrates to the HSP90 molecular chaperoning pathway for their functional stabilization (Young et al, 2004; Hartl et al, 2011). Indeed, AID folding and stabilization shows similarities with the stabilization cycle of steroid hormone receptors (Picard, 2006; Hartl et al, 2011) and our results suggest the identity and function of many of the molecules involved (Orthwein et al, 2010 and this work). DnaJa1 could act as cochaperone of HSC70 by stimulating its ATPase activity to initiate a folding cycle that is completed by HSP70 nucleotide exchange factors (Young et al, 2004; Kampinga and Craig, 2010; Terada and Oike, 2010). We speculate BAG2 could be the HSC70 nucleotide exchange factor in this cycle since it was the only one that copurified with AID (Table 3.1). HSP40–HSP70 and HSP90 are coupled by STI1/HOP, which has been copurified with AID (Okazaki et al, 2011) and may link the ternary AID–HSP40–HSP70 complex to HSP90.

Although DnaJa1 may well be an HSC70 cochaperone during AID folding, the fact that different HSP40s can at least partially substitute for each other in this role (Johnson and Craig, 2001; Cintron and Toft, 2006), combined with the non-redundant function that DnaJa1 has in determining AID cellular levels in vivo, suggest that DnaJa1 may have another, more specific function. There is considerable genetic and biochemical evidence showing that HSP40 is a functional component of some of the complexes during the HSP90 cycle (Caplan et al, 1995; Kimura et al, 1995; Dittmar et al, 1998; Kosano et al, 1998; Hernández et al, 2002; Wegele et al, 2006; Flom et al, 2008). Three observations suggest that DnaJa1 has a specific role in AID stabilization and link this activity to HSP90. First, AID is less stable in cells depleted of DnaJa1. Second, DnaJa1 farnesylation is required for binding to and optimal CSR activity of AID just as YDJ1 farnesylation is required for its interaction with HSP90 clients (Flom et al,

2008). Cytoplasmic type I HSP40s are isoprenylated (Caplan et al, 1992; Kanazawa et al, 1997). Although farnesylation targets a minor proportion of YDJ1 to intracellular membranes (Caplan et al, 1992), this seems to be in no small part by contributing to protein–protein interactions (Marshall, 1993). Indeed, the farnesylated CTDIII domain of DnaJa1 mediates AID binding instead of the CTDI, a characterized YDJ1 substrate-binding domain (Li et al, 2003). Coincidently, the YDJ1 mutant found to compromise HSP90 client stability in yeast had a single point mutation in CTDIII (Kimura et al, 1995). Third, DNAJA1$^{-/-}$ mice can only make 50% of the normal AID protein levels, indicating that no other J-protein is fully redundant with DnaJa1. DnaJa2 would be the obvious backup in *DNAJA1*$^{-/-}$ cells since it is very similar to DnaJa1, well expressed in B cells and interacts with AID in vitro. However, this is not the case since AID and CSR are reduced proportionally to DnaJa1 depletion in CH12F3 cells (despite abundant DnaJa2 expression) while DnaJa2 depletion or overexpression do not change AID levels, nor can DnaJa2 rescue CSR in *DNAJA1*$^{-/-}$ B cells. An analogous specificity was observed for the potassium channel HERG with depletion of DnaJa1, but not DnaJa2, reducing the intracellular trafficking of HERG (Walker et al, 2010). Interestingly, like AID, HERG stability depends on HSP90 (Ficker et al, 2003). It is interesting that most AID–APOBEC2 chimeras disrupt DnaJa1 binding while they all bind to DnaJa2. One could speculate that DnaJa1 recognizes a certain structure, which would be easily altered in the chimeras, while DnaJa2 may recognize less specific hydrophobic motifs present in earlier folding intermediates. Our results are compatible with some specialization of DnaJa1 to work in the HSP90 pathway but defining this will require further work. The experiments with HERG were done in transfected HeLa cells and there is in fact hardly any data about protein levels of endogenous HSP90 clients in the absence of a particular DjA in any system. In yeast, the STE11 kinase levels are reduced by YDJ1 deficiency (Flom et al, 2008). In DNAJA1$^{-/-}$ mice, the androgen and glucocorticoid receptors were increased (Terada et al, 2005) while AID is reduced. This nicely illustrates the existence of different subpathways for folding/stabilization of HSP90 clients. To the best of our knowledge, AID is the first HSP90 client identified in higher eukaryotes that requires a specific HSP40 to maintain its physiological levels in vivo.

If DnaJa2 is not able to complement DnaJa1 deficiency and DnaJa4, the only other cytoplasmic DjA, is not expressed, it is interesting to speculate how the residual AID is folded

and stabilized in vivo in DNAJA1$^{-/-}$ lymphocytes. Whichever pathway forms AID in DNAJA1$^{-/-}$ B cells, it is clearly not fully redundant with DnaJa1. At least in yeast, the DjB Sis1 can partially substitute for YDJ1 (Lu and Cyr, 1998; Johnson and Craig, 2001). Thus, a DjB like DnaJb1 or even DnaJa2 could substitute for DnaJa1 in early HSP70-assisted AID folding; and/or it could proceed via the CCT chaperonin (Young et al, 2004; Hartl et al, 2011). The end result is anyhow much less efficient. Therefore, we hypothesize that a later DnaJa1 role must exist in vivo, probably by linking AID to the HSP90 pathway, and/or helping in assembling some AID complexes. This role would be more specific than, and thereby limiting, compared with protein biogenesis.

The fact that the response of DNAJA1$^{-/-}$ mice to immunization is so similar to the one observed in AID haploinsufficient mice (Sernández et al, 2008; Takizawa et al, 2008) suggests that the defect in CSR in vivo reflects the 50% reduction in AID rather than any other unknown defect on immune cell function. Beyond any small differences, the phenotypes of Aicda$^{+/-}$ and DNAJA1$^{-/-}$ mice indicate that AID can be limiting for antibody diversification and that reduced AID levels, no matter their cause, are detrimental for antibody responses, which could be exploited for therapy. We have shown that HSP90 inhibitors could be used in this way (Orthwein et al, 2010). DnaJa1 now offers alternative possibilities by linking AID protein levels to protein farnesylation. Farnesyltransferase inhibitors have promising anti-cancer activity but their relevant targets are incompletely understood (Sebti and Der, 2003). We show that it is indeed possible to reduce AID levels and function by using farnesyltransferase inhibitors, which could have therapeutic value to modulate AID.

HSP40s are limiting components in chaperone networks. In E. coli, DnaJ is present in a 1:10 ratio with respect to DnaK (HSP70) (Bardwell et al, 1986). In yeast, the relative molecular proportion of HSP82 (HSP90), SSA1 (HSP70) and YDJ1 can be estimated at ~4:2:1, respectively (Ghaemmaghami et al, 2003). HSP40s can also be functionally limiting in mammalian systems (Minami et al, 1996; Dittmar et al, 1998; Heldens et al, 2010). We indeed see a modest increase in AID levels upon DnaJa1 overexpression. We would not expect a dramatic increase since DnaJa1 surely has many substrates and is distributed among all of them and so would be any excess DnaJa1. Considering that we achieve ~2-fold increase in DnaJa1

levels, the fact that we can see an increase in AID levels and activity is significant and suggest that DnaJa1 is indeed limiting for AID folding and/or stabilization. This raises the question of whether DnaJa1 overexpression in certain cases, such as EBV infection (Young et al, 2008) or its association with antibody-mediated autoimmune diseases (Ramos et al, 2011) could contribute to disease by increasing AID levels.

3.6. Materials and methods

3.6.1. Cell lines and drug treatments

The Ramos Burkitt's B-cell lymphoma lines stably expressing GFP, AID–GFP or AID–Flag/HA have been described (Patenaude et al, 2009; Orthwein et al, 2010). Chicken DT40 B-lymphoma cells stably expressing myc–DnaJa1, myc–DnaJa2 or myc–HSP90β were obtained by electroporation as described (Sale et al, 2001). GFP–HSC70 was introduced by retroviral infection. CH12F3 mouse B cells stably expressing DnaJa1, DnaJa2, AID–GFP or empty vectors were generated by retroviral delivery of pMXs-ires–GFP or pMXs constructs and sorted for GFP-expressing cells. FTI-277 (Sigma-Aldrich) was diluted in water at 1 mM and stored at−20°C. Cycloheximide (CHX) (Sigma -Aldrich) was freshly prepared before each experiment and diluted in EtOH at 100 μg/ml.

3.6.2. Identification of AID partners

The yeast two-hybrid screening has been described (Conticello et al, 2008). Ramos B cells stably expressing AID–GFP were lysed on ice in 50 mM Tris–HCl pH 8, 150 mM NaCl, 1% Triton X-100, 5 mM $MgCl_2$, 100 μg/ml RNase, 100 μg/ml DNase and complete protease inhibitors cocktail (Roche) at 3×10^8 cells/ml. AID was immunoprecipitated using anti-GFP-coated magnetic microbeads and MACS separation columns (Miltenyi Biotec) following the manufacturer's instructions. Eluted proteins were separated by SDS–PAGE and silver stained. Differential bands compared with the pattern obtained from Ramos cells expressing GFP only were excised and submitted to mass spectrometry for protein identification as described (Orthwein et al, 2010).

3.6.3. DNA constructs

AID–GFP, AID–Flag/HA, APOBECs and Myc–HSP90β expression vectors have been

described (Orthwein et al, 2010). Human DnaJa1 in pFlag–CMV2 was a kind gift of Dr HY Zoghbi (Baylor College of Medicine, Houston). Human HSC70 in pEGFP-C1 was a kind gift from Dr U Stochaj (McGill University, Montreal). Human DnaJa2, DnaJa4, DnaJb1 and DnaJb11 were obtained from the I.M.A.G.E consortium. Details on DNA constructs are provided in Supplementary data.

3.6.4. Retroviral and lentiviral infections

Retroviral transduction of mouse primary B cells and DT40 cells was as described (Patenaude et al, 2009). CH12F3 B cells were infected with retroviral particles obtained from the supernatant of HEK293T cell cultures cotransfected with pMXs-ires–GFP or pMXs constructs and vectors expressing MLV Gag-Pol and VSV-G envelope (2:1:1 ratio). Briefly, the retroviral supernatant was spun down at 2000 g for 90 min at 32°C in Retronectin® (Takara)-coated plates before adding 5×10^5 CH12F3 cells and spinning at 600 g for 30 min at 32°C and GFP+ cells were sorted. A similar procedure was used for lentiviral infections. Mission® DnaJa1 and DnaJa2 shRNAs (Supplementary Table SII) cloned in pLKO.1-Puro (Sigma-Aldrich) were contransfected with psPAX2 (Addgene plasmid 12260, deposited by Dr D Trono) and pVSG-G into HEK293T cells to produce lentiviral particles. An shRNA targeting luciferase and cloned in pLKO.1-Puro (Addgene plasmid 1864 deposited by Dr D Sabatini) was used as control. Cells were selected in 0.5 μg/ml puromycin 2 days post-infection.

3.6.5. IP and western blot

Cells were homogenized in lysis buffer (20 mM Tris, pH 8.0, 137 mM NaCl, 10% glycerol, 2 mM EDTA, 1% Triton X-100, 20 mM NaF) 48 h after transfection and extracted on ice for 10 min. The lysate was clarified for 10 min at 12 000 g at 4°C and processed for western blot or IP. Typically, $2–5 \times 10^6$ cells were analysed by western blots to detect endogenous proteins. Tagged proteins were immunoprecipitated using either anti-Flag M2 affinity gel (Sigma-Aldrich) or MACS GFP Isolation kit (Miltenyi Biotech) according to the manufacturer's instructions. Eluates and lysates were analysed by western blot developed with SuperSignal West Pico Chemiluminescent substrate (Thermo Fisher Scientific). Antibodies

used are in Supplementary data.

3.6.6. Monitoring of antibody diversification

Ig gene conversion was estimated by fluctuation assay of the proportion of cells undergoing surface IgM^- to IgM^+ reversion in multiple single cell-derived populations of DT40 cells after 3-week expansion at 41°C. IgM expression was measured by flow cytometry using 1:200 PE- (Southern Biotech) or FITC (Bethyl)-conjugated anti-chicken IgM. IgM to IgA switching was assayed in CH12F3-2 cells activated for 3 days with 1 ng/ml TGF-β1, 10 ng/ml IL-4 and 1 μg/ml agonist anti-CD40 (BD). IgA expression was measured by flow cytometry using anti-mouse IgA-PE antibody (1:200; eBioscience). Ex-vivo isotype switching to IgG1 was assayed using resting splenic B cells purified by CD43 depletion, with CFSE loading to monitor cell division where indicated, as described (Orthwein et al, 2010). Cells were stained with anti-IgG1-biotin (1:200; BD) followed by APC-conjugated anti-biotin (Miltenyi Biotech) and 10 μg/ml propidium iodide. For the complementation assays of $DNAJA1^{-/-}$ B cells using retroviral delivery, double infection was performed at days 2 and 3 post-stimulation and isotype switching analysed at day 5.

3.6.7. Mice immunizations and lymphocyte populations

$DNAJA1^{-/-}$ mice (Terada et al, 2005) were backbred to C57Bl/6J background for at least 11 generations. In all experiments, 2- to 4-month-old, sex-matched littermates were used. $DNAJA1^{+/+}$ and $DNAJA1^{+/-}$ served as controls as they were indistinguishable (our results and Terada et al, 2005). Mice were immunized i.p. with 100 μg of NP_{15}-CGG (Biosearch Technologies Inc., # N5055-5) in 100 μl PBS+100 μl of Imject Alum (Thermo Scientific) and boosted at day 30. Blood samples were collected at -1 day (preimmune), day 11 post-immunization (primary response) and day 37 (secondary response). Anti-isotype-specific antibodies were used to capture and detect total serum IgM and IgG1 in serum by ELISA. Concentrations were estimated from calibration curves made with Ig isotype standards (BD

Pharmingen). Serum levels of total or high affinity anti-NP-specific IgG1 were determined by coating plates with NP_{26}-BSA or NP_4-BSA (5 μg/well), respectively. IgG1 was detected using biotynilated anti-mouse IgG1 (1:1000; BD Pharmingen) followed by HRP-conjugated streptavidin (1:5000; Thermo Scientific) and 2,2 -Azino-bis(3-ethylbenzothiazoline-6-sulfonic acid) substrate, detected by absorbance at 405 nm. Arbitrary units were calculated multiplying OD readings for each point of a curve made of serial twofold dilutions of the serum by the corresponding serum dilution factor. The OD 50% was defined as the anti-NP IgG1 titre for each mouse and plotted divided by 100 (NP_{26}) or 10 (NP_4) to have similar graphing scales. Lymphocyte populations from spleen and thymus were analysed by flow cytometry as detailed in Supplementary data. The IRCM's and Kumamoto University's animal experimentation ethics committees approved all mouse work.

3.6.8. IF and confocal microscopy

HeLa cells were transiently cotransfected with AID in pCDNA3.1 and either pEGFP-C3 DnaJa1 or DnaJa1-C394S using TransIT-LT1 (Mirus). Cells were treated 48 h post-transfection either by heat shocking at 43°C for 90 min, or with 50 ng/ml Leptomycin B or EtOH solvent control for 2 h. Cells were processed for IF and confocal microscopy as described (Patenaude et al, 2009), except that blocking was 5% goat serum 1 mg/ml BSA in PBS overnight at 4°C and we used a mouse anti-AID MAb (clone, 1:500; Invitrogen) for 1 h followed by goat anti-mouse Alexa-680 (1:500; Invitrogen) for 30 min and imaged in an LSM 510 microscope (Zeiss) with a HeNe 633 laser. Control and DnaJa1-depleted CH12F3 cells stably expressing AID–GFP or GFP and DnaJa1 were treated with 10 ng/ml Leptomycin B or EtOH for 2 h. Cells were plated on poly-L-Lysine-treated coverslips and processed for confocal microscopy.

3.7. Acknowlegdments

We thank Drs J Chaudhuri, HY Zoghbi and U Stochaj for reagents, E Massicotte (IRCM flow cytometry facility) and D Faubert (IRCM Proteomics facility) for assistance and Dr C Kosan for discussions. We thank Drs J Young and C Buscaglia for critical reading of the manuscript. This work was funded by a grant from the Canadian Institutes of Health Research (MOP-84543) and supported by a Canadian Fund for Innovation LOF equipment grant to JMDN. AO was supported by a Cole Foundation doctoral fellowship, SPM by a CIHR Master's scholarship. JMDN was supported by a Canada Research Chair Tier 2.

The authors declare that they have no conflict of interest.

3.8. References

1. Aoufouchi S, Faili A, Zober C, D'Orlando O, Weller S, Weill J-C, Reynaud C-A (2008) Proteasomal degradation restricts the nuclear lifespan of AID. J Exp Med 205: 1357–1368
2. Arakawa H, Hauschild J, Buerstedde J-M (2002) Requirement of the activation-induced deaminase (AID) gene for immunoglobulin gene conversion. Science 295: 1301–1306
3. Bardwell JC, Tilly K, Craig E, King J, Zylicz M, Georgopoulos C (1986) The nucleotide sequence of the Escherichia coli K12 dnaJ+ gene. A gene that encodes a heat shock protein. J Biol Chem 261: 1782–1785
4. Bhangoo MK, Tzankov S, Fan ACY, Dejgaard K, Thomas DY, Young JC (2007) Multiple 40-kDa heat-shock protein chaperones function in Tom70-dependent mitochondrial import. Mol Biol Cell 18: 3414–3428
5. Brar SS, Watson M, Diaz M (2004) Activation-induced cytosine deaminase (AID) is actively exported out of the nucleus but retained by the induction of DNA breaks. J Biol Chem 279: 26395–26401
6. Caplan AJ, Langley E, Wilson EM, Vidal J (1995) Hormone-dependent transactivation by the human androgen receptor is regulated by a dnaJ protein. J Biol Chem 270: 5251–5257
7. Caplan AJ, Tsai J, Casey PJ, Douglas MG (1992) Farnesylation of YDJ1p is required for function at elevated growth temperatures in Saccharomyces cerevisiae. J Biol Chem 267: 18890–18895
8. Cintron NS, Toft DO (2006) Defining the requirements for HSP40 and HSP70 in the HSP90 chaperone pathway. J Biol Chem 281: 26235–26244
9. Conticello SG, Ganesh K, Xue K, Lu M, Rada C, Neuberger MS (2008) Interaction between antibody-diversification enzyme AID and spliceosome-associated factor CTNNBL1. Mol Cell 31: 474–484
10. Di Noia JM, Neuberger MS (2007) Molecular mechanisms of antibody somatic hypermutation. Annu Rev Biochem 76: 1–22
11. Dittmar KD, Banach M, Galigniana MD, Pratt WB (1998) The role of DnaJ-like proteins in glucocorticoid receptor.HSP90 heterocomplex assembly by the reconstituted HSP90.p60.HSP70 foldosome complex. J Biol Chem 273: 7358–7366
12. Ficker E, Dennis AT, Wang L, Brown AM (2003) Role of the cytosolic chaperones HSP70 and HSP90 in maturation of the cardiac potassium channel HERG. Circ Res 92: e87–e100
13. Flom GA, Lemieszek M, Fortunato EA, Johnson JL (2008) Farnesylation of Ydj1 is required for *in vivo* interaction with HSP90 client proteins. Mol Biol Cell 19: 5249–5258
14. Ghaemmaghami S, Huh WK, Bower K, Howson RW, Belle A, Dephoure N, O'Shea EK, Weissman JS (2003) Global analysis of protein expression in yeast. Nature 425: 737–741
15. Gur E, Katz C, Ron EZ (2005) All three J-domain proteins of the Escherichia coli DnaK chaperone machinery are DNA binding proteins. FEBS Lett 579: 1935–1939

16. Hartl FU, Bracher A, Hayer-Hartl M (2011) Molecular chaperones in protein folding and proteostasis. Nature 475: 324–332
17. Heldens L, Dirks RP, Hensen SMM, Onnekink C, van Genesen ST, Rustenburg F, Lubsen NH (2010) Co-chaperones are limiting in a depleted chaperone network. Cell Mol Life Sci 67: 4035–4048
18. Hernández MP, Chadli A, Toft DO (2002) HSP40 binding is the first step in the HSP90 chaperoning pathway for the progesterone receptor. J Biol Chem 277: 11873–11881
19. Ito S, Nagaoka H, Shinkura R, Begum NA, Muramatsu M, Nakata M, Honjo T (2004) Activation-induced cytidine deaminase shuttles between nucleus and cytoplasm like apolipoprotein B mRNA editing catalytic polypeptide 1. Proc Natl Acad Sci USA 101: 1975–1980
20. Johnson JL, Craig EA (2001) An essential role for the substrate-binding region of HSP40s in Saccharomyces cerevisiae. J Cell Biol 152: 851–856
21. Kampinga HH, Craig EA (2010) The HSP70 chaperone machinery: J proteins as drivers of functional specificity. Nat Rev Mol Cell Biol 11: 579–592
22. Kanazawa M, Terada K, Kato S, Mori M (1997) HSDJ, a human homolog of DnaJ, is farnesylated and is involved in protein import into mitochondria. J Biochem 121: 890–895
23. Kimura Y, Yahara I, Lindquist S (1995) Role of the protein chaperone YDJ1 in establishing HSP90-mediated signal transduction pathways. Science 268: 1362–1365
24. Kosano H, Stensgard B, Charlesworth MC, McMahon N, Toft D (1998) The assembly of progesterone receptor-HSP90 complexes using purified proteins. J Biol Chem 273: 32973–32979
25. Kuraoka M, Holl TM, Liao D, Womble M, Cain DW, Reynolds AE, Kelsoe G (2011) Activation-induced cytidine deaminase mediates central tolerance in B cells. Proc Natl Acad Sci USA 108: 11560–11565
26. Langer T, Lu C, Echols H, Flanagan J, Hayer MK, Hartl FU (1992) Successive action of DnaK, DnaJ and GroEL along the pathway of chaperone-mediated protein folding. Nature 356: 683–689
27. Li J, Qian X, Sha B (2003) The crystal structure of the yeast HSP40 Ydj1 complexed with its peptide substrate. Structure 11: 1475–1483
28. Liu M, Duke JL, Richter DJ, Vinuesa CG, Goodnow CC, Kleinstein SH, Schatz DG (2008) Two levels of protection for the B cell genome during somatic hypermutation. Nature 451: 841–845
29. Lu Z, Cyr DM (1998) Protein folding activity of HSP70 is modified differentially by the HSP40 co-chaperones Sis1 and Ydj1. J Biol Chem 273: 27824–27830
30. Macduff D, Demorest Z, Harris R (2009) AID can restrict L1 retrotransposition suggesting a dual role in innate and adaptive immunity. Nucleic Acids Res 37: 1854–1867
31. Marshall CJ (1993) Protein prenylation: a mediator of protein-protein interactions. Science

259: 1865–1866
32. Matsumoto Y, Marusawa H, Kinoshita K, Endo Y, Kou T, Morisawa T, Azuma T, Okazaki IM, Honjo T, Chiba T (2007) Helicobacter pylori infection triggers aberrant expression of activation-induced cytidine deaminase in gastric epithelium. Nat Med 13: 470–476
33. McBride KM, Barreto V, Ramiro AR, Stavropoulos P, Nussenzweig MC (2004) Somatic hypermutation is limited by CRM1-dependent nuclear export of activation-induced deaminase. J Exp Med 199: 1235–1244
34. Minami Y, Höhfeld J, Ohtsuka K, Hartl FU (1996) Regulation of the heat-shock protein 70 reaction cycle by the mammalian DnaJ homolog, HSP40. J Biol Chem 271: 19617–19624
35. Morgan HD, Dean W, Coker HA, Reik W, Petersen-Mahrt SK (2004) Activation-induced cytidine deaminase deaminates 5-methylcytosine in DNA and is expressed in pluripotent tissues: implications for epigenetic reprogramming. J Biol Chem 279: 52353–52360
36. Muramatsu M, Kinoshita K, Fagarasan S, Yamada S, Shinkai Y, Honjo T (2000) Class switch recombination and hypermutation require activation-induced cytidine deaminase (AID), a potential RNA editing enzyme. Cell 102: 553–563
37. Muramatsu M, Sankaranand VS, Anant S, Sugai M, Kinoshita K, Davidson NO, Honjo T (1999) Specific expression of activation-induced cytidine deaminase (AID), a novel member of the RNA-editing deaminase family in germinal center B cells. J Biol Chem 274: 18470–18476
38. Nakamura M, Kondo S, Sugai M, Nazarea M, Imamura S, Honjo T (1996) High frequency class switching of an IgM+ B lymphoma clone CH12F3 to IgA+ cells. Int Immunol 8: 193–201
39. Okazaki IM, Hiai H, Kakazu N, Yamada S, Muramatsu M, Kinoshita K, Honjo T (2003) Constitutive expression of AID leads to tumorigenesis. J Exp Med 197: 1173–1181 |
40. Okazaki IM, Okawa K, Kobayashi M, Yoshikawa K, Kawamoto S, Nagaoka H, Shinkura R, Kitawaki Y, Taniguchi H, Natsume T, Iemura S-I, Honjo T (2011) Histone chaperone Spt6 is required for class switch recombination but not somatic hypermutation. Proc Natl Acad Sci USA 108: 7920–7925
41. Orthwein A, Patenaude A-M, Affar EB, Lamarre A, Young JC, Di Noia JM (2010) Regulation of activation-induced deaminase stability and antibody gene diversification by HSP90. J Exp Med 207: 2751–2765
42. Pasqualucci L, Bhagat G, Jankovic M, Compagno M, Smith P, Muramatsu M, Honjo T, Morse III HC, Nussenzweig MC, Dalla-Favera R (2008) AID is required for germinal center-derived lymphomagenesis. Nat Genet 40: 108–112
43. Pasqualucci L, Guglielmino R, Houldsworth J, Mohr J, Aoufouchi S, Polakiewicz R, Chaganti RS, Dalla-Favera R (2004) Expression of the AID protein in normal and neoplastic B cells. Blood 104: 3318–3325
44. Pasqualucci L, Neumeister P, Goossens T, Nanjangud G, Chaganti RS, Kuppers R, Dalla-Favera R (2001) Hypermutation of multiple proto-oncogenes in B-cell diffuse large-cell

lymphomas. Nature 412: 341–346
45. Patenaude AM, Di Noia JM (2010) The mechanisms regulating the subcellular localization of AID. Nucleus 1: 325–331
46. Patenaude AM, Orthwein A, Hu Y, Campo VA, Kavli B, Buschiazzo A, Di Noia JM (2009) Active nuclear import and cytoplasmic retention of activation-induced deaminase. Nat Struct Mol Biol 16: 517–527
47. Pauklin S, Sernández I, Bachmann G, Ramiro AR, Petersen-Mahrt SK (2009) Estrogen directly activates AID transcription and function. J Exp Med 206: 99–111
48. Peled JU, Kuang FL, Iglesias-Ussel MD, Roa S, Kalis SL, Goodman MF, Scharff MD (2008) The biochemistry of somatic hypermutation. Annu Rev Immunol 26: 481–511
49. Picard D (2006) Chaperoning steroid hormone action. Trends Endocrinol Metab 17: 229–235
50. Qiu X-B, Shao Y-M, Miao S, Wang L (2006) The diversity of the DnaJ/HSP40 family, the crucial partners for HSP70 chaperones. Cell Mol Life Sci 63: 2560–2570
51. Rada C, Di Noia JM, Neuberger MS (2004) Mismatch recognition and uracil excision provide complementary paths to both Ig switching and the A/T-focused phase of somatic mutation. Mol Cell 16: 163–171
52. Ramiro AR, Jankovic M, Eisenreich T, Difilippantonio S, Chen-Kiang S, Muramatsu M, Honjo T, Nussenzweig A, Nussenzweig MC (2004) AID is required for c-myc/IgH chromosome translocations *in vivo*. Cell 118: 431–438
53. Ramos PS, Williams AH, Ziegler JT, Comeau ME, Guy RT, Lessard CJ, Li H, Edberg JC, Zidovetzki R, Criswell LA, Gaffney PM, Graham DC, Graham RR, Kelly JA, Kaufman KM, Brown EE, Alarcón GS, Petri MA, Reveille JD, Mcgwin G *et al* (2011) Genetic analyses of interferon pathway-related genes reveal multiple new loci associated with systemic lupus erythematosus. Arthritis Rheum 63: 2049–2057
54. Revy P, Muto T, Levy Y, Geissmann F, Plebani A, Sanal O, Catalan N, Forveille M, Dufourcq-Labelouse R, Gennery A, Tezcan I, Ersoy F, Kayserili H, Ugazio AG, Brousse N, Muramatsu M, Notarangelo LD, Kinoshita K, Honjo T, Fischer A *et al* (2000) Activation-induced cytidine deaminase (AID) deficiency causes the autosomal recessive form of the Hyper-IgM syndrome (HIGM2). Cell 102: 565–575
55. Robbiani DF, Bothmer A, Callen E, Reina-San-Martin B, Dorsett Y, Difilippantonio S, Bolland DJ, Chen HT, Corcoran AE, Nussenzweig A, Nussenzweig MC (2008) AID is required for the chromosomal breaks in c-myc that lead to c-myc/IgH translocations. Cell 135: 1028–1038
56. Robbiani DF, Bunting S, Feldhahn N, Bothmer A, Camps J, Deroubaix S, McBride KM, Klein IA, Stone G, Eisenreich TR, Ried T, Nussenzweig A, Nussenzweig MC (2009) AID produces DNA double-strand breaks in non-Ig genes and mature B cell lymphomas with reciprocal chromosome translocations. Mol Cell 36: 631–641

57. Sale JE, Calandrini DM, Takata M, Takeda S, Neuberger MS (2001) Ablation of XRCC2/3 transforms immunoglobulin V gene conversion into somatic hypermutation. Nature 412: 921–926
58. Sebti SM, Der CJ (2003) Opinion: searching for the elusive targets of farnesyltransferase inhibitors. Nat Rev Cancer 3: 945–951
59. Sernández IV, De Yébenes VG, Dorsett Y, Ramiro AR (2008) Haploinsufficiency of activation-induced deaminase for antibody diversification and chromosome translocations both *in vitro* and *in vivo*. PLoS ONE 3: e3927
60. Sha B, Lee S, Cyr DM (2000) The crystal structure of the peptide-binding fragment from the yeast HSP40 protein Sis1. Structure 8: 799–807
61. Stavnezer J (2011) Complex regulation and function of activation-induced cytidine deaminase. Trends Immunol 32: 194–201
62. Stavnezer J, Guikema JEJ, Schrader CE (2008) Mechanism and regulation of class switch recombination. Annu Rev Immunol 26: 261–292
63. Storck S, Aoufouchi S, Weill J-C, Reynaud C-A (2011) AID and partners: for better and (not) for worse. Curr Opin Immunol 23: 337–344
64. Takizawa M, Tolarová H, Li Z, Dubois W, Lim S, Callen E, Franco S, Mosaico M, Feigenbaum L, Alt FW, Nussenzweig A, Potter M, Casellas R (2008) AID expression levels determine the extent of cMyc oncogenic translocations and the incidence of B cell tumor development. J Exp Med 205: 1949–1957
65. Teng G, Hakimpour P, Landgraf P, Rice A, Tuschl T, Casellas R, Papavasiliou FN (2008) MicroRNA-155 is a negative regulator of activation-induced cytidine deaminase. Immunity 28: 621–629
66. Terada K, Mori M (2000) Human DnaJ homologs dj2 and dj3, and bag-1 are positive cochaperones of HSC70. J Biol Chem 275: 24728–24734
67. Terada K, Oike Y (2010) Multiple molecules of HSC70 and a dimer of DjA1 independently bind to an unfolded protein. J Biol Chem 285: 16789–16797
68. Terada K, Yomogida K, Imai T, Kiyonari H, Takeda N, Kadomatsu T, Yano M, Aizawa S, Mori M (2005) A type I DnaJ homolog, DjA1, regulates androgen receptor signaling and spermatogenesis. EMBO J 24: 611–622
69. Tzankov S, Wong MJH, Shi K, Nassif C, Young JC (2008) Functional divergence between co-chaperones of HSC70. J Biol Chem 283: 27100–27109
70. Uchiyama Y, Takeda N, Mori M, Terada K (2006) Heat shock protein 40/DjB1 is required for thermotolerance in early phase. J Biochem 140: 805–812
71. Walker VE, Wong MJ, Atanasiu R, Hantouche C, Young JC, Shrier A (2010) HSP40 chaperones promote degradation of the HERG potassium channel. J Biol Chem 285: 3319–3329
72. Walsh P, saæ D, Law YC, Cyr DM, Lithgow T (2004) The J-protein family: modulating protein assembly, disassembly and translocation. EMBO Rep 5: 567–571

73. Wegele H, Wandinger SK, Schmid AB, Reinstein J, Buchner J (2006) Substrate transfer from the chaperone HSP70 to HSP90. J Mol Biol 356: 802–811
74. Wu Y, Li J, Jin Z, Fu Z, Sha B (2005) The crystal structure of the C-terminal fragment of yeast HSP40 Ydj1 reveals novel dimerization motif for HSP40. J Mol Biol 346: 1005–1011
75. Yamane A, Resch W, Kuo N, Kuchen S, Li Z, Sun H-W, Robbiani DF, McBride K, Nussenzweig MC, Casellas R (2011) Deep-sequencing identification of the genomic targets of the cytidine deaminase AID and its cofactor RPA in B lymphocytes. Nat Immunol 12: 62–69
76. Young JC, Agashe VR, Siegers K, Hartl FU (2004) Pathways of chaperone-mediated protein folding in the cytosol. Nat Rev Mol Cell Biol 5: 781–791
77. Young P, Anderton E, Paschos K, White R, Allday MJ (2008) Epstein-Barr virus nuclear antigen (EBNA) 3A induces the expression of and interacts with a subset of chaperones and co-chaperones. J Gen Virol 89: 866–877
78. Zaheen A, Martin A (2011) Activation-induced cytidine deaminase and aberrant germinal center selection in the development of humoral autoimmunities. Am J Pathol 178: 462–471

3.9. Supplementary figures

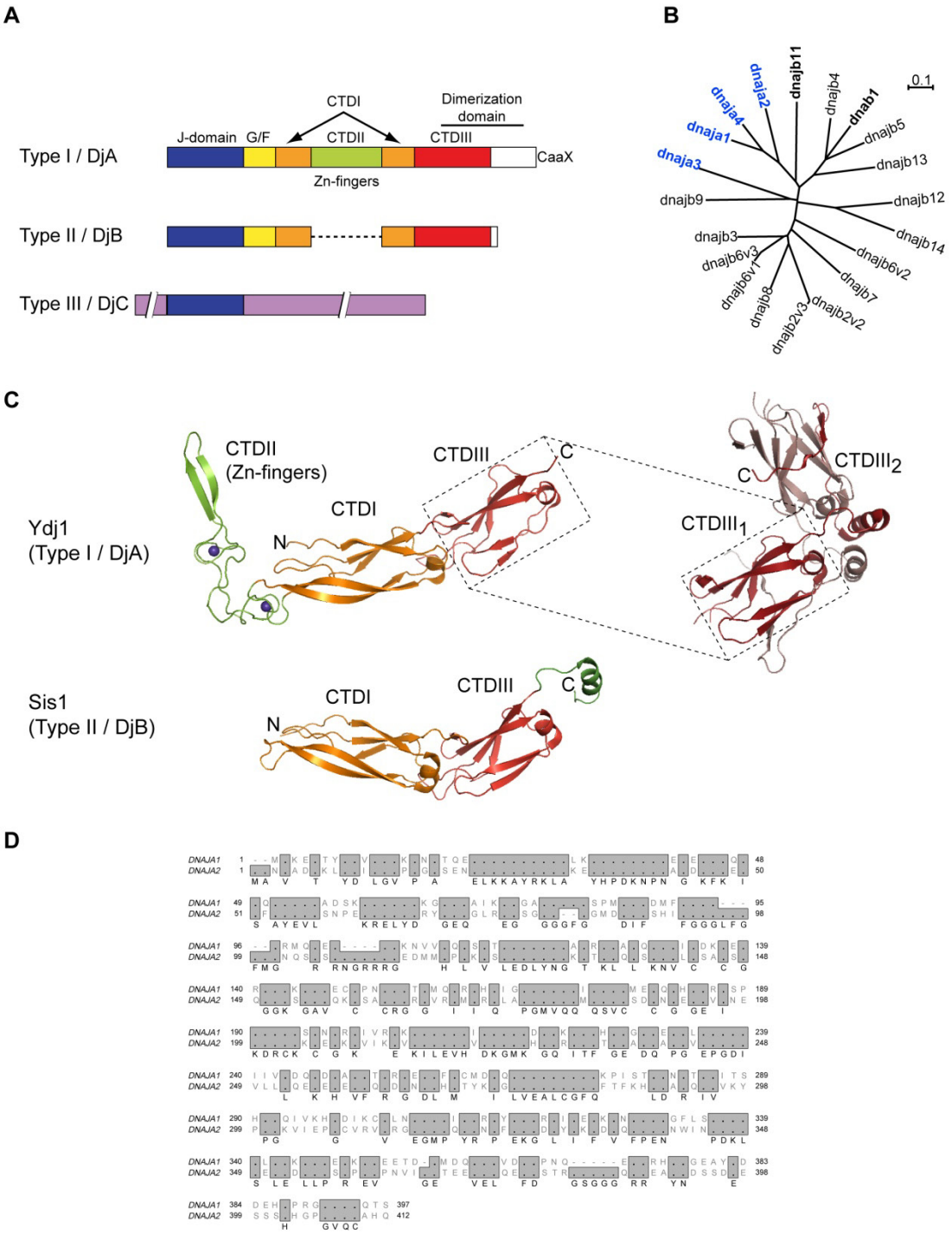

Supplementary Figure S3.1. J-protein family structure and comparison between relevant J-proteins. *(A) Schematic structure of the three types of J-proteins indicating their different domains (except for type IIIs, which do not share a common organization). CaaX indicates the farnesylation motif present in type I J-proteins. CTD, C-terminal domain (B) Similarity between all the mouse type I and II J-proteins was estimated from full length protein alignments using ClustalX (Thompson et al, 2002) and illustrated by a neighbour-joining tree constructed using Seaview 4.2.8 (Gouy et al, 2010). All nodes have significant boostraps (>0.5). Type I HSP40s are in red. Type II HSP40s are in black with the ones used in this work highlighted in bold. (C) Comparison of the three dimensional structure of the yeast type I HSP40 YDJ1 and type II HSP40 Sis1 C-terminal region domains drawn using the same color coding as in (A) drawn in MacPymol using pdbs 1NLT (Li et al, 2003) and 3AGZ (Sha et al, 2000), respectively. The dimerization domain of YDJ1 involving many interspersed hydrophobic residues in CTDIII was drawn from pdb 1XAO (Wu et al, 2005). (D) Protein alignment of mouse DnaJa1 and DnaJa2 with identities shown as grey boxes to highlight the extensive similarity between the two proteins.*

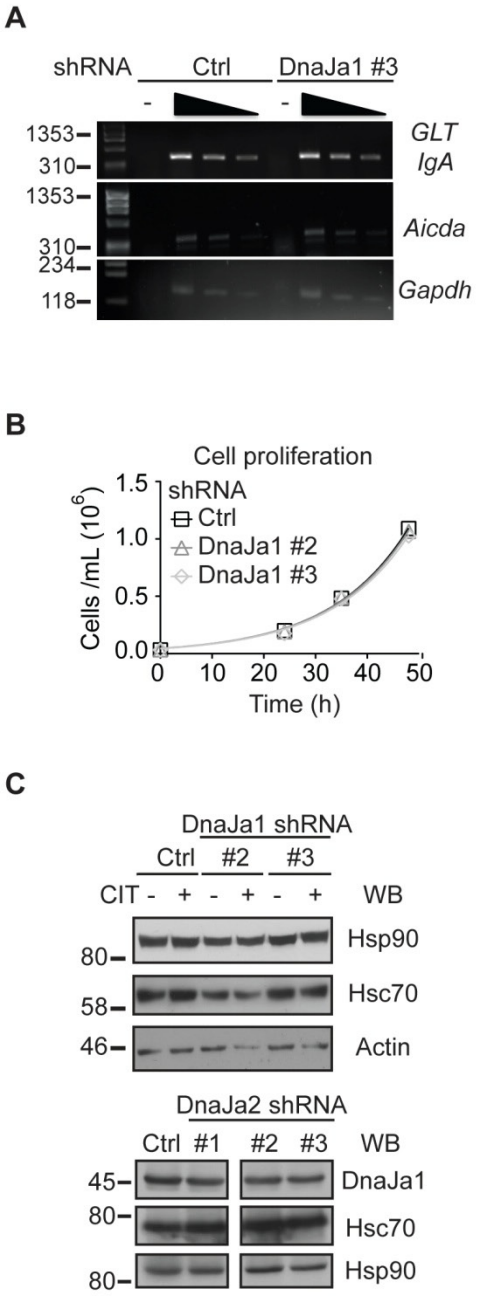

Supplementary Figure S3.2. Analysis of DnaJa1- or DnaJa2-depleted CH12F3 cells. *(A) IgA germline transcript (Iα GLT) and Aicda transcript levels were estimated by semiquantitative RT-PCR on serial two-fold dilution of cDNA made from CH12F3 transduced with control or DnaJa1 shRNA, 24h post-CIT. Gapdh was used as control; – ,reverse transcriptase was*

omitted. (B) Growth curves of the indicated CH12F3 populations starting from 5 x 104 cells/ml were determined by counting live cells in a haemocytometer. Mean ± SEM of duplicate cultures are plotted over time. (C) The effect of DnaJa1 or DnaJa2 downregulation on the levels of HSP90 and HSC70 was monitored by western blot for the indicated CH12F3 populations using actin as loading control.

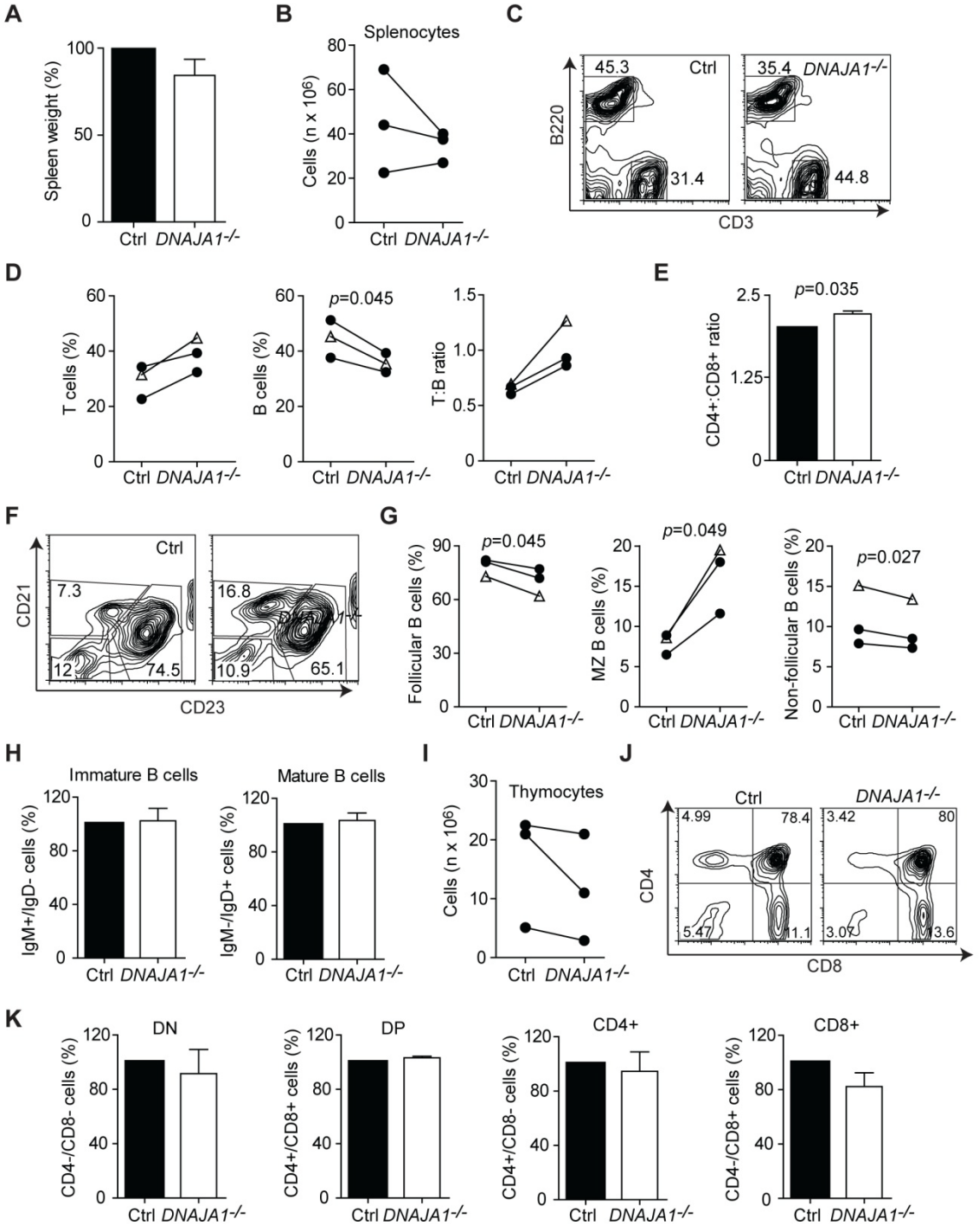

Supplementary Figure S3.3. Analysis of lymphocyte populations in DNAJA1-/- mice. *(A) Mean ± SD spleen weight of three DNAJA1-/- mice normalized to their respective littermate controls. (B) Total number of splenocytes per spleen for three littermate mice pairs. (C)*

Representative flow cytometry profile of splenocytes from DNAJA1-/- and littermate control stained for B and T cells with anti-B220-APC and anti-CD3-PercPCy5.5, respectively. (D) Proportion of T cells (CD3+ B220-), B cells (CD3- B220+) and their ratio in splenic leukocytes for 3 pairs of control and DNAJA1-/- littermates. Each female (triangles) and male (circles) pair is linked by a line. (E) Splenic CD4 to CD8 T cell ratio for three DNAJA1-/- mice calculated from flow cytometry data and plotted as mean ± SD of the value normalized to their littermate controls set at 2. (F) Representative flow cytometry profile of B220+ splenic B cell subpopulations from DNAJA1-/- and littermate control mice. Anti-CD21-FITC versus anti-CD23-PE plot of B220+-gated cells is shown. Marginal zone (MZ) (CD21+ CD23-), follicular (Fo) (CD21+ CD23+) and non-follicular (NF) (CD21- CD23-) B cells are indicated. (G) Proportion of follicular, marginal zone and non-follicular B cells in splenic B cells calculated from flow cytometry data of 3 littermate pairs. (H) Relative proportion of immature and mature B cells in splenic B220+ cells plotted as mean ± SD of the DNAJA1-/- mice values normalized to their littermate controls set as 100%. (I) Total number of thymocytes per thymus for 3 mouse littermate pairs. (J) Representative flow cytometry profile of CD3+ thymic T cells stained with anti-CD4 and anti-CD8. (K) Relative proportion of thymic T cell subpopulations plotted as mean ± SD of three DNAJA1-/- mice normalized to their respective littermate controls set as 100%. In all panels, paired, two-tailed t-test was used with p values indicated where the differences are statistically significant ($p<0.05$).

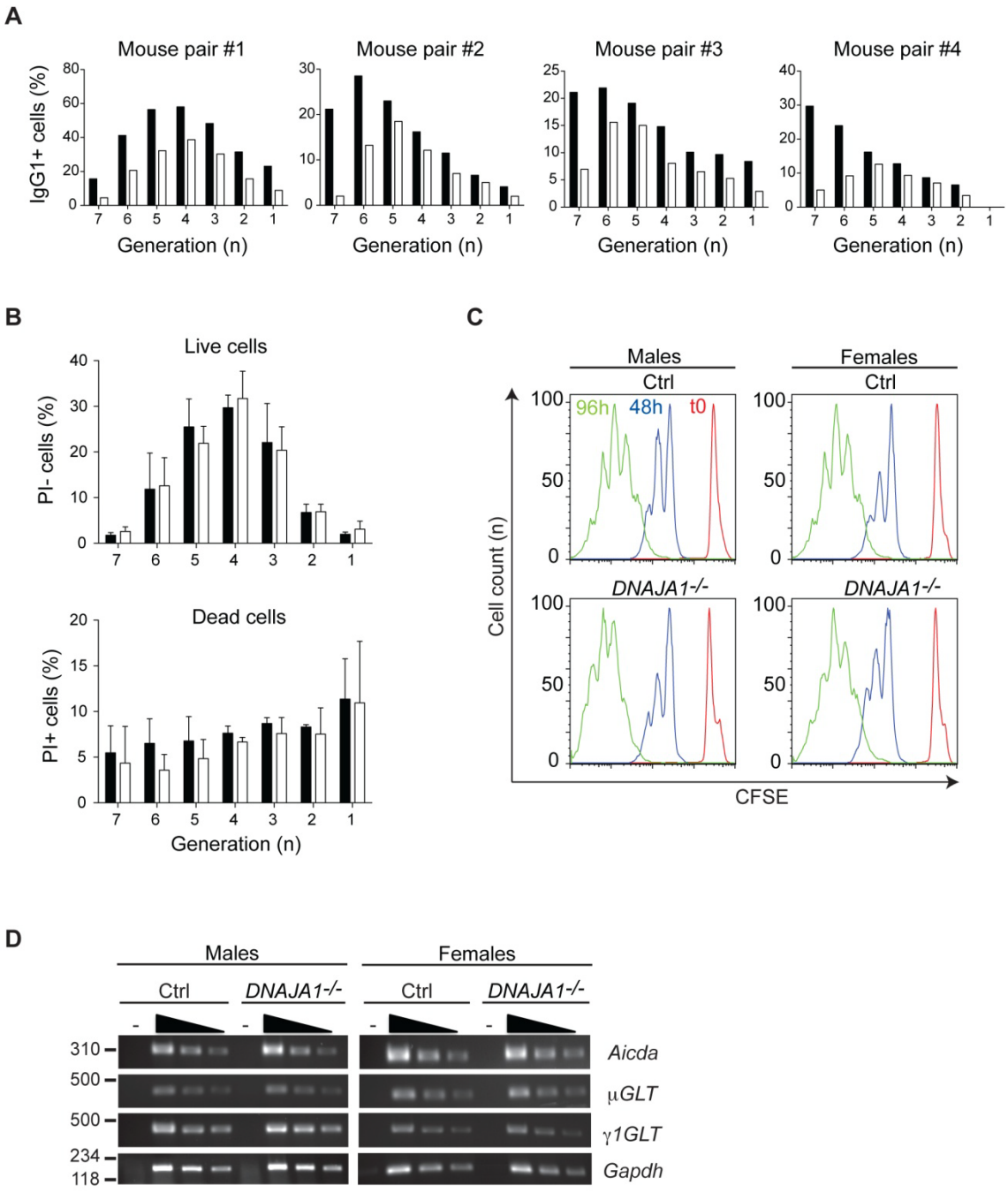

Supplementary Figure S3.4. DNAJA1-/- B cell proliferation, Aicda and IgH sterile transcripts. *(A) Proportion of IgG1+ cells at each generation, as determined from CFSE staining, for four littermate pairs of DNAJA1-/- and control mice. (B) Mean proportion + SD of live (top panel) and dead (bottom panel) cells in each generation for the four DNAJA1-/- (white*

bars) and the four control (black bars) mice shown in (A). The proportion of live cells was calculated by flow cytometry as the proportion of cells at each CFSE peak after gating cells on forward and side scatter and excluding dead cells by propidium iodide (PI) staining. Dead cell proportion was calculated by gating cells on forward and side scatter, then plotting CFSE versus PI and determining the proportion of PI+ cells for each generation. (C) Resting splenic B cells from DNAJA1-/- and littermate control mice were loaded with CFSE and analyzed at 0, 48 and 96 h poststimulation by flow cytometry. Profiles from all time points are plotted superimposed in the same histogram. (D) Aicda transcript and IgM (μ) and IgG1 (γ1) germline transcripts (GLT) estimated by semi-quantitative RT-PCR using 2-fold serial dilutions of cDNA made from DNAJA1-/- and littermate control mice B cells. Gapdh was used as control; –, samples in which reverse transcriptase was omitted.

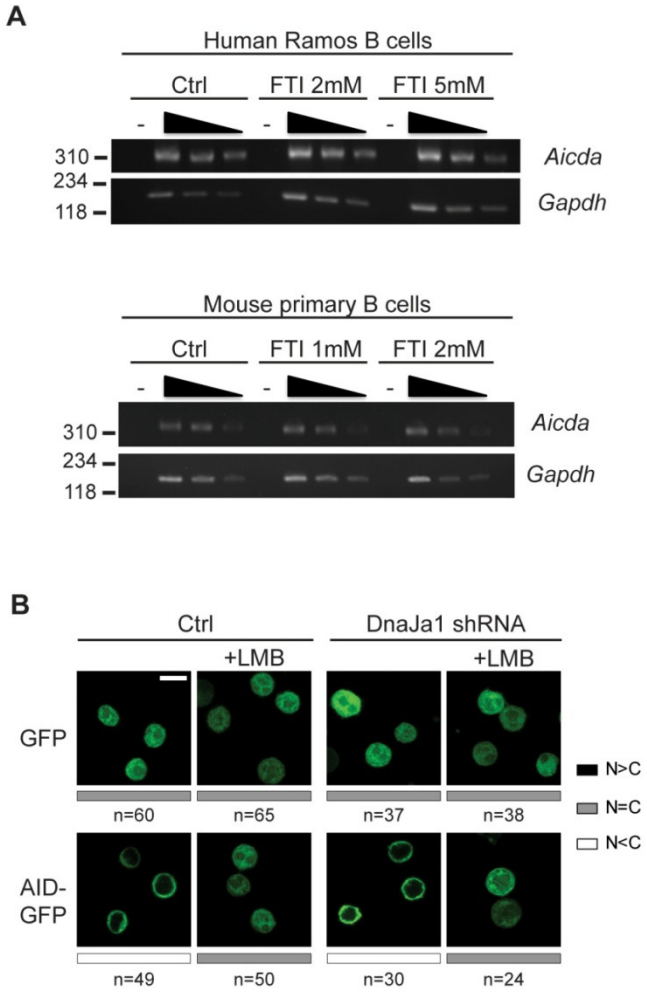

Supplementary Figure S3.5. DNAJA1-/- B cell proliferation, Aicda and IgH sterile transcripts. *(A) Aicda transcript levels were estimated by semi-quantitative RT-PCR using 2-fold serial dilutions of cDNA prepared from mock or FTI-277-treated Ramos and mouse primary B cells. (B) Control or DnaJa1-depleted CH12F3 cells expressing AID-GFP or GFP and DnaJa1 were treated with leptomycin B to monitor the effect of DnaJa1depletion on AID subcellular localization. Representative confocal images are shown, scale bar 10 μm. The cellular localization of each protein was classified and the proportion of cells showing each distribution is plotted as bars with the number of cells counted indicated (n). C, cytoplasm; N, nuclear.*

3.10. Supplementary materials and methods

3.10.1. DNA constructs.

DnaJa1 was subcloned as a BglII-BamHI fragment into pEGFP-C1 and pcDNA3.1-myc by using oligonucleotides AO14 and AO6 (see oligonucleotide sequences in Supplementary Table SI). DnaJa1 C394S (ΔF) point mutation was introduced by Quickchange (Stratagene) using oligonucleotides AO58 and AO59. DnaJa1 truncations were generated by using internal restriction site: HindIII-BamHI fragment subcloned into pEGFP-C3 for DnaJa1ΔN1(50-397) and EcoRI-BamHI fragment subcloned into pEGFP-C1 for DnaJa1ΔN2(161-397). hDnaJa2 was subcloned into pEGFP-C1 as a SalI-BamHI fragment or into pcDNA3.1-myc as BglII-BamHI fragment. hDnaJa4 was subcloned as a BlgII-BamHI fragment, hDnaJb1 and hDnaJb11 as BamHI-EcoRI fragments into pcDNA3.1-myc using oligonucleotides AO16-AO17, AO18-AO19 and OJ110-OJ111 respectively. hDnaJa1 and its respective ΔF mutant were subcloned as a BamHI-NotI fragment into pMX-iresGFP using oligonucleotides AO66- AO67 and AO66-AO68 respectively. hDnaJa2 was excised from pcDNA3.1-myc as a BamHI-EcoRI fragment and subcloned into pMX-iresGFP. GFP-HSC70 was excised as a HindIII-XhoI fragment and subcloned in pMXs vector.

3.10.2. Antibodies used for western blot.

Anti–EGFP–HRP (1:3,000; Miltenyi Biotec), anti– Myc-HRP (1:3,000 Miltenyi Biotec), anti–Flag-HRP (1:3,000 Sigma-Aldrich), anti- HSP90 (1:3,000 sees both isoforms; BD), anti-AID (1:1,000 Cell Signaling Technology), anti-actin (1:3,000; Sigma-Aldrich), anti-PCNA (1:5,000 PC-10; Abcam), anti-DnaJa1 (1:3000 KA2A5; Thermo Scientific), anti-HA (1:3000 CAB3872; Thermo Scientific), anti-HSC70 (1:2000 SMC-106A; Stressmarq). Polyclonal rabbit serum recognizing mouse AID (1:500) was a kind gift from Dr J. Chaudhuri (Sloan-Kettering Institute, New York). Specific antibodies against DnaJa2, -a4 and –b1 have been described (Abdul et al, 2002; Terada & Mori, 2000). Secondary antibodies used were goat anti–mouse Ig-HRP and anti–rabbit Ig-HRP (1:10,000; Dako) and goat anti–rat Ig-HRP

(1:5,000; Millipore).

3.10.3. Lymphocyte population analysis.

Mice were euthanized, organs collected and grinded through a 70 μm cell strainer. Splenocytes were centrifuged at 400 x *g* for 10 min at RT and resuspended in 1 ml erythrocytes lysis buffer for 5 min at RT, washed and resuspended in PBS. Aliquots of 5 x 105 cells were stained for 15 min using combinations of the following antibodies (BD Pharmingen): anti-B220APC, anti-CD3PerCCPCy5.5, anti- CD4PE, anti-CD8APC, anti-CD21FITC and anti-CD23PE (all 1:200); anti-IgMPE and anti- IgDFITC (both 1:100). Dead cells were excluded by staining with 10 μg/ml propidium iodide. Data was acquired in a FACSCalibur (BD Biosciences) and analyzed using FlowJo (Tree Star, Inc).

3.10.4. Semi-quantitative RT-PCR.

Total RNA was extracted with TRIzol® (Invitrogen). cDNA was synthesized by random priming using the ProtoScript® M-MuLV Taq RTPCR kit (NEB). Mouse and human *Aicda* transcripts were amplified using oligonucleotides AO43/AO44 and OJ500/OJ538 respectively. IgM (μ), IgA (Iα) and IgG1 (γ1) germline transcripts were amplified using oligonucleotides OJ530/OJ531, AO45/AO46 and AO39/AO40 respectively. *Gapdh* transcripts were amplified using oligonucleotides provided by the manufacturer.

3.11. Supplementary references

1. Abdul KM, Terada K, Gotoh T, Hafizur RM, Mori M (2002) Characterization and functional analysis of a heart-enriched DnaJ/ HSP40 homolog dj4/DjA4. *Cell Stress Chaperones* **7:** 156-166
2. Gouy M, Guindon S, Gascuel O (2010) SeaView version 4: A multiplatform graphical user interface for sequence alignment and phylogenetic tree building. *Mol Biol Evol* **27:** 221-224
3. Li J, Qian X, Sha B (2003) The crystal structure of the yeast HSP40 Ydj1 complexed with its peptide substrate. *Structure* **11:** 1475-1483
4. Sha B, Lee S, Cyr DM (2000) The crystal structure of the peptide-binding fragment from the yeast HSP40 protein Sis1. *Structure* **8:** 799-807
5. Terada K, Mori M (2000) Human DnaJ homologs dj2 and dj3, and bag-1 are positive cochaperones of HSC70. *J Biol Chem* **275:** 24728-24734
6. Thompson JD, Gibson TJ, Higgins DG (2002) Multiple sequence alignment using ClustalW and ClustalX. *Curr Protoc Bioinformatics* **Chapter 2:** Unit 2 3
7. Wu Y, Li J, Jin Z, Fu Z, Sha B (2005) The crystal structure of the C-terminal fragment of yeast HSP40 Ydj1 reveals novel dimerization motif for HSP40. *J Mol Biol* **346:** 1005-101

CHAPTER 4: INSTRINSIC DETERMINANTS OF PROTEIN STABILITY LIMITING AID ACTIVITY IN ANTIBODY DIVERSIFICATION

Alexandre Orthwein, Stephen P. Methot, Anil Eranki, Anne-Marie Patenaude

and Javier M. Di Noia

This manuscript is formatted for the *Journal of Biological Chemistry*

4.1. Authors contribution

Alexandre Orthwein designed and performed most of the experiments. Stephen P. Methot and Anne-Marie Patenaude performed the experiments of confocal microscopy. Anil Eranki performed the *E.coli* assay experiments. Alexandre Orthwein and Dr Javier M. Di Noia conceived the project and wrote the paper. All authors discussed and interpreted the data and contributed to the final manuscript.

4.2. Abstract

Activation Induced Deaminase (AID) and the APOBEC proteins constitute a group of cytidine deaminases acting on DNA and/or RNA with diverse physiological functions. AID targets the immunoglobulin genes thereby initiating antibody somatic hypermutation and isotype class switching during immune responses. Regulation of AID protein levels is central to balancing efficient immunity with AID pathological roles in cancer and autoimmunity. In this study, we report that AID is instrinsically less stable than its APOBEC paralogs. This, at least partially explains why AID stability depends on constant chaperoning by the HSP90 system, while we find that APOBEC1, 2 and 3G are not even indirectly depending on HSP90. We identify AID N-terminal aspartic acid residue and an internal PEST-like motif as destabilizing modulators of AID protein turnover. Disruption of these motifs impacts AID levels by increasing its stability and concomitantly upregulates antibody diversification. Moreover, we find that cytoplamic polyubiquitination and proteasomal degradation of AID is not dependent on its internal lysine residues. Furthermore, the addition of a HA tag at the N-terminus of AID did not prevent its cytoplasmic protein turnover, suggesting a non-canonical way of targeting AID to the proteasome. Thus, we show that there is a direct contribution of AID intrinsic instability to regulate the efficiency of antibody diversification.

4.3. Introduction

The Activation Induced Deaminase (AID)/APOBEC family comprises several members that act as DNA and/or RNA mutators to perform their biological roles (1). While the functions of APOBEC2 and APOBEC4 are still unclear, AID, which is considered to be one of the ancestral members of this family, plays a central role in adaptive immunity by initiating the diversification of the peripheral antibody repertoire during the GC reaction (2, 3). APOBEC1, on the other hand, edits apolipoprotein B mRNA, which generates a premature stop codon and leads to the expression of a tissue-specific truncated apolipoprotein B polypeptide chain (4, 5). Finally, the APOBEC3 subgroup is important for the innate immune response to retroviruses and protects against the transposition of endogenous retroelements by deaminating their cDNA (6).

AID catalyzes the deamination of deoxycytidine to deoxyuridine at defined regions of the immunoglobulin (Ig) genes, initiates somatic hypermutation (SHM) and class switch recombination (CSR) (7-9). SHM entails the introduction of point mutations within the IgV region and underpins affinity maturation of the antibody response (8, 9). In addition, AID targets the DNA regions immediately preceding the constant exons that encode for the different antibody isotypes. Processing of the deoxyuridine leads to the generation of a double-strand break intermediate and results in CSR, replacing the default IgM isotype for either IgG, IgE or IgA (7). AID deficiency compromises the antibody response leading to a hyper-IgM immunodeficiency syndrome and to a susceptibility to specific autoimmune manifestations (3, 10-12). On the other hand, AID overexpression contributes to other types of antibody-mediated autoimmune diseases such as lupus (13). Finally, physiologically or aberrantly expressed AID predisposes to cancer (14, 15) due to some off-target activity which leads to mutations in tumor suppressor and/or (proto)-oncogenes (16-18) and chromosomal translocations (19-23). Beyond its role in antibody diversification, physiological expression of AID outside the GC B cells is well documented but the role and the regulation of AID in these contexts are virtually unknown (11, 12, 24-31).

Ensuring that AID is expressed appropriately and in the right context is critical to favor its physiological functions over its pathological effects. However, the growing number of instances in which AID is expressed outside of the GC B cells in physiological or pathological conditions highlights the importance of post-transcriptional and post-translational regulation. In this context, regulatory pathways controling AID at the mRNA and protein levels as well as restricting its access to the nucleus are extremely important (32, 33). AID stability is directly linked to its subcellular localization. AID is a nucleo-cytoplasmic shuttling protein with predominantly cytoplasmic steady-state localization (34-38). AID is much more stable in the cytoplasm than in the nucleus (39, 40), but the molecular explanation for this differential stability is only partially known. We have shown that AID interacts with and is stabilized by the HSP90 molecular chaperoning pathway in the cytoplasm (40, 41). Nuclear AID may be unstable in part of a lack of chaperoning but the finding that AID is targeted for degradation by REGγ suggests also some active destabilization (42). It remains unclear why AID requires the assistance of chaperones in comparison to the APOBEC proteins, which share conserved three-dimensional structure and much sequence similarity but do not bind the same chaperones (40, 41).

This study aimed at identifying putative intrinsic sequence or structure that determines AID stability. Although the general steps implicated in protein turnover are well characterized, it is unclear what are the actual signals dictating protein stability. Several biochemical and biophysical properties of proteins have been described as determinants of protein turnover including molecular weight (43), isoelectric point (44, 45), hydrophobicity (46, 47) and the presence of certain motifs (48-51). The presence of unstructured regions has also been implicated in protein stability (52, 53). In several subsets of proteins, motifs also called degrons that predispose a protein to increased instability have been identified including the APC/C-dependent D- and KEN boxes (49, 54-57), the TrCP recognition box (DSGXXS) (58-61), and the PEST motifs (50, 62). The simpler N-degron has also been extensively described in which the nature of a protein N-terminal amino acid determines its half-life (51, 63). Newly synthesized proteins contain an N-terminal methionine which is considered as a stabilizing residue according to the N-end rule, but proteins can be enzymatically modified at their N-terminus to reveal a primary, secondary or tertiary destabilizing residue depending on the

number of steps required before its polyubiquitination starts (63). Proteins degraded by the ubiquitin-proteasome pathway not only require the presence of degrons, but also the availability of free residues for attachment of polyubiquitin chains for targeting to the proteasomal degradation (64, 65).

Here, we report that AID is intrinsically less stable than its paralogs, the APOBECs. This is in good part determined by the N-end rule and an internal PEST-like motif. Disruption of these degrons modulates AID protein turnover and directly impacts antibody diversification, without affecting AID subcellular localization. Strikingly cytoplasmic AID protein turnover and polyubiquitination state is independent of its internal lysine residues. In conclusion, we report for the first time a direct contribution of AID intrinsic instability in the regulation of its biological activity and antibody diversification, independently of its subcellular localization.

4.4. Experimental procedures

4.4.1. DNA constructs

AID-GFP, GFP-AID, AID-A2 chimeras and APOBEC constructs have been described previously (66). The AID Kzero mutant in which every lysines were mutated to arginines and fused to GFP was a kind gift of Dr Reynaud (INSERM, Paris). AID-D2A was cloned in pGEM-T vector as a BamHI-EcoRI fragment by using oligonucleotides OJ251 (5'-AAGGATCCCAAATGTTCAGCCTCTT GATGAA-3') and OJ166 (5'-CGAATTCCCAAGTC CCAAAGTACGAAATGC-3') and subcloned into pEGFP-N3 as a BglI-EcoRI fragment. AID-D2A-GFP fragment was subsequently subcloned into pTRC vector as a Nhe-NotI fragment or in pMX vector as a NotI-EcoRI fragment. The same procedure was performed with AID-D2F using oligonucleotides OJ252 (5'-AAGGATCCCAAATGTTCAGCCTCTTG ATGAA-3') and OJ166. D67A/D69A double mutation was introduced into pAID-GFP by quickchange using oligo-nucleotides OJ343 (5'-GCTACATCTCGGCCTGGGCCCTAGACCCTGG-3') and OJ344 (5'-CCAGGGTCTAGGGCCCAGGCCGAGATGTAGC-3'). AID-D67/69A-GFP was subcloned into pTRC vector or pMX vector as previously described.

4.4.2. Drug treatments

Stock aliquots of 2 mM GA were made in DMSO. Stocks of 5 mM MG132 (EMD) and 25 µg/ml LMB (LC Laboratories) were made in ethanol. CHX (Sigma-Aldrich) was freshly prepared before each experiment (100 µg/ml) in EtOH. All drugs were stored at −20°C protected from light.

4.4.3. Confocal microscopy

HeLa cells were transiently transfected with AID and its mutants in pEGFP-N3 using TransIT-LT1 (Mirus). Cells were treated 48 h post transfection with 50 ng/ml Leptomycin B or EtOH solvent control for 2 h. Cells were processed for confocal microscopy as described (38).

4.4.4. AID stability assays

The GFP signal of cell lines expressing AID-GFP variants was measured by flow cytometry at various time points after the indicated treatments as previously described (38, 40). Dead cells were excluded by propidium iodide staining.

4.4.5. AID mutagenic activity

AID catalytic activity was measured by a mutation assay as previously described (67) using the ung-deficient *E. coli* strain BW310 expressing AID-GFP and derived mutants.

4.4.6. Retroviral infection

The Ramos Burkitt's B cell lymphoma lines stably expressing AID-GFP or GFP-tagged APOBEC proteins were generated as previously described (38, 66). Retroviral transduction of mouse $AID^{-/-}$ primary B cells has been described (38). DT40 IgM^{+} ψV^{-} $AID^{-/-}$ chicken B and Ramos B cells were infected with retroviral particles obtained from the supernatant of HEK293T cell cultures cotransfected with pMX and vectors expressing MLV Gag-Pol and VSV-G envelope (2:1:1 ratio) as previously described (38). GFP+ cells were FACS-sorted.

4.4.7. Monitoring of antibody diversification

AID-mediated somatic hypermutation was estimated by fluctuation assay of the proportion of cells undergoing surface IgM+ to IgM- reversion in multiple subcloned populations of $sIgM^{+}$ ψV^{-} $AID^{-/-}$ DT40 cells complemented with various GFP-tagged AID constructs after 4 weeks of expansion at 41°C (68). IgM expression was measured by flow cytometry using 1:200 PE-conjugated anti–chicken IgM (Southern Biotech). *Ex vivo* isotype switching to IgG1 was assayed using resting splenic $AID^{-/-}$ B cells purified by CD43 depletion as described (38). Cells were stained with anti–IgG1-biotin (1:200; BD) followed by APC-conjugated anti-biotin (Miltenyi Biotech) and 10 μg/ml propidium iodide.

4.4.8. Western blot

Cells were homogenized in lysis buffer as previously indicated (40). The lysate was

clarified for 10 min at 12,000 x *g* at 4°C and processed for western blot. Typically, 2 x 10^6 cell equivalents were analyzed by western blots. Tagged proteins were immunoprecipitated using MACS GFP Isolation kit (Miltenyi Biotech) according to the manufacturer's instructions. Eluates and lysates were analyzed by western blot developed with SuperSignal West Pico Chemiluminescent substrate (Thermo Fisher Scientific). Antibodies used for western blot were anti–EGFP–HRP (1:3,000; Miltenyi Biotec), anti-AID (1:1,000 Cell Signaling Technology), anti-PCNA (1:5,000 PC-10; Abcam), and anti-monoubiquitinated and -polyubiquitinated conjugates antibody (1:1,000; Enzo Life Sciences, Inc.).

4.5. Results

4.5.1. Unlike AID, the APOBEC enzymes are independent of HSP90

We have previously shown that AID interacts with several members of the HSP90 molecular chaperoning pathway including the HSP40 DnaJa1, HSC70 and HSP90 (40, 69). None of the APOBEC1, 2 or 3G was able to bind to any of these chaperones, which is puzzling given the phylogenetic and high sequence and structure similarities among AID/APOBEC members. This could be due to a more transient interaction or an indirect dependence on HSP90 of the APOBECs. The AID-HSP90 interaction is functionally important to stabilize and maintain the steady-state levels of cytoplasmic AID and can be monitored by stably expressing GFP-tagged proteins in a human B cell line and measuring the mean fluorescence intensity (MFI) of the GFP signal over time after inhibiting HSP90 with geldanamycin (GA) (40). We used stable transfectants of the Ramos B cell lymphoma line because at least AID and APOBEC3G are endogenously expressed in B cells (2, 70). We found that, unlike AID, APOBEC1 (A1), APOBEC2 (A2) and APOBEC3G (A3G) levels did not change over time after HSP90 inhibition (Figure 4.1A). AID nuclear accumulation upon treatment with the CRM1 nuclear export inhibitor leptomycin B (LMB) leads to its degradation in the nucleaus (Figure 4.1A and 4.1B) (39, 40). A3G is exclusively cytoplasmic but A2 is distributed throughout the cell; A1 shuttles in and out of the nucleus and accumulates in the nucleus of Ramos cells after LMB treatment (Figure 4.1B). However, neither A2 nor A1 are destabilized by LMB treatment, in fact A1 levels increased after CRM1 inhibition (Figure 4.1A). We then measured the stability of AID and its paralogs by treating cells with cycloheximide (CHX) to block protein synthesis and followed the decay of GFP-tagged proteins in Ramos B cells (Figure 4.1C). AID displayed the fastest decay with a half-life of 13.6 hours; A3G demonstrated a longer half-life with 24 hours. As expected, HSP90 inhibition led to a significant decrease in AID half-life but did not affect the APOBECs (Figure 4.1C). We conclude that none of the APOBECs directly or indirectly requires HSP90 activity. These results also suggest that AID requires constant chaperoning by HSP90, a chaperone that stabilizes nearly-folded proteins rather than participating in protein biogenesis, because it bears

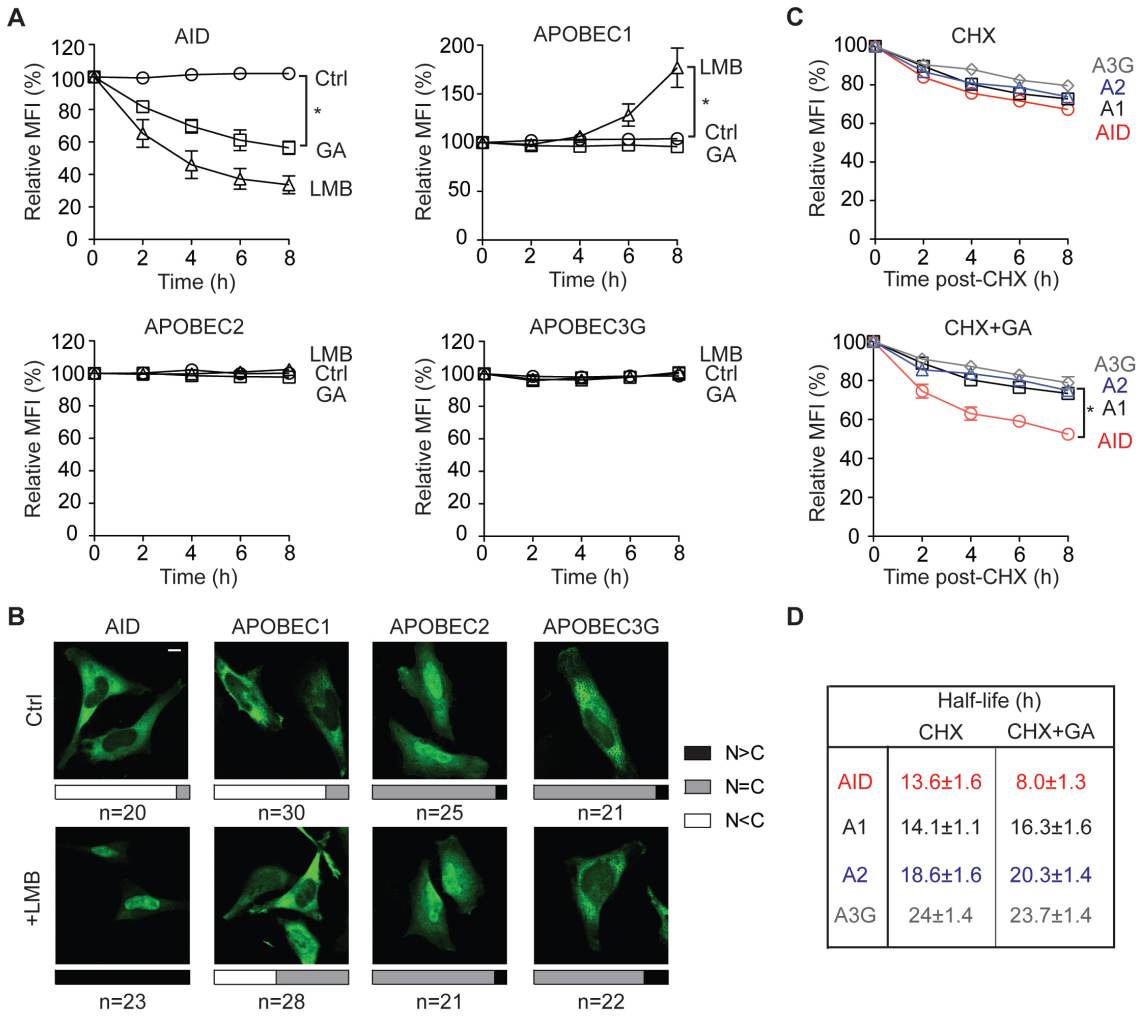

Figure 4.1. The protein half-life of AID is shorter than the other APOBECs. *(A) GFP-tagged AID, APOBEC1 (A1), APOBEC2 (A2) and APOBEC3G (3G) were stably expressed in Ramos B cells and GFP mean fluorescence intensity (MFI) was monitored by flow cytometry at different times after treatment with 2μM geldanamycin (GA), 50 ng/ml leptomycin B (LMB) or DMSO control (Ctrl) and normalized to t_0 = 100%. One of two independent experiments is shown. Average MFI ± SD of duplicates is plotted over time (*, $p<0.05$, paired two-tailed t-test). (B) Hela cells transfected with GFP-tagged AID, A1, A2 or A3G were treated with leptomycin B fixed and imaged by confocal microscopy. Representative confocal images are shown, scale bar 10 μM. The cellular localization of each protein was classified and the proportion of transfected cells showing each distribution is plotted as bars with the number of*

cells quantified indicated (n). C, cytoplasm; N, nuclear.(C) Stable transfected Ramos cells were treated with 100 ng/ml cycloheximide (CHX; upper panel) alone or before HSP90 inhibition (lower panel) and GFP-tagged protein levels were followed as in (A). One of two independent experiments is shown. Average MFI ± SD of duplicates is plotted over time (, $p<0.05$, paired two-tailed t-test). The half-life of each AID/APOBEC proteins was calculated by linear regression. Half-life in hours ± SD is indicated.*

intrinsic instability features that destabilize AID both in the cytoplasm as well as in the nucleus.

4.5.2. Survey of putative destabilizing sequences in AID

We asked whether there were domains in AID that could cause instability. We used AID-APOBEC2 chimeras, in which 30-50 amino acid-long AID regions were replaced by the corresponding homologous APOBEC2 residues (Figure 4.2A), to screen for regions of AID that could be implicated in its intrinsic instability. A caveat of this strategy is that the structure of AID is not known and these AID-A2 chimeric proteins could simply be unstable because they are not folded properly. Indeed, chimeras #3 and #4, in which amino acids 88-116 and 118-150 of AID were respectively replaced, displayed shorter half-lives than wild-type AID (Figure 4.2B-C). However, chimeras #1 and #2, replacing AID N-terminal residues (19-57 or 59-84 amino acids, respectively), showed significantly longer half-lives than AID (Figure 4.2B-C). These could be explained by a defect in AID subcellular trafficking since we have shown previously that chimera #1 fails to enter the nucleus and chimera #2 has a reduced kinetic of nuclear import compared to AID (38). However, N-terminal GFP tagging of AID also entirely blocks its nuclear import (38) and still had a shorter half-life than chimera #1 (Figure 4.2B-C). These results suggested that the AID regions replaced in chimeras #1 and #2 contained motifs destabilizing AID.

As a first approach to define AID destabilizing residues, we performed a sequence analysis for known destabilizing structures and motifs (degrons). Several HSP90 client proteins are intrinsically unstructured proteins (IUP) (71-76). Furthermore, several studies have highlighted the importance of unstructured regions for protein degradation by the ubiquitin-dependent and independent proteasome (52, 64, 77, 78). We compared AID and APOBEC proteins for the presence of disordered regions using two different prediction algorithms (DisEMBL^{TM} (79) and PONDR$^{®}$ (80)) which report unstructured residues based on the protein sequence. In both analyses, AID presented the largest proportion of disordered regions (31% and 18% of AID, respectively) (Table 4.1). Interestingly, several of these regions are predicted as hot loops (defined as loops with a high degree of mobility) and indeed coincide with predicted loops in the three-dimensional model of AID (Figure 4.2D). Analysis of AID protein

Table 4.1. Predicted intrinsic protein disorder and unstructured regions within human AID/ APOBEC proteins.

HUGO name	Description	Hot loops Predicted by DisEMBL™		Disordered regions predicted by PONDR®	
		Position (aminoacid)	Unstructured coverage (%)	Position (aminoacid)	Unstructured coverage (%)
AICDA	activation-induced cytidine deaminase	14-29 38-51 120-130 179-198	31	1-6 13-19 25-33 125-128 188-195	18
APOBEC1	apolipoprotein B mRNA editing enzyme, catalytic polypeptide 1	1-32 51-62	19	1-14 48-55	10
APOBEC2	apolipoprotein B mRNA editing enzyme, catalytic polypeptide-like 2	10-24 197-207	12	10-24	7
APOBEC3G	apolipoprotein B mRNA editing enzyme, catalytic polypeptide-like 3G	1-31 40-52 204-214	14	1-3 48-52 138-147 326-330 373-381	8

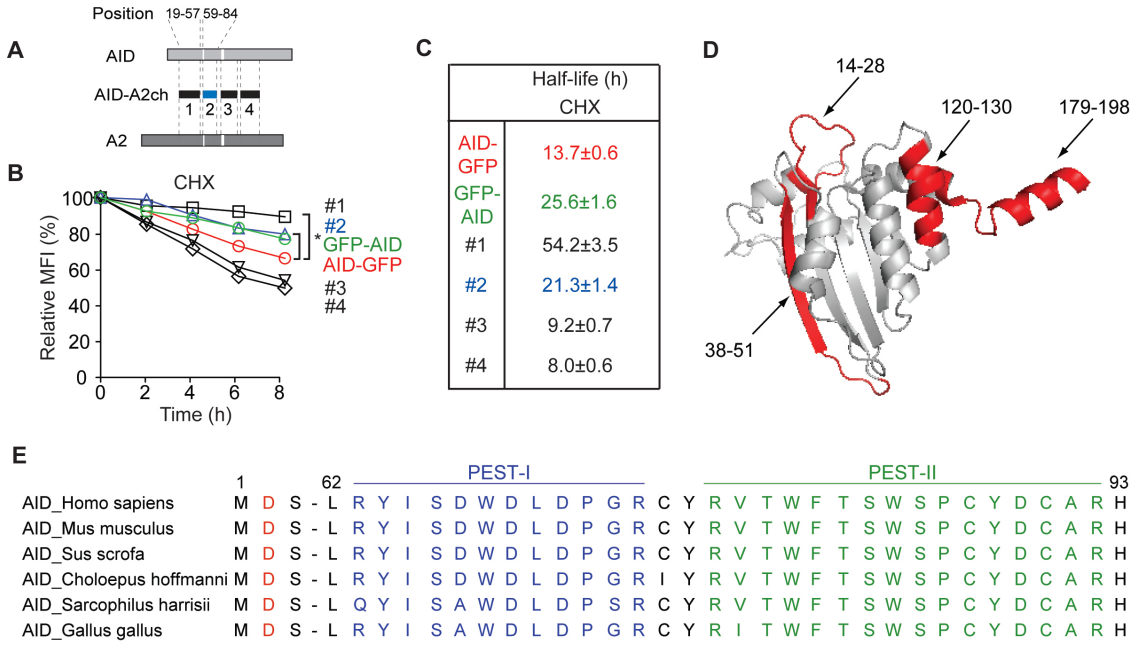

Figure 4.2. N-terminal region of AID modulates its stability. ***(A)*** *Schematic representation of AID-APOBEC2 chimeric proteins (AID-A2ch1-4) in which either one of the regions from A2 indicated between dotted lines was substituted for the homologous AID region.* ***(B)*** *GFP-tagged AID and AID-A2 chimeras were stably expressed in Ramos B cells and GFP MFI was monitored as previously indicated after CHX treatment and normalized to t_0 = 100%. One of two independent experiments is shown. Average MFI ± SD of duplicates is plotted over time (*, $p<0.05$, paired two-tailed t-test).* ***(C)*** *Half-life in hours ± SD of each AID and AID-A2 proteins calculated from linear regression projection of the data obtained in (B) is indicated.* ***(D)*** *DisEMBL™ prediction of AID hot loops are indicated in red in AID three-dimensional model (38).* ***(E)*** *Multispecies alignment of AID N-terminal region containing a conserved aspartic acid at position two (in red) and two conserved PEST-like motifs (highlighted in blue for the PEST-I (score: -10.81) and in green for the PEST-II (score: -15.23)).*

sequence for the presence of degrons failed to identify any significant TrCP recognition box (81), KEN box or D-box motif usually present in cell-cycle regulated proteins (49). Unfolded regions have been shown to be enriched in PEST motifs, which are stretches of amino acids enriched in proline (P), glutamic (E) or aspartic acid (D), serine (S), and threonine (T) and are implicated in protein turnover of many unstable proteins (50, 62). PEST motifs are usually located in solvent-exposed loops or extensions that are preferentially targeted for proteolytic cleavage by the proteasome (82, 83). Analysis of human AID protein sequence using the pestfind algorithm identified two putative PEST sequences with poor scores (Figure 4.2E), located between amino acids 63-74 (PEST-I) and amino acids 77-92 (PEST-II). These domains are highly conserved in AID orthologs (Figure 4.2E), PEST-I was only absent in Xenopus AID.

Several others destabilizing motifs have been described previously. N-terminal unstructured proteins are also associated with N-degrons that regulate protein stability by the proteasome through the N-end rule pathway (63). Some of these proteins have their N-terminal methionine enzymatically removed. The nature of the second N-terminal residue influences the stability of these proteins by making it more or less susceptible to the N-end rule pathway. Amino acids are divided between primary, secondary or tertiary destabilizing for this pathway. Interestingly, AID displays a secondary destabilizing aspartic acid residue at position two, which is conserved throughout evolution (Figure 4.2E). This raised the possibility that AID could be subjected to the N-end rule. Although none of these predictions is conclusive, they all prompted to the N-terminal region of AID for possible intrinsic determinants of its stability.

4.5.3. Altering AID cytoplasmic stability impacts its physiological activity

There is no evidence that AID N-terminus is modified but the influence of the N-terminal residue in half-life can be tested by mutating it to a more stabilizing or destabilizing residue. We replaced AID D2 residue with either a more destabilizing residue, we chose phenylalanine (D2F), or a more stabilizing one, alanine (D2A), and analyzed their impact on AID stability. We first confirmed that D2A or D2F mutation did not affect AID subcellular

localization and shuttling, which are important for AID stability (Figure 4.3A). We also measured the catalytic activity of these mutants using the *E.coli*-based rifampicin-resistance assay (67). D2A catalytic activity was reduced by ~25% compared to AID and D2F was equally active than wild-type (Figure 4.3B). Conserved enzymatic activity and nucleo-cytoplasmic shuttling are good indications that these single point mutants of AID do not have any major structural alteration. We then analyzed their half-lives in Ramos B cell. In steady-state, D2A showed a mild but significantly longer half-life than AID while D2F was less stable than wild-type AID (Figure 4.3C). Interestingly, modification of the AID N-terminal residue impacts its stability in the cytoplasm, but not in the nucleus since both mutants show equal decay kinetics after LMB treatment (Figure 4.3C lower left and upper right panels). Analysis of AID variants expression in 293 cells by western blot correlates with stability data obtained in Ramos B cells : D2A showed higher steady-state levels whereas D2F was less expressed compared to AID (Figure 4.3D). Unlike the AID-A2 chimeras, these mutants provided useful enzymes to analyse the impact of AID cytoplasmic stability on its biological function. Therefore, we performed CSR assays on *Aicda*$^{-/-}$ mouse B cells complemented by retroviral delivery with GFP-tagged AID variants. D2A and D2F showed significantly reduced isotype switching to IgG1 (Figure 4.3E). We also assayed AID-mediated SHM in an *Aicda*$^{-/-}$ chicken DT40 cell line that diversifies the IgVλ by SHM (68) and can be monitored by the appearance of sIgM-loss cells from originally sIgM^{+} populations. There was also a reduction for both D2A and D2F mutants, although, in this case, D2A reduction was non-significantly different from wild-type AID (Figure 4.3F). The compromised CSR and SHM of the D2A mutant could be simply explained by its reduced catalytic activity. However, D2F mutant shows that the introduction of a primary destabilizing residue in AID N-terminus had no impact on its catalytic activity, therefore the decrease in CSR and SHM must be due to the change in stability. We conclude that AID stability in the cytoplasm is important for antibody diversification.

4.5.4. A PEST-like motif influences AID stability and function

Although our data suggest that the N-degron contributes to AID instability, it cannot

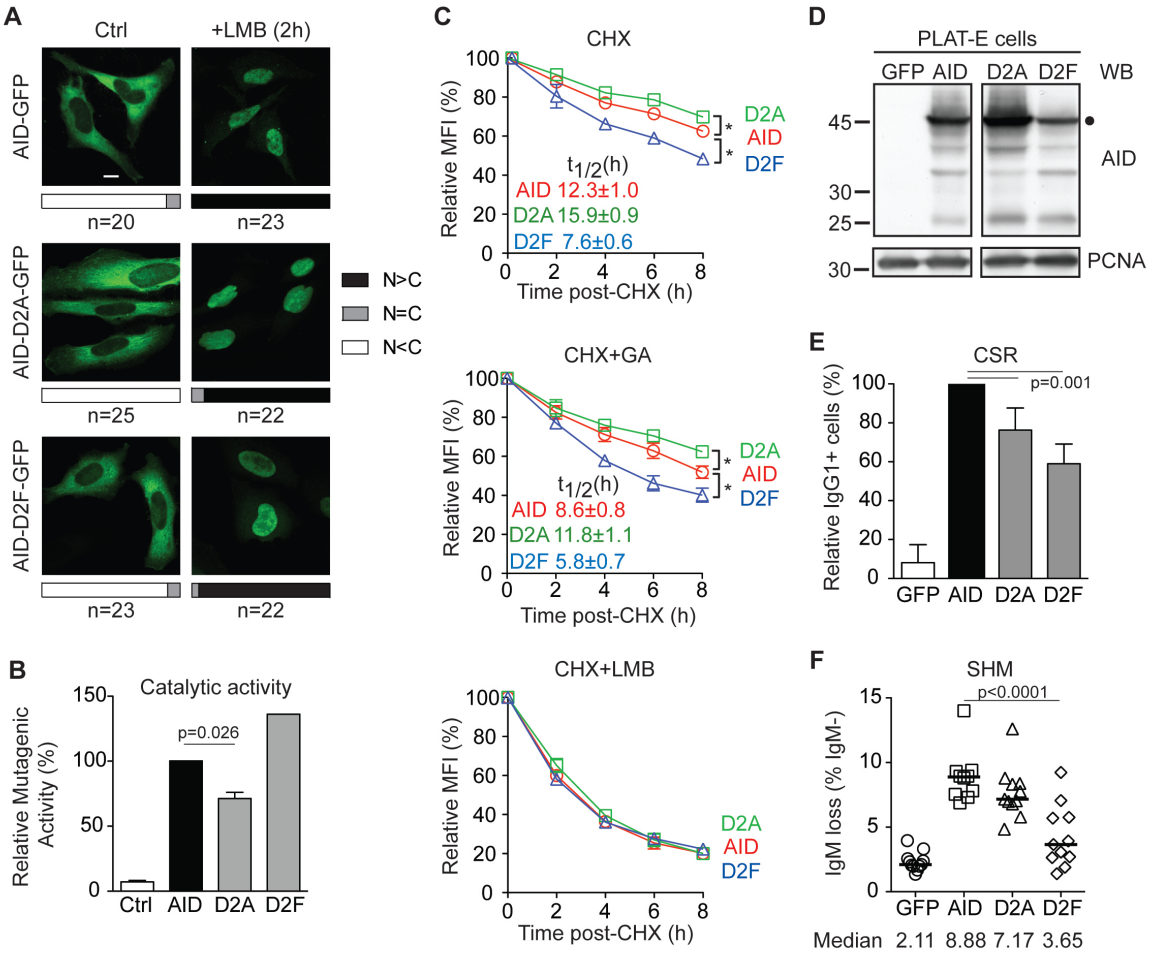

Figure 4.3. Altering AID N-terminal aspartic acid residue impacts both its stability and function. *(**A**) Hela cells transfected with GFP-tagged AID mutated at position 2 either for a more stabilizing residue alanine (D2A), or a primary destabilizing residue phenylalanine (D2F) with regard to the N-end rule were treated with LMB and processed as previously indicated (Figure 1B). Representative confocal images are shown; scale bar 10 µM. n, number of cells counted indicated; C, cytoplasm; N, nuclear. (**B**) The catalytic activity of GFP-tagged AID and the indicated mutants was monitored by E. coli mutation assay. The number of rifampicilline-resistant colonies/10^9 viables colonies obtained for AID-GFP construct was set as 100%. Ctrl, pTRC empty vector. (**C**) GFP-tagged AID and its mutants D2A and D2F were stably expressed in Ramos B cells and analyzed as previously described. One of two*

independent experiments is shown. Average MFI ± SD of duplicates is plotted over time (, $p<0.05$, paired two-tailed t-test). Half-life in hours ± SD is indicated. (**D**) 293 retroviral producing cells transfected with the indicated AID-GFP contruct or GFP control in pMX were harvested, lyzed and the expression level of the indicated proteins was analyzed by WB using anti-AID antibody. GFP-tagged AID contructs migrate at an approximate size of 45 kDa. PCNA was used as a loading control. Expected AID-GFP band was identified by a circle. (**E**) B cells from AID-deficient mice were infected with retroviruses encoding GFP-tagged AID, the indicated AID-GFP variants or GFP control in pMX. The proportion of infected (GFP positive) cells that have switched to IgG1 was measured by flow cytometry in non-saturating conditions of stimulation (5 ng/mL IL-4 and 25 μg/mL LPS) and summarized in the bar graphs. Means ± SD values from seven independent mice for each construct are plotted relative to AID-GFP value set as 100%. (**F**) SHM was monitored in analogous experiments to (E) except that a $sIgM^+$ ψV^- $AID^{-/-}$ DT40 chicken cell line, which uses SHM to diversify the Ig genes, was used. IgM-loss cells arise as a consequence of SHM with a certain frequency, and so the proportion of sIgM-loss cells arising over time provides an estimate of SHM rate. DT40 cells infected with the indicated retroviral GFP-tagged AID contruct were sorted for GFP+ cells. The proportion of infected (GFP positive) cells that have lost IgM was measured for several subclones by flow cytometry and summarized in the graphs. Median values from twelve subclones for each construct are indicated. In all panels, p values from paired, two-tailed t-test are indicated only for significant differences ($p<0.05$).*

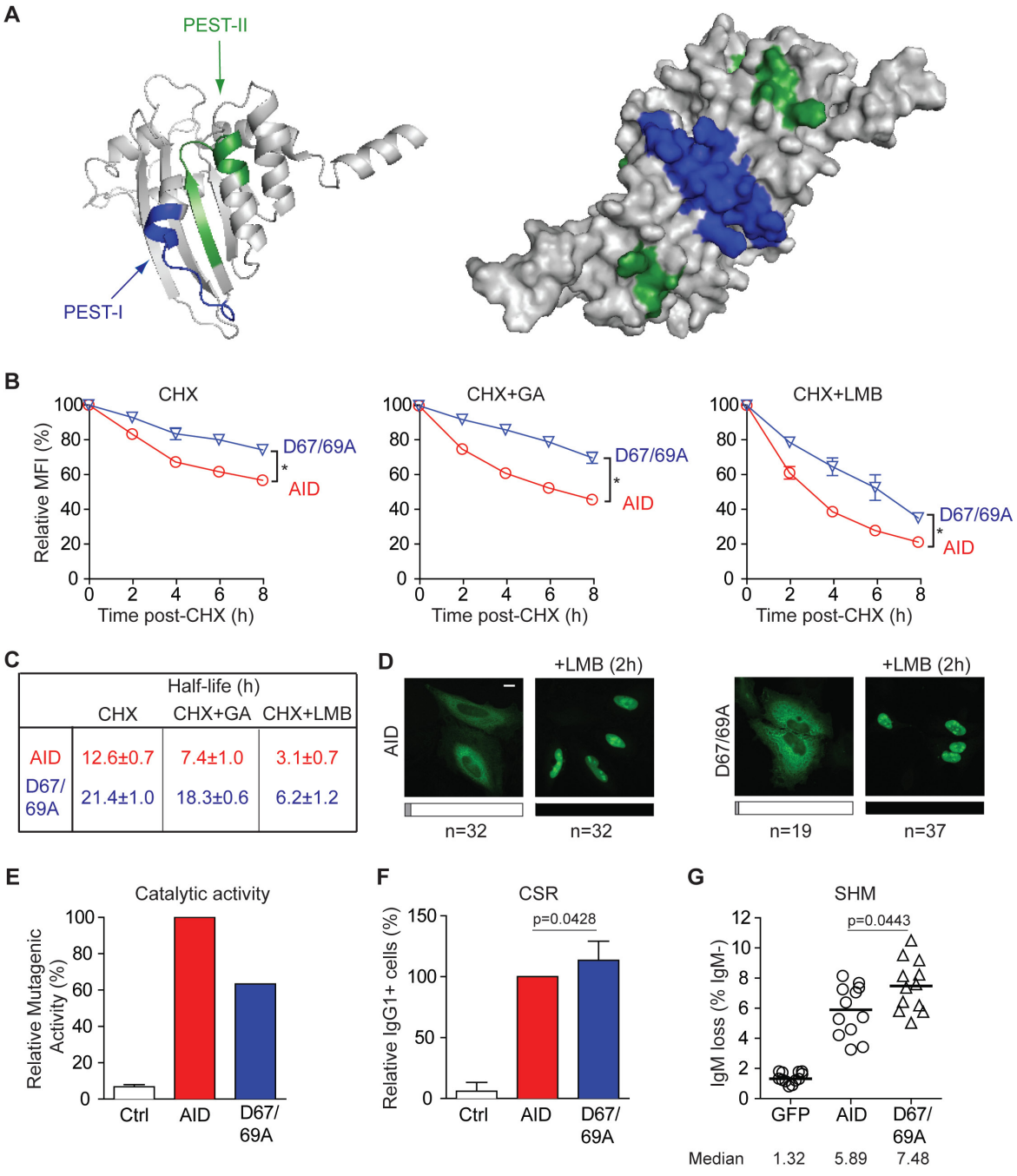

Figure 4.4. Disruption of a PEST-like motif in AID results in increased stability and antibody diversification. *(A) Detailed location in a putative AID monomer (left panel) and*

*dimer (right panel) of PEST domains present in its N-terminus. For clarity, the same colors as in figure 2E were used to deliminate PEST domains. The right panel shows a predicted solvent-accessible surface of the putative PEST. (**B**) GFP-tagged AID and its mutant were stably expressed in Ramos B cells and analyzed as previously described. One of two independent experiments is shown. Average MFI ± SD of duplicates is plotted over time (*, $p<0.05$, paired two-tailed t-test). (**C**) Half-life in hours ± SD of AID and D67/69A mutant calculated from linear regression projection of the data obtained in (B) is indicated. (**D**) Hela cells transfected with GFP-tagged AID or its mutant D67/69A which affects the putative PEST-I domain were treated with LMB and processed as before as in Figure 1B. Representative confocal images are shown; scale bar 10 μM. n, number of cells counted indicated; C, cytoplasm; N, nuclear. (**E**) The catalytic activity of GFP-tagged AID and the indicated mutant was monitored as previously indicated. AID-GFP catalytic activity was set as 100%. Ctrl, pTRC empty vector. (**F**) CSR was measured as previously indicated. Means ± SD values from six independent mice for each construct are plotted relative to AID-GFP value set as 100%. (**G**) SHM was monitored as previously indicated. Median values from twelve subclones for each construct are indicated.In panels (F) and (H), p values from paired, one-tailed Student's t-test are indicated only for statistically significant differences ($p<0.05$)*

explain the difference in protein turnover between AID and chimeras #1 and #2, which do not affect AID N-terminal end. We asked whether the PEST-like motifs present in AID contribute to its intrinsic instability. The PEST-I domain overlapped a solvent-exposed loop in our AID model (Figure 4.4A), while the PEST-II domain would be less accessible for proteolytic cleavage in the folded protein. Despite their low score in pestfinder, two PEST-I motifs would be in close proximity to each other in a putative AID dimer, which might result in a stronger motif. Thus, we focused on the PEST-I and mutated D67 and D69 to alanines to destroy the PEST-I.

D67/69A GFP-tagged mutant showed significantly increased half-life when compared to AID (Figure 4.4B-C). In addition, D67/69A was less responsive to GA suggesting that this mutant is more stable in the cytoplasm where AID stability highly depends on HSP90. Interestingly D67/69A mutation also increased AID half-life in the nucleus (Figure 4.4B right panel and 4.4C). Importantly, these differences in protein turnover could not be explained by any defect in subcellular localization that was equivalent for AID and D67/69A mutant in steady-state and after LMB treatment (Figure 4.4D). Our results suggest that the PEST-I is an intrinsic destabilizing motif for AID in the cytoplasm and in the nucleus. Using the E.coli mutation assay, the D67/69A mutant showed 60% catalytic activity compared to wild-type AID (Figure 4.4E). Despite this, disruption of the PEST-I led to a significant increase in CSR and SHM (Figure 4.4F-G). We conclude that a PEST-like motif influences AID stability in both the cytoplasm and in the nucleus as well as its function in antibody diversification.

4.5.5. AID internal lysine residues are not required for its cytoplasmic polyubiquitination and degradation by the proteasome

We have shown that cytoplasmic AID gets polyubiquinated and degraded by the proteasome after HSP90 inhibition (40). Others have described that nuclear AID is both polyubiquitinated but also targeted by an ubiquitin-independent pathway involving REGγ to the proteasome (39, 42). To verify whether internal AID lysine residues were required for its polyubiquitination and cytoplasmic degradation by the proteasome, we used a construct

previously described (39) in which all AID lysines were mutated to arginines (Kzero; Figure 4.5A). AID-Kzero showed delayed degradation in the nucleus compared to AID (39), which we confirmed in our system using stably transfected Ramos cells treated with LMB (Figure 4.5B). Inversely, HSP90 inhibitor GA treatment led to a faster decay of the lysineless mutant than wild-type AID in our assay (Figure 4.5B). Furthermore, addition of proteasomal inhibitor MG132 blocked Kzero decay, confirming the requirement of the proteasome for AID Kzero degradation after HSP90 inhibition (Figure 4.5B). CHX treatment showed that internal lysines residues are structurally important for AID, since Kzero displayed a significant shorter half-life compared to wild-type AID (Figure 4.5C). However, only a small portion of AID or AID Kzero are polyubiquitinated in steady-state as observed by inhibiting the proteasome with MG132 (Figure 4.5D). Strikingly, proteasome inhibitor combined with the HSP90 inhibitor GA led to a significant increase in the proportion of both AID and AID Kzero polyubiquitinated forms (Figure 4.5D). We therefore investigated the presence of alternative sites for AID polyubiquitination. Free α-NH_2 terminus can serve as the conjugation site for ubiquitin by a poorly understood mechanism and addition of N-terminal tags has been shown to stabilize proteins which are N-terminally ubiquitinated including the AID paralog APOBEC3G (84-87). To verify whether AID α-NH2 terminus is implicated in its protein turnover in the cytoplasm, we added an HA tag to AID Kzero N-terminus. As shown previously, N-terminal tagging of AID prevents its nuclear import which explains why HA-Kzero-GFP levels were not affected by LMB treatment (Figure 4.5E) (38). However, HA-Kzero-GFP was still responsive to GA (Figure 4.5E). We therefore conclude that cytoplasmic AID degradation could occur through the polyubiquitination of non-lysine residues.

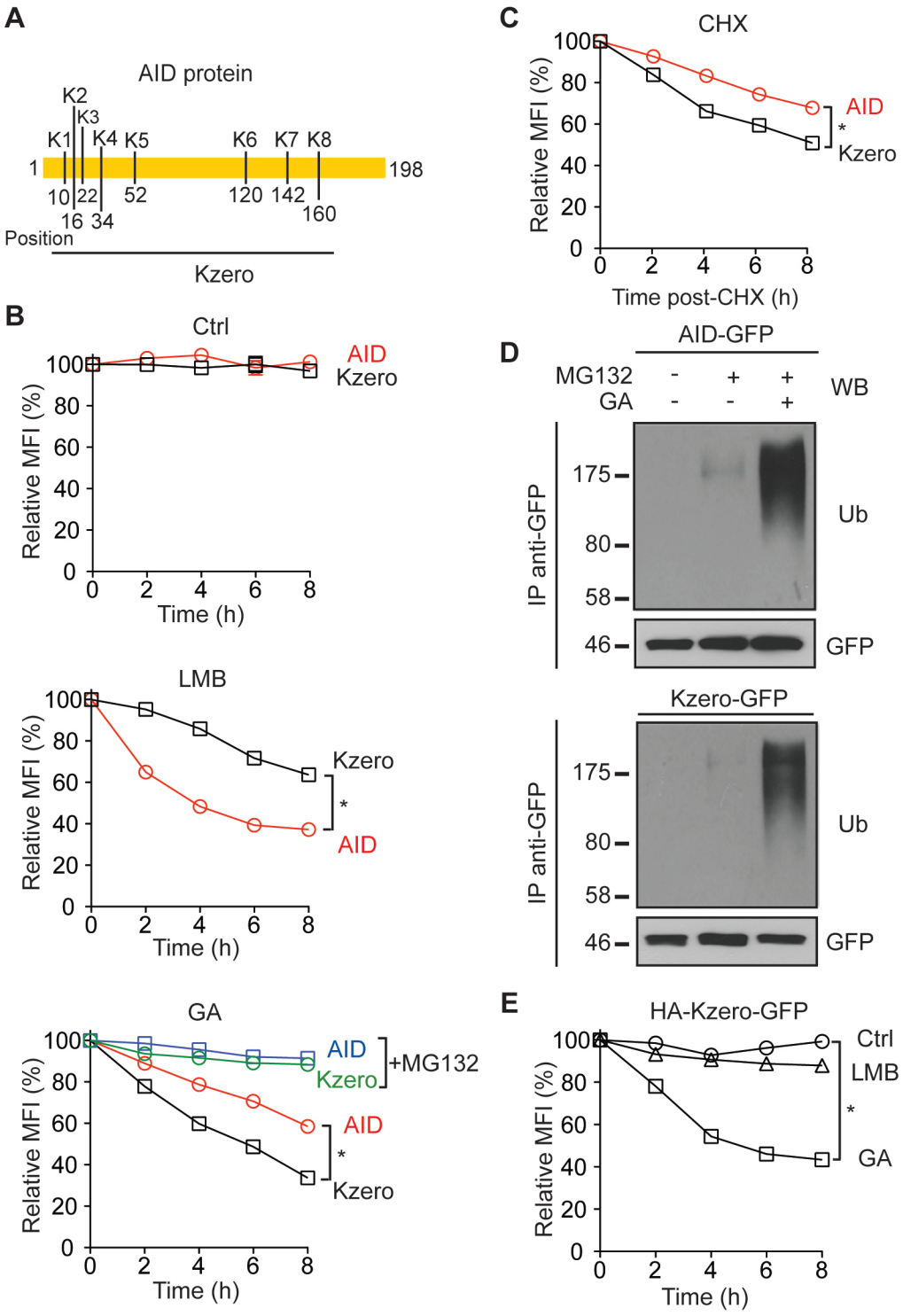
A
AID protein
K2
K3
K1
K4
K5
K6
K7
K8
1
198
10
22
52
120
142
160
16
34
Position
Kzero
B
Ctrl
AID
Kzero
Relative MFI (%)
Time (h)
LMB
Kzero
AID
GA
AID
Kzero
+MG132
AID
Kzero
C
CHX
AID
Kzero
Time post-CHX (h)
D
AID-GFP
MG132
GA
WB
IP anti-GFP
175
80
58
46
Ub
GFP
Kzero-GFP
E
HA-Kzero-GFP
Ctrl
LMB
GA

Figure 4.5. AID lysine residues are dispensable for its polyubiquitination and degradation after HSP90 inhibition. *(**A**) Schematic representation of AID and the positions of its eight lysine residues. All lysines were mutated to arginines in the GFP-tagged Kzero construct. Data from (39). (**B**) GFP-tagged AID and its lysineless mutant (Kzero) were stably expressed in Ramos cells and GFP MFI was monitored after treatment with 50 ng/ml leptomycin B (LMB), 2μM geldanamycin (GA), 10 μM MG132 or DMSO control (Ctrl) and normalized to t_0 = 100%. One of two independent experiments is shown. Average MFI ± SD of duplicates is plotted over time (*, p<0.05, paired two-tailed t-test). (**C**) Stable transfected Ramos cells were treated with 100 ng/ml cycloheximide (CHX; upper panel) alone or before HSP90 inhibition (lower panel) and GFP-tagged protein levels were followed as in (B). One of two independent experiments is shown. Average MFI ± SD of duplicates is plotted over time (*, p<0.05, paired two-tailed t-test). (**D**) GFP-tagged AID and its lysineless mutant Kzero were immunoprecipated using anti-GFP from extracts of stably expressing Ramos cells treated with 2μM Geldanamycin (GA) and/or 10 μM MG132 as indicated and analyzed by western blot to detect ubiquitinated forms of AID. Anti-GFP western blot confirmed similar immunoprecipitation levels of the bait. (**E**) A N-terminal HA tag was added to AID lysineless mutant (HA-Kzero), stably expressed in Ramos cells and analyzed as in (B). (*, p<0.05, paired two-tailed t-test).*

4.6. Discussion

There is ample evidence correlating AID localization and its stability (38-40, 88). Because of this interdependence, it has been difficult to test the contribution of each one to regulate AID and antibody diversification. We identify here mutations that stabilize AID by increasing its half-life without impacting its subcellular localization. These mutations serve to define instrinsic destabilizing regions or motifs in AID. But more importantly, they allow to experimentally proving that the stability of AID in the cytoplasm and in the nucleus is limiting for antibody diversification.

4.6.1. Instrinsic unstructured regions in AID

Our results show that, while AID and the APOBECs show apparently similar stability, AID depends on the HSP90 molecular chaperoning pathway whereas the APOBECs do not. We hypothesize that one of the reasons for this difference could be their different content of unstructured regions. This is speculative in the absence of an AID three-dimensional structure but many HSP90 clients are considered to be instrinsically unstructured proteins such as the neuronal ∝-synuclein (73, 74), the microtubule stabilizing tau protein (71, 72), the cyclin-dependent kinase inhibitor $p21^{(WAF1/CIP1)}$ (75, 89) and the steroid hormone receptors (90-93). Unstructured regions confer useful properties to these proteins such as rapid and specific interaction potential without excessive binding strength at the cost of some instability, versatility in the nature of its partners and susceptibility to post-translational regulation (94). Indeed, AID interacts with multiple partners including DNA replication factor A (RPA) (95), chromatin-associated and transcription factors (KAP1/HP1, RNA pol II, SPT5/SPT6, RNA exosome) (96-100), RNA processing proteins (CTNNLB1, GANP, PTBP2) (101-103) and subcellular localization mediators (importin-α, CRM1, eEF1α) (38, 88). AID is also post-translationally modified by PKA/PKC and PP2A (104-106). Association to these factors is either through the N-terminal or the C-terminal region of AID when it has been mapped, which are the regions predicted to be unstructured (Figure 4.2D and Table 4.1). A recent study suggests that intrinsically unstructured proteins require the chaperones for assistance in the

association to other proteins, rather than for folding (107). The fact that AID is present in different pools in the cytoplasm and the nucleus as revealed recently (88, 96), indicates that HSP90 stabilization could be a transitory state before moving on to another complex (i.e cytoplasmic retention or nuclear import complex), preventing AID from aggregating and/or being targeted to the ubiquitin-proteasome system due to exposed degradation motifs.

4.6.2. Nature of these intrinsic determinants and their impact on AID stability

In an attempt to identify the domains implicated in AID intrinsic instability, we show that changing the amino acid in position two of AID affects its protein stability as it would be predicted by the N-end rule. Although there is no direct evidence that the N-terminal methionine of AID is processed to reveal the destabilizing aspartic acid, this is quite a common N-terminal modification that can affect between 55 and 70% of the proteins depending on the organism and the subcellular compartment (108). Of note, others have reported a methionine aminopeptidase (methionine aminopeptidase 1, MetAP1) copurifying with AID (101). We show that replacing AID aspartic acid at position two for a more stabilizing residue (alanine) delays its turnover and results in higher steady-state levels. This mutation also reduces its catalytic activity by 25% and proportionally its ability to perform antibody diversification. Other stabilizing residues have been described including proline, serine, threonine, glycine and valine. Mutating aspartic acid to a serine may be an alternative to conserve the charged environment at the N-terminus of AID and should be tested to confirm the implication of the N-end rule pathway in AID turnover. The introduction of a more destabilizing amino acid at the second position of AID leads to increased destabilization and reduced antibody diversification confirming the importance of this position for AID stability. Furthermore, it suggests a direct contribution of AID stability for its biological function.

Our results show that disrupting a PEST-like motif in AID N-terminal region stabilizes AID both in the cytoplasm and in the nucleus. These regions enriched in proline, aspartic/glutamic acid, serine and threonine, are generally flanked by positive residues and have been predicted to be solvent-exposed regions more susceptible to proteolysis (62). In fact,

PEST motifs are abundant in intrinsically unstructured proteins (82, 83). Whether the PEST-I is an actual PEST domain or not is secondary. The identification of an additional destabilizing motif suggests that AID intrinsic instability results from the combination of at least two degradation motifs. Indeed, there is no direct correlation between the presence of any specific degradation signal and the *in vivo* half-lives of proteins (53). It is rather the combination of multiple factors including protein disorder and degrons that would influence the rate of a protein turnover (53). Our data show that a PEST-like motif by destabilizing AID influences its function in antibody diversification. Controlling AID protein turnover through the presence of destabilizing motifs could be an additional post-translation regulation to limit its biological function.

4.6.3. AID degradation in the cytoplasm

The turnover of most of the proteins is mediated by the ubiquitin-proteasome pathway. In agreement with this, we showed previously that cytoplasmic AID gets polyubiquitinated and degraded by the proteasome after HSP90 inhibition (40). Surprisingly, we report here that AID polyubiquitination is independent of its lysine residues, which are usually the typical acceptor of ubiquitin moieties. Lysineless ubiquitination has been reported for a small group of proteins including p21 $^{(WAF1/CIP1)}$(86, 109), p14/19^{ARF} (84), ERK3 (86), Id1 and Id2 (110, 111), MyoD (87) as well as APOBEC3G (112, 113). Instead, these proteins are polyubiquitinated at their α-NH_2 group. Addition of an N-terminal tag prevented their stabilization by an unclear mechanism. The high sequence and structure similarities among AID/APOBEC members would predict that they use similar pathway of degradation. However, attachment of an HA tag at AID N-terminus has no impact on its stability after HSP90 inhibition, suggesting an alternative way for targeting AID to the proteasome. Several viral proteins including the HIV-1 Vpu protein and the KSHV K3 and K5 proteins utilize non-canonical ubiquitin acceptors (serine and threonine) to target cellular proteins for proteasomal degradation (114-118). AID could therefore be polyubiquitinated on serine and threonine residues. However, we cannot exclude that the absence of available lysines in the Kzero mutant forces the ubiquitin-

proteasome pathway to use noncanonical residues for AID degradation. It is also possible that AID degradation is mediated by an ubiquitin-independent proteasomal pathway. Indeed, nuclear AID is actively destabilized by the ubiquitin-independent REGγ-proteasome pathway (42).

In conclusion, our data suggest a direct contribution of destabilizing motifs in AID protein turnover and antibody diversification. They are consistent with a model in which AID presents unstructured regions requiring the assistance of the HSP90 molecular chaperoning pathway to prevent its aggregation. Therefore, limiting AID protein levels through the presence of destabilizing motifs is an additional way to regulate antibody diversification.

4.7. Acknowledgments

We thank Dr Claude-Agnès Reynaud (INSERM, Paris) for construct and Eric Massicotte (IRCM flow cytometry facility) for assistance. This work was funded by a grant from the Canadian Institutes of Health Research (MOP-84543) and supported by a Canadian Fund for Innovation LOF equipment grant to JMDN. AO was supported by a Cole Foundation doctoral fellowship, SM by a CIHR Master's scholarship. JMDN is supported by a Canada Research Chair Tier 2. AO designed and performed the majority of the experiments and wrote the paper. SPM, AE and AMP performed experiments. JMDN conceived the project and wrote the paper. All authors discussed and interpreted the data and contributed to the final manuscript.

4.8. References

1. Conticello SG (2008) The AID/APOBEC family of nucleic acid mutators. (Translated from eng) *Genome Biol* 9(6):229 (in eng).
2. Muramatsu M*, et al.* (1999) Specific expression of activation-induced cytidine deaminase (AID), a novel member of the RNA-editing deaminase family in germinal center B cells. (Translated from eng) *J Biol Chem* 274(26):18470-18476 (in eng).
3. Revy P*, et al.* (2000) Activation-induced cytidine deaminase (AID) deficiency causes the autosomal recessive form of the Hyper-IgM syndrome (HIGM2). (Translated from eng) *Cell* 102(5):565-575 (in eng).
4. Teng B, Burant CF, & Davidson NO (1993) Molecular cloning of an apolipoprotein B messenger RNA editing protein. (Translated from eng) *Science* 260(5115):1816-1819 (in eng).
5. Navaratnam N*, et al.* (1993) The p27 catalytic subunit of the apolipoprotein B mRNA editing enzyme is a cytidine deaminase. (Translated from eng) *J Biol Chem* 268(28):20709-20712 (in eng).
6. Turelli P & Trono D (2005) Editing at the crossroad of innate and adaptive immunity. (Translated from eng) *Science* 307(5712):1061-1065 (in eng).
7. Stavnezer J, Guikema JE, & Schrader CE (2008) Mechanism and regulation of class switch recombination. (Translated from eng) *Annu Rev Immunol* 26:261-292 (in eng).
8. Peled JU*, et al.* (2008) The biochemistry of somatic hypermutation. (Translated from eng) *Annu Rev Immunol* 26:481-511 (in eng).
9. Di Noia JM & Neuberger MS (2007) Molecular mechanisms of antibody somatic hypermutation. (Translated from eng) *Annu Rev Biochem* 76:1-22 (in eng).
10. Hase K*, et al.* (2008) Activation-induced cytidine deaminase deficiency causes organ-specific autoimmune disease. (Translated from eng) *PLoS One* 3(8):e3033 (in eng).
11. Kuraoka M*, et al.* (2011) Activation-induced cytidine deaminase mediates central tolerance in B cells. (Translated from eng) *Proc Natl Acad Sci U S A* 108(28):11560-11565 (in eng).
12. Meyers G*, et al.* (2011) Activation-induced cytidine deaminase (AID) is required for B-cell tolerance in humans. (Translated from eng) *Proc Natl Acad Sci U S A* 108(28):11554-11559 (in eng).
13. Zaheen A & Martin A (2011) Activation-induced cytidine deaminase and aberrant germinal center selection in the development of humoral autoimmunities. (Translated from eng) *Am J Pathol* 178(2):462-471 (in eng).
14. Pasqualucci L*, et al.* (2008) AID is required for germinal center-derived lymphomagenesis. (Translated from eng) *Nat Genet* 40(1):108-112 (in eng).
15. Okazaki IM*, et al.* (2003) Constitutive expression of AID leads to tumorigenesis. (Translated from eng) *J Exp Med* 197(9):1173-1181 (in eng).

16. Yamane A, *et al.* (2011) Deep-sequencing identification of the genomic targets of the cytidine deaminase AID and its cofactor RPA in B lymphocytes. (Translated from eng) *Nat Immunol* 12(1):62-69 (in eng).
17. Liu M, *et al.* (2008) Two levels of protection for the B cell genome during somatic hypermutation. (Translated from eng) *Nature* 451(7180):841-845 (in eng).
18. Pasqualucci L, *et al.* (2001) Hypermutation of multiple proto-oncogenes in B-cell diffuse large-cell lymphomas. (Translated from eng) *Nature* 412(6844):341-346 (in eng).
19. Ramiro AR, *et al.* (2004) AID is required for c-myc/IgH chromosome translocations in vivo. (Translated from eng) *Cell* 118(4):431-438 (in eng).
20. Robbiani DF, *et al.* (2009) AID produces DNA double-strand breaks in non-Ig genes and mature B cell lymphomas with reciprocal chromosome translocations. (Translated from eng) *Mol Cell* 36(4):631-641 (in eng).
21. Robbiani DF, *et al.* (2008) AID is required for the chromosomal breaks in c-myc that lead to c-myc/IgH translocations. (Translated from eng) *Cell* 135(6):1028-1038 (in eng).
22. Jankovic M, *et al.* (2010) Role of the translocation partner in protection against AID-dependent chromosomal translocations. (Translated from eng) *Proc Natl Acad Sci U S A* 107(1):187-192 (in eng).
23. Dorsett Y, *et al.* (2007) A role for AID in chromosome translocations between c-myc and the IgH variable region. (Translated from eng) *J Exp Med* 204(9):2225-2232 (in eng).
24. Shinmura K, *et al.* (2011) Aberrant expression and mutation-inducing activity of AID in human lung cancer. (Translated from eng) *Ann Surg Oncol* 18(7):2084-2092 (in eng).
25. Takai A, *et al.* (2011) Targeting activation-induced cytidine deaminase prevents colon cancer development despite persistent colonic inflammation. (Translated from Eng) *Oncogene* (in Eng).
26. Morita S, *et al.* (2011) Bile acid-induced expression of activation-induced cytidine deaminase during the development of Barrett's oesophageal adenocarcinoma. (Translated from eng) *Carcinogenesis* 32(11):1706-1712 (in eng).
27. Pauklin S, Sernandez IV, Bachmann G, Ramiro AR, & Petersen-Mahrt SK (2009) Estrogen directly activates AID transcription and function. (Translated from eng) *J Exp Med* 206(1):99-111 (in eng).
28. Pasqualucci L, *et al.* (2004) Expression of the AID protein in normal and neoplastic B cells. (Translated from eng) *Blood* 104(10):3318-3325 (in eng).
29. Morgan HD, Dean W, Coker HA, Reik W, & Petersen-Mahrt SK (2004) Activation-induced cytidine deaminase deaminates 5-methylcytosine in DNA and is expressed in pluripotent tissues: implications for epigenetic reprogramming. (Translated from eng) *J Biol Chem* 279(50):52353-52360 (in eng).
30. Matsumoto Y, *et al.* (2007) Helicobacter pylori infection triggers aberrant expression of activation-induced cytidine deaminase in gastric epithelium. (Translated from eng) *Nat*

Med 13(4):470-476 (in eng).
31. MacDuff DA, Demorest ZL, & Harris RS (2009) AID can restrict L1 retrotransposition suggesting a dual role in innate and adaptive immunity. (Translated from eng) *Nucleic Acids Res* 37(6):1854-1867 (in eng).
32. Storck S, Aoufouchi S, Weill JC, & Reynaud CA (2011) AID and partners: for better and (not) for worse. (Translated from eng) *Curr Opin Immunol* 23(3):337-344 (in eng).
33. Stavnezer J (2011) Complex regulation and function of activation-induced cytidine deaminase. (Translated from eng) *Trends Immunol* 32(5):194-201 (in eng).
34. Patenaude AM & Di Noia JM (2010) The mechanisms regulating the subcellular localization of AID. (Translated from eng) *Nucleus* 1(4):325-331 (in eng).
35. Ito S*, et al.* (2004) Activation-induced cytidine deaminase shuttles between nucleus and cytoplasm like apolipoprotein B mRNA editing catalytic polypeptide 1. (Translated from eng) *Proc Natl Acad Sci U S A* 101(7):1975-1980 (in eng).
36. Brar SS, Watson M, & Diaz M (2004) Activation-induced cytosine deaminase (AID) is actively exported out of the nucleus but retained by the induction of DNA breaks. (Translated from eng) *J Biol Chem* 279(25):26395-26401 (in eng).
37. McBride KM, Barreto V, Ramiro AR, Stavropoulos P, & Nussenzweig MC (2004) Somatic hypermutation is limited by CRM1-dependent nuclear export of activation-induced deaminase. (Translated from eng) *J Exp Med* 199(9):1235-1244 (in eng).
38. Patenaude AM*, et al.* (2009) Active nuclear import and cytoplasmic retention of activation-induced deaminase. (Translated from eng) *Nat Struct Mol Biol* 16(5):517-527 (in eng).
39. Aoufouchi S*, et al.* (2008) Proteasomal degradation restricts the nuclear lifespan of AID. (Translated from eng) *J Exp Med* 205(6):1357-1368 (in eng).
40. Orthwein A*, et al.* (2010) Regulation of activation-induced deaminase stability and antibody gene diversification by HSP90. (Translated from eng) *J Exp Med* 207(12):2751-2765 (in eng).
41. Orthwein A*, et al.* (2011) Optimal functional levels of activation induced deaminase specifically require the HSP40 DnaJa1. *Embo J*.
42. Uchimura Y, Barton LF, Rada C, & Neuberger MS (2011) REG-gamma associates with and modulates the abundance of nuclear activation-induced deaminase. (Translated from Eng) *J Exp Med* (in Eng).
43. Dice JF & Goldberg AL (1975) A statistical analysis of the relationship between degradative rates and molecular weights of proteins. (Translated from eng) *Arch Biochem Biophys* 170(1):213-219 (in eng).
44. Dice JF, Hess EJ, & Goldberg AL (1979) Studies on the relationship between the degradative rates of proteins in vivo and their isoelectric points. (Translated from eng) *Biochem J* 178(2):305-312 (in eng).
45. Dice JF & Goldberg AL (1975) Relationship between in vivo degradative rates and

isoelectric points of proteins. (Translated from eng) *Proc Natl Acad Sci U S A* 72(10):3893-3897 (in eng).

46. Goldberg AL & St John AC (1976) Intracellular protein degradation in mammalian and bacterial cells: Part 2. (Translated from eng) *Annu Rev Biochem* 45:747-803 (in eng).
47. Goldberg AL & Dice JF (1974) Intracellular protein degradation in mammalian and bacterial cells. (Translated from eng) *Annu Rev Biochem* 43(0):835-869 (in eng).
48. Frescas D & Pagano M (2008) Deregulated proteolysis by the F-box proteins SKP2 and beta-TrCP: tipping the scales of cancer. (Translated from eng) *Nat Rev Cancer* 8(6):438-449 (in eng).
49. Barford D (2011) Structure, function and mechanism of the anaphase promoting complex (APC/C). (Translated from eng) *Q Rev Biophys* 44(2):153-190 (in eng).
50. Rogers S, Wells R, & Rechsteiner M (1986) Amino acid sequences common to rapidly degraded proteins: the PEST hypothesis. (Translated from eng) *Science* 234(4774):364-368 (in eng).
51. Bachmair A, Finley D, & Varshavsky A (1986) In vivo half-life of a protein is a function of its amino-terminal residue. (Translated from eng) *Science* 234(4773):179-186 (in eng).
52. Prakash S, Tian L, Ratliff KS, Lehotzky RE, & Matouschek A (2004) An unstructured initiation site is required for efficient proteasome-mediated degradation. (Translated from eng) *Nat Struct Mol Biol* 11(9):830-837 (in eng).
53. Tompa P, Prilusky J, Silman I, & Sussman JL (2008) Structural disorder serves as a weak signal for intracellular protein degradation. (Translated from eng) *Proteins* 71(2):903-909 (in eng).
54. Pfleger CM & Kirschner MW (2000) The KEN box: an APC recognition signal distinct from the D box targeted by Cdh1. (Translated from eng) *Genes Dev* 14(6):655-665 (in eng).
55. Yamano H, Gannon J, & Hunt T (1996) The role of proteolysis in cell cycle progression in Schizosaccharomyces pombe. (Translated from eng) *Embo J* 15(19):5268-5279 (in eng).
56. King RW, Glotzer M, & Kirschner MW (1996) Mutagenic analysis of the destruction signal of mitotic cyclins and structural characterization of ubiquitinated intermediates. (Translated from eng) *Mol Biol Cell* 7(9):1343-1357 (in eng).
57. Glotzer M, Murray AW, & Kirschner MW (1991) Cyclin is degraded by the ubiquitin pathway. (Translated from eng) *Nature* 349(6305):132-138 (in eng).
58. Glickman MH & Ciechanover A (2002) The ubiquitin-proteasome proteolytic pathway: destruction for the sake of construction. (Translated from eng) *Physiol Rev* 82(2):373-428 (in eng).
59. Margottin F*, et al.* (1998) A novel human WD protein, h-beta TrCp, that interacts with HIV-1 Vpu connects CD4 to the ER degradation pathway through an F-box motif. (Translated from eng) *Mol Cell* 1(4):565-574 (in eng).

60. Hart M*, et al.* (1999) The F-box protein beta-TrCP associates with phosphorylated beta-catenin and regulates its activity in the cell. (Translated from eng) *Curr Biol* 9(4):207-210 (in eng).
61. Yaron A*, et al.* (1998) Identification of the receptor component of the IkappaBalpha-ubiquitin ligase. (Translated from eng) *Nature* 396(6711):590-594 (in eng).
62. Rechsteiner M & Rogers SW (1996) PEST sequences and regulation by proteolysis. (Translated from eng) *Trends Biochem Sci* 21(7):267-271 (in eng).
63. Varshavsky A (2011) The N-end rule pathway and regulation by proteolysis. (Translated from Eng) *Protein Sci* (in Eng).
64. Schrader EK, Harstad KG, & Matouschek A (2009) Targeting proteins for degradation. (Translated from eng) *Nat Chem Biol* 5(11):815-822 (in eng).
65. Pickart CM & Eddins MJ (2004) Ubiquitin: structures, functions, mechanisms. (Translated from eng) *Biochim Biophys Acta* 1695(1-3):55-72 (in eng).
66. Orthwein A*, et al.* (2010) Regulation of activation-induced deaminase stability and antibody gene diversification by HSP90. (Translated from eng) *J Exp Med* 207(12):2751-2765 (in eng).
67. Petersen-Mahrt SK, Harris RS, & Neuberger MS (2002) AID mutates E. coli suggesting a DNA deamination mechanism for antibody diversification. (Translated from eng) *Nature* 418(6893):99-103 (in eng).
68. Arakawa H, Saribasak H, & Buerstedde JM (2004) Activation-induced cytidine deaminase initiates immunoglobulin gene conversion and hypermutation by a common intermediate. (Translated from eng) *PLoS Biol* 2(7):E179 (in eng).
69. Orthwein A*, et al.* (2011) Optimal functional levels of activation-induced deaminase specifically require the HSP40 DnaJa1. (Translated from Eng) *Embo J* (in Eng).
70. Koning FA*, et al.* (2009) Defining APOBEC3 expression patterns in human tissues and hematopoietic cell subsets. (Translated from eng) *J Virol* 83(18):9474-9485 (in eng).
71. Dickey CA*, et al.* (2007) The high-affinity HSP90-CHIP complex recognizes and selectively degrades phosphorylated tau client proteins. (Translated from eng) *J Clin Invest* 117(3):648-658 (in eng).
72. Schweers O, Schonbrunn-Hanebeck E, Marx A, & Mandelkow E (1994) Structural studies of tau protein and Alzheimer paired helical filaments show no evidence for beta-structure. (Translated from eng) *J Biol Chem* 269(39):24290-24297 (in eng).
73. Falsone SF, Kungl AJ, Rek A, Cappai R, & Zangger K (2009) The molecular chaperone HSP90 modulates intermediate steps of amyloid assembly of the Parkinson-related protein alpha-synuclein. (Translated from eng) *J Biol Chem* 284(45):31190-31199 (in eng).
74. Uversky VN (2003) A protein-chameleon: conformational plasticity of alpha-synuclein, a disordered protein involved in neurodegenerative disorders. (Translated from eng) *J Biomol Struct Dyn* 21(2):211-234 (in eng).
75. Kriwacki RW, Hengst L, Tennant L, Reed SI, & Wright PE (1996) Structural studies of

p21Waf1/Cip1/Sdi1 in the free and Cdk2-bound state: conformational disorder mediates binding diversity. (Translated from eng) *Proc Natl Acad Sci U S A* 93(21):11504-11509 (in eng).

76. Jascur T*, et al.* (2005) Regulation of p21(WAF1/CIP1) stability by WISp39, a HSP90 binding TPR protein. (Translated from English) *Mol Cell* 17(2):237-249 (in English).
77. Babu MM, van der Lee R, de Groot NS, & Gsponer J (2011) Intrinsically disordered proteins: regulation and disease. (Translated from eng) *Curr Opin Struct Biol* 21(3):432-440 (in eng).
78. Tsvetkov P, Reuven N, & Shaul Y (2009) The nanny model for IDPs. (Translated from eng) *Nat Chem Biol* 5(11):778-781 (in eng).
79. Linding R*, et al.* (2003) Protein disorder prediction: implications for structural proteomics. (Translated from eng) *Structure* 11(11):1453-1459 (in eng).
80. Xue B, Dunbrack RL, Williams RW, Dunker AK, & Uversky VN (2010) PONDR-FIT: a meta-predictor of intrinsically disordered amino acids. (Translated from eng) *Biochim Biophys Acta* 1804(4):996-1010 (in eng).
81. Nakayama KI & Nakayama K (2005) Regulation of the cell cycle by SCF-type ubiquitin ligases. (Translated from eng) *Semin Cell Dev Biol* 16(3):323-333 (in eng).
82. Gsponer J, Futschik ME, Teichmann SA, & Babu MM (2008) Tight regulation of unstructured proteins: from transcript synthesis to protein degradation. (Translated from eng) *Science* 322(5906):1365-1368 (in eng).
83. Singh GP, Ganapathi M, Sandhu KS, & Dash D (2006) Intrinsic unstructuredness and abundance of PEST motifs in eukaryotic proteomes. (Translated from eng) *Proteins* 62(2):309-315 (in eng).
84. Kuo ML, den Besten W, Bertwistle D, Roussel MF, & Sherr CJ (2004) N-terminal polyubiquitination and degradation of the Arf tumor suppressor. (Translated from eng) *Genes Dev* 18(15):1862-1874 (in eng).
85. Li H, Okamoto K, Peart MJ, & Prives C (2009) Lysine-independent turnover of cyclin G1 can be stabilized by B'alpha subunits of protein phosphatase 2A. (Translated from eng) *Mol Cell Biol* 29(3):919-928 (in eng).
86. Coulombe P, Rodier G, Bonneil E, Thibault P, & Meloche S (2004) N-Terminal ubiquitination of extracellular signal-regulated kinase 3 and p21 directs their degradation by the proteasome. (Translated from eng) *Mol Cell Biol* 24(14):6140-6150 (in eng).
87. Breitschopf K, Bengal E, Ziv T, Admon A, & Ciechanover A (1998) A novel site for ubiquitination: the N-terminal residue, and not internal lysines of MyoD, is essential for conjugation and degradation of the protein. (Translated from eng) *Embo J* 17(20):5964-5973 (in eng).
88. Hasler J, Rada C, & Neuberger MS (2011) Cytoplasmic activation-induced cytidine deaminase (AID) exists in stoichiometric complex with translation elongation factor

1alpha (eEF1A). (Translated from Eng) *Proc Natl Acad Sci U S A* (in Eng).
89. Jascur T, *et al.* (2005) Regulation of p21(WAF1/CIP1) stability by WISp39, a HSP90 binding TPR protein. (Translated from eng) *Mol Cell* 17(2):237-249 (in eng).
90. Sanchez ER, Toft DO, Schlesinger MJ, & Pratt WB (1985) Evidence that the 90-kDa phosphoprotein associated with the untransformed L-cell glucocorticoid receptor is a murine heat shock protein. (Translated from eng) *J Biol Chem* 260(23):12398-12401 (in eng).
91. Schuh S, *et al.* (1985) A 90,000-dalton binding protein common to both steroid receptors and the Rous sarcoma virus transforming protein, pp60v-src. (Translated from eng) *J Biol Chem* 260(26):14292-14296 (in eng).
92. Joab I, *et al.* (1984) Common non-hormone binding component in non-transformed chick oviduct receptors of four steroid hormones. (Translated from eng) *Nature* 308(5962):850-853 (in eng).
93. Kumar R, *et al.* (2004) TATA box binding protein induces structure in the recombinant glucocorticoid receptor AF1 domain. (Translated from eng) *Proc Natl Acad Sci U S A* 101(47):16425-16430 (in eng).
94. Dyson HJ & Wright PE (2005) Intrinsically unstructured proteins and their functions. (Translated from eng) *Nat Rev Mol Cell Biol* 6(3):197-208 (in eng).
95. Chaudhuri J, Khuong C, & Alt FW (2004) Replication protein A interacts with AID to promote deamination of somatic hypermutation targets. (Translated from eng) *Nature* 430(7003):992-998 (in eng).
96. Jeevan-Raj BP, *et al.* (2011) Epigenetic tethering of AID to the donor switch region during immunoglobulin class switch recombination. (Translated from eng) *J Exp Med* 208(8):1649-1660 (in eng).
97. Basu U, *et al.* (2011) The RNA exosome targets the AID cytidine deaminase to both strands of transcribed duplex DNA substrates. (Translated from eng) *Cell* 144(3):353-363 (in eng).
98. Okazaki IM, *et al.* (2011) Histone chaperone Spt6 is required for class switch recombination but not somatic hypermutation. (Translated from eng) *Proc Natl Acad Sci U S A* 108(19):7920-7925 (in eng).
99. Pavri R, *et al.* (2010) Activation-induced cytidine deaminase targets DNA at sites of RNA polymerase II stalling by interaction with Spt5. (Translated from eng) *Cell* 143(1):122-133 (in eng).
100. Nambu Y, *et al.* (2003) Transcription-coupled events associating with immunoglobulin switch region chromatin. (Translated from eng) *Science* 302(5653):2137-2140 (in eng).
101. Nowak U, Matthews AJ, Zheng S, & Chaudhuri J (2011) The splicing regulator PTBP2 interacts with the cytidine deaminase AID and promotes binding of AID to switch-region DNA. (Translated from eng) *Nat Immunol* 12(2):160-166 (in eng).
102. Maeda K, *et al.* (2010) GANP-mediated recruitment of activation-induced cytidine

deaminase to cell nuclei and to immunoglobulin variable region DNA. (Translated from eng) *J Biol Chem* 285(31):23945-23953 (in eng).

103. Conticello SG*, et al.* (2008) Interaction between antibody-diversification enzyme AID and spliceosome-associated factor CTNNBL1. (Translated from eng) *Mol Cell* 31(4):474-484 (in eng).
104. Gazumyan A*, et al.* (2011) Amino-terminal phosphorylation of activation-induced cytidine deaminase suppresses c-myc/IgH translocation. (Translated from eng) *Mol Cell Biol* 31(3):442-449 (in eng).
105. McBride KM*, et al.* (2008) Regulation of class switch recombination and somatic mutation by AID phosphorylation. (Translated from eng) *J Exp Med* 205(11):2585-2594 (in eng).
106. Pasqualucci L, Kitaura Y, Gu H, & Dalla-Favera R (2006) PKA-mediated phosphorylation regulates the function of activation-induced deaminase (AID) in B cells. (Translated from eng) *Proc Natl Acad Sci U S A* 103(2):395-400 (in eng).
107. Hegyi H & Tompa P (2008) Intrinsically disordered proteins display no preference for chaperone binding in vivo. (Translated from English) *Plos Comput Biol* 4(3) (in English).
108. Giglione C, Boularot A, & Meinnel T (2004) Protein N-terminal methionine excision. (Translated from eng) *Cell Mol Life Sci* 61(12):1455-1474 (in eng).
109. Bloom J, Amador V, Bartolini F, DeMartino G, & Pagano M (2003) Proteasome-mediated degradation of p21 via N-terminal ubiquitinylation. (Translated from eng) *Cell* 115(1):71-82 (in eng).
110. Sun L, Trausch-Azar JS, Muglia LJ, & Schwartz AL (2008) Glucocorticoids differentially regulate degradation of MyoD and Id1 by N-terminal ubiquitination to promote muscle protein catabolism. (Translated from eng) *Proc Natl Acad Sci U S A* 105(9):3339-3344 (in eng).
111. Fajerman I, Schwartz AL, & Ciechanover A (2004) Degradation of the Id2 developmental regulator: targeting via N-terminal ubiquitination. (Translated from eng) *Biochem Biophys Res Commun* 314(2):505-512 (in eng).
112. Shao Q, Wang Y, Hildreth JE, & Liu B (2010) Polyubiquitination of APOBEC3G is essential for its degradation by HIV-1 Vif. (Translated from eng) *J Virol* 84(9):4840-4844 (in eng).
113. Wang Y*, et al.* (2011) N-terminal hemagglutinin tag renders lysine-deficient APOBEC3G resistant to HIV-1 Vif-induced degradation by reduced polyubiquitination. (Translated from eng) *J Virol* 85(9):4510-4519 (in eng).
114. Wang X*, et al.* (2007) Ubiquitination of serine, threonine, or lysine residues on the cytoplasmic tail can induce ERAD of MHC-I by viral E3 ligase mK3. (Translated from eng) *J Cell Biol* 177(4):613-624 (in eng).
115. Cadwell K & Coscoy L (2008) The specificities of Kaposi's sarcoma-associated herpesvirus-encoded E3 ubiquitin ligases are determined by the positions of lysine or

cysteine residues within the intracytoplasmic domains of their targets. (Translated from eng) *J Virol* 82(8):4184-4189 (in eng).

116. Cadwell K & Coscoy L (2005) Ubiquitination on nonlysine residues by a viral E3 ubiquitin ligase. (Translated from eng) *Science* 309(5731):127-130 (in eng).
117. Tokarev AA, Munguia J, & Guatelli JC (2011) Serine-threonine ubiquitination mediates downregulation of BST-2/tetherin and relief of restricted virion release by HIV-1 Vpu. (Translated from eng) *J Virol* 85(1):51-63 (in eng).
118. Magadan JG*, et al.* (2010) Multilayered mechanism of CD4 downregulation by HIV-1 Vpu involving distinct ER retention and ERAD targeting steps. (Translated from eng) *PLoS Pathog* 6(4):e1000869 (in eng).

CHAPTER 5: DISCUSSION

This thesis described the identification of new cytoplasmic partners and determinants of AID that modulate/affect its stability and contribute in regulating antibody diversification. We have found that cytoplasmic AID is stabilized by the HSP90 molecular chaperoning pathway, which we have described in much detail (Chapters 2 and 3). This regulatory pathway is important to set up the necessary AID levels for efficient antibody diversification, while limiting AID oncogenic potential. We were also able to initiate a study which points toward intrinsic destabilizing determinants in AID protein sequence that could explain the need for chaperoning, and toward a direct contribution of AID stability to antibody diversification (Chapter 4).

5.1. AID association with the HSP90 molecular chaperoning pathway

During the course of this thesis, Aoufouchi *et al.* described that AID is much more stable in the cytoplasm than in the nucleus [522], but the molecular explanation for this differential stability was unknown. We identified and functionally characterized AID as a novel HSP90 client [523] and we showed that AID interacts with several factors that are part of the HSP90 molecular chaperoning pathway, in particular the HSP40 DnaJa1, HSC70 and HSP90 [523, 524]. AID requirement for these chaperones is evolutionary conserved, as HSP90 inhibition or modulation of DnaJa1 levels affected both endogenous AID levels and AID-mediated antibody diversification in chicken, mouse and human B cells [523, 524]. Intriguingly, none of AID paralog APOBECs, which share high sequence and structure similarities, were able to bind to any of these chaperones [523, 524]. APOBEC1 was reported to associate with a type II HSP40/DnaJ protein, DnaJb11, and downregulation of DnaJb11 inhibited APOBEC1-mediated ApoB mRNA editing [525]. This observation was surprising at first since DnaJb11 is an endoplasmic reticulum (ER)-resident protein [526] while APOBEC1 is a nucleo-cytoplasmic shuttling protein [157, 314, 527]. In fact, a truncated form of DnaJb11 lacking its ER localization signal was used and therefore it is likely that the observated interaction is not physiologically relevant. However, convincing evidence showed that zebrafish APOBEC2 interacts with the chaperone UNC45B but not with HSP90-α [149].

Disruption of *unc45b* in zebrafish showed the same dystrophic phenotype as downregulation of APOBEC2 [149]. UNC45B interacts with HSP90 [528], but our data showed that, unlike AID, APOBEC proteins do not depend on the HSP90 pathway for their stabilization (Chapter 4). It remains unclear whether any other chaperones are involved in the stabilization of APOBEC proteins.

Since HSP90 stabilizes nearly-folded proteins rather than participating in protein biogenesis, the AID-HSP90 association could be due to the presence of intrinsically unstructured domains that make AID partially unfolded unless stabilized by an interacting partner. Indeed, early reports suggested that recombinant AID purification is quite challenging and only yields a low amount of active/soluble protein (~5%), with the rest being found in complexes that are inactive [187, 190]. In the absence of an AID crystal structure, we can only speculate about the position and the extent of these partially unfolded regions. The presence of unstructured domains in AID would fit with the fact that several intrinsically unstructured proteins such as α-synuclein [529, 530], tau [531, 532], $p21^{(WAF1/CIP1)}$ [533, 534], and the steroid hormone receptors [535-538], also require HSP90 assistance for their stabilization. But the absence of any canonical sequence or structural motif that dictate HSP90 association to its clients makes it difficult to identify domain(s) controlling AID-HSP90 interaction [375]. We mapped this interaction to AID N-terminal region spanning residues 19 to 84 [523]. This region contains 2-3 putative unstructured domains as predicted by two different algorithms, DisEMBL™ and PONDR® (Chapter 4). Together, these domains could confer to AID a partially unfolded face and require its binding to HSP90. Indeed, several lines of evidence suggest that recognition of HSP90 clients is related to their conformation and stability [375]. This is exemplified by the cellular and viral forms of the SRC tyrosine kinase (c- and v-SRC), which share high sequence similarities (~95%) but depend differently on HSP90. V-SRC is intrinsically unstable and associates strongly to HSP90, while c-SRC is more resistant to denaturating conditions *in vitro* and only transiently associates with this molecular chaperone [376-378]. Similarly, the differential dependence of AID/APOBEC on the HSP90 pathway may be related to their different contents in unstructured regions. Although this is a hypothesis, it is suggestive that replacing these regions with the homologuous APOBEC2 regions or mutating

them to disrupt the PEST-like motif result in less responsiveness to HSP90 inhibitors (Chapter 4 and data not shown). Altogether, we showed that AID requires the assistance of the HSP90 molecular chaperoning pathway. We suspect this process to be determined by AID intrinsic instability conferred by unstructured regions containing destabilizing motifs such as a PEST-like motif.

5.2. The role of the HSP90 pathway in AID stability and its interdependence with subcellular localization

Our studies provide mechanistic insight into the link between AID subcellular localization and stability. Indeed, the HSP90 molecular chaperoning pathway stabilizes cytoplasmic AID and determines the overall AID steady-state levels [523], thus at least partially explaining why cytoplasmic AID is much more stable than its nuclear counterpart. HSP90 protects cytoplasmic AID from degradation since HSP90 inhibition resulted in the polyubiquitination and the proteasomal degradation of AID in the cytoplasm (Figure 5.1). This recapitulates the major function of HSP90 as a modulator of the stability and the functional maturation of its clients [375, 409, 539], such as the steroid hormone receptors [540, 541].

In general, HSP90 client stabilization is initiated by the interaction with the HSP40 and HSP70 system [524, 540, 541] (Figure 5.1), but only a subset of HSP40-HSP70 substrates is delivered to HSP90 for stabilization [541, 542]. Different HSP40 proteins can have a redundant role in this initial substrate recognition and association with HSP70. Indeed, several HSP40s (f.i. DnaJa1 and –b1 for the progesterone receptor [416] , DnaJa1 and -a2 for the potassium channel protein HERG [420]) can bind to the same substrate *in vitro* [416, 421, 423, 543, 544], as we found to be the case for AID [524]. Nonetheless, AID specifically depends on DnaJa1 for its stabilization since its deficiency results in reduced endogenous AID levels and decreased AID half-life, accompanied by reduced biological activity [524]. The requirement of DnaJa1 farnesylation for binding and biological activity of AID supports a non-redundant role for this co-chaperone in linking AID to the HSP90 pathway. This is based on a previous report showing that the farnesylation of DnaJa1 ortholog YDJ1 is required for its interaction with HSP90 clients *in vitro* [400] and *in vivo* in yeast [401]. To our knowledge, AID is the first endogenous

HSP90 client in higher eukaryotes for which a specific HSP40 has been identified to be involved in its stabilization *in vivo*. The only other known example for an endogenous protein is the mitogen-activated kinase kinase kinase (MAPKKK) STE11 in yeast [400], but in this case the diversity of HSP40/DnaJ proteins is limited as yeast only expresses one type I- and one type II- cytosolic DnaJ proteins [545, 546].

It remains unclear whether additional HSP40 proteins are implicated in AID stabilization, since *DNAJA1*-/- mice can make up to 50% of normal AID protein levels. The first candidate for this DnaJa1-independent pathway would be DnaJa2, given its high similarity with DnaJa1 (~95%), but our data exclude this possibility [524]. In yeast, the type II HSP40 SIS1 protein can partially substitute for the DnaJa1 ortholog YDJ1 [394, 544], which suggests that DnaJb1 could potentially contribute to AID stabilization in the absence of DnaJa1. Partially folded AID could also skip the stabilization by HSP90 altogether and become stable in complex with others factors such as eEF1α [325] or importins [315] (Figure 5.2). The nature of this DnaJa1-independent pathway for AID stabilization remains unclear and requires further investigations but it is clearly much less efficient than the DnaJa1-dependent pathway.

In any case, the cytoplasmic stabilization by the DnaJa1–HSP90 pathway is critical for producing the physiological maximal levels of AID. Overexpression experiments suggest that DnaJa1 is the limiting factor in AID stabilization [524], in line with previous studies showing that HSP40 co-chaperones, especially DnaJa1, are limiting components in the HSP90 molecular chaperoning pathway in *E. coli*, yeast, but also in mammalian systems [390, 412-415]. DnaJa1 overexpression increases both AID protein levels and AID biological activity in B cell lines [524]. Interestingly, mice in which higher levels of AID were achieved by either overexpression AID through a transgene [199-202] or removing the negative post-transcriptional regulation of AID by miR-155 [203, 204] all showed increased CSR and SHM *in vitro* but did not display increased levels of switched serum Ig. In particular, loss of AID

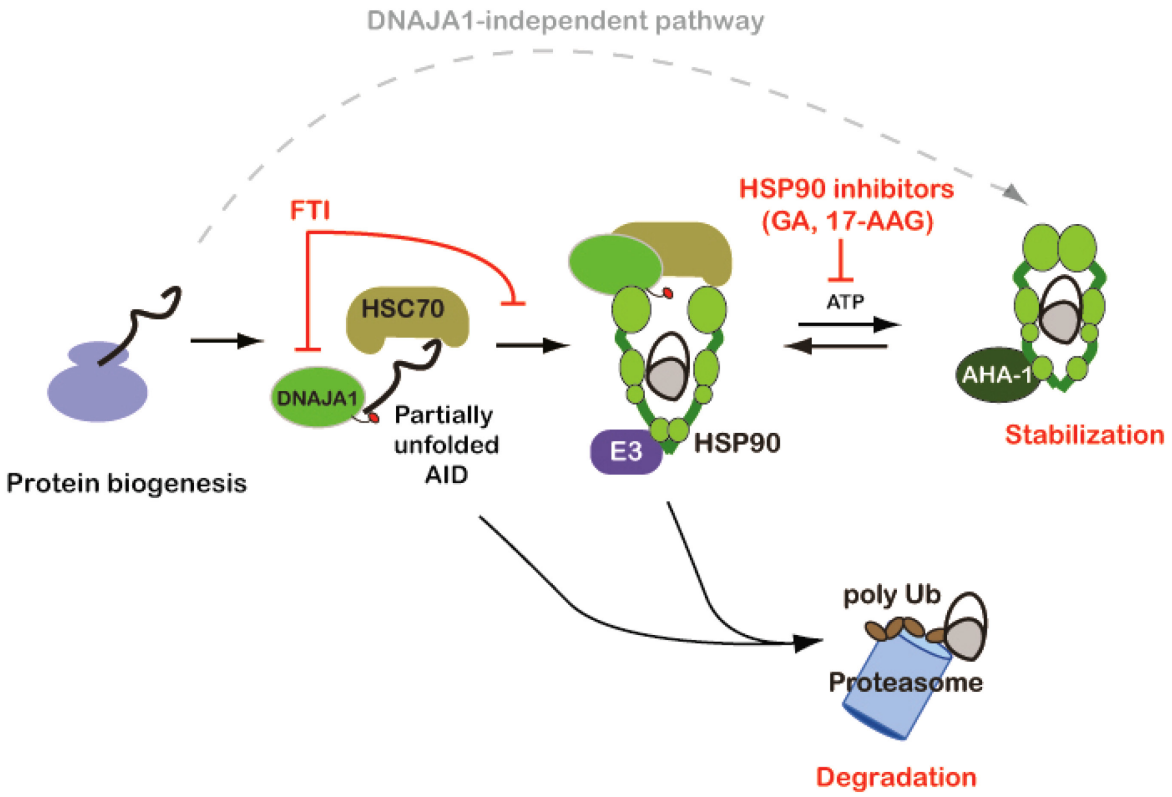

Figure 5.1. AID stabilization by the DnaJa1-HSP90 pathway and drugs that can inhibit it. *Detailed schematic representation with each step participating in the stabilization of AID. AID is synthesized in the cytoplasm where unfolded AID is met by the HSP40-HSC70 system; the specific action of DnaJa1 allows transferring AID into the HSP90 molecular chaperoning stabilization cycle. AID stabilization can also occur through a DnaJa1-independent pathway, as DNAJA1-/- B cells still display up to 50% of normal AID levels. HSP90 inhibitors, such as geldanamycin (GA) and its derivative 17-AAG, prevent the ATP hydrolysis cycle of the chaperone. FTI, farnesyltransferase inhibitors, prevent farnesylation of DnaJa1, which is required for binding to and stabilization of AID. Both inhibitors lead to polyubiquitination and proteasomal degradation of cytoplasmic AID.*

regulation by mi-R155 resulted in impaired affinity maturation *in vivo* [203]. It may be that the upper limit for AID physiological levels could be influenced by the increased apoptosis that elevated AID can bring about [547]. Thus, it is unlikely that DnaJa1 overexpression, which is predicted to increase steady-state AID levels in B cells, results in a more efficient antibody diversification. It may rather affect AID oncogenic potential as increased levels of AID in B cells have been reported to increase IgH-cMyc translocations [201, 204] and mutations in some non-Ig targets [201, 203, 257].

Our data also suggests that there is very little turnover of cytoplasmic AID, with stabilization being the default pathway. Indeed, inhibiting the proteasome does not produce much polyubiquitinated AID in B cells while simultaneous inhibition of HSP90 and the proteasome results in massive accumulation of polyubiquitinated AID [523]. Furthermore, downregulation of the HSP90-associated E3 ubiquitin ligase CHIP does not impact the overall steady-state AID levels in a mouse B cell line (data not shown), suggesting that only a very small proportion of cytoplasmic AID is targeted for degradation under normal steady-state conditions. Conversely, nuclear AID is much less stable and seems to be constantly targeted to the proteasome by Ub-dependent and –independent pathways [331, 333]. It remains unclear whether AID nuclear degradation results from the loss of stabilizing interactions and/or an active program of destabilization. HSP90 is mostly found in the cytoplasm, where it constitutes 1-2% of the total protein levels [375]. Nuclear AID could therefore loose this stabilizing interaction and be exposed to rapid degradation after import. However, there is still some HSP90 in the nucleus in normal and cancer cells [548, 549] and some evidence suggests that HSP90 can translocate into the nucleus in response to stress or other stimuli [550-553]. Since HSP90 does not have a nuclear localization sequence, its nuclear import may only occur by co-transport with its clients. Indeed, HSP90 can be co-imported with the glucocorticoid receptor (GR) into the nucleus [554-556]. But whether HSP90 is localized in the nucleus in the context of B cell stimulation and whether nuclear AID is at any stage associated with this chaperone is unknown.

A common feature of nuclear and cytoplasmic AID is the fact that they do not depend on internal lysines for polyubiquitination. AID with all lysine residues mutated to arginines

(Kzero) is still significantly polyubiquitinated in both the cytoplasm and the nucleus ([331] and chapter 4), suggesting either a N-terminal ligation or a non-canonical ubiquitination site. Our data indicates that AID degradation through N-terminal ligation is unlikely to occur in the cytoplasm, but further work is required to definitively exclude this possibility. Due to AID's intrinsic instability, it is possible that the absence of available lysines in the Kzero mutant forces the Ub-proteasome pathway to use noncanonical residues for AID degradation. This could also have some unknown physiological relevance.

5.3. Direct impact of AID stability in antibody diversification

Because of the interdependence between AID subcellular localization and stability [315, 325, 329, 331, 332], it has been difficult to evaluate the direct contribution of AID protein turnover in regulating antibody diversification. Here we could show that modulating AID stability, without visibly affecting its subcellular localization, influences the efficiency of antibody diversification *in vitro* (Chapter 4). AID intrinsic instability seems to depend at least on an N-degron and an internal PEST-like motif. The N-end rule, which depends on the Ub-proteasome pathway for protein turnover, requires N-terminal proteolytic processing of its substrates [500]. While N-terminal methionine cleavage is an evolutionary conserved modification, affecting up to 70 % of the proteins in plant plastids [503], we have no direct evidence that AID is processed in such a way to reveal the destabilizing aspartic acid at position two. Analysis of purified AID by mass spectrometry or N-end sequencing of purified endogenous protein could reveal whether AID is post-translationally cleaved at its N-terminus. Similarly, it remains unclear whether the AID internal destabilizing motif we described (Chapter 4) is an actual PEST motif. These regions enriched in proline, aspartic/glutamic acid, serine and threonine, are generally found in short-lived proteins [508-511]. Interestingly, it has been hypothesized that PEST motifs confer increased susceptibility to proteolysis by recruiting both the Ub-dependent and -independent proteasomal degradation pathway [512]. It is possible that the AID PEST-like motif is recognized by REG-γ in the nucleus, thus targeting AID for Ub-independent proteasomal degradation but this has not been confirmed. Indeed, AID-REGγ interaction requires the first 140 amino acids of AID that encompass the PEST-like motif [484].

Whether modulating AID's instrinsic stability may affect antibody diversification *in vivo* also requires more investigation. But it is now clear that destabilizing motifs in AID directly contribute to its biological functions by modulating AID protein turnover and limiting its presence in the nucleus.

5.4. Cytoplasmic pools of AID

Differential AID stability between the cytoplasm and the nucleus is an additional way of restricting its access to the nucleus. Indeed, inhibiting HSP90 or DnaJa1 farnesylation (which prevents binding to AID), as well as *DNAJA1* knockdown, do not affect cytoplasmic retention of AID [523, 524]. Both nuclear destabilization and cytoplasmic retention contribute to AID nuclear exclusion [315, 484, 522]. Cytoplasmic retention may involve the participation of the eEF1α translation factor, since it is stoichiometrically associated with AID in the cytoplasm and mutating the proposed AID cytoplasmic retention motif can disrupt this interaction [315, 325]. This step would logically be after AID is stabilized by and released from HSP90. AID would therefore coexist in different cytoplasmic pools [557]. We could envision that these regulatory mechanisms form a circuit (f.i. release from HSP90 is always followed by AID associated to cytoplasmic retention, which precedes nuclear import, etc; Figure 5.2A). Preliminary immunofluorescence experiments suggest that AID stabilization by HSP90 is a prerequisite for its nuclear import [523]. It is also likely that the transmission of AID from the meta-stable complex with HSP90 may require some maturation step such as post-translational modifications or oligomerization [327, 332]. This would therefore allow mechanisms with apparently the same effect to play distinct roles.

Alternatively, unstructured regions may confer to AID useful properties such as rapid and specific interaction potential without excessive binding strength [558]. In fact, unstructured proteins require the assistance of chaperones for interacting with other co-factors [559]. HSP90 stabilization could therefore be a transitory state, where AID is subsequently transferred to several competing destinations (f.i. release from HSP90 could be followed by cytoplasmic retention or nuclear import or degradation; Figure 5.2B). This network model would prevent

AID from aggregating/or being targeted to the Ub-proteasome system while having the flexibility to bind multiple alternative partners. Of course, AID regulation may be a mixture of both models. Nevertheless, it remains unclear what dictates AID dissociation from HSP90 and what is the relative distribution of AID between the HSP90 stabilizing pool and the cytoplasmic retention pool. But altogether these mechanisms greatly contribute in determining the appropriate steady-state and nuclear levels of AID during antibody diversification.

5.5. Pharmacological modulation of AID levels.

Modulating AID stability seems to be one way of controlling AID expression levels and, thereby an important mechanism regulating antibody diversification. On the one hand, AID stabilization by the DnaJa1-HSP90 chaperoning pathway is important to obtain sufficiently high AID protein levels for efficient antibody diversification. On the other hand, AID pathological outcomes are restricted by both DnaJa1 levels and nuclear destabilization of AID, which limit the functional levels of this mutagenic enzyme. In fact, AID is oncogenic, which is likely a consequence of its capacity to mutate and generate DNA breaks, thus initiating chromosomal translocations and mutations in tumor suppressor genes and proto-oncogenes [261-265]. Oncogenic AID lesions are directly correlated to AID protein levels as increased expression of AID in B cells leads to a large increase in IgH-cMyc translocations [201, 204] and increased mutations in some non-Ig targets [201, 203, 257]. Ectopic expression of AID in Ph+ CML promotes the progression into a fatal B lymphoid blast crisis as AID activity leads to the acquisition of mutations in BCR-ABL1 and the development of resistance to the therapeutic drug imatinib [129]. We have shown that HSP90 inhibitors such as geldanamycin derivates, which are already in clinical trials [444], could be exploited to indirectly target AID. Indeed, destabilization of AID with HSP90 inhibitors prevented AID-mediated mutations in BCR-ABL and the generation of resistance to imatinib in CML cells. Farnesyltransferase inhibitors, which prevent the binding of AID to DnaJa1, could also serve as a pharmacological tool to decrease

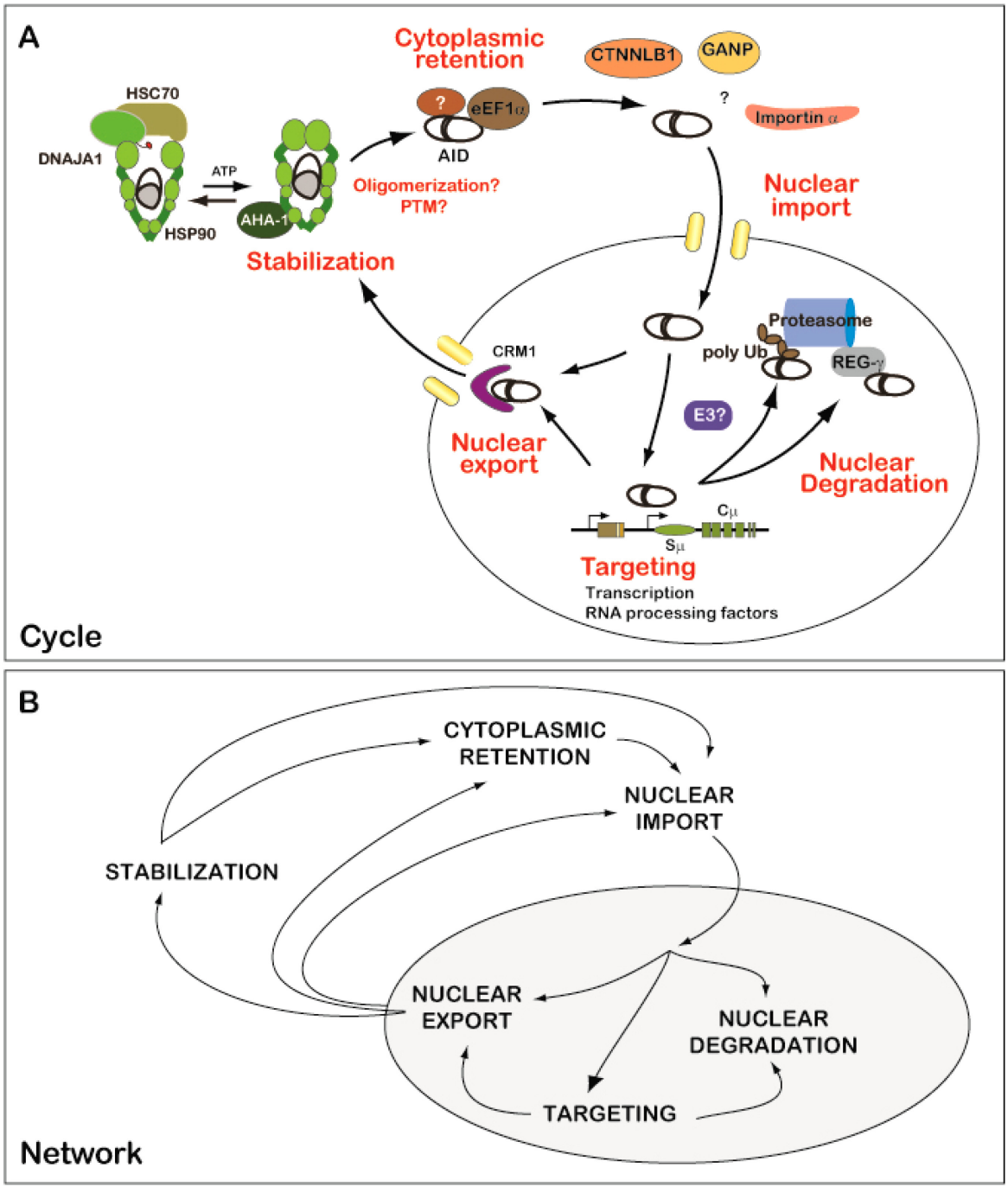
A
Cytoplasmic retention
CTNNLB1
GANP
HSC70
DNAJA1
ATP
HSP90
AHA-1
?
eEF1α
AID
Oligomerization?
PTM?
?
Importin α
Nuclear import
Stabilization
CRM1
poly Ub
Proteasome
REG-γ
E3?
Nuclear export
Nuclear Degradation
Cμ
Sμ
Targeting
Transcription
RNA processing factors
Cycle
B
CYTOPLASMIC RETENTION
NUCLEAR IMPORT
STABILIZATION
NUCLEAR EXPORT
NUCLEAR DEGRADATION
TARGETING
Network

Figure 5.2. Major post-translational regulation steps affecting AID levels. (A) *Detailed schematic representation with each step participating in the stability and the subcellular localization regulation represented within a cycle. Only selected AID interacting factors are shown. After AID stabilization by the HSP90 molecular chaperoning pathway, some undefined maturation step or conformational change can allow AID to pass onto eEF1α and/or other cytoplasmic retention factors before active nuclear import. A number of factors could be implicated, alternatively or jointly, in AID nuclear import. Once inside the nucleus, AID is either exported by CRM1 or targeted to the Ig loci by interacting with a number of RNA processing factor, where it is phosphorylated by PKA. AID is (subsequently?) degraded in the nucleus either through Ub- or REGγ-dependent proteasomal degradation.* ***(B)*** *Simplified schematic representation of the same steps as in* ***A*** *but in the form of a network in which most pools of AID are interconnected.*

AID protein levels. Whether increased expression of limiting factors of the HSP90 pathway, especially DnaJa1, could favour the development of AID-associated lymphomas/leukemias is unknown. Increased expression of members of the HSP90 pathway has been reported in solid tumors and haematological malignancies [408, 409], but little is known about DnaJa1 expression profiles between healthy subjects and lymphoma/leukemia-affected patients. We also know very little about whether DnaJa1 levels correlate with AID levels in B cells and other relevant cell types/tissues.

AID is also implicated in the onset of autoimmune diseases [242, 285-287] and could be an interesting target to treat pathologies such as rheumatoid arthristis and systemic lupus erythematosus, which are associated with exacerbated antibody diversification. Interestingly, several reports have shown a differential expression of *DNAJA1* between healthy controls and patients affected with autoimmune diseases. *DNAJA1* is overexpressed in synovial tissues of patients affected by rheumatoid arthritis [560]. Furthermore, differential expression of *DNAJA1* in peripheral blood of systemic lupus erythematosus patients has been reported and two single nucleotide polymorphisms in *DNAJA1* are associated with the onset and the progression of this autoimmune disease [561, 562]. Mouse models recapitulating lupus and rheumatoid arthritis display increased levels of AID, which correlate with higher levels of autoantibodies [242, 285-287]. Moreover, AID deficiency, or even haploinsufficiency, results in a more moderate disease [195, 242-244]. The challenge here, similar to AID involvement in cancer development, is to identify a disease and a mouse model where AID implication and onset can be predicted in order to target AID at the right time. In the absence of specific inhibitors of AID, exploiting HSP90 and farnesyltransferase inhibitors as described in this thesis (Chapter 2 and 3) proved to be a reasonable alternative to pharmacologically targeting AID.

CHAPTER 6: CONCLUSION

Our results show that AID is stabilized in the cytoplasm by the HSP90 molecular chaperoning pathway. This requires the participation of the HSP40 DnaJa1, which is a limiting step in AID stabilization. AID stability and protein levels directly modulate its biological functions. Increased AID stability, by introducing stabilizing mutations, or increased AID protein levels by overexpressing DnaJa1, result in a more efficient antibody diversification. Conversely, inhibiting HSP90 or farnesyltransferases as well as reducing DnaJa1 levels result in less antibody diversification and off-target mutations.

We show this in particular for the BCR-ABL oncogene, in which HSP90 inhibitors prevent the emergence of an AID-dependent imatinib-resistant subpopulation of CML cells. Thus, pharmacological modulation of AID protein levels is an interesting possibility to treat AID-related cancers and/or pathologies associated with exacerbated antibody diversification. Mouse models, where AID has been directly implicated in the development of ALL or CML, are great tools to investigate whether this strategy could prevent or slow down the onset of these diseases. Preliminary work in patients affected by CML blast crisis suggested that the use of arsenic trioxide, a drug that downregulates AID mRNA and protein levels, combined to imatinib, could achieve better therapeutic effects by reducing drug resistance [563]. Similarly, disruption of *Aicda* in the mouse model of IBD reduces the incidence of colon cancer development [564], which could be another therapeutic opportunity. Downregulating AID protein levels could also minimize AID contribution to autoimmune diseases, as AID overexpression correlates with the production of autoantibodies and the onset of autoimmune diseases such as lupus and rheumatoid arthritis [242, 285-287]. Therefore, modulating AID levels, systematically or locally, could minimize its pathological contribution to both cancer and autoimmune diseases. Targeting the farnesylation of DnaJa1 by using farnesyltransferase inhibitors may reduce AID pathological outcomes as well and could serve as an alternative to HSP90 inhibitors.

Our work raises the question of whether the HSP90 molecular chaperoning pathway could be a predisposing element in the development of AID-associated diseases. Since DnaJa1 is a limiting factor in AID stabilization, one could hypothesize that upregulation of this co-chaperones may result in higher steady-state AID levels, thus increasing the susceptibility to off-target mutations, chromosomal translocations, and antibody-associated autoimmune

diseases. It is also unclear whether AID is as dependent on HSP90 stabilization in normal versus transformed cells. Further experimental work is also needed to explore whether AID stabilization by the HSP90 molecular chaperoning pathway is as critical for its demethylation function as it is for antibody diversification.

CHAPTER 7: BIBLIOGRAPHY

[1] Bartl S, Baish M, Weissman IL, Diaz M. Did the molecules of adaptive immunity evolve from the innate immune system? Integr Comp Biol. 2003;43:338-346.
[2] Butler JE, Zhao Y, Sinkora M, Wertz N, Kacskovics I. Immunoglobulins, antibody repertoire and B cell development. Dev Comp Immunol. 2009;33:321-333.
[3] Wang W, Singh S, Zeng DL, King K, Nema S. Antibody structure, instability, and formulation. J Pharm Sci. 2007;96:1-26.
[4] Schroeder HW, Jr., Cavacini L. Structure and function of immunoglobulins. J Allergy Clin Immunol. 2010;125:S41-52.
[5] Skvaril F, Barandun S, MoreIl A, Kuffer F, Probst M. Imbalances of K/A immunoglobulin light chain ratios in normal individuals and in immunodeficient patients. Twenty-second Colloquium, Bruges, Protides of the Biological Fluids 1975.
[6] Low JM, Chauhan AK, Moore TL. Abnormal kappa:lambda light chain ratio in circulating immune complexes as a marker for B cell activity in juvenile idiopathic arthritis. Scand J Immunol. 2007;65:76-83.
[7] Wardemann H, Hammersen J, Nussenzweig MC. Human autoantibody silencing by immunoglobulin light chains. J Exp Med. 2004;200:191-199.
[8] Gharavi AE, Harris EN, Lockshin MD, Hughes GR, Elkon KB. IgG subclass and light chain distribution of anticardiolipin and anti-DNA antibodies in systemic lupus erythematosus. Ann Rheum Dis. 1988;47:286-290.
[9] Chen K, Xu W, Wilson M, He B, Miller NW, Bengten E, et al. Immunoglobulin D enhances immune surveillance by activating antimicrobial, proinflammatory and B cell-stimulating programs in basophils. Nat Immunol. 2009;10:889-898.
[10] Clynes R, Ravetch JV. Cytotoxic antibodies trigger inflammation through Fc receptors. Immunity. 1995;3:21-26.
[11] Sylvestre D, Clynes R, Ma M, Warren H, Carroll MC, Ravetch JV. Immunoglobulin G-mediated inflammatory responses develop normally in complement-deficient mice. J Exp Med. 1996;184:2385-2392.
[12] Nimmerjahn F, Ravetch JV. Divergent immunoglobulin g subclass activity through selective Fc receptor binding. Science. 2005;310:1510-1512.
[13] Woof JM, Russell MW. Structure and function relationships in IgA. Mucosal Immunol. 2011;4:590-597.
[14] Gould HJ, Sutton BJ. IgE in allergy and asthma today. Nat Rev Immunol. 2008;8:205-217.
[15] van Gent DC, McBlane JF, Ramsden DA, Sadofsky MJ, Hesse JE, Gellert M. Initiation of V(D)J recombination in a cell-free system. Cell. 1995;81:925-934.
[16] McBlane JF, van Gent DC, Ramsden DA, Romeo C, Cuomo CA, Gellert M, et al. Cleavage at a V(D)J recombination signal requires only RAG1 and RAG2 proteins and occurs in two steps. Cell. 1995;83:387-395.
[17] Mombaerts P, Iacomini J, Johnson RS, Herrup K, Tonegawa S, Papaioannou VE. RAG-1-deficient mice have no mature B and T lymphocytes. Cell. 1992;68:869-877.
[18] Shinkai Y, Rathbun G, Lam KP, Oltz EM, Stewart V, Mendelsohn M, et al. RAG-2-deficient mice lack mature lymphocytes owing to inability to initiate V(D)J rearrangement. Cell. 1992;68:855-867.
[19] Rooney S, Chaudhuri J, Alt FW. The role of the non-homologous end-joining pathway in lymphocyte development. Immunol Rev. 2004;200:115-131.

[20] Benedict CL, Gilfillan S, Thai TH, Kearney JF. Terminal deoxynucleotidyl transferase and repertoire development. Immunol Rev. 2000;175:150-157.
[21] Jung D, Giallourakis C, Mostoslavsky R, Alt FW. Mechanism and control of V(D)J recombination at the immunoglobulin heavy chain locus. Annu Rev Immunol. 2006;24:541-570.
[22] Lentz VM, Manser T. Cutting edge: germinal centers can be induced in the absence of T cells. J Immunol. 2001;167:15-20.
[23] de Vinuesa CG, Cook MC, Ball J, Drew M, Sunners Y, Cascalho M, et al. Germinal centers without T cells. J Exp Med. 2000;191:485-494.
[24] Lopes-Carvalho T, Kearney JF. Development and selection of marginal zone B cells. Immunol Rev. 2004;197:192-205.
[25] Martin F, Kearney JF. Marginal-zone B cells. Nat Rev Immunol. 2002;2:323-335.
[26] Reif K, Ekland EH, Ohl L, Nakano H, Lipp M, Forster R, et al. Balanced responsiveness to chemoattractants from adjacent zones determines B-cell position. Nature. 2002;416:94-99.
[27] Garside P, Ingulli E, Merica RR, Johnson JG, Noelle RJ, Jenkins MK. Visualization of specific B and T lymphocyte interactions in the lymph node. Science. 1998;281:96-99.
[28] Forster R, Schubel A, Breitfeld D, Kremmer E, Renner-Muller I, Wolf E, et al. CCR7 coordinates the primary immune response by establishing functional microenvironments in secondary lymphoid organs. Cell. 1999;99:23-33.
[29] Gatto D, Brink R. The germinal center reaction. J Allergy Clin Immunol. 2010;126:898-907; quiz 908-899.
[30] Han S, Hathcock K, Zheng B, Kepler TB, Hodes R, Kelsoe G. Cellular interaction in germinal centers. Roles of CD40 ligand and B7-2 in established germinal centers. J Immunol. 1995;155:556-567.
[31] Foy TM, Laman JD, Ledbetter JA, Aruffo A, Claassen E, Noelle RJ. gp39-CD40 interactions are essential for germinal center formation and the development of B cell memory. J Exp Med. 1994;180:157-163.
[32] Neuberger MS, Milstein C. Somatic hypermutation. Curr Opin Immunol. 1995;7:248-254.
[33] Rajewsky K. Clonal selection and learning in the antibody system. Nature. 1996;381:751-758.
[34] Rajewsky K, Forster I, Cumano A. Evolutionary and somatic selection of the antibody repertoire in the mouse. Science. 1987;238:1088-1094.
[35] Goossens T, Klein U, Kuppers R. Frequent occurrence of deletions and duplications during somatic hypermutation: implications for oncogene translocations and heavy chain disease. Proc Natl Acad Sci U S A. 1998;95:2463-2468.
[36] Di Noia JM, Neuberger MS. Molecular mechanisms of antibody somatic hypermutation. Annu Rev Biochem. 2007;76:1-22.
[37] Peled JU, Kuang FL, Iglesias-Ussel MD, Roa S, Kalis SL, Goodman MF, et al. The biochemistry of somatic hypermutation. Annu Rev Immunol. 2008;26:481-511.
[38] Smith DS, Creadon G, Jena PK, Portanova JP, Kotzin BL, Wysocki LJ. Di- and trinucleotide target preferences of somatic mutagenesis in normal and autoreactive B cells. J Immunol. 1996;156:2642-2652.

[39] Golding GB, Gearhart PJ, Glickman BW. Patterns of somatic mutations in immunoglobulin variable genes. Genetics. 1987;115:169-176.
[40] Rogozin IB, Diaz M. Cutting edge: DGYW/WRCH is a better predictor of mutability at G:C bases in Ig hypermutation than the widely accepted RGYW/WRCY motif and probably reflects a two-step activation-induced cytidine deaminase-triggered process. J Immunol. 2004;172:3382-3384.
[41] Wagner SD, Milstein C, Neuberger MS. Codon bias targets mutation. Nature. 1995;376:732.
[42] Revy P, Muto T, Levy Y, Geissmann F, Plebani A, Sanal O, et al. Activation-induced cytidine deaminase (AID) deficiency causes the autosomal recessive form of the Hyper-IgM syndrome (HIGM2). Cell. 2000;102:565-575.
[43] Muramatsu M, Kinoshita K, Fagarasan S, Yamada S, Shinkai Y, Honjo T. Class switch recombination and hypermutation require activation-induced cytidine deaminase (AID), a potential RNA editing enzyme. Cell. 2000;102:553-563.
[44] Martin A, Bardwell PD, Woo CJ, Fan M, Shulman MJ, Scharff MD. Activation-induced cytidine deaminase turns on somatic hypermutation in hybridomas. Nature. 2002;415:802-806.
[45] Petersen-Mahrt SK, Harris RS, Neuberger MS. AID mutates E. coli suggesting a DNA deamination mechanism for antibody diversification. Nature. 2002;418:99-103.
[46] Seki M, Gearhart PJ, Wood RD. DNA polymerases and somatic hypermutation of immunoglobulin genes. EMBO Rep. 2005;6:1143-1148.
[47] Tippin B, Goodman MF. A new class of errant DNA polymerases provides candidates for somatic hypermutation. Philos Trans R Soc Lond B Biol Sci. 2001;356:47-51.
[48] Imai K, Slupphaug G, Lee WI, Revy P, Nonoyama S, Catalan N, et al. Human uracil-DNA glycosylase deficiency associated with profoundly impaired immunoglobulin class-switch recombination. Nat Immunol. 2003;4:1023-1028.
[49] Rada C, Williams GT, Nilsen H, Barnes DE, Lindahl T, Neuberger MS. Immunoglobulin isotype switching is inhibited and somatic hypermutation perturbed in UNG-deficient mice. Curr Biol. 2002;12:1748-1755.
[50] Di Noia J, Neuberger MS. Altering the pathway of immunoglobulin hypermutation by inhibiting uracil-DNA glycosylase. Nature. 2002;419:43-48.
[51] Saribasak H, Maul RW, Cao Z, McClure RL, Yang W, McNeill DR, et al. XRCC1 suppresses somatic hypermutation and promotes alternative nonhomologous end joining in Igh genes. J Exp Med. 2011;208:2209-2216.
[52] Faili A, Aoufouchi S, Flatter E, Gueranger Q, Reynaud CA, Weill JC. Induction of somatic hypermutation in immunoglobulin genes is dependent on DNA polymerase iota. Nature. 2002;419:944-947.
[53] Simpson LJ, Sale JE. Rev1 is essential for DNA damage tolerance and non-templated immunoglobulin gene mutation in a vertebrate cell line. Embo J. 2003;22:1654-1664.
[54] Zeng X, Winter DB, Kasmer C, Kraemer KH, Lehmann AR, Gearhart PJ. DNA polymerase eta is an A-T mutator in somatic hypermutation of immunoglobulin variable genes. Nat Immunol. 2001;2:537-541.
[55] Diaz M, Verkoczy LK, Flajnik MF, Klinman NR. Decreased frequency of somatic hypermutation and impaired affinity maturation but intact germinal center formation in mice expressing antisense RNA to DNA polymerase zeta. J Immunol. 2001;167:327-335.

[56] Zan H, Komori A, Li Z, Cerutti A, Schaffer A, Flajnik MF, et al. The translesion DNA polymerase zeta plays a major role in Ig and bcl-6 somatic hypermutation. Immunity. 2001;14:643-653.
[57] Wu X, Tsai CY, Patam MB, Zan H, Chen JP, Lipkin SM, et al. A role for the MutL mismatch repair Mlh3 protein in immunoglobulin class switch DNA recombination and somatic hypermutation. J Immunol. 2006;176:5426-5437.
[58] Li Z, Peled JU, Zhao C, Svetlanov A, Ronai D, Cohen PE, et al. A role for Mlh3 in somatic hypermutation. DNA Repair (Amst). 2006;5:675-682.
[59] Bardwell PD, Woo CJ, Wei K, Li Z, Martin A, Sack SZ, et al. Altered somatic hypermutation and reduced class-switch recombination in exonuclease 1-mutant mice. Nat Immunol. 2004;5:224-229.
[60] Shen HM, Tanaka A, Bozek G, Nicolae D, Storb U. Somatic hypermutation and class switch recombination in Msh6(-/-)Ung(-/-) double-knockout mice. J Immunol. 2006;177:5386-5392.
[61] Li Z, Zhao C, Iglesias-Ussel MD, Polonskaya Z, Zhuang M, Yang G, et al. The mismatch repair protein Msh6 influences the in vivo AID targeting to the Ig locus. Immunity. 2006;24:393-403.
[62] Roa S, Li Z, Peled JU, Zhao C, Edelmann W, Scharff MD. MSH2/MSH6 complex promotes error-free repair of AID-induced dU:G mispairs as well as error-prone hypermutation of A:T sites. PLoS One. 2010;5:e11182.
[63] Martin A, Li Z, Lin DP, Bardwell PD, Iglesias-Ussel MD, Edelmann W, et al. Msh2 ATPase activity is essential for somatic hypermutation at a-T basepairs and for efficient class switch recombination. J Exp Med. 2003;198:1171-1178.
[64] Wiesendanger M, Kneitz B, Edelmann W, Scharff MD. Somatic hypermutation in MutS homologue (MSH)3-, MSH6-, and MSH3/MSH6-deficient mice reveals a role for the MSH2-MSH6 heterodimer in modulating the base substitution pattern. J Exp Med. 2000;191:579-584.
[65] Rada C, Ehrenstein MR, Neuberger MS, Milstein C. Hot spot focusing of somatic hypermutation in MSH2-deficient mice suggests two stages of mutational targeting. Immunity. 1998;9:135-141.
[66] Phung QH, Winter DB, Cranston A, Tarone RE, Bohr VA, Fishel R, et al. Increased hypermutation at G and C nucleotides in immunoglobulin variable genes from mice deficient in the MSH2 mismatch repair protein. J Exp Med. 1998;187:1745-1751.
[67] Langerak P, Nygren AO, Krijger PH, van den Berk PC, Jacobs H. A/T mutagenesis in hypermutated immunoglobulin genes strongly depends on PCNAK164 modification. J Exp Med. 2007;204:1989-1998.
[68] Roa S, Avdievich E, Peled JU, Maccarthy T, Werling U, Kuang FL, et al. Ubiquitylated PCNA plays a role in somatic hypermutation and class-switch recombination and is required for meiotic progression. Proc Natl Acad Sci U S A. 2008;105:16248-16253.
[69] Arakawa H, Moldovan GL, Saribasak H, Saribasak NN, Jentsch S, Buerstedde JM. A role for PCNA ubiquitination in immunoglobulin hypermutation. PLoS Biol. 2006;4:e366.
[70] Krijger PH, Langerak P, van den Berk PC, Jacobs H. Dependence of nucleotide substitutions on Ung2, Msh2, and PCNA-Ub during somatic hypermutation. J Exp Med. 2009;206:2603-2611.

[71] Reynaud CA, Anquez V, Grimal H, Weill JC. A hyperconversion mechanism generates the chicken light chain preimmune repertoire. Cell. 1987;48:379-388.
[72] Reynaud CA, Dahan A, Anquez V, Weill JC. Somatic hyperconversion diversifies the single Vh gene of the chicken with a high incidence in the D region. Cell. 1989;59:171-183.
[73] Parvari R, Avivi A, Lentner F, Ziv E, Tel-Or S, Burstein Y, et al. Chicken immunoglobulin gamma-heavy chains: limited VH gene repertoire, combinatorial diversification by D gene segments and evolution of the heavy chain locus. Embo J. 1988;7:739-744.
[74] Reynaud CA, Anquez V, Dahan A, Weill JC. A single rearrangement event generates most of the chicken immunoglobulin light chain diversity. Cell. 1985;40:283-291.
[75] Carlson LM, McCormack WT, Postema CE, Humphries EH, Thompson CB. Templated insertions in the rearranged chicken IgL V gene segment arise by intrachromosomal gene conversion. Genes Dev. 1990;4:536-547.
[76] Arakawa H, Hauschild J, Buerstedde JM. Requirement of the activation-induced deaminase (AID) gene for immunoglobulin gene conversion. Science. 2002;295:1301-1306.
[77] Harris RS, Sale JE, Petersen-Mahrt SK, Neuberger MS. AID is essential for immunoglobulin V gene conversion in a cultured B cell line. Curr Biol. 2002;12:435-438.
[78] McCormack WT, Thompson CB. Chicken IgL variable region gene conversions display pseudogene donor preference and 5' to 3' polarity. Genes Dev. 1990;4:548-558.
[79] Arakawa H, Kuma K, Yasuda M, Furusawa S, Ekino S, Yamagishi H. Oligoclonal development of B cells bearing discrete Ig chains in chicken single germinal centers. J Immunol. 1998;160:4232-4241.
[80] Arakawa H, Furusawa S, Ekino S, Yamagishi H. Immunoglobulin gene hyperconversion ongoing in chicken splenic germinal centers. Embo J. 1996;15:2540-2546.
[81] Arakawa H, Saribasak H, Buerstedde JM. Activation-induced cytidine deaminase initiates immunoglobulin gene conversion and hypermutation by a common intermediate. PLoS Biol. 2004;2:E179.
[82] Saribasak H, Saribasak NN, Ipek FM, Ellwart JW, Arakawa H, Buerstedde JM. Uracil DNA glycosylase disruption blocks Ig gene conversion and induces transition mutations. J Immunol. 2006;176:365-371.
[83] Hatanaka A, Yamazoe M, Sale JE, Takata M, Yamamoto K, Kitao H, et al. Similar effects of Brca2 truncation and Rad51 paralog deficiency on immunoglobulin V gene diversification in DT40 cells support an early role for Rad51 paralogs in homologous recombination. Mol Cell Biol. 2005;25:1124-1134.
[84] Sale JE, Calandrini DM, Takata M, Takeda S, Neuberger MS. Ablation of XRCC2/3 transforms immunoglobulin V gene conversion into somatic hypermutation. Nature. 2001;412:921-926.
[85] Nakahara M, Sonoda E, Nojima K, Sale JE, Takenaka K, Kikuchi K, et al. Genetic evidence for single-strand lesions initiating Nbs1-dependent homologous recombination in diversification of Ig v in chicken B lymphocytes. PLoS Genet. 2009;5:e1000356.
[86] Yabuki M, Fujii MM, Maizels N. The MRE11-RAD50-NBS1 complex accelerates somatic hypermutation and gene conversion of immunoglobulin variable regions. Nat Immunol. 2005;6:730-736.
[87] Schrader CE, Linehan EK, Mochegova SN, Woodland RT, Stavnezer J. Inducible DNA breaks in Ig S regions are dependent on AID and UNG. J Exp Med. 2005;202:561-568.

[88] Guikema JE, Linehan EK, Tsuchimoto D, Nakabeppu Y, Strauss PR, Stavnezer J, et al. APE1- and APE2-dependent DNA breaks in immunoglobulin class switch recombination. J Exp Med. 2007;204:3017-3026.
[89] Kunkel TA, Erie DA. DNA mismatch repair. Annu Rev Biochem. 2005;74:681-710.
[90] Martomo SA, Yang WW, Gearhart PJ. A role for Msh6 but not Msh3 in somatic hypermutation and class switch recombination. J Exp Med. 2004;200:61-68.
[91] Li Z, Scherer SJ, Ronai D, Iglesias-Ussel MD, Peled JU, Bardwell PD, et al. Examination of Msh6- and Msh3-deficient mice in class switching reveals overlapping and distinct roles of MutS homologues in antibody diversification. J Exp Med. 2004;200:47-59.
[92] Ehrenstein MR, Rada C, Jones AM, Milstein C, Neuberger MS. Switch junction sequences in PMS2-deficient mice reveal a microhomology-mediated mechanism of Ig class switch recombination. Proc Natl Acad Sci U S A. 2001;98:14553-14558.
[93] Schrader CE, Edelmann W, Kucherlapati R, Stavnezer J. Reduced isotype switching in splenic B cells from mice deficient in mismatch repair enzymes. J Exp Med. 1999;190:323-330.
[94] Ehrenstein MR, Neuberger MS. Deficiency in Msh2 affects the efficiency and local sequence specificity of immunoglobulin class-switch recombination: parallels with somatic hypermutation. Embo J. 1999;18:3484-3490.
[95] Rada C, Di Noia JM, Neuberger MS. Mismatch recognition and uracil excision provide complementary paths to both Ig switching and the A/T-focused phase of somatic mutation. Mol Cell. 2004;16:163-171.
[96] van den Bosch M, Bree RT, Lowndes NF. The MRN complex: coordinating and mediating the response to broken chromosomes. EMBO Rep. 2003;4:844-849.
[97] Demuth I, Digweed M. The clinical manifestation of a defective response to DNA double-strand breaks as exemplified by Nijmegen breakage syndrome. Oncogene. 2007;26:7792-7798.
[98] Kracker S, Bergmann Y, Demuth I, Frappart PO, Hildebrand G, Christine R, et al. Nibrin functions in Ig class-switch recombination. Proc Natl Acad Sci U S A. 2005;102:1584-1589.
[99] Reina-San-Martin B, Nussenzweig MC, Nussenzweig A, Difilippantonio S. Genomic instability, endoreduplication, and diminished Ig class-switch recombination in B cells lacking Nbs1. Proc Natl Acad Sci U S A. 2005;102:1590-1595.
[100] Bekker-Jensen S, Mailand N. Assembly and function of DNA double-strand break repair foci in mammalian cells. DNA Repair (Amst). 2010;9:1219-1228.
[101] Loizou JI, Sancho R, Kanu N, Bolland DJ, Yang F, Rada C, et al. ATMIN is required for maintenance of genomic stability and suppression of B cell lymphoma. Cancer Cell. 2011;19:587-600.
[102] Reina-San-Martin B, Chen HT, Nussenzweig A, Nussenzweig MC. ATM is required for efficient recombination between immunoglobulin switch regions. J Exp Med. 2004;200:1103-1110.
[103] Lumsden JM, McCarty T, Petiniot LK, Shen R, Barlow C, Wynn TA, et al. Immunoglobulin class switch recombination is impaired in Atm-deficient mice. J Exp Med. 2004;200:1111-1121.
[104] Derheimer FA, Kastan MB. Multiple roles of ATM in monitoring and maintaining DNA integrity. FEBS Lett. 2010;584:3675-3681.

[105] Al-Hakim A, Escribano-Diaz C, Landry MC, O'Donnell L, Panier S, Szilard RK, et al. The ubiquitous role of ubiquitin in the DNA damage response. DNA Repair (Amst). 2010;9:1229-1240.
[106] Ward IM, Reina-San-Martin B, Olaru A, Minn K, Tamada K, Lau JS, et al. 53BP1 is required for class switch recombination. J Cell Biol. 2004;165:459-464.
[107] Reina-San-Martin B, Difilippantonio S, Hanitsch L, Masilamani RF, Nussenzweig A, Nussenzweig MC. H2AX is required for recombination between immunoglobulin switch regions but not for intra-switch region recombination or somatic hypermutation. J Exp Med. 2003;197:1767-1778.
[108] Bohgaki T, Bohgaki M, Cardoso R, Panier S, Zeegers D, Li L, et al. Genomic instability, defective spermatogenesis, immunodeficiency, and cancer in a mouse model of the RIDDLE syndrome. PLoS Genet. 2011;7:e1001381.
[109] Ramachandran S, Chahwan R, Nepal RM, Frieder D, Panier S, Roa S, et al. The RNF8/RNF168 ubiquitin ligase cascade facilitates class switch recombination. Proc Natl Acad Sci U S A. 2010;107:809-814.
[110] Li L, Halaby MJ, Hakem A, Cardoso R, El Ghamrasni S, Harding S, et al. Rnf8 deficiency impairs class switch recombination, spermatogenesis, and genomic integrity and predisposes for cancer. J Exp Med. 2010;207:983-997.
[111] Wu X, Tschumper RC, Gutierrez A, Jr., Mihalcik SA, Nowakowski GS, Jelinek DF. Selective induction of DNA repair pathways in human B cells activated by CD4+ T cells. PLoS One. 2010;5:e15549.
[112] Park K, Kim J, Kim HS, Shin HS. Isolated human germinal center centroblasts have an intact mismatch repair system. J Immunol. 1998;161:6128-6132.
[113] Casellas R, Nussenzweig A, Wuerffel R, Pelanda R, Reichlin A, Suh H, et al. Ku80 is required for immunoglobulin isotype switching. Embo J. 1998;17:2404-2411.
[114] Manis JP, Gu Y, Lansford R, Sonoda E, Ferrini R, Davidson L, et al. Ku70 is required for late B cell development and immunoglobulin heavy chain class switching. J Exp Med. 1998;187:2081-2089.
[115] Soulas-Sprauel P, Le Guyader G, Rivera-Munoz P, Abramowski V, Olivier-Martin C, Goujet-Zalc C, et al. Role for DNA repair factor XRCC4 in immunoglobulin class switch recombination. J Exp Med. 2007;204:1717-1727.
[116] Cook AJ, Oganesian L, Harumal P, Basten A, Brink R, Jolly CJ. Reduced switching in SCID B cells is associated with altered somatic mutation of recombined S regions. J Immunol. 2003;171:6556-6564.
[117] Bosma GC, Kim J, Urich T, Fath DM, Cotticelli MG, Ruetsch NR, et al. DNA-dependent protein kinase activity is not required for immunoglobulin class switching. J Exp Med. 2002;196:1483-1495.
[118] Rooney S, Alt FW, Sekiguchi J, Manis JP. Artemis-independent functions of DNA-dependent protein kinase in Ig heavy chain class switch recombination and development. Proc Natl Acad Sci U S A. 2005;102:2471-2475.
[119] Manis JP, Dudley D, Kaylor L, Alt FW. IgH class switch recombination to IgG1 in DNA-PKcs-deficient B cells. Immunity. 2002;16:607-617.
[120] Callen E, Jankovic M, Wong N, Zha S, Chen HT, Difilippantonio S, et al. Essential role for DNA-PKcs in DNA double-strand break repair and apoptosis in ATM-deficient lymphocytes. Mol Cell. 2009;34:285-297.

[121] Boboila C, Yan C, Wesemann DR, Jankovic M, Wang JH, Manis J, et al. Alternative end-joining catalyzes class switch recombination in the absence of both Ku70 and DNA ligase 4. J Exp Med. 2010;207:417-427.
[122] Pan-Hammarstrom Q, Jones AM, Lahdesmaki A, Zhou W, Gatti RA, Hammarstrom L, et al. Impact of DNA ligase IV on nonhomologous end joining pathways during class switch recombination in human cells. J Exp Med. 2005;201:189-194.
[123] Yan CT, Boboila C, Souza EK, Franco S, Hickernell TR, Murphy M, et al. IgH class switching and translocations use a robust non-classical end-joining pathway. Nature. 2007;449:478-482.
[124] Robert I, Dantzer F, Reina-San-Martin B. Parp1 facilitates alternative NHEJ, whereas Parp2 suppresses IgH/c-myc translocations during immunoglobulin class switch recombination. J Exp Med. 2009;206:1047-1056.
[125] Pan-Hammarstrom Q, Lahdesmaki A, Zhao Y, Du L, Zhao Z, Wen S, et al. Disparate roles of ATR and ATM in immunoglobulin class switch recombination and somatic hypermutation. J Exp Med. 2006;203:99-110.
[126] Lee-Theilen M, Matthews AJ, Kelly D, Zheng S, Chaudhuri J. CtIP promotes microhomology-mediated alternative end joining during class-switch recombination. Nat Struct Mol Biol. 2011;18:75-79.
[127] Peled JU, Sellers RS, Iglesias-Ussel MD, Shin DM, Montagna C, Zhao C, et al. Msh6 protects mature B cells from lymphoma by preserving genomic stability. Am J Pathol. 2010;177:2597-2608.
[128] Shen Y, Iqbal J, Xiao L, Lynch RC, Rosenwald A, Staudt LM, et al. Distinct gene expression profiles in different B-cell compartments in human peripheral lymphoid organs. BMC Immunol. 2004;5:20.
[129] Klemm L, Duy C, Iacobucci I, Kuchen S, von Levetzow G, Feldhahn N, et al. The B cell mutator AID promotes B lymphoid blast crisis and drug resistance in chronic myeloid leukemia. Cancer Cell. 2009;16:232-245.
[130] Allman D, Jain A, Dent A, Maile RR, Selvaggi T, Kehry MR, et al. BCL-6 expression during B-cell activation. Blood. 1996;87:5257-5268.
[131] Cattoretti G, Chang CC, Cechova K, Zhang J, Ye BH, Falini B, et al. BCL-6 protein is expressed in germinal-center B cells. Blood. 1995;86:45-53.
[132] Ranuncolo SM, Polo JM, Melnick A. BCL6 represses CHEK1 and suppresses DNA damage pathways in normal and malignant B-cells. Blood Cells Mol Dis. 2008;41:95-99.
[133] Phan RT, Saito M, Basso K, Niu H, Dalla-Favera R. BCL6 interacts with the transcription factor Miz-1 to suppress the cyclin-dependent kinase inhibitor p21 and cell cycle arrest in germinal center B cells. Nat Immunol. 2005;6:1054-1060.
[134] Phan RT, Dalla-Favera R. The BCL6 proto-oncogene suppresses p53 expression in germinal-centre B cells. Nature. 2004;432:635-639.
[135] Shaffer AL, Yu X, He Y, Boldrick J, Chan EP, Staudt LM. BCL-6 represses genes that function in lymphocyte differentiation, inflammation, and cell cycle control. Immunity. 2000;13:199-212.

[136] Ranuncolo SM, Polo JM, Dierov J, Singer M, Kuo T, Greally J, et al. Bcl-6 mediates the germinal center B cell phenotype and lymphomagenesis through transcriptional repression of the DNA-damage sensor ATR. Nat Immunol. 2007;8:705-714.
[137] Strasser A, Jost PJ, Nagata S. The many roles of FAS receptor signaling in the immune system. Immunity. 2009;30:180-192.
[138] Conticello SG, Thomas CJ, Petersen-Mahrt SK, Neuberger MS. Evolution of the AID/APOBEC family of polynucleotide (deoxy)cytidine deaminases. Mol Biol Evol. 2005;22:367-377.
[139] Muramatsu M, Sankaranand VS, Anant S, Sugai M, Kinoshita K, Davidson NO, et al. Specific expression of activation-induced cytidine deaminase (AID), a novel member of the RNA-editing deaminase family in germinal center B cells. Journal of Biological Chemistry. 1999;274:18470-18476.
[140] Conticello SG. The AID/APOBEC family of nucleic acid mutators. Genome Biol. 2008;9:229.
[141] Kedzierski P, Sokalski WA, Cheng HS, Mitchell J, Leszczynski J. DFT study of the reaction proceeding in the cytidine deaminase. Chem Phys Lett. 2003;381:660-665.
[142] Teng B, Burant CF, Davidson NO. Molecular cloning of an apolipoprotein B messenger RNA editing protein. Science. 1993;260:1816-1819.
[143] Rogozin IB, Basu MK, Jordan IK, Pavlov YI, Koonin EV. APOBEC4, a new member of the AID/APOBEC family of polynucleotide (deoxy)cytidine deaminases predicted by computational analysis. Cell Cycle. 2005;4:1281-1285.
[144] Mukhopadhyay D, Anant S, Lee RM, Kennedy S, Viskochil D, Davidson NO. C-->U editing of neurofibromatosis 1 mRNA occurs in tumors that express both the type II transcript and apobec-1, the catalytic subunit of the apolipoprotein B mRNA-editing enzyme. Am J Hum Genet. 2002;70:38-50.
[145] Liao W, Hong SH, Chan BH, Rudolph FB, Clark SC, Chan L. APOBEC-2, a cardiac- and skeletal muscle-specific member of the cytidine deaminase supergene family. Biochem Biophys Res Commun. 1999;260:398-404.
[146] Matsumoto T, Marusawa H, Endo Y, Ueda Y, Matsumoto Y, Chiba T. Expression of APOBEC2 is transcriptionally regulated by NF-kappaB in human hepatocytes. FEBS Lett. 2006;580:731-735.
[147] Mikl MC, Watt IN, Lu M, Reik W, Davies SL, Neuberger MS, et al. Mice deficient in APOBEC2 and APOBEC3. Mol Cell Biol. 2005;25:7270-7277.
[148] Sato Y, Probst HC, Tatsumi R, Ikeuchi Y, Neuberger MS, Rada C. Deficiency in APOBEC2 leads to a shift in muscle fiber type, diminished body mass, and myopathy. J Biol Chem. 2010;285:7111-7118.
[149] Etard C, Roostalu U, Strahle U. Lack of Apobec2-related proteins causes a dystrophic muscle phenotype in zebrafish embryos. J Cell Biol. 2010;189:527-539.
[150] Navaratnam N, Morrison JR, Bhattacharya S, Patel D, Funahashi T, Giannoni F, et al. The p27 catalytic subunit of the apolipoprotein B mRNA editing enzyme is a cytidine deaminase. J Biol Chem. 1993;268:20709-20712.
[151] Hirano K, Young SG, Farese RV, Jr., Ng J, Sande E, Warburton C, et al. Targeted disruption of the mouse apobec-1 gene abolishes apolipoprotein B mRNA editing and eliminates apolipoprotein B48. J Biol Chem. 1996;271:9887-9890.

[152] Morrison JR, Paszty C, Stevens ME, Hughes SD, Forte T, Scott J, et al. Apolipoprotein B RNA editing enzyme-deficient mice are viable despite alterations in lipoprotein metabolism. Proc Natl Acad Sci U S A. 1996;93:7154-7159.
[153] Yamanaka S, Balestra ME, Ferrell LD, Fan J, Arnold KS, Taylor S, et al. Apolipoprotein B mRNA-editing protein induces hepatocellular carcinoma and dysplasia in transgenic animals. Proc Natl Acad Sci U S A. 1995;92:8483-8487.
[154] Rosenberg BR, Hamilton CE, Mwangi MM, Dewell S, Papavasiliou FN. Transcriptome-wide sequencing reveals numerous APOBEC1 mRNA-editing targets in transcript 3' UTRs. Nat Struct Mol Biol. 2011;18:230-236.
[155] Harris RS, Petersen-Mahrt SK, Neuberger MS. RNA editing enzyme APOBEC1 and some of its homologs can act as DNA mutators. Mol Cell. 2002;10:1247-1253.
[156] Lau PP, Xiong WJ, Zhu HJ, Chen SH, Chan L. Apolipoprotein B mRNA editing is an intranuclear event that occurs posttranscriptionally coincident with splicing and polyadenylation. J Biol Chem. 1991;266:20550-20554.
[157] Chester A, Somasekaram A, Tzimina M, Jarmuz A, Gisbourne J, O'Keefe R, et al. The apolipoprotein B mRNA editing complex performs a multifunctional cycle and suppresses nonsense-mediated decay. Embo J. 2003;22:3971-3982.
[158] Yang Y, Smith HC. Multiple protein domains determine the cell type-specific nuclear distribution of the catalytic subunit required for apolipoprotein B mRNA editing. Proc Natl Acad Sci U S A. 1997;94:13075-13080.
[159] Harris RS, Bishop KN, Sheehy AM, Craig HM, Petersen-Mahrt SK, Watt IN, et al. DNA deamination mediates innate immunity to retroviral infection. Cell. 2003;113:803-809.
[160] Sheehy AM, Gaddis NC, Choi JD, Malim MH. Isolation of a human gene that inhibits HIV-1 infection and is suppressed by the viral Vif protein. Nature. 2002;418:646-650.
[161] Stenglein MD, Harris RS. APOBEC3B and APOBEC3F inhibit L1 retrotransposition by a DNA deamination-independent mechanism. J Biol Chem. 2006;281:16837-16841.
[162] Muckenfuss H, Hamdorf M, Held U, Perkovic M, Lower J, Cichutek K, et al. APOBEC3 proteins inhibit human LINE-1 retrotransposition. J Biol Chem. 2006;281:22161-22172.
[163] Chiu YL, Witkowska HE, Hall SC, Santiago M, Soros VB, Esnault C, et al. High-molecular-mass APOBEC3G complexes restrict Alu retrotransposition. Proc Natl Acad Sci U S A. 2006;103:15588-15593.
[164] Yu X, Yu Y, Liu B, Luo K, Kong W, Mao P, et al. Induction of APOBEC3G ubiquitination and degradation by an HIV-1 Vif-Cul5-SCF complex. Science. 2003;302:1056-1060.
[165] Kobayashi M, Takaori-Kondo A, Miyauchi Y, Iwai K, Uchiyama T. Ubiquitination of APOBEC3G by an HIV-1 Vif-Cullin5-Elongin B-Elongin C complex is essential for Vif function. J Biol Chem. 2005;280:18573-18578.
[166] Conticello SG, Harris RS, Neuberger MS. The Vif protein of HIV triggers degradation of the human antiretroviral DNA deaminase APOBEC3G. Curr Biol. 2003;13:2009-2013.
[167] Cullen BR. Role and mechanism of action of the APOBEC3 family of antiretroviral resistance factors. J Virol. 2006;80:1067-1076.

[168] Newman EN, Holmes RK, Craig HM, Klein KC, Lingappa JR, Malim MH, et al. Antiviral function of APOBEC3G can be dissociated from cytidine deaminase activity. Curr Biol. 2005;15:166-170.
[169] Bishop KN, Holmes RK, Malim MH. Antiviral potency of APOBEC proteins does not correlate with cytidine deamination. J Virol. 2006;80:8450-8458.
[170] Shirakawa K, Takaori-Kondo A, Yokoyama M, Izumi T, Matsui M, Io K, et al. Phosphorylation of APOBEC3G by protein kinase A regulates its interaction with HIV-1 Vif. Nat Struct Mol Biol. 2008;15:1184-1191.
[171] Demorest ZL, Li M, Harris RS. Phosphorylation directly regulates the intrinsic DNA cytidine deaminase activity of activation-induced deaminase and APOBEC3G protein. J Biol Chem. 2011;286:26568-26575.
[172] Kozak SL, Marin M, Rose KM, Bystrom C, Kabat D. The anti-HIV-1 editing enzyme APOBEC3G binds HIV-1 RNA and messenger RNAs that shuttle between polysomes and stress granules. J Biol Chem. 2006;281:29105-29119.
[173] Gallois-Montbrun S, Kramer B, Swanson CM, Byers H, Lynham S, Ward M, et al. Antiviral protein APOBEC3G localizes to ribonucleoprotein complexes found in P bodies and stress granules. J Virol. 2007;81:2165-2178.
[174] Chiu YL, Greene WC. APOBEC3G: an intracellular centurion. Philos Trans R Soc Lond B Biol Sci. 2009;364:689-703.
[175] Severi F, Chicca A, Conticello SG. Analysis of reptilian APOBEC1 suggests that RNA editing may not be its ancestral function. Mol Biol Evol. 2011;28:1125-1129.
[176] Holden LG, Prochnow C, Chang YP, Bransteitter R, Chelico L, Sen U, et al. Crystal structure of the anti-viral APOBEC3G catalytic domain and functional implications. Nature. 2008;456:121-124.
[177] Chen KM, Harjes E, Gross PJ, Fahmy A, Lu Y, Shindo K, et al. Structure of the DNA deaminase domain of the HIV-1 restriction factor APOBEC3G. Nature. 2008;452:116-119.
[178] Prochnow C, Bransteitter R, Klein MG, Goodman MF, Chen XS. The APOBEC-2 crystal structure and functional implications for the deaminase AID. Nature. 2007;445:447-451.
[179] McDougall WM, Okany C, Smith HC. Deaminase activity on single-stranded DNA (ssDNA) occurs in vitro when APOBEC3G cytidine deaminase forms homotetramers and higher-order complexes. J Biol Chem. 2011;286:30655-30661.
[180] Huthoff H, Autore F, Gallois-Montbrun S, Fraternali F, Malim MH. RNA-dependent oligomerization of APOBEC3G is required for restriction of HIV-1. PLoS Pathog. 2009;5:e1000330.
[181] Wu X, Darce JR, Chang SK, Nowakowski GS, Jelinek DF. Alternative splicing regulates activation-induced cytidine deaminase (AID): implications for suppression of AID mutagenic activity in normal and malignant B cells. Blood. 2008;112:4675-4682.
[182] Saunders HL, Magor BG. Cloning and expression of the AID gene in the channel catfish. Dev Comp Immunol. 2004;28:657-663.
[183] Bascove M, Frippiat JP. Molecular characterization of Pleurodeles waltl activation-induced cytidine deaminase. Mol Immunol. 2010;47:1640-1649.
[184] Verma S, Goldammer T, Aitken R. Cloning and expression of activation induced cytidine deaminase from Bos taurus. Vet Immunol Immunopathol. 2010;134:151-159.

[185] Zhao Y, Pan-Hammarstrom Q, Zhao Z, Hammarstrom L. Identification of the activation-induced cytidine deaminase gene from zebrafish: an evolutionary analysis. Dev Comp Immunol. 2005;29:61-71.
[186] Ramiro AR, Stavropoulos P, Jankovic M, Nussenzweig MC. Transcription enhances AID-mediated cytidine deamination by exposing single-stranded DNA on the nontemplate strand. Nat Immunol. 2003;4:452-456.
[187] Dickerson SK, Market E, Besmer E, Papavasiliou FN. AID mediates hypermutation by deaminating single stranded DNA. J Exp Med. 2003;197:1291-1296.
[188] Bransteitter R, Pham P, Scharff MD, Goodman MF. Activation-induced cytidine deaminase deaminates deoxycytidine on single-stranded DNA but requires the action of RNase. Proc Natl Acad Sci U S A. 2003;100:4102-4107.
[189] Pham P, Bransteitter R, Petruska J, Goodman MF. Processive AID-catalysed cytosine deamination on single-stranded DNA simulates somatic hypermutation. Nature. 2003;424:103-107.
[190] Chaudhuri J, Tian M, Khuong C, Chua K, Pinaud E, Alt FW. Transcription-targeted DNA deamination by the AID antibody diversification enzyme. Nature. 2003;422:726-730.
[191] Sohail A, Klapacz J, Samaranayake M, Ullah A, Bhagwat AS. Human activation-induced cytidine deaminase causes transcription-dependent, strand-biased C to U deaminations. Nucleic Acids Res. 2003;31:2990-2994.
[192] Yu K, Huang FT, Lieber MR. DNA substrate length and surrounding sequence affect the activation-induced deaminase activity at cytidine. J Biol Chem. 2004;279:6496-6500.
[193] Takizawa M, Tolarova H, Li Z, Dubois W, Lim S, Callen E, et al. AID expression levels determine the extent of cMyc oncogenic translocations and the incidence of B cell tumor development. J Exp Med. 2008;205:1949-1957.
[194] Sernandez IV, de Yebenes VG, Dorsett Y, Ramiro AR. Haploinsufficiency of activation-induced deaminase for antibody diversification and chromosome translocations both in vitro and in vivo. PLoS One. 2008;3:e3927.
[195] Jiang C, Zhao ML, Diaz M. Activation-induced deaminase heterozygous MRL/lpr mice are delayed in the production of high-affinity pathogenic antibodies and in the development of lupus nephritis. Immunology. 2009;126:102-113.
[196] McBride KM, Gazumyan A, Woo EM, Schwickert TA, Chait BT, Nussenzweig MC. Regulation of class switch recombination and somatic mutation by AID phosphorylation. J Exp Med. 2008;205:2585-2594.
[197] Rada C, Jarvis JM, Milstein C. AID-GFP chimeric protein increases hypermutation of Ig genes with no evidence of nuclear localization. Proc Natl Acad Sci U S A. 2002;99:7003-7008.
[198] Woo CJ, Martin A, Scharff MD. Induction of somatic hypermutation is associated with modifications in immunoglobulin variable region chromatin. Immunity. 2003;19:479-489.
[199] Rush JS, Liu M, Odegard VH, Unniraman S, Schatz DG. Expression of activation-induced cytidine deaminase is regulated by cell division, providing a mechanistic basis for division-linked class switch recombination. Proc Natl Acad Sci U S A. 2005;102:13242-13247.
[200] Muto T, Okazaki IM, Yamada S, Tanaka Y, Kinoshita K, Muramatsu M, et al. Negative regulation of activation-induced cytidine deaminase in B cells. Proc Natl Acad Sci U S A. 2006;103:2752-2757.

[201] Robbiani DF, Bunting S, Feldhahn N, Bothmer A, Camps J, Deroubaix S, et al. AID produces DNA double-strand breaks in non-Ig genes and mature B cell lymphomas with reciprocal chromosome translocations. Molecular Cell. 2009;36:631-641.
[202] Okazaki IM, Hiai H, Kakazu N, Yamada S, Muramatsu M, Kinoshita K, et al. Constitutive expression of AID leads to tumorigenesis. J Exp Med. 2003;197:1173-1181.
[203] Teng G, Hakimpour P, Landgraf P, Rice A, Tuschl T, Casellas R, et al. MicroRNA-155 is a negative regulator of activation-induced cytidine deaminase. Immunity. 2008;28:621-629.
[204] Dorsett Y, McBride KM, Jankovic M, Gazumyan A, Thai TH, Robbiani DF, et al. MicroRNA-155 suppresses activation-induced cytidine deaminase-mediated Myc-Igh translocation. Immunity. 2008;28:630-638.
[205] Fagarasan S, Kinoshita K, Muramatsu M, Ikuta K, Honjo T. In situ class switching and differentiation to IgA-producing cells in the gut lamina propria. Nature. 2001;413:639-643.
[206] Ramiro A, Di Noia J. Regulatory mechanisms of AID function. In: DNA Deamination and the Immune System. Imperial College Press. 2010.
[207] Crouch EE, Li Z, Takizawa M, Fichtner-Feigl S, Gourzi P, Montano C, et al. Regulation of AID expression in the immune response. J Exp Med. 2007;204:1145-1156.
[208] Shaffer AL, Lin KI, Kuo TC, Yu X, Hurt EM, Rosenwald A, et al. Blimp-1 orchestrates plasma cell differentiation by extinguishing the mature B cell gene expression program. Immunity. 2002;17:51-62.
[209] Cattoretti G, Büttner M, Shaknovich R, Kremmer E, Alobeid B, Niedobitek G. Nuclear and cytoplasmic AID in extrafollicular and germinal center B cells. Blood. 2006;107:3967-3975.
[210] Pasqualucci L, Guglielmino R, Houldsworth J, Mohr J, Aoufouchi S, Polakiewicz R, et al. Expression of the AID protein in normal and neoplastic B cells. Blood. 2004;104:3318-3325.
[211] MacDuff DA, Demorest ZL, Harris RS. AID can restrict L1 retrotransposition suggesting a dual role in innate and adaptive immunity. Nucleic Acids Res. 2009;37:1854-1867.
[212] Morgan HD, Dean W, Coker HA, Reik W, Petersen-Mahrt SK. Activation-induced cytidine deaminase deaminates 5-methylcytosine in DNA and is expressed in pluripotent tissues: implications for epigenetic reprogramming. Journal of Biological Chemistry. 2004;279:52353-52360.
[213] Pauklin S, Sernandez IV, Bachmann G, Ramiro AR, Petersen-Mahrt SK. Estrogen directly activates AID transcription and function. J Exp Med. 2009;206:99-111.
[214] Babbage G. Immunoglobulin Heavy Chain Locus Events and Expression of Activation-Induced Cytidine Deaminase in Epithelial Breast Cancer Cell Lines. Cancer Research. 2006;66:3996-4000.
[215] Lin C, Yang L, Tanasa B, Hutt K, Ju BG, Ohgi K, et al. Nuclear receptor-induced chromosomal proximity and DNA breaks underlie specific translocations in cancer. Cell. 2009;139:1069-1083.
[216] Gourzi P, Leonova T, Papavasiliou FN. Viral induction of AID is independent of the interferon and the Toll-like receptor signaling pathways but requires NF-kappaB. J Exp Med. 2007;204:259-265.
[217] Gourzi P, Leonova T, Papavasiliou FN. A role for activation-induced cytidine deaminase in the host response against a transforming retrovirus. Immunity. 2006;24:779-786.

[218] Epeldegui M, Breen EC, Hung YP, Boscardin WJ, Detels R, Martinez-Maza O. Elevated expression of activation induced cytidine deaminase in peripheral blood mononuclear cells precedes AIDS-NHL diagnosis. AIDS. 2007;21:2265-2270.
[219] He B, Raab-Traub N, Casali P, Cerutti A. EBV-encoded latent membrane protein 1 cooperates with BAFF/BLyS and APRIL to induce T cell-independent Ig heavy chain class switching. J Immunol. 2003;171:5215-5224.
[220] Meyers G, Ng YS, Bannock JM, Lavoie A, Walter JE, Notarangelo LD, et al. Activation-induced cytidine deaminase (AID) is required for B-cell tolerance in humans. Proc Natl Acad Sci U S A. 2011;108:11554-11559.
[221] Kuraoka M, Holl TM, Liao D, Womble M, Cain DW, Reynolds AE, et al. Activation-induced cytidine deaminase mediates central tolerance in B cells. Proc Natl Acad Sci U S A. 2011;108:11560-11565.
[222] Han JH, Akira S, Calame K, Beutler B, Selsing E, Imanishi-Kari T. Class switch recombination and somatic hypermutation in early mouse B cells are mediated by B cell and Toll-like receptors. Immunity. 2007;27:64-75.
[223] Mao C, Jiang L, Melo-Jorge M, Puthenveetil M, Zhang X, Carroll MC, et al. T cell-independent somatic hypermutation in murine B cells with an immature phenotype. Immunity. 2004;20:133-144.
[224] Lucier MR, Thompson RE, Waire J, Lin AW, Osborne BA, Goldsby RA. Multiple sites of V lambda diversification in cattle. J Immunol. 1998;161:5438-5444.
[225] Reynaud CA, Garcia C, Hein WR, Weill JC. Hypermutation generating the sheep immunoglobulin repertoire is an antigen-independent process. Cell. 1995;80:115-125.
[226] Weinstein PD, Anderson AO, Mage RG. Rabbit IgH sequences in appendix germinal centers: VH diversification by gene conversion-like and hypermutation mechanisms. Immunity. 1994;1:647-659.
[227] Qin H, Suzuki K, Nakata M, Chikuma S, Izumi N, Huong le T, et al. Activation-induced cytidine deaminase expression in CD4+ T cells is associated with a unique IL-10-producing subset that increases with age. PLoS One. 2011;6:e29141.
[228] Zheng B, Xue W, Kelsoe G. Locus-specific somatic hypermutation in germinal centre T cells. Nature. 1994;372:556-559.
[229] Hajkova P, Jeffries SJ, Lee C, Miller N, Jackson SP, Surani MA. Genome-wide reprogramming in the mouse germ line entails the base excision repair pathway. Science. 2010;329:78-82.
[230] Schreck S, Buettner M, Kremmer E, Bogdan M, Herbst H, Niedobitek G. Activation-induced cytidine deaminase (AID) is expressed in normal spermatogenesis but only infrequently in testicular germ cell tumours. J Pathol. 2006;210:26-31.
[231] Bhutani N, Brady JJ, Damian M, Sacco A, Corbel SY, Blau HM. Reprogramming towards pluripotency requires AID-dependent DNA demethylation. Nature. 2010;463:1042-1047.
[232] Popp C, Dean W, Feng S, Cokus SJ, Andrews S, Pellegrini M, et al. Genome-wide erasure of DNA methylation in mouse primordial germ cells is affected by AID deficiency. Nature. 2010;463:1101-1105.

[233] Rai K, Huggins IJ, James SR, Karpf AR, Jones DA, Cairns BR. DNA demethylation in zebrafish involves the coupling of a deaminase, a glycosylase, and gadd45. Cell. 2008;135:1201-1212.
[234] Marr S, Morales H, Bottaro A, Cooper M, Flajnik M, Robert J. Localization and differential expression of activation-induced cytidine deaminase in the amphibian Xenopus upon antigen stimulation and during early development. J Immunol. 2007;179:6783-6789.
[235] Guo JU, Su Y, Zhong C, Ming GL, Song H. Hydroxylation of 5-methylcytosine by TET1 promotes active DNA demethylation in the adult brain. Cell. 2011;145:423-434.
[236] Chen ZX, Riggs AD. DNA methylation and demethylation in mammals. J Biol Chem. 2011;286:18347-18353.
[237] Morgan HD, Santos F, Green K, Dean W, Reik W. Epigenetic reprogramming in mammals. Hum Mol Genet. 2005;14 Spec No 1:R47-58.
[238] Yamazaki Y, Mann MR, Lee SS, Marh J, McCarrey JR, Yanagimachi R, et al. Reprogramming of primordial germ cells begins before migration into the genital ridge, making these cells inadequate donors for reproductive cloning. Proc Natl Acad Sci U S A. 2003;100:12207-12212.
[239] Lee J, Inoue K, Ono R, Ogonuki N, Kohda T, Kaneko-Ishino T, et al. Erasing genomic imprinting memory in mouse clone embryos produced from day 11.5 primordial germ cells. Development. 2002;129:1807-1817.
[240] Hajkova P, Erhardt S, Lane N, Haaf T, El-Maarri O, Reik W, et al. Epigenetic reprogramming in mouse primordial germ cells. Mech Dev. 2002;117:15-23.
[241] Barreto G, Schafer A, Marhold J, Stach D, Swaminathan SK, Handa V, et al. Gadd45a promotes epigenetic gene activation by repair-mediated DNA demethylation. Nature. 2007;445:671-675.
[242] Hsu HC, Yang P, Wu Q, Wang JH, Job G, Guentert T, et al. Inhibition of the catalytic function of activation-induced cytidine deaminase promotes apoptosis of germinal center B cells in BXD2 mice. Arthritis Rheum. 2011;63:2038-2048.
[243] Jiang C, Zhao ML, Scearce RM, Diaz M. Activation-induced deaminase-deficient MRL/lpr mice secrete high levels of protective antibodies against lupus nephritis. Arthritis Rheum. 2011;63:1086-1096.
[244] Jiang C, Foley J, Clayton N, Kissling G, Jokinen M, Herbert R, et al. Abrogation of lupus nephritis in activation-induced deaminase-deficient MRL/lpr mice. J Immunol. 2007;178:7422-7431.
[245] Shen HM, Michael N, Kim N, Storb U. The TATA binding protein, c-Myc and survivin genes are not somatically hypermutated, while Ig and BCL6 genes are hypermutated in human memory B cells. Int Immunol. 2000;12:1085-1093.
[246] Muschen M, Re D, Jungnickel B, Diehl V, Rajewsky K, Kuppers R. Somatic mutation of the CD95 gene in human B cells as a side-effect of the germinal center reaction. J Exp Med. 2000;192:1833-1840.
[247] Pasqualucci L, Migliazza A, Fracchiolla N, William C, Neri A, Baldini L, et al. BCL-6 mutations in normal germinal center B cells: evidence of somatic hypermutation acting outside Ig loci. Proc Natl Acad Sci U S A. 1998;95:11816-11821.
[248] Gordon MS, Kanegai CM, Doerr JR, Wall R. Somatic hypermutation of the B cell receptor genes B29 (Igbeta, CD79b) and mb1 (Igalpha, CD79a). Proc Natl Acad Sci U S A. 2003;100:4126-4131.

[249] Pasqualucci L, Neumeister P, Goossens T, Nanjangud G, Chaganti RS, Kuppers R, et al. Hypermutation of multiple proto-oncogenes in B-cell diffuse large-cell lymphomas. Nature. 2001;412:341-346.
[250] Shen HM, Peters A, Baron B, Zhu X, Storb U. Mutation of BCL-6 gene in normal B cells by the process of somatic hypermutation of Ig genes. Science. 1998;280:1750-1752.
[251] Zan H, Li Z, Yamaji K, Dramitinos P, Cerutti A, Casali P. B cell receptor engagement and T cell contact induce Bcl-6 somatic hypermutation in human B cells: identity with Ig hypermutation. J Immunol. 2000;165:830-839.
[252] Bemark M, Neuberger MS. The c-MYC allele that is translocated into the IgH locus undergoes constitutive hypermutation in a Burkitt's lymphoma line. Oncogene. 2000;19:3404-3410.
[253] Liu M, Duke JL, Richter DJ, Vinuesa CG, Goodnow CC, Kleinstein SH, et al. Two levels of protection for the B cell genome during somatic hypermutation. Nature. 2008;451:841-845.
[254] Yoshikawa K, Okazaki IM, Eto T, Kinoshita K, Muramatsu M, Nagaoka H, et al. AID enzyme-induced hypermutation in an actively transcribed gene in fibroblasts. Science. 2002;296:2033-2036.
[255] Martin A, Scharff MD. Somatic hypermutation of the AID transgene in B and non-B cells. Proc Natl Acad Sci U S A. 2002;99:12304-12308.
[256] Kotani A, Okazaki IM, Muramatsu M, Kinoshita K, Begum NA, Nakajima T, et al. A target selection of somatic hypermutations is regulated similarly between T and B cells upon activation-induced cytidine deaminase expression. Proc Natl Acad Sci U S A. 2005;102:4506-4511.
[257] Yamane A, Resch W, Kuo N, Kuchen S, Li Z, Sun HW, et al. Deep-sequencing identification of the genomic targets of the cytidine deaminase AID and its cofactor RPA in B lymphocytes. Nat Immunol. 2011;12:62-69.
[258] Pasqualucci L, Bhagat G, Jankovic M, Compagno M, Smith P, Muramatsu M, et al. AID is required for germinal center-derived lymphomagenesis. Nat Genet. 2008;40:108-112.
[259] Gruber TA, Chang MS, Sposto R, Muschen M. Activation-induced cytidine deaminase accelerates clonal evolution in BCR-ABL1-driven B-cell lineage acute lymphoblastic leukemia. Cancer Res. 2010;70:7411-7420.
[260] Feldhahn N, Henke N, Melchior K, Duy C, Soh BN, Klein F, et al. Activation-induced cytidine deaminase acts as a mutator in BCR-ABL1-transformed acute lymphoblastic leukemia cells. J Exp Med. 2007;204:1157-1166.
[261] Ramiro AR, Jankovic M, Callen E, Difilippantonio S, Chen HT, McBride KM, et al. Role of genomic instability and p53 in AID-induced c-myc-Igh translocations. Nature. 2006;440:105-109.
[262] Robbiani DF, Bothmer A, Callen E, Reina-San-Martin B, Dorsett Y, Difilippantonio S, et al. AID is required for the chromosomal breaks in c-myc that lead to c-myc/IgH translocations. Cell. 2008;135:1028-1038.
[263] Dorsett Y, Robbiani DF, Jankovic M, Reina-San-Martin B, Eisenreich TR, Nussenzweig MC. A role for AID in chromosome translocations between c-myc and the IgH variable region. J Exp Med. 2007;204:2225-2232.

[264] Chiarle R, Zhang Y, Frock RL, Lewis SM, Molinie B, Ho YJ, et al. Genome-wide translocation sequencing reveals mechanisms of chromosome breaks and rearrangements in B cells. Cell. 2011;147:107-119.
[265] Klein IA, Resch W, Jankovic M, Oliveira T, Yamane A, Nakahashi H, et al. Translocation-capture sequencing reveals the extent and nature of chromosomal rearrangements in B lymphocytes. Cell. 2011;147:95-106.
[266] Jankovic M, Robbiani DF, Dorsett Y, Eisenreich T, Xu Y, Tarakhovsky A, et al. Role of the translocation partner in protection against AID-dependent chromosomal translocations. Proc Natl Acad Sci U S A. 2010;107:187-192.
[267] Gauwerky CE, Huebner K, Isobe M, Nowell PC, Croce CM. Activation of MYC in a masked t(8;17) translocation results in an aggressive B-cell leukemia. Proc Natl Acad Sci U S A. 1989;86:8867-8871.
[268] Hasham MG, Donghia NM, Coffey E, Maynard J, Snow KJ, Ames J, et al. Widespread genomic breaks generated by activation-induced cytidine deaminase are prevented by homologous recombination. Nat Immunol. 2010;11:820-826.
[269] Moldenhauer G, Popov SW, Wotschke B, Bruderlein S, Riedl P, Fissolo N, et al. AID expression identifies interfollicular large B cells as putative precursors of mature B-cell malignancies. Blood. 2006;107:2470-2473.
[270] Smit LA, Bende RJ, Aten J, Guikema JE, Aarts WM, van Noesel CJ. Expression of activation-induced cytidine deaminase is confined to B-cell non-Hodgkin's lymphomas of germinal-center phenotype. Cancer Res. 2003;63:3894-3898.
[271] Lossos IS, Levy R, Alizadeh AA. AID is expressed in germinal center B-cell-like and activated B-cell-like diffuse large-cell lymphomas and is not correlated with intraclonal heterogeneity. Leukemia. 2004;18:1775-1779.
[272] Bodor C, Bognar A, Reiniger L, Szepesi A, Toth E, Kopper L, et al. Aberrant somatic hypermutation and expression of activation-induced cytidine deaminase mRNA in mediastinal large B-cell lymphoma. Br J Haematol. 2005;129:373-376.
[273] Deutsch AJ, Aigelsreiter A, Staber PB, Beham A, Linkesch W, Guelly C, et al. MALT lymphoma and extranodal diffuse large B-cell lymphoma are targeted by aberrant somatic hypermutation. Blood. 2007;109:3500-3504.
[274] McCarthy H, Wierda WG, Barron LL, Cromwell CC, Wang J, Coombes KR, et al. High expression of activation-induced cytidine deaminase (AID) and splice variants is a distinctive feature of poor-prognosis chronic lymphocytic leukemia. Blood. 2003;101:4903-4908.
[275] Palacios F, Moreno P, Morande P, Abreu C, Correa A, Porro V, et al. High expression of AID and active class switch recombination might account for a more aggressive disease in unmutated CLL patients: link with an activated microenvironment in CLL disease. Blood. 2010;115:4488-4496.
[276] Endo Y, Marusawa H, Kou T, Nakase H, Fujii S, Fujimori T, et al. Activation-induced cytidine deaminase links between inflammation and the development of colitis-associated colorectal cancers. Gastroenterology. 2008;135:889-898, 898 e881-883.
[277] Endo Y, Marusawa H, Kinoshita K, Morisawa T, Sakurai T, Okazaki IM, et al. Expression of activation-induced cytidine deaminase in human hepatocytes via NF-kappaB signaling. Oncogene. 2007;26:5587-5595.

[278] Kou T, Marusawa H, Kinoshita K, Endo Y, Okazaki IM, Ueda Y, et al. Expression of activation-induced cytidine deaminase in human hepatocytes during hepatocarcinogenesis. Int J Cancer. 2007;120:469-476.
[279] Komori J, Marusawa H, Machimoto T, Endo Y, Kinoshita K, Kou T, et al. Activation-induced cytidine deaminase links bile duct inflammation to human cholangiocarcinoma. Hepatology. 2008;47:888-896.
[280] Matsumoto Y, Marusawa H, Kinoshita K, Endo Y, Kou T, Morisawa T, et al. Helicobacter pylori infection triggers aberrant expression of activation-induced cytidine deaminase in gastric epithelium. Nat Med. 2007;13:470-476.
[281] Machida K, Cheng KT, Sung VM, Shimodaira S, Lindsay KL, Levine AM, et al. Hepatitis C virus induces a mutator phenotype: enhanced mutations of immunoglobulin and protooncogenes. Proc Natl Acad Sci U S A. 2004;101:4262-4267.
[282] Matsumoto Y, Marusawa H, Kinoshita K, Niwa Y, Sakai Y, Chiba T. Up-regulation of activation-induced cytidine deaminase causes genetic aberrations at the CDKN2b-CDKN2a in gastric cancer. Gastroenterology. 2010;139:1984-1994.
[283] Epeldegui M, Thapa DR, De la Cruz J, Kitchen S, Zack JA, Martinez-Maza O. CD40 ligand (CD154) incorporated into HIV virions induces activation-induced cytidine deaminase (AID) expression in human B lymphocytes. PLoS One. 2010;5:e11448.
[284] Dedeoglu F, Horwitz B, Chaudhuri J, Alt FW, Geha RS. Induction of activation-induced cytidine deaminase gene expression by IL-4 and CD40 ligation is dependent on STAT6 and NFkappaB. Int Immunol. 2004;16:395-404.
[285] Zan H, Zhang J, Ardeshna S, Xu Z, Park SR, Casali P. Lupus-prone MRL/faslpr/lpr mice display increased AID expression and extensive DNA lesions, comprising deletions and insertions, in the immunoglobulin locus: concurrent upregulation of somatic hypermutation and class switch DNA recombination. Autoimmunity. 2009;42:89-103.
[286] White CA, Seth Hawkins J, Pone EJ, Yu ES, Al-Qahtani A, Mai T, et al. AID dysregulation in lupus-prone MRL/Fas(lpr/lpr) mice increases class switch DNA recombination and promotes interchromosomal c-Myc/IgH loci translocations: modulation by HoxC4. Autoimmunity. 2011;44:585-598.
[287] Xu X, Hsu HC, Chen J, Grizzle WE, Chatham WW, Stockard CR, et al. Increased expression of activation-induced cytidine deaminase is associated with anti-CCP and rheumatoid factor in rheumatoid arthritis. Scand J Immunol. 2009;70:309-316.
[288] Hase K, Takahashi D, Ebisawa M, Kawano S, Itoh K, Ohno H. Activation-induced cytidine deaminase deficiency causes organ-specific autoimmune disease. PLoS One. 2008;3:e3033.
[289] Quartier P, Bustamante J, Sanal O, Plebani A, Debre M, Deville A, et al. Clinical, immunologic and genetic analysis of 29 patients with autosomal recessive hyper-IgM syndrome due to Activation-Induced Cytidine Deaminase deficiency. Clin Immunol. 2004;110:22-29.
[290] Aloisi F, Pujol-Borrell R. Lymphoid neogenesis in chronic inflammatory diseases. Nat Rev Immunol. 2006;6:205-217.
[291] Humby F, Bombardieri M, Manzo A, Kelly S, Blades MC, Kirkham B, et al. Ectopic lymphoid structures support ongoing production of class-switched autoantibodies in rheumatoid synovium. PLoS Med. 2009;6:e1.

[292] Coker HA, Durham SR, Gould HJ. Local somatic hypermutation and class switch recombination in the nasal mucosa of allergic rhinitis patients. J Immunol. 2003;171:5602-5610.
[293] Takhar P, Corrigan CJ, Smurthwaite L, O'Connor BJ, Durham SR, Lee TH, et al. Class switch recombination to IgE in the bronchial mucosa of atopic and nonatopic patients with asthma. J Allergy Clin Immunol. 2007;119:213-218.
[294] Vicario M, Blanchard C, Stringer KF, Collins MH, Mingler MK, Ahrens A, et al. Local B cells and IgE production in the oesophageal mucosa in eosinophilic oesophagitis. Gut. 2010;59:12-20.
[295] Takhar P, Smurthwaite L, Coker HA, Fear DJ, Banfield GK, Carr VA, et al. Allergen drives class switching to IgE in the nasal mucosa in allergic rhinitis. J Immunol. 2005;174:5024-5032.
[296] Mechtcheriakova D, Sobanov Y, Holtappels G, Bajna E, Svoboda M, Jaritz M, et al. Activation-induced cytidine deaminase (AID)-associated multigene signature to assess impact of AID in etiology of diseases with inflammatory component. PLoS One. 2011;6:e25611.
[297] Tran TH, Nakata M, Suzuki K, Begum NA, Shinkura R, Fagarasan S, et al. B cell-specific and stimulation-responsive enhancers derepress Aicda by overcoming the effects of silencers. Nat Immunol. 2010;11:148-154.
[298] Park SR, Zan H, Pal Z, Zhang J, Al-Qahtani A, Pone EJ, et al. HoxC4 binds to the promoter of the cytidine deaminase AID gene to induce AID expression, class-switch DNA recombination and somatic hypermutation. Nat Immunol. 2009;10:540-550.
[299] Gonda H, Sugai M, Nambu Y, Katakai T, Agata Y, Mori KJ, et al. The balance between Pax5 and Id2 activities is the key to AID gene expression. J Exp Med. 2003;198:1427-1437.
[300] Yadav A, Olaru A, Saltis M, Setren A, Cerny J, Livak F. Identification of a ubiquitously active promoter of the murine activation-induced cytidine deaminase (AICDA) gene. Mol Immunol. 2006;43:529-541.
[301] Sayegh CE, Quong MW, Agata Y, Murre C. E-proteins directly regulate expression of activation-induced deaminase in mature B cells. Nat Immunol. 2003;4:586-593.
[302] Sherman MH, Kuraishy AI, Deshpande C, Hong JS, Cacalano NA, Gatti RA, et al. AID-induced genotoxic stress promotes B cell differentiation in the germinal center via ATM and LKB1 signaling. Mol Cell. 2010;39:873-885.
[303] de Yebenes VG, Belver L, Pisano DG, Gonzalez S, Villasante A, Croce C, et al. miR-181b negatively regulates activation-induced cytidine deaminase in B cells. J Exp Med. 2008;205:2199-2206.
[304] Basu U, Chaudhuri J, Alpert C, Dutt S, Ranganath S, Li G, et al. The AID antibody diversification enzyme is regulated by protein kinase A phosphorylation. Nature. 2005;438:508-511.
[305] Chatterji M, Unniraman S, McBride KM, Schatz DG. Role of activation-induced deaminase protein kinase A phosphorylation sites in Ig gene conversion and somatic hypermutation. J Immunol. 2007;179:5274-5280.
[306] Gazumyan A, Timachova K, Yuen G, Siden E, Di Virgilio M, Woo EM, et al. Amino-terminal phosphorylation of activation-induced cytidine deaminase suppresses c-myc/IgH translocation. Mol Cell Biol. 2011;31:442-449.

[307] McBride KM, Gazumyan A, Woo EM, Barreto VM, Robbiani DF, Chait BT, et al. Regulation of hypermutation by activation-induced cytidine deaminase phosphorylation. Proc Natl Acad Sci U S A. 2006;103:8798-8803.
[308] Pasqualucci L, Kitaura Y, Gu H, Dalla-Favera R. PKA-mediated phosphorylation regulates the function of activation-induced deaminase (AID) in B cells. Proc Natl Acad Sci U S A. 2006;103:395-400.
[309] Demorest ZL, Li M, Harris RS. Phosphorylation directly regulates the intrinsic DNA cytidine deaminase activity of activation-induced deaminase and APOBEC3G protein. J Biol Chem. 2011;286:26568-26575.
[310] Cheng HL, Vuong BQ, Basu U, Franklin A, Schwer B, Astarita J, et al. Integrity of the AID serine-38 phosphorylation site is critical for class switch recombination and somatic hypermutation in mice. Proc Natl Acad Sci U S A. 2009;106:2717-2722.
[311] Vuong BQ, Lee M, Kabir S, Irimia C, Macchiarulo S, McKnight GS, et al. Specific recruitment of protein kinase A to the immunoglobulin locus regulates class-switch recombination. Nat Immunol. 2009;10:420-426.
[312] Chaudhuri J, Khuong C, Alt FW. Replication protein A interacts with AID to promote deamination of somatic hypermutation targets. Nature. 2004;430:992-998.
[313] Rada C, Jarvis JM, Milstein C. AID-GFP chimeric protein increases hypermutation of Ig genes with no evidence of nuclear localization. Proc Natl Acad Sci USA. 2002;99:7003-7008.
[314] Ito S, Nagaoka H, Shinkura R, Begum N, Muramatsu M, Nakata M, et al. Activation-induced cytidine deaminase shuttles between nucleus and cytoplasm like apolipoprotein B mRNA editing catalytic polypeptide 1. Proc Natl Acad Sci U S A. 2004;101:1975-1980.
[315] Patenaude AM, Orthwein A, Hu Y, Campo VA, Kavli B, Buschiazzo A, et al. Active nuclear import and cytoplasmic retention of activation-induced deaminase. Nat Struct Mol Biol. 2009;16:517-527.
[316] McBride KM, Barreto V, Ramiro AR, Stavropoulos P, Nussenzweig MC. Somatic hypermutation is limited by CRM1-dependent nuclear export of activation-induced deaminase. J Exp Med. 2004;199:1235-1244.
[317] Brar SS, Watson M, Diaz M. Activation-induced cytosine deaminase (AID) is actively exported out of the nucleus but retained by the induction of DNA breaks. J Biol Chem. 2004;279:26395-26401.
[318] Brar SS, Watson M, Diaz M. Activation-induced cytosine deaminase (AID) is actively exported out of the nucleus but retained by the induction of DNA breaks. J Biol Chem. 2004;279:26395-26401.
[319] Ito S, Nagaoka H, Shinkura R, Begum NA, Muramatsu M, Nakata M, et al. Activation-induced cytidine deaminase shuttles between nucleus and cytoplasm like apolipoprotein B mRNA editing catalytic polypeptide 1. Proc Natl Acad Sci USA. 2004;101:1975-1980.
[320] Ellyard JI, Benk AS, Taylor B, Rada C, Neuberger MS. The dependence of Ig class-switching on the nuclear export sequence of AID likely reflects interaction with factors additional to Crm1 exportin. Eur J Immunol. 2011;41:485-490.
[321] Conticello SG, Ganesh K, Xue K, Lu M, Rada C, Neuberger MS. Interaction between antibody-diversification enzyme AID and spliceosome-associated factor CTNNBL1. Mol Cell. 2008;31:474-484.

[322] Ganesh K, Adam S, Taylor B, Simpson P, Rada C, Neuberger MS. CTNNBL1 Is a Novel Nuclear Localization Sequence-binding Protein That Recognizes RNA-splicing Factors CDC5L and Prp31. J Biol Chem. 2011;286:17091-17102.
[323] Han L, Masani S, Yu K. Cutting edge: CTNNBL1 is dispensable for Ig class switch recombination. J Immunol. 2010;185:1379-1381.
[324] Maeda K, Singh SK, Eda K, Kitabatake M, Pham P, Goodman MF, et al. GANP-mediated recruitment of activation-induced cytidine deaminase to cell nuclei and to immunoglobulin variable region DNA. J Biol Chem. 2010;285:23945-23953.
[325] Häsler J, Rada C, Neuberger MS. Cytoplasmic activation-induced cytidine deaminase (AID) exists in stoichiometric complex with translation elongation factor 1α (eEF1A). Proc Natl Acad Sci USA. 2011;108:18366-18371.
[326] Ordinario EC, Yabuki M, Larson RP, Maizels N. Temporal regulation of Ig gene diversification revealed by single-cell imaging. J Immunol. 2009;183:4545-4553.
[327] Patenaude AM, Di Noia JM. The mechanisms regulating the subcellular localization of AID Nucleus. 2010;1:325-331.
[328] Barreto VM, Reina San-Martin BR, Ramiro AR, McBride KM, Nussenzweig MC. C-terminal deletion of AID uncouples class switch recombination from somatic hypermutation and gene conversion. Mol Cell. 2003;12:501-508.
[329] Geisberger R, Rada C, Neuberger MS. The stability of AID and its function in class-switching are critically sensitive to the identity of its nuclear-export sequence. Proc Natl Acad Sci USA. 2009;106:6736-6741.
[330] Kohli RM, Abrams SR, Gajula KS, Maul RW, Gearhart PJ, Stivers JT. A portable hot spot recognition loop transfers sequence preferences from APOBEC family members to activation-induced cytidine deaminase. J Biol Chem. 2009;284:22898-22904.
[331] Aoufouchi S, Faili A, Zober C, D'Orlando O, Weller S, Weill J-C, et al. Proteasomal degradation restricts the nuclear lifespan of AID. J Exp Med. 2008;205:1357-1368.
[332] Orthwein A, Patenaude A-M, Affar EB, Lamarre A, Young JC, Di Noia JM. Regulation of activation-induced deaminase stability and antibody gene diversification by Hsp90. J Exp Med. 2010;207:2751-2765.
[333] Uchimura Y, Barton LF, Rada C, Neuberger MS. REG-gamma associates with and modulates the abundance of nuclear activation-induced deaminase. J Exp Med. 2011;208:2385-2391.
[334] MacDuff DA, Neuberger MS, Harris RS. MDM2 can interact with the C-terminus of AID but it is inessential for antibody diversification in DT40 B cells. Mol Immunol. 2006;43:1099-1108.
[335] Besmer E, Market E, Papavasiliou FN. The transcription elongation complex directs activation-induced cytidine deaminase-mediated DNA deamination. Mol Cell Biol. 2006;26:4378-4385.
[336] Okazaki IM, Kinoshita K, Muramatsu M, Yoshikawa K, Honjo T. The AID enzyme induces class switch recombination in fibroblasts. Nature. 2002;416:340-345.
[337] Tumas-Brundage K, Manser T. The transcriptional promoter regulates hypermutation of the antibody heavy chain locus. J Exp Med. 1997;185:239-250.
[338] Peters A, Storb U. Somatic hypermutation of immunoglobulin genes is linked to transcription initiation. Immunity. 1996;4:57-65.

[339] Fukita Y, Jacobs H, Rajewsky K. Somatic hypermutation in the heavy chain locus correlates with transcription. Immunity. 1998;9:105-114.
[340] Bachl J, Carlson C, Gray-Schopfer V, Dessing M, Olsson C. Increased transcription levels induce higher mutation rates in a hypermutating cell line. J Immunol. 2001;166:5051-5057.
[341] Wang M, Rada C, Neuberger MS. Altering the spectrum of immunoglobulin V gene somatic hypermutation by modifying the active site of AID. J Exp Med. 2010;207:141-153.
[342] Kohli RM, Abrams SR, Gajula KS, Maul RW, Gearhart PJ, Stivers JT. A portable hot spot recognition loop transfers sequence preferences from APOBEC family members to activation-induced cytidine deaminase. J Biol Chem. 2009;284:22898-22904.
[343] Shen HM, Storb U. Activation-induced cytidine deaminase (AID) can target both DNA strands when the DNA is supercoiled. Proc Natl Acad Sci U S A. 2004;101:12997-13002.
[344] Basu U, Meng FL, Keim C, Grinstein V, Pefanis E, Eccleston J, et al. The RNA exosome targets the AID cytidine deaminase to both strands of transcribed duplex DNA substrates. Cell. 2011;144:353-363.
[345] Wang L, Wuerffel R, Feldman S, Khamlichi AA, Kenter AL. S region sequence, RNA polymerase II, and histone modifications create chromatin accessibility during class switch recombination. J Exp Med. 2009;206:1817-1830.
[346] Kuang FL, Luo Z, Scharff MD. H3 trimethyl K9 and H3 acetyl K9 chromatin modifications are associated with class switch recombination. Proc Natl Acad Sci U S A. 2009;106:5288-5293.
[347] Chowdhury M, Forouhi O, Dayal S, McCloskey N, Gould HJ, Felsenfeld G, et al. Analysis of intergenic transcription and histone modification across the human immunoglobulin heavy-chain locus. Proc Natl Acad Sci U S A. 2008;105:15872-15877.
[348] Fraenkel S, Mostoslavsky R, Novobrantseva TI, Pelanda R, Chaudhuri J, Esposito G, et al. Allelic 'choice' governs somatic hypermutation in vivo at the immunoglobulin kappa-chain locus. Nat Immunol. 2007;8:715-722.
[349] Wang L, Whang N, Wuerffel R, Kenter AL. AID-dependent histone acetylation is detected in immunoglobulin S regions. J Exp Med. 2006;203:215-226.
[350] Odegard VH, Kim ST, Anderson SM, Shlomchik MJ, Schatz DG. Histone modifications associated with somatic hypermutation. Immunity. 2005;23:101-110.
[351] Jeevan-Raj BP, Robert I, Heyer V, Page A, Wang JH, Cammas F, et al. Epigenetic tethering of AID to the donor switch region during immunoglobulin class switch recombination. J Exp Med. 2011;208:1649-1660.
[352] Pavri R, Gazumyan A, Jankovic M, Di Virgilio M, Klein I, Ansarah-Sobrinho C, et al. Activation-induced cytidine deaminase targets DNA at sites of RNA polymerase II stalling by interaction with Spt5. Cell. 2010;143:122-133.
[353] Rajagopal D, Maul RW, Ghosh A, Chakraborty T, Khamlichi AA, Sen R, et al. Immunoglobulin switch mu sequence causes RNA polymerase II accumulation and reduces dA hypermutation. J Exp Med. 2009;206:1237-1244.
[354] Nowak U, Matthews AJ, Zheng S, Chaudhuri J. The splicing regulator PTBP2 interacts with the cytidine deaminase AID and promotes binding of AID to switch-region DNA. Nat Immunol. 2011;12:160-166.

[355] Xu Z, Fulop Z, Wu G, Pone EJ, Zhang J, Mai T, et al. 14-3-3 adaptor proteins recruit AID to 5'-AGCT-3'-rich switch regions for class switch recombination. Nat Struct Mol Biol. 2010;17:1124-1135.
[356] Shinkura R, Ito S, Begum NA, Nagaoka H, Muramatsu M, Kinoshita K, et al. Separate domains of AID are required for somatic hypermutation and class-switch recombination. Nat Immunol. 2004;5:707-712.
[357] Barreto V, Reina-San-Martin B, Ramiro AR, McBride KM, Nussenzweig MC. C-terminal deletion of AID uncouples class switch recombination from somatic hypermutation and gene conversion. Mol Cell. 2003;12:501-508.
[358] Ta VT, Nagaoka H, Catalan N, Durandy A, Fischer A, Imai K, et al. AID mutant analyses indicate requirement for class-switch-specific cofactors. Nat Immunol. 2003;4:843-848.
[359] Geisberger R, Rada C, Neuberger MS. The stability of AID and its function in class-switching are critically sensitive to the identity of its nuclear-export sequence. Proc Natl Acad Sci U S A. 2009;106:6736-6741.
[360] Wu X, Geraldes P, Platt JL, Cascalho M. The double-edged sword of activation-induced cytidine deaminase. J Immunol. 2005;174:934-941.
[361] Doi T, Kinoshita K, Ikegawa M, Muramatsu M, Honjo T. De novo protein synthesis is required for the activation-induced cytidine deaminase function in class-switch recombination. Proc Natl Acad Sci U S A. 2003;100:2634-2638.
[362] Reynaud CA, Aoufouchi S, Faili A, Weill JC. What role for AID: mutator, or assembler of the immunoglobulin mutasome? Nat Immunol. 2003;4:631-638.
[363] Kampinga HH, Craig EA. The HSP70 chaperone machinery: J proteins as drivers of functional specificity. Nat Rev Mol Cell Biol. 2010;11:579-592.
[364] Freeman BC, Yamamoto KR. Disassembly of transcriptional regulatory complexes by molecular chaperones. Science. 2002;296:2232-2235.
[365] Picard D, Khursheed B, Garabedian MJ, Fortin MG, Lindquist S, Yamamoto KR. Reduced levels of hsp90 compromise steroid receptor action in vivo. Nature. 1990;348:166-168.
[366] Pratt WB, Toft DO. Regulation of signaling protein function and trafficking by the hsp90/hsp70-based chaperone machinery. Exp Biol Med (Maywood). 2003;228:111-133.
[367] McClellan AJ, Xia Y, Deutschbauer AM, Davis RW, Gerstein M, Frydman J. Diverse cellular functions of the Hsp90 molecular chaperone uncovered using systems approaches. Cell. 2007;131:121-135.
[368] Zhao R, Davey M, Hsu YC, Kaplanek P, Tong A, Parsons AB, et al. Navigating the chaperone network: an integrative map of physical and genetic interactions mediated by the hsp90 chaperone. Cell. 2005;120:715-727.
[369] Millson SH, Truman AW, King V, Prodromou C, Pearl LH, Piper PW. A two-hybrid screen of the yeast proteome for Hsp90 interactors uncovers a novel Hsp90 chaperone requirement in the activity of a stress-activated mitogen-activated protein kinase, Slt2p (Mpk1p). Eukaryot Cell. 2005;4:849-860.
[370] Krukenberg KA, Street TO, Lavery LA, Agard DA. Conformational dynamics of the molecular chaperone Hsp90. Q Rev Biophys. 2011;44:229-255.

[371] Soti C, Racz A, Csermely P. A Nucleotide-dependent molecular switch controls ATP binding at the C-terminal domain of Hsp90. N-terminal nucleotide binding unmasks a C-terminal binding pocket. J Biol Chem. 2002;277:7066-7075.
[372] Meyer P, Prodromou C, Hu B, Vaughan C, Roe SM, Panaretou B, et al. Structural and functional analysis of the middle segment of hsp90: implications for ATP hydrolysis and client protein and cochaperone interactions. Mol Cell. 2003;11:647-658.
[373] Panaretou B, Siligardi G, Meyer P, Maloney A, Sullivan JK, Singh S, et al. Activation of the ATPase activity of hsp90 by the stress-regulated cochaperone aha1. Mol Cell. 2002;10:1307-1318.
[374] Meyer P, Prodromou C, Liao C, Hu B, Mark Roe S, Vaughan CK, et al. Structural basis for recruitment of the ATPase activator Aha1 to the Hsp90 chaperone machinery. Embo J. 2004;23:511-519.
[375] Taipale M, Jarosz DF, Lindquist S. HSP90 at the hub of protein homeostasis: emerging mechanistic insights. Nat Rev Mol Cell Biol. 2010;11:515-528.
[376] Xu Y, Singer MA, Lindquist S. Maturation of the tyrosine kinase c-src as a kinase and as a substrate depends on the molecular chaperone Hsp90. Proc Natl Acad Sci U S A. 1999;96:109-114.
[377] Brugge JS. Interaction of the Rous sarcoma virus protein pp60src with the cellular proteins pp50 and pp90. Curr Top Microbiol Immunol. 1986;123:1-22.
[378] Xu Y, Lindquist S. Heat-shock protein hsp90 governs the activity of pp60v-src kinase. Proc Natl Acad Sci U S A. 1993;90:7074-7078.
[379] Sterrenberg JN, Blatch GL, Edkins AL. Human DNAJ in cancer and stem cells. Cancer Lett. 2011;312:129-142.
[380] Cheetham ME, Caplan AJ. Structure, function and evolution of DnaJ: conservation and adaptation of chaperone function. Cell Stress Chaperones. 1998;3:28-36.
[381] Wall D, Zylicz M, Georgopoulos C. The NH2-terminal 108 amino acids of the Escherichia coli DnaJ protein stimulate the ATPase activity of DnaK and are sufficient for lambda replication. J Biol Chem. 1994;269:5446-5451.
[382] Tsai J, Douglas MG. A conserved HPD sequence of the J-domain is necessary for YDJ1 stimulation of Hsp70 ATPase activity at a site distinct from substrate binding. J Biol Chem. 1996;271:9347-9354.
[383] Qiu XB, Shao YM, Miao S, Wang L. The diversity of the DnaJ/Hsp40 family, the crucial partners for Hsp70 chaperones. Cell Mol Life Sci. 2006;63:2560-2570.
[384] Hageman J, Kampinga HH. Computational analysis of the human HSPH/HSPA/DNAJ family and cloning of a human HSPH/HSPA/DNAJ expression library. Cell Stress Chaperones. 2009;14:1-21.
[385] Wittung-Stafshede P, Guidry J, Horne BE, Landry SJ. The J-domain of Hsp40 couples ATP hydrolysis to substrate capture in Hsp70. Biochemistry. 2003;42:4937-4944.
[386] Horne BE, Li T, Genevaux P, Georgopoulos C, Landry SJ. The Hsp40 J-domain stimulates Hsp70 when tethered by the client to the ATPase domain. J Biol Chem. 2010;285:21679-21688.
[387] Greene MK, Maskos K, Landry SJ. Role of the J-domain in the cooperation of Hsp40 with Hsp70. Proc Natl Acad Sci U S A. 1998;95:6108-6113.

[388] Wall D, Zylicz M, Georgopoulos C. The conserved G/F motif of the DnaJ chaperone is necessary for the activation of the substrate binding properties of the DnaK chaperone. J Biol Chem. 1995;270:2139-2144.
[389] Karzai AW, McMacken R. A bipartite signaling mechanism involved in DnaJ-mediated activation of the Escherichia coli DnaK protein. J Biol Chem. 1996;271:11236-11246.
[390] Minami Y, Hohfeld J, Ohtsuka K, Hartl FU. Regulation of the heat-shock protein 70 reaction cycle by the mammalian DnaJ homolog, Hsp40. J Biol Chem. 1996;271:19617-19624.
[391] Li J, Qian X, Sha B. The crystal structure of the yeast Hsp40 Ydj1 complexed with its peptide substrate. Structure. 2003;11:1475-1483.
[392] Wu Y, Li J, Jin Z, Fu Z, Sha B. The crystal structure of the C-terminal fragment of yeast Hsp40 Ydj1 reveals novel dimerization motif for Hsp40. J Mol Biol. 2005;346:1005-1011.
[393] Sha B, Lee S, Cyr DM. The crystal structure of the peptide-binding fragment from the yeast Hsp40 protein Sis1. Structure. 2000;8:799-807.
[394] Lu Z, Cyr DM. Protein folding activity of Hsp70 is modified differentially by the hsp40 co-chaperones Sis1 and Ydj1. J Biol Chem. 1998;273:27824-27830.
[395] Lu Z, Cyr DM. The conserved carboxyl terminus and zinc finger-like domain of the co-chaperone Ydj1 assist Hsp70 in protein folding. J Biol Chem. 1998;273:5970-5978.
[396] Kanazawa M, Terada K, Kato S, Mori M. HSDJ, a human homolog of DnaJ, is farnesylated and is involved in protein import into mitochondria. J Biochem. 1997;121:890-895.
[397] Caplan AJ, Tsai J, Casey PJ, Douglas MG. Farnesylation of YDJ1p is required for function at elevated growth temperatures in Saccharomyces cerevisiae. J Biol Chem. 1992;267:18890-18895.
[398] Sebti SM. Protein farnesylation: implications for normal physiology, malignant transformation, and cancer therapy. Cancer Cell. 2005;7:297-300.
[399] Marshall CJ. Protein prenylation: a mediator of protein-protein interactions. Science. 1993;259:1865-1866.
[400] Flom GA, Lemieszek M, Fortunato EA, Johnson JL. Farnesylation of Ydj1 is required for in vivo interaction with Hsp90 client proteins. Mol Biol Cell. 2008;19:5249-5258.
[401] Kimura Y, Yahara I, Lindquist S. Role of the protein chaperone YDJ1 in establishing Hsp90-mediated signal transduction pathways. Science. 1995;268:1362-1365.
[402] Young JC. Mechanisms of the Hsp70 chaperone system. Biochem Cell Biol. 2010;88:291-300.
[403] Zuehlke A, Johnson JL. Hsp90 and co-chaperones twist the functions of diverse client proteins. Biopolymers. 2010;93:211-217.
[404] McLaughlin SH, Sobott F, Yao ZP, Zhang W, Nielsen PR, Grossmann JG, et al. The co-chaperone p23 arrests the Hsp90 ATPase cycle to trap client proteins. J Mol Biol. 2006;356:746-758.
[405] Freeman BC, Felts SJ, Toft DO, Yamamoto KR. The p23 molecular chaperones act at a late step in intracellular receptor action to differentially affect ligand efficacies. Genes Dev. 2000;14:422-434.
[406] Young JC, Hartl FU. Polypeptide release by Hsp90 involves ATP hydrolysis and is enhanced by the co-chaperone p23. Embo J. 2000;19:5930-5940.
[407] Pratt WB, Morishima Y, Osawa Y. The Hsp90 chaperone machinery regulates signaling by modulating ligand binding clefts. J Biol Chem. 2008;283:22885-22889.

[408] Trepel J, Mollapour M, Giaccone G, Neckers L. Targeting the dynamic HSP90 complex in cancer. Nat Rev Cancer. 2010;10:537-549.
[409] Whitesell L, Lindquist SL. HSP90 and the chaperoning of cancer. Nat Rev Cancer. 2005;5:761-772.
[410] Cutforth T, Rubin GM. Mutations in Hsp83 and cdc37 impair signaling by the sevenless receptor tyrosine kinase in Drosophila. Cell. 1994;77:1027-1036.
[411] Borkovich KA, Farrelly FW, Finkelstein DB, Taulien J, Lindquist S. hsp82 is an essential protein that is required in higher concentrations for growth of cells at higher temperatures. Mol Cell Biol. 1989;9:3919-3930.
[412] Bardwell JC, Tilly K, Craig E, King J, Zylicz M, Georgopoulos C. The nucleotide sequence of the Escherichia coli K12 dnaJ+ gene. A gene that encodes a heat shock protein. J Biol Chem. 1986;261:1782-1785.
[413] Ghaemmaghami S, Huh WK, Bower K, Howson RW, Belle A, Dephoure N, et al. Global analysis of protein expression in yeast. Nature. 2003;425:737-741.
[414] Heldens L, Dirks RP, Hensen SM, Onnekink C, van Genesen ST, Rustenburg F, et al. Co-chaperones are limiting in a depleted chaperone network. Cell Mol Life Sci. 2010;67:4035-4048.
[415] Dittmar KD, Banach M, Galigniana MD, Pratt WB. The role of DnaJ-like proteins in glucocorticoid receptor.hsp90 heterocomplex assembly by the reconstituted hsp90.p60.hsp70 foldosome complex. J Biol Chem. 1998;273:7358-7366.
[416] Cintron NS, Toft D. Defining the requirements for Hsp40 and Hsp70 in the Hsp90 chaperone pathway. J Biol Chem. 2006;281:26235-26244.
[417] Hernandez MP, Chadli A, Toft DO. HSP40 binding is the first step in the HSP90 chaperoning pathway for the progesterone receptor. J Biol Chem. 2002;277:11873-11881.
[418] Kosano H, Stensgard B, Charlesworth MC, McMahon N, Toft D. The assembly of progesterone receptor-hsp90 complexes using purified proteins. J Biol Chem. 1998;273:32973-32979.
[419] Felts SJ, Karnitz LM, Toft DO. Functioning of the Hsp90 machine in chaperoning checkpoint kinase I (Chk1) and the progesterone receptor (PR). Cell Stress Chaperones. 2007;12:353-363.
[420] Walker VE, Wong MJ, Atanasiu R, Hantouche C, Young JC, Shrier A. Hsp40 chaperones promote degradation of the HERG potassium channel. J Biol Chem. 2010;285:3319-3329.
[421] Tzankov S, Wong MJ, Shi K, Nassif C, Young JC. Functional divergence between co-chaperones of Hsc70. J Biol Chem. 2008;283:27100-27109.
[422] Terada K, Mori M. Human DnaJ homologs dj2 and dj3, and bag-1 are positive cochaperones of hsc70. J Biol Chem. 2000;275:24728-24734.
[423] Bhangoo MK, Tzankov S, Fan AC, Dejgaard K, Thomas DY, Young JC. Multiple 40-kDa heat-shock protein chaperones function in Tom70-dependent mitochondrial import. Mol Biol Cell. 2007;18:3414-3428.
[424] Terada K, Yomogida K, Imai T, Kiyonari H, Takeda N, Kadomatsu T, et al. A type I DnaJ homolog, DjA1, regulates androgen receptor signaling and spermatogenesis. Embo J. 2005;24:611-622.

[425] Lo JF, Hayashi M, Woo-Kim S, Tian B, Huang JF, Fearns C, et al. Tid1, a cochaperone of the heat shock 70 protein and the mammalian counterpart of the Drosophila tumor suppressor l(2)tid, is critical for early embryonic development and cell survival. Mol Cell Biol. 2004;24:2226-2236.
[426] Hayashi M, Imanaka-Yoshida K, Yoshida T, Wood M, Fearns C, Tatake RJ, et al. A crucial role of mitochondrial Hsp40 in preventing dilated cardiomyopathy. Nat Med. 2006;12:128-132.
[427] Uchiyama Y, Takeda N, Mori M, Terada K. Heat shock protein 40/DjB1 is required for thermotolerance in early phase. J Biochem. 2006;140:805-812.
[428] Hunter PJ, Swanson BJ, Haendel MA, Lyons GE, Cross JC. Mrj encodes a DnaJ-related co-chaperone that is essential for murine placental development. Development. 1999;126:1247-1258.
[429] Ladiges WC, Knoblaugh SE, Morton JF, Korth MJ, Sopher BL, Baskin CR, et al. Pancreatic beta-cell failure and diabetes in mice with a deletion mutation of the endoplasmic reticulum molecular chaperone gene P58IPK. Diabetes. 2005;54:1074-1081.
[430] Fernandez-Chacon R, Wolfel M, Nishimune H, Tabares L, Schmitz F, Castellano-Munoz M, et al. The synaptic vesicle protein CSP alpha prevents presynaptic degeneration. Neuron. 2004;42:237-251.
[431] Munster PN, Marchion DC, Basso AD, Rosen N. Degradation of HER2 by ansamycins induces growth arrest and apoptosis in cells with HER2 overexpression via a HER3, phosphatidylinositol 3'-kinase-AKT-dependent pathway. Cancer Res. 2002;62:3132-3137.
[432] Stepanova L, Leng X, Parker SB, Harper JW. Mammalian p50Cdc37 is a protein kinase-targeting subunit of Hsp90 that binds and stabilizes Cdk4. Genes Dev. 1996;10:1491-1502.
[433] Schulte TW, Blagosklonny MV, Romanova L, Mushinski JF, Monia BP, Johnston JF, et al. Destabilization of Raf-1 by geldanamycin leads to disruption of the Raf-1-MEK-mitogen-activated protein kinase signalling pathway. Mol Cell Biol. 1996;16:5839-5845.
[434] DeZwaan DC, Freeman BC. HSP90 manages the ends. Trends Biochem Sci. 2010;35:384-391.
[435] Holt SE, Aisner DL, Baur J, Tesmer VM, Dy M, Ouellette M, et al. Functional requirement of p23 and Hsp90 in telomerase complexes. Genes Dev. 1999;13:817-826.
[436] Basso AD, Solit DB, Chiosis G, Giri B, Tsichlis P, Rosen N. Akt forms an intracellular complex with heat shock protein 90 (Hsp90) and Cdc37 and is destabilized by inhibitors of Hsp90 function. J Biol Chem. 2002;277:39858-39866.
[437] Cerchietti LC, Lopes EC, Yang SN, Hatzi K, Bunting KL, Tsikitas LA, et al. A purine scaffold Hsp90 inhibitor destabilizes BCL-6 and has specific antitumor activity in BCL-6-dependent B cell lymphomas. Nat Med. 2009;15:1369-1376.
[438] Peng C, Li D, Li S. Heat shock protein 90: a potential therapeutic target in leukemic progenitor and stem cells harboring mutant BCR-ABL resistant to kinase inhibitors. Cell Cycle. 2007;6:2227-2231.
[439] Shiotsu Y, Neckers LM, Wortman I, An WG, Schulte TW, Soga S, et al. Novel oxime derivatives of radicicol induce erythroid differentiation associated with preferential G(1) phase accumulation against chronic myelogenous leukemia cells through destabilization of Bcr-Abl with Hsp90 complex. Blood. 2000;96:2284-2291.

[440] Peng C, Brain J, Hu Y, Goodrich A, Kong L, Grayzel D, et al. Inhibition of heat shock protein 90 prolongs survival of mice with BCR-ABL-T315I-induced leukemia and suppresses leukemic stem cells. Blood. 2007;110:678-685.
[441] Rutherford SL, Lindquist S. Hsp90 as a capacitor for morphological evolution. Nature. 1998;396:336-342.
[442] Queitsch C, Sangster TA, Lindquist S. Hsp90 as a capacitor of phenotypic variation. Nature. 2002;417:618-624.
[443] Roe SM, Prodromou C, O'Brien R, Ladbury JE, Piper PW, Pearl LH. Structural basis for inhibition of the Hsp90 molecular chaperone by the antitumor antibiotics radicicol and geldanamycin. J Med Chem. 1999;42:260-266.
[444] Kim YS, Alarcon SV, Lee S, Lee MJ, Giaccone G, Neckers L, et al. Update on Hsp90 inhibitors in clinical trial. Curr Top Med Chem. 2009;9:1479-1492.
[445] Murata S, Minami Y, Minami M, Chiba T, Tanaka K. CHIP is a chaperone-dependent E3 ligase that ubiquitylates unfolded protein. EMBO Rep. 2001;2:1133-1138.
[446] Connell P, Ballinger CA, Jiang J, Wu Y, Thompson LJ, Hohfeld J, et al. The co-chaperone CHIP regulates protein triage decisions mediated by heat-shock proteins. Nat Cell Biol. 2001;3:93-96.
[447] Xu W, Marcu M, Yuan X, Mimnaugh E, Patterson C, Neckers L. Chaperone-dependent E3 ubiquitin ligase CHIP mediates a degradative pathway for c-ErbB2/Neu. Proc Natl Acad Sci U S A. 2002;99:12847-12852.
[448] Morishima Y, Wang AM, Yu Z, Pratt WB, Osawa Y, Lieberman AP. CHIP deletion reveals functional redundancy of E3 ligases in promoting degradation of both signaling proteins and expanded glutamine proteins. Hum Mol Genet. 2008;17:3942-3952.
[449] Ehrlich ES, Wang T, Luo K, Xiao Z, Niewiadomska AM, Martinez T, et al. Regulation of Hsp90 client proteins by a Cullin5-RING E3 ubiquitin ligase. Proc Natl Acad Sci U S A. 2009;106:20330-20335.
[450] Mitra A, Shevde LA, Samant RS. Multi-faceted role of HSP40 in cancer. Clin Exp Metastasis. 2009;26:559-567.
[451] Wang CC, Liao YP, Mischel PS, Iwamoto KS, Cacalano NA, McBride WH. HDJ-2 as a target for radiosensitization of glioblastoma multiforme cells by the farnesyltransferase inhibitor R115777 and the role of the p53/p21 pathway. Cancer Res. 2006;66:6756-6762.
[452] Rechsteiner M, Hill CP. Mobilizing the proteolytic machine: cell biological roles of proteasome activators and inhibitors. Trends Cell Biol. 2005;15:27-33.
[453] Farras R, Bossis G, Andermarcher E, Jariel-Encontre I, Piechaczyk M. Mechanisms of delivery of ubiquitylated proteins to the proteasome: new target for anti-cancer therapy? Crit Rev Oncol Hematol. 2005;54:31-51.
[454] Groll M, Ditzel L, Lowe J, Stock D, Bochtler M, Bartunik HD, et al. Structure of 20S proteasome from yeast at 2.4 A resolution. Nature. 1997;386:463-471.
[455] Lowe J, Stock D, Jap B, Zwickl P, Baumeister W, Huber R. Crystal structure of the 20S proteasome from the archaeon T. acidophilum at 3.4 A resolution. Science. 1995;268:533-539.
[456] Groll M, Bajorek M, Kohler A, Moroder L, Rubin DM, Huber R, et al. A gated channel into the proteasome core particle. Nat Struct Biol. 2000;7:1062-1067.

[457] Peters JM, Franke WW, Kleinschmidt JA. Distinct 19 S and 20 S subcomplexes of the 26 S proteasome and their distribution in the nucleus and the cytoplasm. J Biol Chem. 1994;269:7709-7718.
[458] DeMartino GN, Moomaw CR, Zagnitko OP, Proske RJ, Chu-Ping M, Afendis SJ, et al. PA700, an ATP-dependent activator of the 20 S proteasome, is an ATPase containing multiple members of a nucleotide-binding protein family. J Biol Chem. 1994;269:20878-20884.
[459] Udvardy A. Purification and characterization of a multiprotein component of the Drosophila 26 S (1500 kDa) proteolytic complex. J Biol Chem. 1993;268:9055-9062.
[460] Hoffman P, Rajakumar P, Hoffman B, Heuertz R, Wold WS, Carlin CR. Evidence for intracellular down-regulation of the epidermal growth factor (EGF) receptor during adenovirus infection by an EGF-independent mechanism. J Virol. 1992;66:197-203.
[461] Dubiel W, Pratt G, Ferrell K, Rechsteiner M. Purification of an 11 S regulator of the multicatalytic protease. J Biol Chem. 1992;267:22369-22377.
[462] Ma CP, Slaughter CA, DeMartino GN. Identification, purification, and characterization of a protein activator (PA28) of the 20 S proteasome (macropain). J Biol Chem. 1992;267:10515-10523.
[463] Ustrell V, Hoffman L, Pratt G, Rechsteiner M. PA200, a nuclear proteasome activator involved in DNA repair. Embo J. 2002;21:3516-3525.
[464] McCutchen-Maloney SL, Matsuda K, Shimbara N, Binns DD, Tanaka K, Slaughter CA, et al. cDNA cloning, expression, and functional characterization of PI31, a proline-rich inhibitor of the proteasome. J Biol Chem. 2000;275:18557-18565.
[465] Gao Y, Lecker S, Post MJ, Hietaranta AJ, Li J, Volk R, et al. Inhibition of ubiquitin-proteasome pathway-mediated I kappa B alpha degradation by a naturally occurring antibacterial peptide. J Clin Invest. 2000;106:439-448.
[466] Zwickl P, Voges D, Baumeister W. The proteasome: a macromolecular assembly designed for controlled proteolysis. Philos Trans R Soc Lond B Biol Sci. 1999;354:1501-1511.
[467] Peters JM, Cejka Z, Harris JR, Kleinschmidt JA, Baumeister W. Structural features of the 26 S proteasome complex. J Mol Biol. 1993;234:932-937.
[468] Breitschopf K, Bengal E, Ziv T, Admon A, Ciechanover A. A novel site for ubiquitination: the N-terminal residue, and not internal lysines of MyoD, is essential for conjugation and degradation of the protein. Embo J. 1998;17:5964-5973.
[469] Pickart CM, Eddins MJ. Ubiquitin: structures, functions, mechanisms. Biochim Biophys Acta. 2004;1695:55-72.
[470] Glickman MH, Ciechanover A. The ubiquitin-proteasome proteolytic pathway: destruction for the sake of construction. Physiol Rev. 2002;82:373-428.
[471] Wang X, Herr RA, Chua WJ, Lybarger L, Wiertz EJ, Hansen TH. Ubiquitination of serine, threonine, or lysine residues on the cytoplasmic tail can induce ERAD of MHC-I by viral E3 ligase mK3. J Cell Biol. 2007;177:613-624.
[472] Cadwell K, Coscoy L. The specificities of Kaposi's sarcoma-associated herpesvirus-encoded E3 ubiquitin ligases are determined by the positions of lysine or cysteine residues within the intracytoplasmic domains of their targets. J Virol. 2008;82:4184-4189.
[473] Cadwell K, Coscoy L. Ubiquitination on nonlysine residues by a viral E3 ubiquitin ligase. Science. 2005;309:127-130.

[474] Tokarev AA, Munguia J, Guatelli JC. Serine-threonine ubiquitination mediates downregulation of BST-2/tetherin and relief of restricted virion release by HIV-1 Vpu. J Virol. 2011;85:51-63.
[475] Magadan JG, Perez-Victoria FJ, Sougrat R, Ye Y, Strebel K, Bonifacino JS. Multilayered mechanism of CD4 downregulation by HIV-1 Vpu involving distinct ER retention and ERAD targeting steps. PLoS Pathog. 2010;6:e1000869.
[476] Jariel-Encontre I, Bossis G, Piechaczyk M. Ubiquitin-independent degradation of proteins by the proteasome. Biochim Biophys Acta. 2008;1786:153-177.
[477] Rotin D, Kumar S. Physiological functions of the HECT family of ubiquitin ligases. Nat Rev Mol Cell Biol. 2009;10:398-409.
[478] Christensen DE, Klevit RE. Dynamic interactions of proteins in complex networks: identifying the complete set of interacting E2s for functional investigation of E3-dependent protein ubiquitination. FEBS J. 2009;276:5381-5389.
[479] Rosenberg-Hasson Y, Bercovich Z, Ciechanover A, Kahana C. Degradation of ornithine decarboxylase in mammalian cells is ATP dependent but ubiquitin independent. Eur J Biochem. 1989;185:469-474.
[480] Bercovich Z, Rosenberg-Hasson Y, Ciechanover A, Kahana C. Degradation of ornithine decarboxylase in reticulocyte lysate is ATP-dependent but ubiquitin-independent. J Biol Chem. 1989;264:15949-15952.
[481] Bloom J, Amador V, Bartolini F, DeMartino G, Pagano M. Proteasome-mediated degradation of p21 via N-terminal ubiquitinylation. Cell. 2003;115:71-82.
[482] Coulombe P, Rodier G, Bonneil E, Thibault P, Meloche S. N-Terminal ubiquitination of extracellular signal-regulated kinase 3 and p21 directs their degradation by the proteasome. Mol Cell Biol. 2004;24:6140-6150.
[483] Jariel-Encontre I, Pariat M, Martin F, Carillo S, Salvat C, Piechaczyk M. Ubiquitinylation is not an absolute requirement for degradation of c-Jun protein by the 26 S proteasome. J Biol Chem. 1995;270:11623-11627.
[484] Uchimura Y, Barton LF, Rada C, Neuberger MS. REG-gamma associates with and modulates the abundance of nuclear activation-induced deaminase. J Exp Med. 2011.
[485] Realini C, Jensen CC, Zhang Z, Johnston SC, Knowlton JR, Hill CP, et al. Characterization of recombinant REGalpha, REGbeta, and REGgamma proteasome activators. J Biol Chem. 1997;272:25483-25492.
[486] Baugh JM, Viktorova EG, Pilipenko EV. Proteasomes can degrade a significant proportion of cellular proteins independent of ubiquitination. J Mol Biol. 2009;386:814-827.
[487] Hoyt MA, Coffino P. Ubiquitin-free routes into the proteasome. Cell Mol Life Sci. 2004;61:1596-1600.
[488] Grune T, Merker K, Sandig G, Davies KJ. Selective degradation of oxidatively modified protein substrates by the proteasome. Biochem Biophys Res Commun. 2003;305:709-718.
[489] Liu CW, Corboy MJ, DeMartino GN, Thomas PJ. Endoproteolytic activity of the proteasome. Science. 2003;299:408-411.
[490] Zhou P. REGgamma: a shortcut to destruction. Cell. 2006;124:256-257.
[491] Dice JF, Goldberg AL. A statistical analysis of the relationship between degradative rates and molecular weights of proteins. Arch Biochem Biophys. 1975;170:213-219.

[492] Dice JF, Hess EJ, Goldberg AL. Studies on the relationship between the degradative rates of proteins in vivo and their isoelectric points. Biochem J. 1979;178:305-312.
[493] Dice JF, Goldberg AL. Relationship between in vivo degradative rates and isoelectric points of proteins. Proc Natl Acad Sci U S A. 1975;72:3893-3897.
[494] Goldberg AL, St John AC. Intracellular protein degradation in mammalian and bacterial cells: Part 2. Annu Rev Biochem. 1976;45:747-803.
[495] Goldberg AL, Dice JF. Intracellular protein degradation in mammalian and bacterial cells. Annu Rev Biochem. 1974;43:835-869.
[496] Frescas D, Pagano M. Deregulated proteolysis by the F-box proteins SKP2 and beta-TrCP: tipping the scales of cancer. Nat Rev Cancer. 2008;8:438-449.
[497] Barford D. Structure, function and mechanism of the anaphase promoting complex (APC/C). Q Rev Biophys. 2011;44:153-190.
[498] Rogers S, Wells R, Rechsteiner M. Amino acid sequences common to rapidly degraded proteins: the PEST hypothesis. Science. 1986;234:364-368.
[499] Bachmair A, Finley D, Varshavsky A. In vivo half-life of a protein is a function of its amino-terminal residue. Science. 1986;234:179-186.
[500] Varshavsky A. The N-end rule pathway and regulation by proteolysis. Protein Sci. 2011.
[501] Kanno T, Endo H, Takeuchi K, Morishita Y, Fukayama M, Mori S. High expression of methionine aminopeptidase type 2 in germinal center B cells and their neoplastic counterparts. Lab Invest. 2002;82:893-901.
[502] Priest RC, Spaull J, Buckton J, Grimley RL, Sims M, Binks M, et al. Immunomodulatory activity of a methionine aminopeptidase-2 inhibitor on B cell differentiation. Clin Exp Immunol. 2009;155:514-522.
[503] Giglione C, Boularot A, Meinnel T. Protein N-terminal methionine excision. Cell Mol Life Sci. 2004;61:1455-1474.
[504] Tompa P, Prilusky J, Silman I, Sussman JL. Structural disorder serves as a weak signal for intracellular protein degradation. Proteins. 2008;71:903-909.
[505] Rechsteiner M, Rogers SW. PEST sequences and regulation by proteolysis. Trends Biochem Sci. 1996;21:267-271.
[506] Gsponer J, Futschik ME, Teichmann SA, Babu MM. Tight regulation of unstructured proteins: from transcript synthesis to protein degradation. Science. 2008;322:1365-1368.
[507] Singh GP, Ganapathi M, Sandhu KS, Dash D. Intrinsic unstructuredness and abundance of PEST motifs in eukaryotic proteomes. Proteins. 2006;62:309-315.
[508] Lukov GL, Goodell MA. LYL1 degradation by the proteasome is directed by a N-terminal PEST rich site in a phosphorylation-independent manner. PLoS One. 2010;5.
[509] Tsurumi C, Ishida N, Tamura T, Kakizuka A, Nishida E, Okumura E, et al. Degradation of c-Fos by the 26S proteasome is accelerated by c-Jun and multiple protein kinases. Mol Cell Biol. 1995;15:5682-5687.
[510] Yaglom J, Linskens MH, Sadis S, Rubin DM, Futcher B, Finley D. p34Cdc28-mediated control of Cln3 cyclin degradation. Mol Cell Biol. 1995;15:731-741.
[511] Badi I, Cinquetti R, Frascoli M, Parolini C, Chiesa G, Taramelli R, et al. Intracellular ANKRD1 protein levels are regulated by 26S proteasome-mediated degradation. FEBS Lett. 2009;583:2486-2492.

[512] Belizario JE, Alves J, Garay-Malpartida M, Occhiucci JM. Coupling caspase cleavage and proteasomal degradation of proteins carrying PEST motif. Curr Protein Pept Sci. 2008;9:210-220.
[513] Pfleger CM, Kirschner MW. The KEN box: an APC recognition signal distinct from the D box targeted by Cdh1. Genes Dev. 2000;14:655-665.
[514] Yamano H, Gannon J, Hunt T. The role of proteolysis in cell cycle progression in Schizosaccharomyces pombe. Embo J. 1996;15:5268-5279.
[515] King RW, Glotzer M, Kirschner MW. Mutagenic analysis of the destruction signal of mitotic cyclins and structural characterization of ubiquitinated intermediates. Mol Biol Cell. 1996;7:1343-1357.
[516] Glotzer M, Murray AW, Kirschner MW. Cyclin is degraded by the ubiquitin pathway. Nature. 1991;349:132-138.
[517] Margottin F, Bour SP, Durand H, Selig L, Benichou S, Richard V, et al. A novel human WD protein, h-beta TrCp, that interacts with HIV-1 Vpu connects CD4 to the ER degradation pathway through an F-box motif. Mol Cell. 1998;1:565-574.
[518] Hart M, Concordet JP, Lassot I, Albert I, del los Santos R, Durand H, et al. The F-box protein beta-TrCP associates with phosphorylated beta-catenin and regulates its activity in the cell. Curr Biol. 1999;9:207-210.
[519] Yaron A, Hatzubai A, Davis M, Lavon I, Amit S, Manning AM, et al. Identification of the receptor component of the IkappaBalpha-ubiquitin ligase. Nature. 1998;396:590-594.
[520] Buschhorn BA, Peters JM. How APC/C orders destruction. Nat Cell Biol. 2006;8:209-211.
[521] Fuchs SY, Spiegelman VS, Kumar KG. The many faces of beta-TrCP E3 ubiquitin ligases: reflections in the magic mirror of cancer. Oncogene. 2004;23:2028-2036.
[522] Aoufouchi S, Faili A, Zober C, D'Orlando O, Weller S, Weill JC, et al. Proteasomal degradation restricts the nuclear lifespan of AID. J Exp Med. 2008;205:1357-1368.
[523] Orthwein A, Patenaude AM, Affar el B, Lamarre A, Young JC, Di Noia JM. Regulation of activation-induced deaminase stability and antibody gene diversification by Hsp90. J Exp Med. 2010;207:2751-2765.
[524] Orthwein A, Zahn A, Methot SP, Godin D, Conticello SG, Terada K, et al. Optimal functional levels of activation-induced deaminase specifically require the Hsp40 DnaJa1. Embo J. 2011.
[525] Lau PP, Villanueva H, Kobayashi K, Nakamuta M, Chang BH, Chan L. A DnaJ protein, apobec-1-binding protein-2, modulates apolipoprotein B mRNA editing. J Biol Chem. 2001;276:46445-46452.
[526] Yu M, Haslam RH, Haslam DB. HEDJ, an Hsp40 co-chaperone localized to the endoplasmic reticulum of human cells. J Biol Chem. 2000;275:24984-24992.
[527] Blanc V, Kennedy S, Davidson NO. A novel nuclear localization signal in the auxiliary domain of apobec-1 complementation factor regulates nucleocytoplasmic import and shuttling. J Biol Chem. 2003;278:41198-41204.
[528] Etard C, Behra M, Fischer N, Hutcheson D, Geisler R, Strahle U. The UCS factor Steif/Unc-45b interacts with the heat shock protein Hsp90a during myofibrillogenesis. Dev Biol. 2007;308:133-143.

[529] Falsone SF, Kungl AJ, Rek A, Cappai R, Zangger K. The molecular chaperone Hsp90 modulates intermediate steps of amyloid assembly of the Parkinson-related protein alpha-synuclein. J Biol Chem. 2009;284:31190-31199.
[530] Uversky VN. A protein-chameleon: conformational plasticity of alpha-synuclein, a disordered protein involved in neurodegenerative disorders. J Biomol Struct Dyn. 2003;21:211-234.
[531] Dickey CA, Kamal A, Lundgren K, Klosak N, Bailey RM, Dunmore J, et al. The high-affinity HSP90-CHIP complex recognizes and selectively degrades phosphorylated tau client proteins. J Clin Invest. 2007;117:648-658.
[532] Schweers O, Schonbrunn-Hanebeck E, Marx A, Mandelkow E. Structural studies of tau protein and Alzheimer paired helical filaments show no evidence for beta-structure. J Biol Chem. 1994;269:24290-24297.
[533] Kriwacki RW, Hengst L, Tennant L, Reed SI, Wright PE. Structural studies of p21Waf1/Cip1/Sdi1 in the free and Cdk2-bound state: conformational disorder mediates binding diversity. Proc Natl Acad Sci U S A. 1996;93:11504-11509.
[534] Li H, Okamoto K, Peart MJ, Prives C. Lysine-independent turnover of cyclin G1 can be stabilized by B'alpha subunits of protein phosphatase 2A. Mol Cell Biol. 2009;29:919-928.
[535] Sanchez ER, Toft DO, Schlesinger MJ, Pratt WB. Evidence that the 90-kDa phosphoprotein associated with the untransformed L-cell glucocorticoid receptor is a murine heat shock protein. J Biol Chem. 1985;260:12398-12401.
[536] Schuh S, Yonemoto W, Brugge J, Bauer VJ, Riehl RM, Sullivan WP, et al. A 90,000-dalton binding protein common to both steroid receptors and the Rous sarcoma virus transforming protein, pp60v-src. J Biol Chem. 1985;260:14292-14296.
[537] Joab I, Radanyi C, Renoir M, Buchou T, Catelli MG, Binart N, et al. Common non-hormone binding component in non-transformed chick oviduct receptors of four steroid hormones. Nature. 1984;308:850-853.
[538] Kumar R, Volk DE, Li J, Lee JC, Gorenstein DG, Thompson EB. TATA box binding protein induces structure in the recombinant glucocorticoid receptor AF1 domain. Proc Natl Acad Sci U S A. 2004;101:16425-16430.
[539] Wandinger SK, Richter K, Buchner J. The Hsp90 chaperone machinery. J Biol Chem. 2008;283:18473-18477.
[540] Picard D. Chaperoning steroid hormone action. Trends Endocrinol Metab. 2006;17:229-235.
[541] Hartl FU, Bracher A, Hayer-Hartl M. Molecular chaperones in protein folding and proteostasis. Nature. 2011;475:324-332.
[542] Young JC, Agashe VR, Siegers K, Hartl FU. Pathways of chaperone-mediated protein folding in the cytosol. Nat Rev Mol Cell Biol. 2004;5:781-791.
[543] Young JC, Hoogenraad NJ, Hartl FU. Molecular chaperones Hsp90 and Hsp70 deliver preproteins to the mitochondrial import receptor Tom70. Cell. 2003;112:41-50.
[544] Johnson JL, Craig EA. An essential role for the substrate-binding region of Hsp40s in Saccharomyces cerevisiae. J Cell Biol. 2001;152:851-856.
[545] Reinders J, Zahedi RP, Pfanner N, Meisinger C, Sickmann A. Toward the complete yeast mitochondrial proteome: multidimensional separation techniques for mitochondrial proteomics. J Proteome Res. 2006;5:1543-1554.

[546] Walsh P, Bursac D, Law YC, Cyr D, Lithgow T. The J-protein family: modulating protein assembly, disassembly and translocation. EMBO Rep. 2004;5:567-571.
[547] Zaheen A, Boulianne B, Parsa JY, Ramachandran S, Gommerman JL, Martin A. AID constrains germinal center size by rendering B cells susceptible to apoptosis. Blood. 2009;114:547-554.
[548] Yano M, Naito Z, Tanaka S, Asano G. Expression and roles of heat shock proteins in human breast cancer. Jpn J Cancer Res. 1996;87:908-915.
[549] Gasc JM, Renoir JM, Faber LE, Delahaye F, Baulieu EE. Nuclear localization of two steroid receptor-associated proteins, hsp90 and p59. Exp Cell Res. 1990;186:362-367.
[550] Langer T, Rosmus S, Fasold H. Intracellular localization of the 90 kDA heat shock protein (HSP90alpha) determined by expression of a EGFP-HSP90alpha-fusion protein in unstressed and heat stressed 3T3 cells. Cell Biol Int. 2003;27:47-52.
[551] Biggiogera M, Tanguay RM, Marin R, Wu Y, Martin TE, Fakan S. Localization of heat shock proteins in mouse male germ cells: an immunoelectron microscopical study. Exp Cell Res. 1996;229:77-85.
[552] Akner G, Mossberg K, Sundqvist KG, Gustafsson JA, Wikstrom AC. Evidence for reversible, non-microtubule and non-microfilament-dependent nuclear translocation of hsp90 after heat shock in human fibroblasts. Eur J Cell Biol. 1992;58:356-364.
[553] Pratt WB, Toft DO. Steroid receptor interactions with heat shock protein and immunophilin chaperones. Endocr Rev. 1997;18:306-360.
[554] Yang J, Liu J, DeFranco DB. Subnuclear trafficking of glucocorticoid receptors in vitro: chromatin recycling and nuclear export. J Cell Biol. 1997;137:523-538.
[555] Tago K, Tsukahara F, Naruse M, Yoshioka T, Takano K. Regulation of nuclear retention of glucocorticoid receptor by nuclear Hsp90. Mol Cell Endocrinol. 2004;213:131-138.
[556] Yang J, DeFranco DB. Assessment of glucocorticoid receptor-heat shock protein 90 interactions in vivo during nucleocytoplasmic trafficking. Mol Endocrinol. 1996;10:3-13.
[557] Hasler J, Rada C, Neuberger MS. Cytoplasmic activation-induced cytidine deaminase (AID) exists in stoichiometric complex with translation elongation factor 1alpha (eEF1A). Proc Natl Acad Sci U S A. 2011.
[558] Dyson HJ, Wright PE. Intrinsically unstructured proteins and their functions. Nat Rev Mol Cell Biol. 2005;6:197-208.
[559] Hegyi H, Tompa P. Intrinsically disordered proteins display no preference for chaperone binding in vivo. Plos Comput Biol. 2008;4:e1000017.
[560] Lehr C, Rzepka R, Schick C, Zgaga-Griesz A, Melchers I. PRESENCE OF EXTRACELLULAR HDJ2 IN SYNOVIAL FLUIDS. B cells and autoantibodies: diagnosis and pathophysiology. 2008.
[561] Baechler EC, Batliwalla FM, Karypis G, Gaffney PM, Ortmann WA, Espe KJ, et al. Interferon-inducible gene expression signature in peripheral blood cells of patients with severe lupus. Proc Natl Acad Sci U S A. 2003;100:2610-2615.
[562] Ramos PS, Williams AH, Ziegler JT, Comeau ME, Guy RT, Lessard CJ, et al. Genetic analyses of interferon pathway-related genes reveal multiple new loci associated with systemic lupus erythematosus. Arthritis Rheum. 2011;63:2049-2057.

[563] Liu Z, Wu X, Duan Y, Wang Y, Shan B, Kong J, et al. AID expression is correlated with Bcr-Abl expression in CML-LBC and can be down-regulated by As2O3 and/or imatinib. Leuk Res. 2011;35:1355-1359.
[564] Takai A, Marusawa H, Minaki Y, Watanabe T, Nakase H, Kinoshita K, et al. Targeting activation-induced cytidine deaminase prevents colon cancer development despite persistent colonic inflammation. Oncogene. 2011.